THE UNIVERSITY *of* EDINBURGH

HYDROLOGY AND DYNAMICS OF A LAND-TERMINATING GREENLAND OUTLET GLACIER

Ian D Bartholomew

Thesis submitted in fulfilment of the requirements for the degree of

Doctor of Philosophy to the University of Edinburgh

2011

Abstract

The purpose of this thesis is to investigate the hydrology and dynamics of a land-terminating outlet glacier on the western margin of the Greenland Ice Sheet (GrIS). The investigations are motivated by uncertainty about the effect of meltwater on rates of ice flow in the GrIS and the possibility that hydrologically forced changes in ice velocity might increase mass loss from the ice sheet significantly in response to climate warming. The impact of meltwater on fluctuations in ice flow has been a research focus for glaciologists studying Alpine and Arctic glaciers for decades. In these settings, one of the main controls on the relationship between surface melting and ice velocity is the structure of the subglacial drainage system, which evolves spatially and temporally on a seasonal basis in response to inputs of meltwater from the glacier surface. In this thesis we present three years of field observations of glacier velocity, surface ablation and hydrology from a land-terminating glacier in west Greenland. These data are supplemented by satellite data and the use of simple models to constrain surface melting.

We find that hydrologically forced ice acceleration occurs each year along a ∼115 km transect, first at sites nearest the ice sheet margin and at locations further inland following the onset of surface melting at higher elevations. At sites near the ice sheet margin, the relationship between surface melting and ice velocity is not consistent throughout the melt season, and ice velocity becomes less sensitive to inputs of meltwater later in the summer. This is explained by development in the efficiency of the subglacial drainage system, in a manner similar to Alpine glaciers. We perform a hydrological study which indicates that an efficient subglacial drainage system expands upglacier over the course of the melt season, in response to inputs of water from the ice sheet surface. At higher elevation sites, however, thicker ice and colder temperatures mean that it is harder to generate enough water to reach the ice-bed interface and this only occurs once enough water has accumulated to propagate fractures through thick ice to the bed. One mechanism which allows this is drainage of supraglacial lakes.

Inter-annual comparison shows that increased rates of annual ablation lead to higher annual ice velocities. At high elevation sites (>1000 m), timing of drainage of meltwater to the ice-bed interface appears to be the main control on the the overall magnitude of summer acceleration. At lower elevations, although development in the structure of the

subglacial drainage system limits the overall summer acceleration signal, short-term variability in meltwater input can sustain high ice velocities even once the subglacial drainage system has become channelised. Overall, the research presented in this thesis suggests that hydrologically-forced acceleration can increase mass loss from the GrIS in a warmer climate due to inland expansion of the area of the ice sheet bed which is subject to inputs of meltwater from the ice sheet surface. The relationship between surface melting and ice velocity is mediated, however, by the structure of the subglacial drainage system and variations in the rate of meltwater drainage to the ice bed interface. Insights from this work can help in the development of numerical ice sheet models which aim to predict the future contribution to sea-level rise from the Greenland Ice Sheet.

Acknowledgements

I am much indebted to Peter Nienow, my main supervisor, for his guidance and support throughout this project. This work is the result of his vision for the fieldwork in Greenland and his diligent input has helped to shape endless drafts of the chapters which appear in this thesis. At the same time, I have been allowed the freedom to work in my own way and responsibility for research that reaches further than my own project. Pete's equanimity has helped us to avoid chaos on each of three field seasons and, above all, our work together has been a lot of fun.

This work would not have been possible without the efforts of a number of people. I would particularly like to thank: Doug Mair, for providing thoughtful advice since the very beginning and excellent times while on fieldwork; Andrew Sole who has been a consistent source of help and entertainment, as well as friendship through long stints in the field; Tom Cowton for his company and good humour in Greenland, and for pointing out to us our most basic errors; Matt King at Newcastle University for invaluable guidance in processing GPS data; and Jemma Wadham and Alun Hubbard for their supervision which has mostly taken place in tents. In addition, we have had numerous field assistants, including undergraduates, postgraduates, family and friends, without whom the summer-long field seasons wouldn't have been possible.

Thanks are also due to the staff at Kangerlussuaq International Scientific Support, VECO Polar Resources (now CH2M Hill), the NEEM Ice Core research project and helicopter pilots from Air Greenland and Heli Greenland for their logistical support and generosity. Michael Studinger and colleagues at NASA who are involved in Operation IceBridge kindly diverted a flight-line to collect ice surface elevation data along our transect and Steve Palmer allowed us to use his digital elevation model of the study area. Thanks also to Paul Kearney and Alan Hobbs from the NERC Geophysical Equipment Facility for loan and training in the use of GPS equipment.

I reserve special thanks for Derek and Maureen Moss. Without their generous financial support, through a University of Edinburgh Moss Centenary Scholarship, the fieldwork in Greenland could never have got off the ground and the scope of this thesis would have been greatly restricted. My PhD has been funded by a Natural Environment Research Council studentship and I received a Royal Society Dudley Stamp Memorial Fund award to support fieldwork in 2008.

Lastly, I would like to thank my family and friends for their support over the past few years. My greatest thanks are to Rosie for her unselfish support, even during long periods of absence, which has kept me going from the first day until the end.

Author's declaration

The work presented in this thesis is original and my own, unless indicated otherwise. No part of the thesis has been submitted for any other academic award or professional qualification.

SIGNED:..... DATE:.....

Contents

CHAPTER 1

Introduction

The purpose of this thesis is to investigate the hydrology and dynamics of a land-terminating outlet glacier on the western margin of the Greenland Ice Sheet (GrIS). The investigations are motivated by uncertainty about the effect of meltwater on rates of ice flow in the GrIS and the possibility that hydrologically forced changes in ice velocity might increase mass loss from the ice sheet significantly in response to climate warming.

1.1 The Greenland Ice Sheet and climate change

The GrIS covers an area of 1.7 million km^2 and contains enough freshwater to increase global sea level by approximately 7 m if it were to melt completely (*Bamber et al.*, 2001, 2003; *Church et al.*, 2001). The most recent IPCC report (AR4) estimated that the GrIS contribution to global sea level rise had increased from 0.05 $\pm$ 0.12 mm yr^{-1} for the period 1961 - 2003, to 0.21 $\pm$ 0.07 mm yr^{-1} between 1993 and 2003 (*Bindoff et al.*, 2007) in response to late 20th century climate warming (*Meehl et al.*, 2007). In addition

to concerns over the socio-economic impacts of global sea level rise (e.g. *Nicholls et al.*, 2007; *Dasgupta et al.*, 2009), increased freshwater flux from the GrIS has the potential to inhibit key areas of North Atlantic Deepwater (NADW) production (*Dickson and Brown*, 1994), affecting the turnover of large scale ocean circulation and, in turn, global heat transfer and regional climate (e.g. *Rahmstorf*, 1995; *Fichefet et al.*, 2003).

The GrIS gains mass through precipitation and loses it primarily by runoff of meltwater from the ice sheet surface, calving of icebergs where outlet glaciers meet the sea and submarine melting of floating ice tongues. Recently reported estimates of the GrIS mass balance (the net sum of mass gained and lost from the ice sheet over a balance year) vary from modest loss during the 1990s (47 - 97 Gt yr^{-1}, which is $\simeq$0.13 - 0.27 mm yr^{-1} sea-level equivalent (s.l.e); *Krabill et al.*, 2000) and near equilibrium for the period 1992 - 2002 (*Zwally et al.*, 2005), to mass losses of >200 Gt yr^{-1} ($\simeq$0.55 mm yr^{-1} s.l.e) since 2002 (*Rignot and Kanagaratnam*, 2006; *Velicogna and Wahr*, 2006; *Chen et al.*, 2006; *Rignot et al.*, 2008; *Van Den Broeke et al.*, 2009; *Rignot et al.*, 2011). This evidence that GrIS mass loss has accelerated in the last decade is substantiated by independent calculations of the GrIS mass balance using different techniques (e.g. *Van Den Broeke et al.*, 2009; *Rignot et al.*, 2011).

Traditional consensus had suggested that climate warming over the coming centuries (*Meehl et al.*, 2007) would lead to gradual interplay between marginal mass loss in the ablation zone and increased mass gain in the accumulation zone of the GrIS, resulting in a slow retreat of the ice sheet over the course of a few millennia, and that changes in ice dynamics (controlled either thermodynamically or by changes in ice geometry) would respond over glacial-interglacial timescales (e.g. *Huybrechts et al.*, 1991; *Oerlemans*, 1991; *Van de Wal and Oerlemans*, 1994; *Huybrechts and de Wolde*, 1999; *Church et al.*, 2001). Recent observations of accelerated ice flow in outlet glaciers which drain from the GrIS interior (*Joughin et al.*, 2004; *Rignot and Kanagaratnam*, 2006; *Luckman and Murray*, 2005; *Howat et al.*, 2005, 2007; *Luckman et al.*, 2006; *Stearns and Hamilton*, 2007; *Pritchard et al.*, 2009) suggest, however, that ice dynamic responses to climate warming may play a much greater role in the future mass balance of the GrIS than had been previously considered (*Pritchard et al.*, 2009; *Howat et al.*, 2007; *Krabill et al.*, 2004; *Alley et al.*, 2005a; *Zwally et al.*, 2002; *Parizek and Alley*, 2004). Annual rates of

dynamic mass loss are now roughly equal to ablation at the ice sheet surface (*Rignot and Kanagaratnam*, 2006; *Van Den Broeke et al.*, 2009) and if recent increases in ice discharge continue, sea level rise predictions for the next few centuries will need to be revised upward (*Krabill et al.*, 2004; *Alley et al.*, 2005a; *Shepherd and Wingham*, 2007).

Although this shortcoming was recognised in AR4, mechanisms that allow rapid coupling between ice dynamics and climatic forcing are not currently included in large scale ice sheet models used to predict future sea level change (*Meehl et al.*, 2007). This is partly a consequence of computational limitations, but also because the processes which control these changes are relatively poorly understood (*Alley et al.*, 2005a).

Where outlet glaciers drain into the ocean, changes in ice dynamics may result from processes that act at the glacier terminus to trigger a retreat, thereby reducing resistance to ice flow. Proposed mechanisms include a reduction in the buttressing resistance provided by an ice shelf (*Joughin et al.*, 2004), increased calving rates sustained by rapid melting (*Thomas*, 2004; *Holland et al.*, 2008) or glacier retreat and associated ungrounding (*Howat et al.*, 2005). These mechanisms are often termed 'marine' and are thought to result from warmer ocean temperatures (e.g. *Thomas*, 2004; *Holland et al.*, 2008), although the initial forcing could also be driven by surface melting at the glacier terminus. Dynamic thinning of marine-terminating outlet glaciers now reaches all latitudes in Greenland (*Rignot and Kanagaratnam*, 2006; *Pritchard et al.*, 2009) and, although these glaciers only represent a small fraction of the GrIS margin, they drain ice from large inland basins (*Rignot and Kanagaratnam*, 2006) and are responsible for virtually all of the recent acceleration in dynamic mass loss that has been observed in the GrIS (*Rignot and Kanagaratnam*, 2006; *Sole et al.*, 2008; *Van Den Broeke et al.*, 2009; *Thomas et al.*, 2009; *Joughin et al.*, 2010).

In land-terminating sections of the GrIS, variations in ice velocity are initiated when surface meltwater drains to the ice-bed interface, via moulins and crevasses, lubricating basal motion (*Zwally et al.*, 2002; *Van de Wal et al.*, 2008; *Joughin et al.*, 2008a; *Shepherd et al.*, 2009). Inputs of meltwater from the ice sheet surface act to raise subglacial water pressure, which weakens the coupling between ice and the bed to allow faster sliding (*Iken and Bindschadler*, 1986; *Iverson et al.*, 1999; *Schoof*, 2005). Initial observations show that summer velocities in land-terminating sections of the GrIS can

be >50% faster than in winter (*Van de Wal et al.*, 2008; *Joughin et al.*, 2008a). *Zwally et al.* (2002) recorded summer acceleration of 5 - 25 %, ~35 km from the ice margin in west Greenland, in four consecutive years that was directly correlated with the magnitude of local surface melting (parameterised by the positive degree-day method (*Braithwaite*, 1995)).

Such observations suggest that GrIS dynamics may also respond to atmospheric forcing over short timescales (*Zwally et al.*, 2002; *Joughin et al.*, 2008a; *Das et al.*, 2008; *Van de Wal et al.*, 2008; *Shepherd et al.*, 2009). Although this atmospheric forcing mechanism has not led to rates of ice thinning in land-terminating sections of the GrIS margin that can be resolved using remote sensing techniques (*Sole et al.*, 2008; *Van Den Broeke et al.*, 2009), numerical simulations indicate that the widespread effect of increased surface melting on ice velocities would lead to an additional sea level rise of 0.15 - 0.4 m by 2500 AD, should there be a direct correlation between rates of surface melting and the magnitude of ice acceleration (*Parizek and Alley*, 2004). In these simulations, acceleration near the ice sheet margin draws ice to lower elevations where ablation rates are higher, leading to a positive feedback between enhanced surface melting and ice velocity (*Parizek and Alley*, 2004).

The ice-motion response to seasonal variations in meltwater inputs remains poorly constrained, however, both spatially and temporally. Observations from near the ice sheet margin show that summer acceleration is widespread <30 km from the ice margin in west Greenland (*Joughin et al.*, 2008a). However, we lack datasets which extend further inland to regions where the ice sheet is thicker and melt rates are lower. Both of these factors make it more difficult for surface meltwater to reach the ice-bed interface and may limit the spatial extent of seasonal velocity variation. Drainage of supraglacial lakes is known to be common in the ablation zone of the GrIS (*Box and Ski*, 2007; *McMillan et al.*, 2007; *Sundal et al.*, 2009) and does provide a mechanism by which water can drain through ice >1 km thick (*Das et al.*, 2008; *Krawczynski et al.*, 2009). Nonetheless, while dramatic changes in vertical and horizontal components of ice motion have been observed in response to a lake drainage event in Greenland (*Das et al.*, 2008), it is not certain that the integrated effect of many individual lake drainage events is a sustained and significant increase in ice velocity.

Simultaneous measurements of ice velocity and air temperature have established, over short-time scales, a correlation between local surface melting and velocity fluctuations over a widespread area (*Joughin et al.*, 2008a; *Van de Wal et al.*, 2008; *Shepherd et al.*, 2009). A longer-term study found, however, that higher annual ablation does not necessarily lead to increased annual ice velocities (*Van de Wal et al.*, 2008) and the importance of this relationship for large-scale dynamic behaviour of the GrIS therefore remains equivocal (e.g. *Sundal et al.*, 2011).

The link between subglacial water pressure and variations in the basal sliding component of glacier motion has been long recognised in temperate glaciers (e.g. *Iken et al.*, 1983; *Iken and Bindschadler*, 1986). *Shepherd et al.* (2009) suggest that Alpine glaciers may provide an appropriate analogue for the evolution of the GrIS in a warming climate. In Alpine and High Arctic polythermal valley glaciers ice motion depends on variations in the structure, hydraulic-capacity and efficiency of the subglacial drainage system (*Iken et al.*, 1983), each of which evolve spatially and temporally on a seasonal basis (*Kamb*, 1987; *Bingham et al.*, 2003; *Anderson et al.*, 2004; *Kessler and Anderson*, 2004; *Mair et al.*, 2002a). Until now, limited datasets have been unable to confirm this hypothesis for the GrIS and it is not clear whether our understanding of the behaviour of smaller glaciers can be scaled-up to large ice sheet systems.

1.2 Research objectives

The aim of this project is to investigate the relationship between meltwater production and variations in summer ice velocity in a land-terminating outlet glacier in west Greenland. This is achieved primarily through field studies, supplemented by use of satellite data and simple modelling. The research has a particular focus on behaviour at different elevations along a transect and the mediatory role of the subglacial drainage system. We hope that this will provide a better framework to understand whether meltwater-forced ice acceleration is an important component of GrIS mass balance, and to provide insights for the modelling community who are tasked with representing these mechanisms in large scale ice sheet models through collaborations such as the European Union funded Ice2Sea programme.

Investigation of a land-terminating section of the GrIS margin allows us to focus on atmospheric forcing of ice acceleration because the simpler system isolates the mechanism from the complex interactions associated with marine forcing. The extent to which meltwater forcing contributes to changes in marine-terminating outlet glacier dynamics, by weakening the coupling between ice and its bed, is not fully resolved (e.g. *Van der Veen et al.*, 2011; *Howat et al.*, 2010; *Sole et al.*, 2011). Recent modelling work suggests that while the marine-terminating glacier response to climate warming may be large and rapid, it is also likely to be transient and contemporary changes cannot be simply projected into the future. Roughly half of the ice which calves off the GrIS into the ocean drains through only twelve of these fast flowing outlet glaciers (*Rignot and Kanagaratnam*, 2006), and the greatest changes are observed in those glaciers which have the deepest marine troughs (*Thomas et al.*, 2009). In contrast with the Antarctic ice sheet, however, the GrIS is grounded mostly above sea level (*Bamber et al.*, 2001, 2003). If marine-terminating glaciers continue their retreat (e.g. *Howat et al.*, 2008) then it is possible that the entire GrIS margin will become land-terminating within hundreds of years or less, and the marine forcing will be short-lived (*Bamber et al.*, 2007).

1.3 Thesis structure

The presentation of research in this thesis is structured as a series of papers, each of which comprises a chapter which can be read as an independent piece of work. This approach has been adopted because a large part of the research has been published in peer-reviewed journals. Chapters 4 and 6 are reproduced from articles that were published during the course of my doctoral study, in 2010 and 2011 respectively. In addition, chapter 5 is a slightly extended version of an article that was also published in 2011 and chapter 7 has been submitted for consideration. In order to maintain a coherent structure, and because it is intended that the work is submitted for publication, chapter 8 is also written in paper format.

The research is based on field observations of an outlet glacier in west Greenland that were made over a three year period, from 2008 to 2010. The papers which make up

the thesis reflect chronological development of insights from new data and continuing work. A brief description of how each chapter follows on from the work already presented is provided between each research chapter, along with a statement of the author contributions.

The relationship between surface meltwater production and ice dynamics in the GrIS is an active research focus for a large number of glaciology researchers. Over the course of this study, new data have been reported in the literature and hypotheses have been extended that were not available when the earlier papers were published. This work has played its part in these developments, which often draw directly on findings presented in papers that form this thesis (e.g. *Schoof*, 2010; *Sundal et al.*, 2011; *Pimentel and Flowers*, 2011). As such, later chapters comment on and respond to work that did not exist when earlier chapters were written. Where appropriate, these developments are made clear in the preamble to the research chapters.

Chapter 2 discusses the background and context of the thesis research, and chapter 3 provides a description of the field site and a summary of the data that were collected. Due to the format of the thesis, however, a large part of the discussion about data limitations and uncertainties is incorporated within each chapter at the relevant point. Chapter 9 summarises the main findings of the research and outlines its contribution to our understanding of the relationship between surface melting, glacier hydrology and ice dynamics in land-terminating sections of the GrIS.

The published versions of the three papers that make up chapters 4 - 6 are included in the thesis as appendices. A fourth paper that was produced by our research group during my PhD studies, and on which I am also an author, investigates hydrological controls on ice dynamics in a marine-terminating outlet glacier in SW Greenland. This paper is also included as an appendix.

CHAPTER 2

Background

Current understanding of glacier hydrology and its relationship with ice dynamics is derived mainly from theoretical considerations (e.g. *Röthlisberger*, 1972; *Iken*, 1981) and observations of temperate glaciers in Europe and Alaska (e.g. *Iken et al.*, 1983; *Kamb*, 1987). Recent studies have extended their scope onto High Arctic polythermal glaciers which contain both ice that is at, and ice that is below, the pressure-melting temperature (e.g. *Skidmore and Sharp*, 1999; *Copland et al.*, 2003; *Bingham et al.*, 2003). Our knowledge of the hydrology of large ice sheets, however, is much less complete. This reflects both their scale and inaccessibility, as well as the realisation only recently that meltwater can reach the ice-bed interface in Greenland and that this causes ice acceleration which might have an important impact on the future mass balance of the GrIS (*Zwally et al.*, 2002). The purpose of this section is to build a conceptual model of water flow through an ice mass and the consequences for glacier dynamics. I extend the scope of previous reviews (e.g. *Röthlisberger and Lang*, 1987; *Hubbard and Nienow*,

1997; *Fountain and Walder*, 1998) by relating classical theory of glacier hydrology to larger ice sheet systems.

2.1 Glacier motion and water pressure

Glacier motion occurs through a combination of three components: plastic deformation of the ice, sliding of ice over its bed, and deformation within underlying sediments (*Paterson*, 1994). The presence of subglacial meltwater is a necessary condition for basal motion as it facilitates both of two basic sliding mechanisms (regelation and enhanced plastic flow around bedrock obstacles (*Weertman*, 1957)) and deformation of saturated sediments (*Boulton and Hindmarsh*, 1987; *Alley et al.*, 1989; *Tulaczyk et al.*, 2000) as well as mechanisms that cause enhanced basal motion such as ice-bed separation (e.g. *Bindschadler*, 1983). As a result it is expected that the motion of cold-based glaciers will be dominated by internal deformation as the ice is frozen to its bed. Conversely, in glaciers where the ice-bed interface is at the pressure melting point basal motion will occur and can account for a significant proportion of ice flow (e.g. *Kamb et al.*, 1985).

One of the most important controls on rates of basal motion is the subglacial water pressure. In classical theories of sliding over a hard bed, higher basal water pressure encourages the growth of subglacial cavities in the lee of bedrock undulations (*Lliboutry*, 1968; *Iken*, 1981; *Fowler*, 1986; *Schoof*, 2005). Growth of subglacial cavities leads to local separation of the ice and its bed, causing a reduction in basal drag thus allowing higher sliding velocities (*Bindschadler*, 1983). Surface measurements of glacier movement have repeatedly shown short-term (days to weeks) accelerations that are related to variations in melt or rain-water supply (e.g. *Iken et al.*, 1983; *Hooke et al.*, 1989; *Raymond et al.*, 1995; *Mair et al.*, 2002a; *Nienow et al.*, 2005; *Bartholomaus et al.*, 2007). Since short-term variations in ice motion cannot result from changes in ice deformation rates, because ice thickness and surface slope cannot change significantly over such short time periods, such observations confirm the link between increases in subglacial water pressure and variations in the basal component of glacier motion (e.g. *Iken et al.*, 1983; *Iken and Bindschadler*, 1986; *Kamb*, 1987; *Kamb et al.*, 1994; *Nienow et al.*, 2005).

An influential modelling study by *Iken* (1981) showed that the sliding velocity of ice over bedrock depends not only on effective pressure (equal to the ice overburden minus the subglacial water pressure), but on the stage of subglacial cavity growth. In her experiments which described sliding across an idealised undulating bed, the highest horizontal ice velocities were achieved while subglacial cavities were expanding and maximum horizontal speeds were also associated with vertical movement of ice, out from the growing cavities (*Iken*, 1981). This finding was supported by subsequent field observations of ice uplift at the surface of Unteraargletscher, by up to 0.6 m, at the same time as horizontal acceleration, up to six times its normal value (*Iken et al.*, 1983). Uplift of a glacier surface that coincides with horizontal acceleration has been reproduced in numerous further studies (e.g. *Anderson et al.*, 2004; *Bartholomaus et al.*, 2007) and is widely viewed as diagnostic of subglacial cavity growth caused by increased water pressure (*Mair et al.*, 2002a).

Where the glacier bed is comprised of sediments, higher water pressures are also associated with faster rates of basal motion. Basal motion of an ice mass over a sedimentary bed can arise from pervasive deformation of the bed, shearing across discrete planes in the bed or ploughing of clasts through the upper layer of the bed (*Alley et al.*, 1989) as well as sliding of the ice over its bed (*Iverson et al.*, 1995). High basal water pressures promote glacier sliding by weakening coupling between the ice and its bed, and also has the potential to weaken basal sediments allowing the bed to deform (*Fischer and Clarke*, 2001).

Although effective pressure beneath the glacier features dominantly in most sliding theories, there is no formulation of a sliding law which is universally applicable to all glaciers (*Van der Veen*, 1999). This reflects the complexity and interdependence of factors which control rates of basal motion, such as glacier bed roughness, the strength of the underlying substrate, rheology and temperature of ice and the amount of subglacial water (*Weertman*, 1979), as well as uncertainty about the spatial scales over which variations in basal drag must occur to allow widespread changes in ice motion (*Harbor et al.*, 1997; *Nienow et al.*, 2005)

A major obstacle is the difficulty of making direct observations at the glacier bed at appropriate temporal and spatial scales. While measurements of basal water pressure

at a single point can be made using boreholes (e.g. *Fountain*, 1994; *Hubbard et al.*, 1995; *Gordon et al.*, 1998) ice velocity might reflect water pressure averaged over a larger area (*Iken*, 1981; *Kamb*, 1987). As a result it has proved difficult to reconcile observations of ice velocity and subglacial water pressure in order to make inferences about the mechanisms which control basal motion. For example, *Iken and Bindschadler* (1986) captured simultaneous measurements of borehole water level and surface velocity at Findelengletscher in the Swiss Alps. Multi-day variations in horizontal velocity were strongly correlated to borehole water levels and maximum velocities coincided with maximum water pressure. Other field studies have found, however, that maxima in sliding velocity occur on the rising limb of subglacial water pressure, rather than at its peak (*Blake et al.*, 1994; *Fischer and Clarke*, 1997; *Nienow et al.*, 2005) leading to the suggestion that the relationship between high water pressures and ice acceleration operates via a 'stick-slip' mechanism, where water pressures increase until a local strain build-up in the ice is is released (*Fischer and Clarke*, 1997; *Nienow et al.*, 2005).

On the basis of field observations of the water budget of Columbia Glacier, *Kamb et al.* (1994) found that ice velocity fluctuations were better correlated with water storage beneath the glacier rather than peak water pressure. A similar observation was made later on Kennicott Glacier, Alaska (*Bartholomaus et al.*, 2007). *Iken and Bindschadler* (1986) argue, however, that ''the subglacial water pressure can affect the sliding velocity only if it acts on a large proportion of the bed''. It is possible, then, that the correlation of ice velocity with water storage can be reconciled with previous predictions if higher subglacial water storage reflects an increase in the spatial extent of raised subglacial water pressures.

Overall, although the conditions at the ice-bed interface that result in transient ice acceleration may vary, it is generally believed that high subglacial water pressure is required to initiate faster rates of basal motion. Discrepancy between observations of ice velocity and water pressure likely reflects spatial and temporal variability in basal conditions (*Hubbard et al.*, 1995; *Murray and Clarke*, 1995; *Stone and Clarke*, 1996) and competition between different mechanisms that allow ice to move over its bed (e.g. *Iken et al.*, 1983; *Fischer and Clarke*, 2001).

2.2 Subglacial drainage system structure

One of the major controls on spatial and temporal patterns in subglacial water pressure (and therefore rates of basal motion) is the structure of the drainage system, which, in turn, reflects the recent water flux (*Hubbard and Nienow*, 1997; *Nienow et al.*, 1998). Meltwater necessary for basal motion can be generated at the ice bed interface by frictional heating and the geothermal heat flux (*Paterson*, 1994). In practice, however, large quantities of surface meltwater also penetrate to the beds of temperate and polythermal glaciers, dominating the water budget of the subglacial drainage system under all or part of the glacier, and determine the drainage system structure, at least during the summer months (e.g. *Röthlisberger*, 1972; *Röthlisberger and Lang*, 1987; *Hubbard and Nienow*, 1997; *Fountain and Walder*, 1998).

There is presently broad agreement among glaciologists that, in temperate glaciers, water flows at the glacier bed in one or both of two qualitatively different flow systems, commonly termed 'channelised' or 'distributed', which exhibit contrasting pressure-discharge characteristics (e.g. *Hubbard and Nienow*, 1997; *Fountain and Walder*, 1998). The existence of these drainage configurations has been established empirically on the basis of proglacial bedrock mapping (e.g. *Walder and Hallet*, 1979; *Sharp et al.*, 1989), dye-tracer studies (e.g. *Seaberg et al.*, 1988; *Nienow et al.*, 1998) and meltwater hydrochemistry (e.g. *Collins*, 1979; *Tranter et al.*, 1993; *Brown*, 2002). A channelised system is composed of relatively large, hydraulically efficient channels that cover a relatively small proportion of the glacier bed and results from higher water flux (*Röthlisberger*, 1972; *Shreve*, 1972; *Röthlisberger and Lang*, 1987). By contrast, distributed drainage systems are composed of more tortuous and resistive flow pathways that cover a greater proportion of the glacier bed. A distributed drainage system may comprise several morphologically distinct flow pathways that include discharge through cavities that are linked by short channels (*Walder*, 1986; *Kamb*, 1987) and flow through subglacial sediments (*Clarke*, 1987; *Hubbard et al.*, 1995) and flow within a thin water film (*Weertman*, 1972).

The relationship between drainage system structure and its pressure-discharge characteristics is generally understood in terms of the theoretical steady-state behaviour

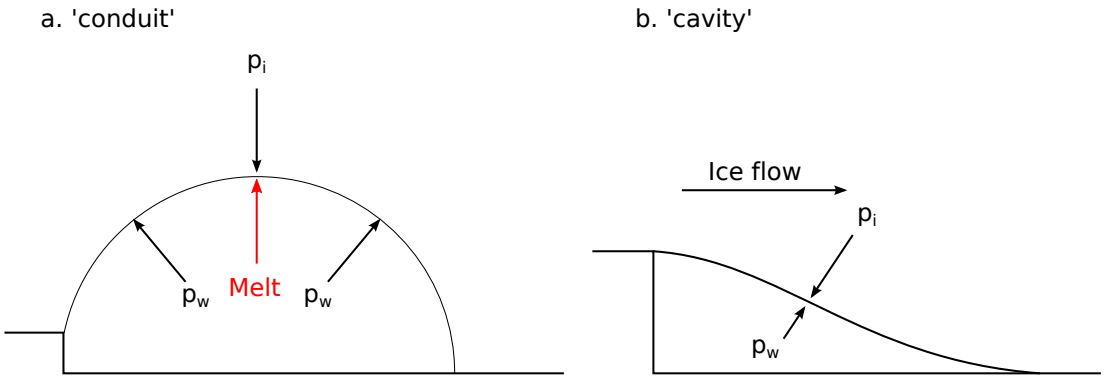

Figure 2.1: Schematic view of subglacial conduit cross-sections: a. The size of channels primarily reflects balance between closure under the weight of overlying ice (p_i) and opening of the walls by melting and the pressure of water within the conduit (p_w). In the largest channels, which carry higher discharge, a greater proportion of channel opening can be maintained by melting of the walls, resulting in lower steady-state water pressure (*Röthlisberger*, 1972). b. In a cavity discharge is not as high, and rates of cavity wall melting are less significant. The size of cavity is maintained by horizontal flow of ice past bedrock obstacles and water pressure increases with cavity size (*Walder*, 1986). Diagram based on *Schoof* (2010) after *Röthlisberger* (1972) and *Walder* (1986).

of subglacial conduits (*Röthlisberger*, 1972; *Walder*, 1986; *Schoof*, 2010). Overall, the size of subglacial conduits is determined by the balance between the tendency for conduit closure by collapse under the weight of overlying ice, and opening due to frictional melting of the walls by water, horizontal flow of the ice past bedrock obstacles and the pressure of water within the conduits (Figure 2.1; *Röthlisberger*, 1972; *Walder*, 1986; *Schoof*, 2010). Larger water flux therefore leads to faster rates of conduit opening and a drainage system dominated by larger conduits (channelised), while lower water flux means that conduits remain small and large channels do not develop (distributed).

In small conduits, opening of conduit walls by frictional melting is small due to the low water flux and conduit size is maintained largely by flow of ice past bedrock obstacles (Figure 2.1). In conduits of this type, generally described as 'cavities', the tendency for creep closure is balanced by an increase in water pressure to maintain equilibrium (*Walder*, 1986; *Schoof*, 2010). In a drainage system which is dominated by cavity-type drainage there is a positive relationship between conduit size, subglacial discharge and water pressure. In larger conduits where the water flux is much greater (known as 'R-channels'), closure is principally offset by higher rates of wall melting, which is controlled by the conduit discharge (Figure 2.1; *Röthlisberger*, 1972). The

largest channels have the highest closure rates (greatest effective pressure) and therefore require the highest discharge to maintain conduit size by melting. Above a critical discharge, the melting of walls relieves water pressure as a channel grows in a way that is not possible in cavities where flux is low (*Schoof*, 2010). As a result, in a predominantly channelised subglacial drainage system in steady-state, there is an inverse relationship between drainage system discharge and mean subglacial water pressure (*Röthlisberger*, 1972; *Schoof*, 2010).

Where the glacier bed is comprised of a sediment layer, distributed drainage is more likely to occur by Darcian porewater flow or through a thin film than through interconnected bedrock cavities (*Alley*, 1989; *Walder and Fowler*, 1994; *Flowers and Clarke*, 2002). *Walder and Fowler* (1994) also predicted the development of 'canals' incised down into the sediment layer, in response to higher water flux, that would exhibit a positive relationship between water flux and pressure. Since the analysis does not rule out the development of R-channels at the same time, however, it is likely that conduits of this type could only exist when water flux is relatively low. Leakage of water through permeable sediments will drain water away from canals towards lower pressure R-channels, causing their collapse (Fountain and Walder, 1998). It is expected, therefore, that the pressure-discharge behaviour of the subglacial drainage system remains qualitatively similar whether the glacier is underlain by sediments or bedrock.

In a drainage system where R-channels predominate, the largest channels, which operate at lower mean pressure, will tend to capture water from smaller channels, leading to concentration of flow into fewer channels and development of a dendritic drainage pattern (*Röthlisberger*, 1972; *Shreve*, 1972). Conversely, in a system where there is a positive relationship between conduit discharge and water pressure there is no tendency for one conduit to outgrow others by capturing water across a hydraulic gradient. As a result, cavity-type drainage systems with low water flux are spatially distributed across the glacier bed (*Walder*, 1986). Since a channelised drainage system occupies a small portion of the bed, however, the two drainage configurations may co-exist once a channelised drainage system has developed, with a distributed system filling the space between channels (*Fountain*, 1994; *Hubbard et al.*, 1995; *Hubbard and*

Nienow, 1997). Under these circumstances the two types of drainage system do not operate in isolation and R-channels can interact with the surrounding distributed system to alter water pressure over a wider area (*Hubbard et al.*, 1995; *Gordon et al.*, 1998).

2.3 Temporal and spatial development in subglacial drainage

Routing of meltwater has an important influence on subglacial drainage system development as it controls spatial and temporal patterns of meltwater delivery to the ice-bed interface. Water input to the subglacial drainage system is driven by seasonal variations in air temperature but the delivery is mediated by supraglacial conditons and englacial pathways.

The key features of meltwater drainage in a temperate glacier are shown in Figure 2.2. Early in the summer melt season, the whole of the glacier surface is likely to be covered by snow and, above the ablation zone, this will be underlain by a firn layer (*Nienow and Hubbard*, 2006). The primary hydrological effects of the seasonal snowpack and firn layers on glacier hydrology are to temporarily store water (*Jansson et al.*, 2003), to delay its passage to the interior of the glacier, and to smooth out diurnal variations in meltwater input (*Campbell et al.*, 2006). After the seasonal snowpack has melted in the ablation zone, meltwater can be routed more quickly across the glacier surface. Channels develop on the glacier surface that drain meltwater directly into crevasses and moulins, and water can be routed more quickly into the body of the glacier. On temperate glaciers, supraglacial streams rarely flow for more than a kilometre before intersecting a crevasse (*Nienow and Hubbard*, 2006). On cold or polythermal ice masses, deeply incised (>3 m) supraglacial streams (*Thomsen et al.*, 1988; *Bingham et al.*, 2003) may flow for many kilometres because of the lack of crevasses, and individual catchment basins may reach up to several hundred square kilometres (*Sugden and John*, 1976).

For temperate glaciers, meltwaters typically flow to the bed via moulins and crevasses. Pathways to the bed develop through downcutting of streams at the bottom of crevasses, which are subsequently isolated by creep closure above (*Fountain and Walder*, 1998). *Shreve* (1972) argued that englacial conduits should form an upward branching arborescent network, with the mean flow direction orientated steeply downglacier, as

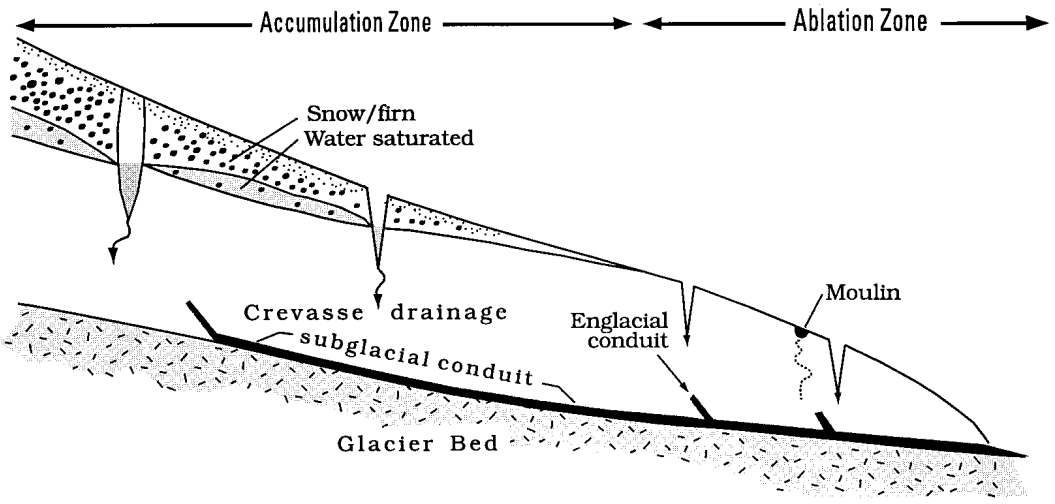

Figure 2.2: Idealised longitudinal cross-section of a temperate alpine glacier showing the important hydrological components. In the accumulation zone, water percolates downward through snow and firn to the top of the nearly impermeable ice, and then flows into crevasses (open fractures). In the ablation zone, once the seasonal snow has melted, water flows directly across the glacier surface into crevasses and moulins. Figure: *Röthlisberger and Lang* (1987).

determined by the gradient of the total potential (gravity and ice pressure) driving the flow. Englacial conduits which form under open conditions are able connect to the glacier bed even when ice is >200 m thick (*Hooke et al.*, 1984). An important consequence of englacial drainage through moulins is that inputs of meltwater to the subglacial drainage system are concentrated at discrete locations, favouring the development of a channelised drainage system (*Röthlisberger and Lang*, 1987; *Hubbard and Nienow*, 1997; *Fountain and Walder*, 1998).

Spatial and temporal variations in meltwater input to the ice-bed interface force the subglacial drainage system to develop over the course of a melt season, from a spatially distributed inefficient system to a discrete network of efficient channels (*Hubbard and Nienow*, 1997). The winter subglacial hydrological system is dominated by water produced by melting at the bed, creating a relatively low volume, high pressure, distributed system. Dye-tracer studies at Haut Glacier d'Arolla indicate that channelised drainage develops when water drains to the ice-bed interface in late spring, destabilising the winter drainage pattern (*Nienow et al.*, 1998). As surface melting and subglacial discharge increase through the summer, headward growth of channels replaces distributed flow and the channelised system migrates upglacier, growing in

extent and efficiency. The boundary between the two systems is broadly associated with the retreat of the snow line at the glacier surface (*Nienow et al.*, 1998). Analysis of subglacial piezometric surfaces indicates that such replacement is laterally variable, with distributed drainage surviving the melt season in areas of the glacier bed separating the channels (*Fountain*, 1994). Late in the melt season, however, all but the upper reaches of the glacier are drained by a distributed flow network that feeds into, and interacts with, large R-channels (*Hubbard et al.*, 1995; *Hubbard and Nienow*, 1997; *Nienow et al.*, 1998) and the behaviour of the channelised drainage system dominates subglacial water pressure patterns (*Gordon et al.*, 1998). Inputs into the subglacial hydrological system end with the suppression of surface melting in the autumn. Large channels, that can no longer maintain their size by frictional heating, gradually close by deformation of the overlying ice. Rates of channel closure are dependent on variables such as ice thickness, viscosity and conduit shape (e.g. *Nye*, 1953; *Hooke et al.*, 1990) as well as the size of the conduit; plausible timescales for the closure of efficient subglacial channels are in the range of days to weeks. During the winter, therefore, the background high-pressure system becomes widely established once again (*Hubbard and Nienow*, 1997).

2.4 Impact of subglacial drainage on ice dynamics

Interplay between development of the subglacial drainage system and variations in meltwater drainage to the ice-bed interface leads to temporal and spatial variations in subglacial water pressure that cause ice velocity changes on timescales ranging from 1 year to <1 day.

Low volumes of meltwater input to the winter subglacial drainage system result in steady and relatively slow rates of ice motion (e.g. *Hooke et al.*, 1989; *Anderson et al.*, 2004). During the early stages of a melt season, when subglacial channels are poorly developed, delivery of large volumes of surface meltwater to the ice bed result in a temporary incapacity of the subglacial drainage system to match outputs to inputs, creating high subglacial water pressures. The associated glacier speed-up is often termed the 'spring event' and may last a few hours or days. Spring-events are common features in valley glaciers, marking initial drainage of meltwaters to the ice bed, and have

been recorded in detail on Unteraargletscher and Findelengletscher (*Iken et al.*, 1983; *Iken and Bindschadler*, 1986) in Switzerland, the polythermal Störglaciaren in Sweden (*Hooke et al.*, 1989) and Haut Glacier d'Arolla (*Mair et al.*, 2001, 2003).

As the season progresses, however, the development of a channelised subglacial drainage system causes basal motion to become less sensitive to changes in water input. A progressive transition from a predominantly distributed to well-developed channelised drainage system causes lower mean subglacial water pressures. In the early stages of channelisation, discharge through incipient channels below moulins, not yet connected to the main channel, cause more localised basal forcing and slightly increased glacier velocity as higher water pressures are transferred to the surrounding distributed system (*Iken and Truffer*, 1997; *Mair et al.*, 2002a). Later in the melt season, however, increasing discharge through a fully channelised drainage system has less effect as waters are efficiently routed through discrete channels and late summer glacier velocity has often been found to be similar to the annual deformation flow pattern (*Hooke et al.*, 1989; *Iken and Truffer*, 1997; *Hanson et al.*, 1998; *Mair et al.*, 2002a; *Anderson et al.*, 2004).

Observations of surface motion and water balance on Bench Glacier, Alaska, also show that spatial patterns in seasonal evolution of the subglacial drainage system result in up-glacier development of changes in ice velocity (*MacGregor et al.*, 2005). A short-lived pulse of surface acceleration, which raised velocities up to four times the annual mean velocity, propagated up-glacier from the terminus at a rate of 200 - 250 m day^{-1}. The speed-up event is caused by the pressurisation of a poorly connected subglacial linked-cavity system (*Mair et al.*, 2002b, 2003), while its termination can be explained by an increase in efficiency of the subglacial hydrologic system through the up-glacier evolution of an efficient subglacial drainage system (*Nienow et al.*, 1998).

Water pressure variations recorded in boreholes located close to a subglacial conduit at Haut Glacier d'Arolla, Switzerland, show that diurnal variations in water pressure continue to occur even once a channelised system has been established (*Hubbard et al.*, 1995). Pressure variations within a large subglacial conduit resulted in a transverse pressure gradient that drove water laterally into the distributed system during high pressures, and back to the channel when levels dropped at night and the pressure

gradient reversed. The observations demonstrate interconnection between the two types of drainage system (*Hubbard et al.*, 1995). Subsequent observations of diurnal cycles in ice velocity suggest that a channelised system can raise subglacial water pressure, and ice velocities, over a wider area (*Hubbard et al.*, 1995; *Nienow et al.*, 2005). While subglacial conduits adjust in size to accommodate meltwater discharge over timescales of days or more (e.g. *Röthlisberger*, 1972; *Röthlisberger and Lang*, 1987; *Cutler*, 1998; *Schoof*, 2010), variability in meltwater delivery can vary significantly over much shorter periods. Although steady-state analysis indicates that a channelised drainage system will operate at lower *mean* pressure than a distributed one (*Röthlisberger*, 1972), temporary imbalance between the volume of water delivered to a subglacial drainage system and its ability to evacuate that water are accommodated by short-term spikes in subglacial water pressure which lead to transient ice acceleration (*Röthlisberger and Lang*, 1987; *Schoof*, 2010). Short-term ice velocity variations can therefore be explained by time-varying water input to a channelised subglacial drainage system.

2.5 Polythermal glaciers

Observations have shown seasonal velocity variations that are linked to changes in subglacial water pressure in High Arctic polythermal glaciers (*Muller and Iken*, 1973; *Andreasen*, 1985; *Rabus and Echelmeyer*, 1997; *Bingham et al.*, 2003, 2006). *Bingham et al.* (2003) observed a spring event at John Evans Glacier at 80°N on Ellesmere Island where increased basal water pressures induced a velocity speed-up 50 - 100% above winter velocities and rates of ice motion remained up to 50% above winter velocities whilst surface derived meltwaters enhanced rates of basal sliding. During the course of the summer, meltwaters accessed the glacier bed at increasing distances upglacier thereby impacting on the glacier wide dynamics.

Observations of water drainage and ice acceleration in polythermal glaciers are particularly significant since it had been thought that supraglacial meltwaters would be unlikely to penetrate through thick layers of cold (below pressure-melting temperature) ice to the glacier bed (*Boon and Sharp*, 2003). At John Evans Glacier, multiple, relatively abrupt, drainage events occurred over a period of about one week during

which a crevasse was water-filled or overfilled. After eight such events the surface reservoir which had been feeding water into the crevasse drained completely within one hour, suggesting that a hydraulic connection had been established through the entire 150 m ice thickness (*Boon and Sharp*, 2003). It is proposed that a hydrofracture mechanism is responsible for propagating cracks from the bottom of crevasses to the bottom surface of a glacier (*Van der Veen*, 1998; *Boon and Sharp*, 2003). Because the density of water is slightly greater than that of ice, provided a crevasse or moulin remains water-filled, theoretical calculations show that the weight of the water can overcome the lithostatic (resistive) stress in the ice, to deliver supraglacial meltwater through layers of cold ice to a glacier bed (*Weertman*, 1973; *Van der Veen*, 1998; *Alley et al.*, 2005b; *Van der Veen*, 2007). At John Evans glacier, multiple drainage events were necessary in order to deliver water through the full ice thickness because refreezing of surface meltwater penetrating the initial fractures exceeded water inflow (*Van der Veen*, 2007). The rate of crevasse penetration is dominantly controlled by the rate at which water is supplied to the crevasse (*Van der Veen*, 2007) and a water-filled crevasse has unlimited capacity, acting under gravity, to force water to the bottom surface of a glacier (*Weertman*, 1973; *Van der Veen*, 1998; *Alley et al.*, 2005b).

The thermal regime of polythermal glaciers means that there are differences in the mechanisms and evolution of subglacial hydraulics compared with temperate glaciers. For example, in many polythermal glaciers, the presence of cold ice under the glacier snout creates a 'thermal dam' which delays subglacial outburst (*Skidmore and Sharp*, 1999; *Rippin et al.*, 2003) and may prolong the spring velocity event. However, the evidence for links between meltwater production, drainage of water by hydrofracture, and ice acceleration raise the possibility of similar behaviour in larger ice sheet systems.

2.6 Hydrology and dynamics of ice sheets

By comparison with temperate and polythermal glaciers, our understanding of the hydrology and dynamics of larger ice sheets is far less complete. In marginal parts of the ablation zone, it may be reasonable to suggest that the hydraulic regime is similar to a temperate glacier. Summer temperatures are warm and field observations

from Jakobshavns Isbræ, a marine-terminating glacier in west Greenland, indicate that meltwater streams drain through crevasses up to approximately 10 km from the ice sheet margin (*Echelmeyer et al.*, 1991). Numerous meltwater streams and moulins are also reported further inland (*Echelmeyer et al.*, 1991), although they become rarer at higher elevations and have not been found above the equilibrium line (*Catania et al.*, 2008). The Quaternary geologic record contains strong evidence of channelised subglacial water flow beneath former ice sheets in the form of tunnel valleys (e.g. *Brennand and Shaw*, 1994), bedrock channels (*Denton and Sugden*, 2005) and eskers (e.g *Clark and Walder*, 1994; *Brennand*, 2000). These features are usually restricted to marginal areas of former ice sheets (*Boulton et al.*, 2001) and it has been suggested that they delimit the ablation zone (*Clark and Walder*, 1994).

Initial observations of summer ice acceleration ∼35 km from the ice sheet margin in west Greenland (*Zwally et al.*, 2002) indicate that surface meltwater does penetrate to the GrIS bed and causes acceleration of the ice sheet. *Zwally et al.* (2002) recorded summer acceleration of 5 - 25 % in four consecutive years that was directly correlated with the magnitude of local surface melting (parameterised by the positive degree-day method (*Braithwaite*, 1995)). Numerical simulations using a flowline model showed that meltwater forced acceleration of ice flow has the potential to increase the GrIS contrbution to sea level rise by 0.15 - 0.4 m by 2500 AD, should there be a direct correlation between rates of surface melting and the magnitude of ice acceleration (*Parizek and Alley*, 2004).

In these simulations, it is assumed that ice basal sliding rates are positively related to air temperature, parameterised using the data from *Zwally et al.* (2002), and by the driving stress which is determined by the evolving ice sheet surface slope. External temperature forcing for the model was based on projections from the 3^{rd} IPCC assessment (*Cubasch et al.*, 2001), and was then also used to determine variations in precipitation patterns (*Parizek and Alley*, 2004). A number of simulations of GrIS evolution under different global warming scenarios and parameter configurations were performed. These demonstrated the following typical scenario, indicating the potential significance of meltwater induced sliding for the future mass balance of the GrIS (*Parizek and Alley*, 2004):

Rising air temperatures over the GrIS increase melting in the ablation zone and cause retreat of the ice sheet margin. Meanwhile, increased precipitation in the ice sheet interior maintains the ice thickness there, leading to higher mean ice sheet thickness. This increase in mean ice thickness, and in surface slope in the ablation zone, leads to higher driving stresses. Following from this change in driving stress, a redistribution of mass from the accumulation to the ablation zone occurs. This redistribution is initially driven by higher surface slopes but ice flow velocity is also increased within the region that water is able to drain to the ice-bed interface. The increase in ice flux from the ice sheet interior to the ablation zone reduces the rate of ice front retreat, but lowers the elevation of the surface inland. Elevated ice flux is sustained until the surface slope and ice thickness have been sufficiently reduced to offset the additional sliding allowed by meltwater. As the ice surface falls (with continued climate warming) the area of the ice sheet subject to basal lubrication migrates inland. With surface ablation attacking more and more of the ice sheet, the period of slowed marginal retreat is followed by faster than standard retreat predicted by ice sheet models which do not account for the basal sliding mechanism (*Parizek and Alley*, 2004).

The feedback between surface lowering of the GrIS and increases in the area which is subject to meltwater enhanced basal sliding is exacerbated by the hypsometry of the ice sheet which flattens inland, exposing a greater area of the ice sheet surface to melting as temperatures increase (*Bamber et al.*, 2001). Sensitivity testing of the model employed by *Parizek and Alley* (2004) indicates that, beyond inclusion of a meltwater related sliding law, parameterisation of the onset location of meltwater induced sliding is the most important factor in determining the sensitivity of ice volume projections in a climate warming scenario, even above the climate warming scenario that is used itself. In the context of the research presented in this thesis, then, understanding the relationship between meltwater production and factors controlling its spatial and temporal evolution can be considered particularly important.

Satellite observations from west Greenland show that summer acceleration in land-terminating sections of the GrIS margin is widespread up to ∼30 km inland (*Joughin et al.*, 2008a). A short study used ground-based and satellite observations from sites further inland (up to 72 km from the margin) to detect large diurnal and longer-term

variations in ice flow during late summer that were strongly coupled with changes in surface hydrology (*Shepherd et al.*, 2009). The diurnal signals were associated with periodic changes in surface melting, and the less frequent signals were associated with the episodic drainage of supra-glacial lakes. Overall, they found that the ice sheet accelerated by 35% per positive degree-day of melting. The close link between surface melting and enhanced flow suggests that Alpine glacier behaviour may provide an appropriate analogue for the interplay between hydrology and dynamics in the GrIS (*Shepherd et al.*, 2009).

A longer-term study of ice velocity at 8 sites along the 'K-transect', which extends inland from the west margin of the GrIS at $\sim 67°$N, found that higher rates of annual ablation did not necessarily lead to faster ice flow (*Van de Wal et al.*, 2008). *Truffer et al.* (2005) caution that, similar to Alpine glaciers, the development of efficient water drainage networks in times of high runoff may tend to reduce basal motion in larger ice sheet systems. The results from the K-transect indicate, then, that the subglacial drainage system beneath the GrIS may become channelised over the course of a melt season to accommodate larger volumes of water at lower pressure. As a result, higher levels of surface melting do not result in higher water pressures and ice velocity (cf. *Zwally et al.*, 2002; *Parizek and Alley*, 2004) and the importance of this relationship for large-scale dynamic behaviour of the GrIS therefore remains uncertain (*Truffer et al.*, 2005; *Van de Wal et al.*, 2008).

Despite the evidence that the relationship between surface meltwater production, subglacial hydrology and ice dynamics in land-terminating sections of the GrIS is analogous to smaller temperate and polythermal glacier systems, two critical issues remain unresolved. Firstly, without hydrological data or detailed observations of the seasonal structure of ice velocity variations from the GrIS, there is no direct evidence which can confirm that seasonal development of the hydrological system occurs, or that this process is responsible for the lack of correlation between rates of annual ablation and ice velocity. For example, the study along the 'K-transect' only compares velocity with ablation on yearly timescales (*Van de Wal et al.*, 2008), while the short-term study further inland confirms that meltwater is responsible for the ice acceleration, but can only provide a snapshot of the relationship between hydrology and ice dynamics

(*Shepherd et al.*, 2009). Secondly, it is not clear whether inputs of meltwater from the surface of the GrIS are sufficiently large to establish an efficient drainage system that remains open for the entire melt season, or whether the large overburden pressure of thick ice causes any subglacial tunnel networks to collapse after each drainage event, making the subglacial environment of the GrIS less able to accommodate large volumes of water and more sensitive to repeated hydrological perturbations than in smaller glaciers.

Since the GrIS is much thicker and colder than temperate glaciers, it seems likely that hydrofracture (e.g. *Van der Veen*, 1998; *Boon and Sharp*, 2003) plays an important role in allowing water to reach the ice bed, particularly further inland from the ice sheet margin. Satellite imagery shows seasonal development of large numbers of supraglacial lakes which fill and subsequently drain from the surface of the GrIS over the course of each summer (*McMillan et al.*, 2007; *Sundal et al.*, 2009). Supraglacial lake drainage events have an obvious potential to supply large volumes of water to the ice sheet bed (*Alley et al.*, 2005b; *Box and Ski*, 2007; *Sneed and Hamilton*, 2007) and to provide the large water fluxes necessary for crevasse hydrofracture (*Van der Veen*, 2007). *Das et al.* (2008) recently reported drainage of a 2.7 km diameter lake, holding approximately 0.03 km^3 of water, draining entirely through 1 km of ice thickness in less than 2 hours. The peak rate of water flow during this event exceeded 8700 m^3 and coincided with rapid glacier uplift of 1.2 m and horizontal acceleration to nearly 8 km yr^{-1}. Subsequent subsidence and deceleration of the ice sheet occurred over the following 24 hours.

The coincidence of lake drainage, ice surface uplift and horizontal acceleration is consistent with the propagation of a conduit linking the ice sheet surface and basal hydraulics. These observations provide evidence for the injection of surface melt water directly to the ice sheet bed, in a region where the ice $\sim$1 km thick; significantly thicker than sites which are nearer the ice sheet margin. With increased summer temperatures and an expanded ablation zone, it is likely that a greater area of the GrIS will have surface lakes in future years, increasing the area of the bed that meltwaters have the potential to access (*Box and Ski*, 2007; *Sundal et al.*, 2009). The dynamic effect of this lake drainage event was short-lived, however, and the factors which control the initiation and timing of this process are currently not well understood (*Alley et al.*,

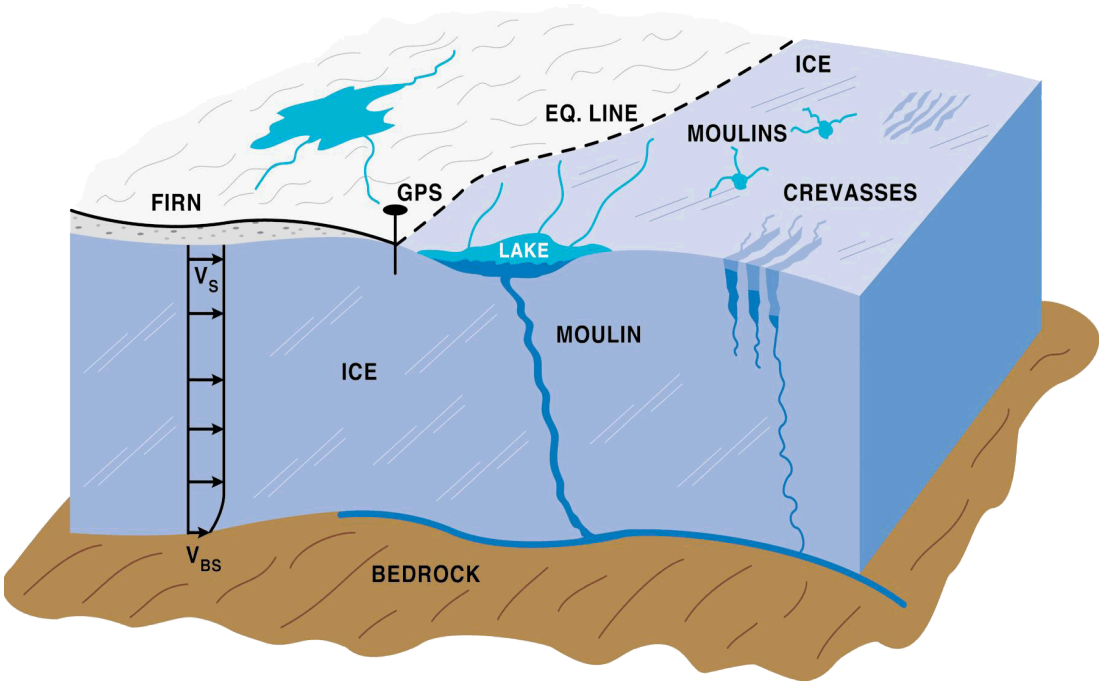

Figure 2.3: Schematic of drainage features in the equilibrium and ablation zones of the GrIS, including lakes, supraglacial streams, crevasses and moulins. Figure: *Zwally et al.* (2002)

2005b; *Van der Veen*, 2007). It is not clear, therefore, whether the integrated effect of widespread lake drainages can explain the net regional summer ice speed-up as observed by satellite and ground-based observations (*Das et al.*, 2008; *Joughin et al.*, 2008a).

Given the temporal correlation between horizontal ice acceleration and ice sheet surface uplift observed in a number of studies (*Das et al.*, 2008; *Shepherd et al.*, 2009), it appears summer velocity increases are local events that are triggered by inputs of surface meltwater directly to the bed. It is possible, however, if behaviour similar to Alpine glaciers does occur (e.g. *Zwally et al.*, 2002; *Van de Wal et al.*, 2008; *Shepherd et al.*, 2009) that it is confined to a narrow marginal zone where the ice sheet is thinner and surface ablation is higher, while lake drainage events dominate at higher elevations (Figure 2.3).

Whilst theoretical considerations suggest that longitudinal stress gradients do not have a large effect on whole ice sheet profiles, they may be important closer to the margin, or where basal sliding is the dominant mode of ice flow (*Van der Veen*, 1999). *Price et al.* (2008) argue it is important to investigate how a zone of fast flowing ice at the ice sheet margin can affect ice velocity further upglacier. In a numerical

study designed to investigate the mechanisms responsible for the summer acceleration observed by *Zwally et al.* (2002) in the Swiss Camp region in west Greenland, *Price et al.* (2008) suggested that larger surface meltwater induced seasonal accelerations (>2x those observed at Swiss Camp) in a region <20 km from the ice sheet margin can induce significant speed-ups further inland by longitudinal (along-flow) coupling. Since the region nearer the ice sheet margin is heavily crevassed as a result of extending ice flow, it is proposed that abundant meltwater access to the ice-bed interface in this region results in behaviour similar to Alpine glaciers, and that coupling to ice upglacier is a more plausible explanation for ice acceleration further inland (>35km) than local hydrological forcing (cf. *Zwally et al.*, 2002; *Parizek and Alley*, 2004; *Das et al.*, 2008).

This 'coupling-hypothesis' suggests that increased sliding as a function of increased surface melt will be limited by evolution of the subglacial water system which operates like an Alpine glacier, and that the effects of meltwater induced acceleration in a warming climate will therefore have a smaller impact on the mass balance of the ice sheet than has been implicated (*Price et al.*, 2008). Without field observations, however, it is not known over what distance longitudinal coupling can be effective and including longitudinal stress gradients in ice sheet models of basal sliding remains an important challenge (*Marshall*, 2005). Even if not wholly responsible for upglacier acceleration, longitudinal (tensile) stress gradients that propagate from downglacier could contribute to a feedback which would favour the hydrofracture of water-filled crevasses to the glacier bed (*Boon and Sharp*, 2003).

In light of concerns about the future contribution of the GrIS to sea level change, there has been significant recent interest in modelling of large-scale glacial hydrology and coupling with models of ice sheet evolution (*Arnold and Sharp*, 2002; *Flowers and Clarke*, 2002; *Marshall*, 2005; *Pimentel and Flowers*, 2010). These efforts are limited, however, by fundamental shortcomings in available datasets and understanding of the processes that control the relationship between melting at the surface of the GrIS and seasonal changes in ice dynamics (*Alley et al.*, 2005a). The purpose of this thesis, therefore, is to investigate factors which control the relationship between the hydrology and dynamics of a land-terminating section of the GrIS margin in order to provide insights that improve our ability to make robust predictions about the future GrIS mass

balance.

CHAPTER 3

Study area, data and methods

The research presented in this thesis is based on field observations of the hydrology and dynamics of a land-terminating outlet glacier in west Greenland. The aim of the project is to use a suite of different observations in order to compare temporal and upglacier variability in the relationship between surface meltwater production, subglacial drainage system development and ice velocity over the course of a summer melt season. This section describes the study area and outlines the main data that were collected. It is not intended as an exhaustive methodological review, however, and specific discussions of data limitations and errors are provided in the individual chapters where they are most relevant.

3.1 Study area

Fieldwork was carried out at Leverett Glacier, a land-terminating outlet glacier located at ∼67.10°N on the western margin of the GrIS (Figure 3.1). The glacier tongue extends

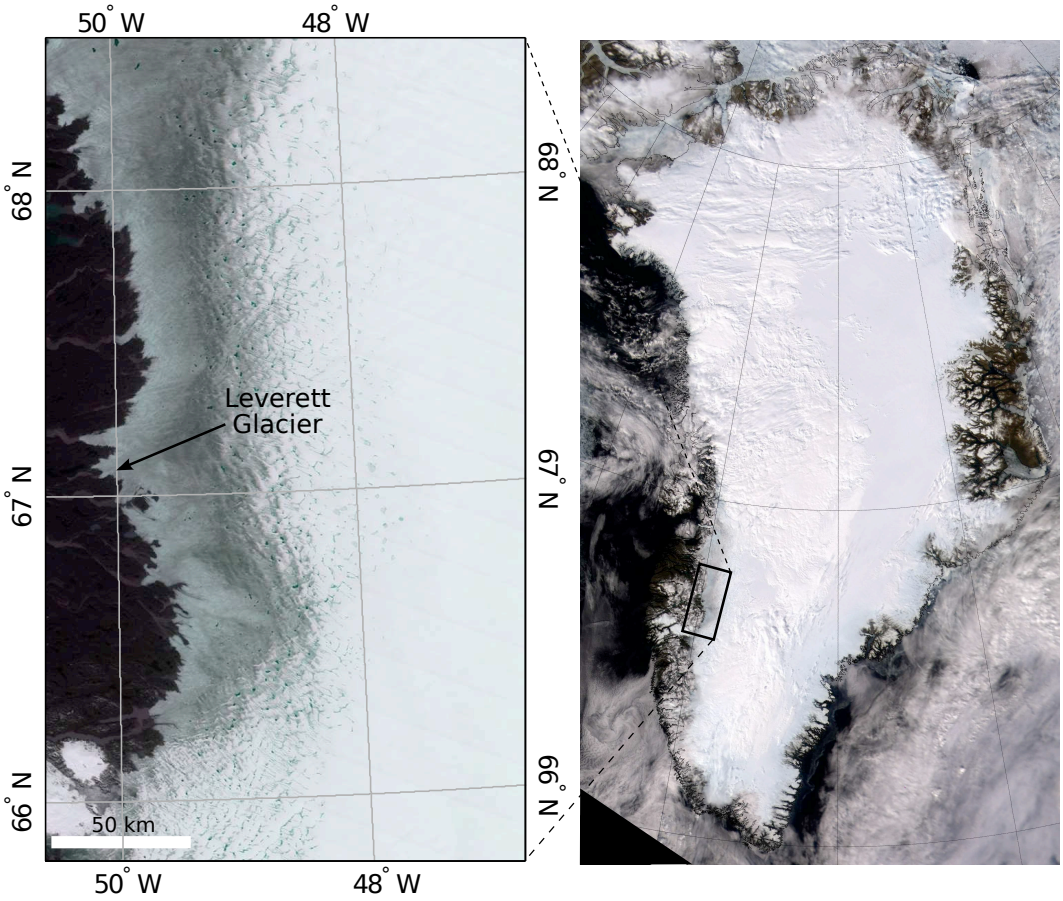

Figure 3.1: Location of Leverett Glacier on the western margin of the GrIS. The ice sheet margin in this region is mostly land-terminating (Figure 3.1; cf. e.g. SE Greenland) and therefore provides an appropriate glaciological setting in which to begin investigations into the relationship between surface melting, glacier hydrology and ice dynamics in the GrIS. Satellite images from the Moderate Resolution Imaging Spectroradiometer (MODIS).

approximately 2 km from the south part of Russell Glacier, a slightly larger outlet glacier which forms part of the same lobe, and drains ice from the main ice sheet.

Measurements of surface mass balance have been collected along a transect close to Leverett Glacier (K-transect) at ∼67°N since 1990 (*Van de Wal et al.*, 1995; *Greuell et al.*, 2001; *Van de Wal et al.*, 2005). The region is characterised by relatively high ablation (4-5 m yr^{-1}) near the margin and low accumulation (∼0.3 m w.e. yr^{-1}; *Van de Wal and Russell*, 1994; *Van de Wal et al.*, 2005). At a site 3 km from the ice sheet margin, which is at an altitude of 340 m a.s.l, the mean annual surface mass balance was -4.03 m w.e. for the period 1990 - 2003 (*Van de Wal et al.*, 2005). The mass balance increased with elevation at a rate of ∼3.7 x 10^{-3} m m^{-1} and these data indicate

that the mean equilibrium-line altitude (ELA) in this region is 1534 m (*Van de Wal et al.*, 2005). Satellite interferometry and ground-based observations have shown that this section of the ice sheet experiences summer ice acceleration which is attributed to meltwater forcing (*Joughin et al.*, 2008a; *Van de Wal et al.*, 2008; *Shepherd et al.*, 2009). Seasonal development and subsequent drainage of supraglacial lakes has also been observed at elevations up to ∼1600 m using optical satellite imagery (*McMillan et al.*, 2007; *Sundal et al.*, 2009).

Large volumes of meltwater drain each summer from Leverett Glacier. Peak discharge is estimated to be hundreds of $m^2s{-}1$, suggesting that water is delivered from a large catchment, perhaps several hundred km^2 in area, within the ice sheet. Drainage at the glacier snout emerges from a discrete portal and flows along a single channel for approximately 2 km before reaching a bedrock cross-section (Figure 3.2; location shown by green triangle, Figure 3.3), making an ideal setting in which to investigate hydrological parameters in water emerging from the subglacial drainage system. The ice sheet margin in this region is mostly land-terminating (compared with, for example, SE Greenland) and therefore provides an appropriate glaciological setting in which to begin investigations into the relationship between surface melting, glacier hydrology and ice dynamics in the GrIS.

The field site was also chosen partly for practical reasons. Leverett Glacier is approximately 25 km east from the town Kangerlussuaq which lies at the head of Søndre Strømfjord and most of the distance can be covered by vehicle. Access for personnel and equipment is therefore relatively easy compared with most sites in Greenland.

3.2 Data and methods

Data were collected over three field seasons from 2008 - 2010. In spring 2008 we established a transect of four global positioning system (GPS) receivers which were used to monitor rates of surface motion approximately along a glacier flowline, as determined using interferometric synthetic aperture radar observations (InSAR; *Palmer et al.*, 2008, 2011). This transect extended ∼35 km inland across an alitudinal range of 390 - 1060 m (Figure 3.3). Simultaneous measurements of air temperature were made at each

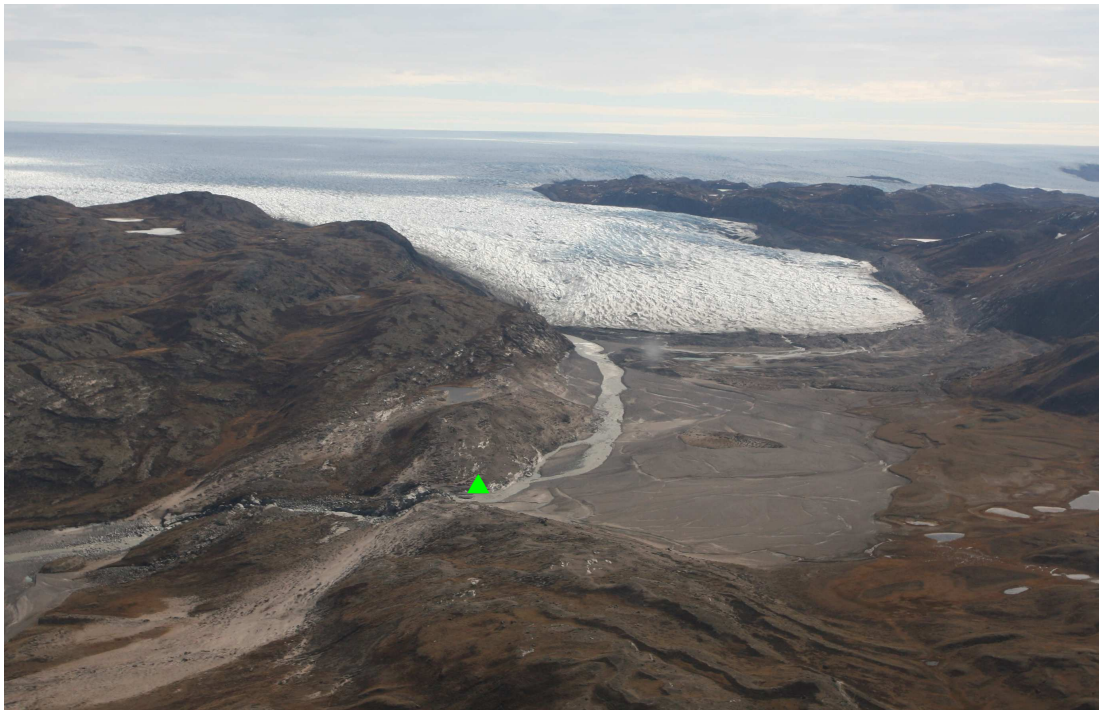

Figure 3.2: Leverett Glacier viewed from the east. The proglacial stream emerges from the north side of the glacier snout through a single outlet. The outlet is fed by a large subglacial channel which is expressed as a depression on the surface of the glacier which extends several kilometres upglacier. The gauging site where hydrological measurements were made in the proglacial stream is marked by a green triangle.

of these sites in order to constrain melt rates.

Hydrological monitoring began in 2009 in the proglacial stream that emerges from the Leverett Glacier snout. This site was chosen because Leverett Glacier has much higher proglacial meltwater discharge than its close neighbours, implying that meltwater drains from a larger portion of the ice sheet. In this season the GPS transect was also expanded to include seven sites extending ∼115 km inland to ∼1700 m elevation and more detailed measurements of surface ablation were made (Figure 3.4). The GPS at site 1 was transferred to the Leverett Glacier tongue from neighbouring Russell Glacier, where it had been placed in 2008 for access reasons, in order to be able to compare changes in ice velocity with hydrological parameters (Figure 3.3). Sites 2 - 4 remained in the positions indicated in figure 3.3.

The ice velocity, air temperature and surface ablation measurements were continued in 2010 along with basic hydrological measurements. In the spring of 2010, an airborne geophysical survey also collected ice surface elevation data from a flightline which passed

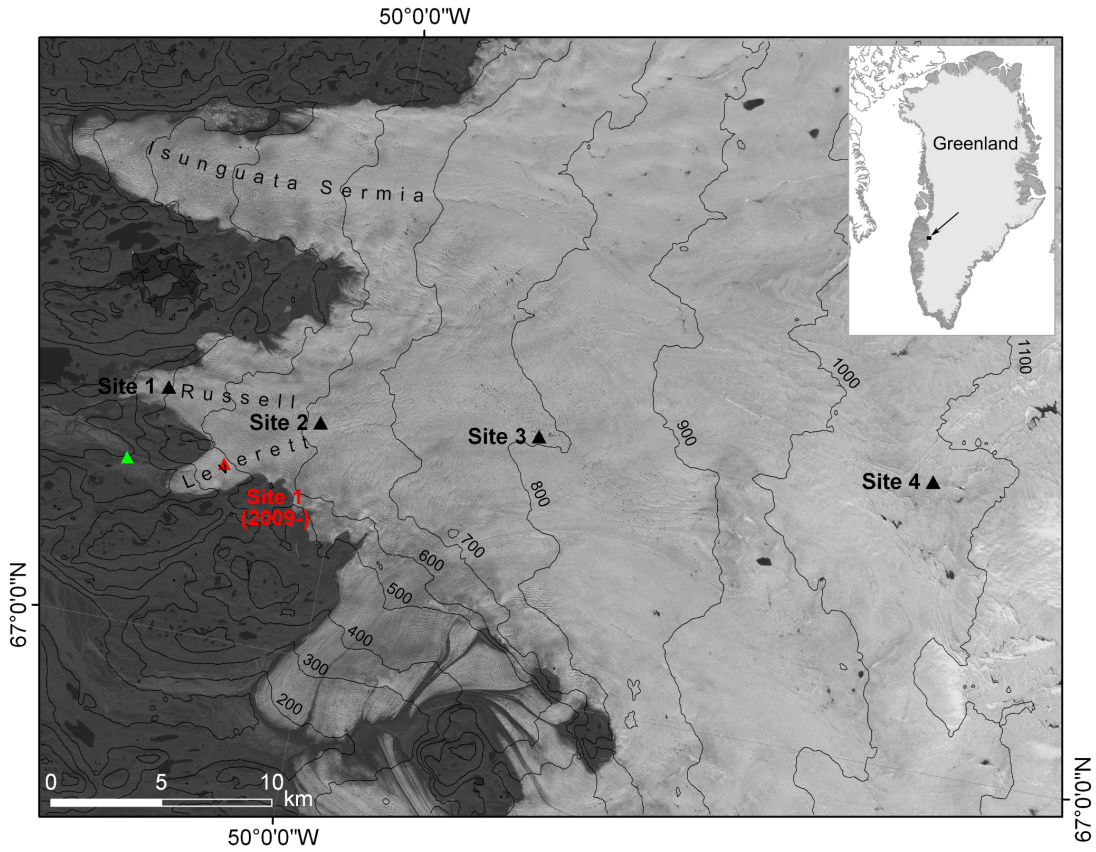

Figure 3.3: Map showing the GPS transect in 2008 (black triangles). Four GPS sites are located in the ablation zone of the GrIS across an altitudinal range of 395-1060 m a.s.l., where ice thickness ranges from 270-920 m (*Bamber et al.*, 2001). Simultaneous measurements of air temperature were made at each site to constrain surface melt-rates. The hydrological monitoring site from 2009 is shown by the green triangle. Site 1 was relocated from Russell Glacier to the Leverett Glacier tongue in 2009 in order to be able to compare the hydrological record with changes in ice dynamics.

directly over the transect (Figure 3.4; *Krabill*, 2010). Combined with a lower resolution digital elevation model (DEM) of the GrIS bed (*Bamber et al.*, 2001) the cross-profile shows that ice thickness along the transect ranges from ∼270 m at site 1 to ∼1400 m at site 7 (Figure 3.5).

3.2.1 Global Positioning System observations

GPS observations have been used since the 1980s to provide measurements of glacier surface velocities (e.g. *Hinze and Seeber*, 1988). Satellites in the GPS constellation continuously orbit the Earth, broadcasting radio signals with an embedded code which allows computation of the signal transit time and therefore the distance from an antenna

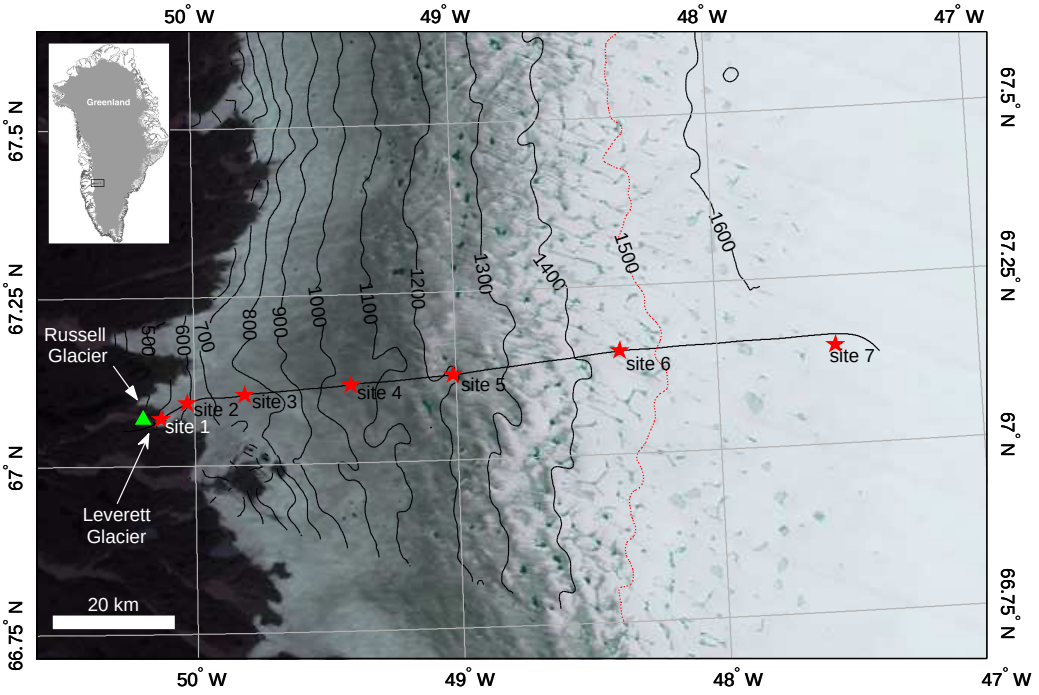

Figure 3.4: Map showing the extended GPS transect in 2009 & 2010. The transect consists of seven sites which extend from 450 - 1700 m a.s.l. (red stars). The ELA in this region is at ∼1500 m (red; *Van de Wal et al.*, 2005). In 2010, an airborne geophysical survey collected surface elevation data along the transect (*Krabill*, 2010). The flightline for this survey is shown by the black line and the data are presented in Figure 3.5. The hydrological monitoring site from 2009 is shown by the green triangle. Contours on this map are produced at 100 m intervals from a digital elevation model derived from InSAR (*Palmer et al.*, 2011).

to each satellite. Precise coordinates of the antenna position can then be calculated by trilateration (as opposed to triangulation, which uses angles), typically using four or more satellites (e.g. *Leick*, 2004). The use of GPS holds significant advantages over traditional survey techniques, particularly in polar regions where distances from stable reference points are prohibitively large and continuous manual operation is impractical. Achievable accuracies can be reduced to millimetres or centimetres by using high temporal resolution sampling and appropriate processing techniques (*King*, 2004).

In ice sheet applications, use of GPS provides highly detailed timeseries of the antenna position, and therefore ice motion, at a single point. A drawback of GPS systems is their cost, both in terms of equipment and in deploying a station in a remote area. In addition, the low spatial coverage (i.e. one point) necessitates use of multiple stations. The observations therefore represent one extreme of a trade-off between spatial

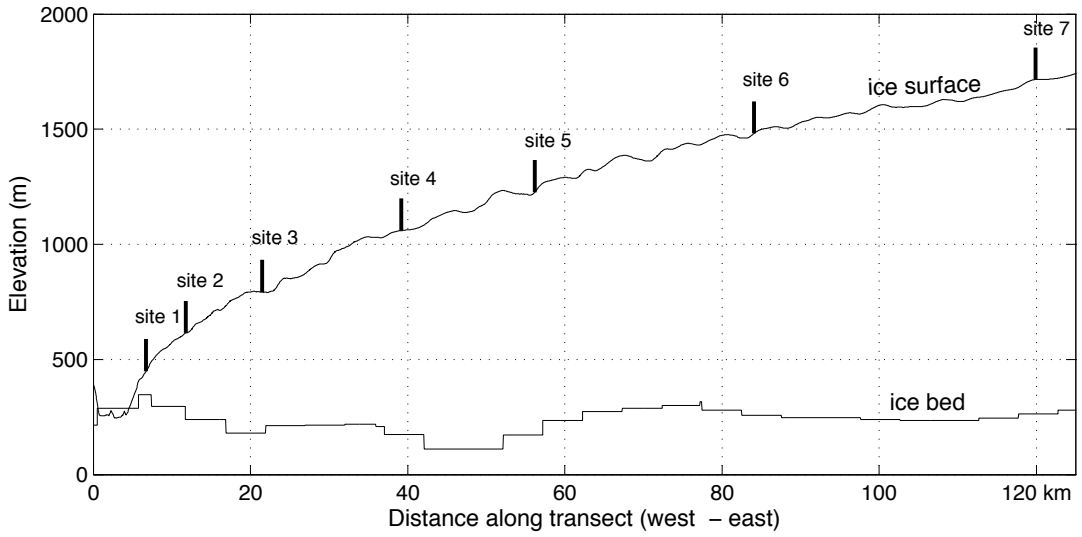

Figure 3.5: Ice thickness profile along the GPS transect. Ice surface elevation data were acquired during an airborne geophysical survey (*Krabill*, 2010) and bed elevation were sampled from a coarser resolution DEM of the GrIS bed (*Bamber et al.*, 2001)

coverage and temporal resolution. At the other end are satellite observations, which can provide snapshots of ice velocity over wide areas (e.g. *Joughin et al.*, 2010), but whose temporal resolution is limited by the repeat period of satellite orbits. For this study, however, the high temporal resolution provided by GPS observations is critical in order to understand how atmospheric forcing controls short-term variability in ice motion.

We used dual-frequency Leica 500 and 1200 series GPS receivers to collect season long records of ice motion at each site. Each GPS antenna was mounted on a pole drilled several metres into the ice, which froze in subsequently, providing measurements of ice motion that were independent of ablation (Figure 3.6). The GPS receivers were powered by solar panels which were mounted on the same pole as the antenna. The GPS receivers were housed in an insulated box that also contained the batteries and was loosely attached to the bottom of the pole. This allowed the box to remain near the pole as the ice sheet surface lowered during the summer ablation period. Each site was visited twice a year, at the start and end of the melt season, to collect data, redrill the poles and perform any necessary maintenance.

The GPS receivers collected data continuously at 30 second intervals that were processed using a kinematic approach relative to an off-ice base station (*King*, 2004)

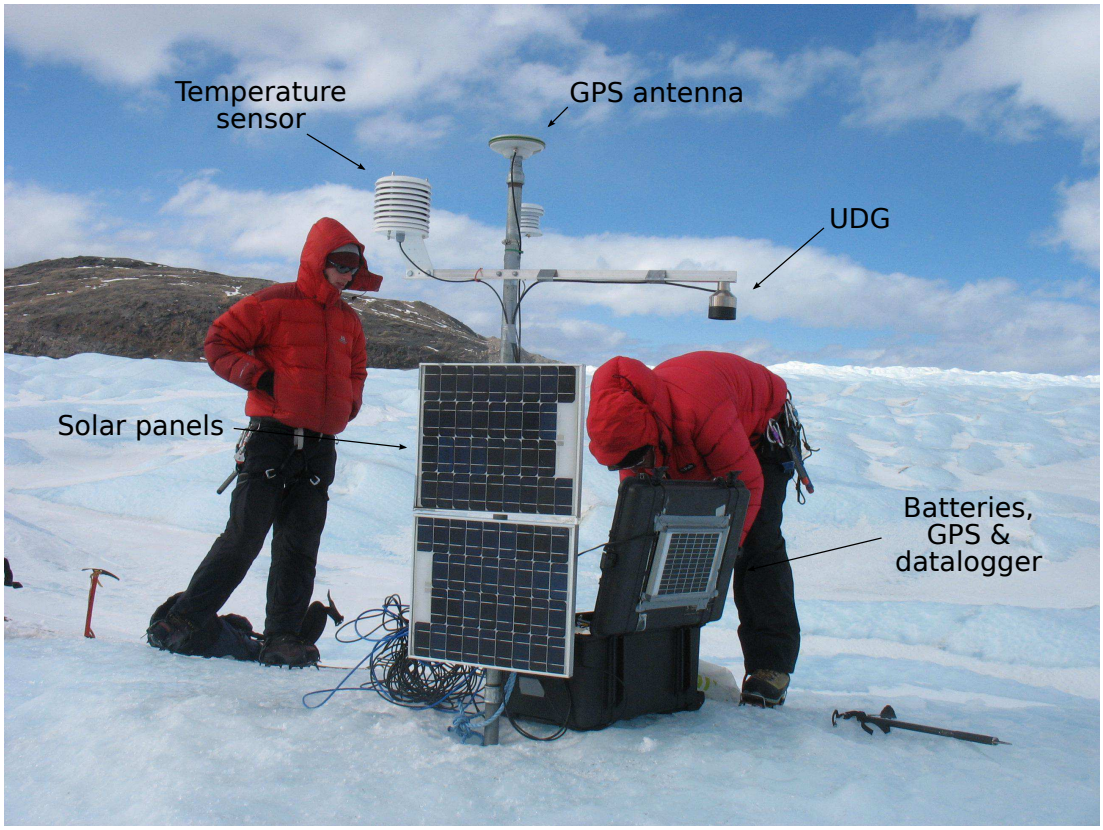

Figure 3.6: The GPS monitoring station at site 1. The GPS antenna is mounted on the top of a support pole which is drilled ∼4 m into the ice. At this site, a shielded temperature sensor and UDG are attached to a cross-bar which is also mounted on the pole. The GPS is powered by the large solar panels. Data are collected by the GPS receiver and a datalogger (which records the temperature and ablation data) which are housed in an insulated box at the base of the pole along with the batteries. At sites where no ablation data was collected, a shielded HOBO temperature sensor with integrated logger was attached directly to the support pole.

using the Track 1.21 software (*Chen*, 1999; *King and Bock*, 2006). Data from an International GNSS Service (IGS) base station located in Kelyville, approximately 30 km east from Leverett Glacier, were used for processing data in 2008, 2009 and the first part of 2010. In 2010 we also established an off-ice base station at the snout of Leverett Glacier and reduced the sampling interval to 10s in order to improve the accuracy of the ice motion observations. Conservative estimates of the uncertainty associated with positioning at each epoch in the GPS record are approximately ± 1 cm in the horizontal direction and ± 2 cm in the vertical direction. Rates of ice motion along the transect range from approximately 0.3 - >1 m day^{-1}. We can therefore resolve variations in ice velocity over timescales of 1 day or less. Specific discussion of the uncertainty in each GPS timeseries is provided in the methods sections of chapters 4, 6, 7 and 8.

3.2.2 Temperature and surface ablation data

Simultaneous measurements of air temperature and surface ablation were made at each GPS site in order to constrain melt rates using the positive degree-day method (e.g. *Braithwaite and Olesen*, 1989; *Ohmura*, 2001). This method rests on an empirical relationship between snow or ice melt and air temperatures and has been widely used in glaciological studies. The popularity of degree-day (also known as temperature-index) models is due to the relative ease of collecting temperature data and generally good performance despite their simplicity (*Hock*, 2003). In its simplest application we use positive air temperature values as a proxy for local melt rates (e.g. in Chapters 4 and 6). This approach is improved upon, however, by using a simple model which uses observed lapse rates and a surface DEM (*Palmer et al.*, 2008, 2011) to calculate rates of surface melting distributed across a catchment (discussed in chapter 5).

Degree-day models often match the performance of energy balance models (which quantify melt as residual in the heat balance equation) on a catchment scale (*Hock*, 2003). This success is explained by high correlation of temperature with several energy balance components (*Braithwaite and Olesen*, 1990; *Lang and Braun*, 1990; *Ohmura*, 2001). It is recognised that there are important limitations of degree-day melt models compared with more complex methods. For example, two major shortcomings are decreasing accuracy with increasing temporal resolution and difficulty in accurately representing spatial variability in melt rates, which may vary substantially due to topographic effects such as shading, slope and aspect (*Hock*, 2003). In addition, it is also challenging to capture relevant data, such as the lapse rate, on appropriate scales. For the purposes of our investigations, however, where we wish to compare temporal patterns of surface melting with variations in ice velocity, this method can provide a simple first-approximation of bulk meltwater production at the ice sheet surface within the Leverett Glacier catchment.

Measurements of air temperature were made using shielded Campbell Scientific T107 temperature sensors connected to Campbell Scientific CR800 dataloggers (sites 1, 3 and 6) or shielded HOBO U21-004 temperature sensors (sites 2, 4, 5 and 7) at 15 minute intervals throughout the survey period, and were mounted on the same poles as the

GPS antennae (Figure 3.6). Seasonal melt totals were measured using the GPS support pole as an ablation stake at each site. In addition, detailed measurements of local surface ablation were made at sites 1, 3 and 6 from spring 2009 using a Campbell SR-50 ultra-sonic depth gauge (UDG; Figure 3.6). The datalogger for both the temperature and ablation measurements was housed in the same box as the GPS equipment and powered by a small solar panel mounted on the top of the box. Winter snow depth was also measured before the onset of melt at each site using an avalanche probe. Combined with the detailed surface ablation record, this allows us to improve the parameterisation of melt production by calculating different degree-day factors for snow and ice.

3.2.3 Hydrological data

Drainage from Leverett Glacier occurs through one large portal on the North side of the glacier snout, which is the outlet for runoff from a large subglacial conduit (Figure 3.7). This conduit grows to >20 m wide over the course of the melt season and its route is expressed on the glacier surface as a large depression which extends several kilometres inland (Figure 3.2; *Van Tatenhove et al.*, 1995). Meltwater flows in a single channel for ∼2 km before reaching a stable bedrock cross-section prior to drainage over a large waterfall. Water stage, electrical conductivity (EC) and turbidity were monitored continuously in the proglacial stream at the bedrock section (Figures 3.8 & 3.9).

Detailed analysis of the form and timing of variability in proglacial discharge parameters may reveal characteristics of the flow pathways followed by the meltwater and therefore the structure and extent of the subglacial drainage system (e.g. *Collins*, 1979; *Fenn*, 1987; *Swift et al.*, 2002). Studies of sediment evacuation by subglacial drainage system have demonstrated high variability in sediment yield at both seasonal and annual timescales (e.g. *Collins*, 1990; *Bogen*, 1996; *Swift et al.*, 2002). This variability in sediment yield has previously been related to sediment availability (*Bogen*, 1996; *Collins*, 1996), changes in the basal area accessed by subglacial meltwater due to flood events or drainage system expansion (*Gurnell*, 1995; *Collins*, 1996; *Denner et al.*, 1999), and drainage instabilities, including flowpath migration and drainage system reorganisation (*Gurnell*, 1987; *Collins*, 1990; *Gurnell and Warburton*, 1990; *Humphrey*

Figure 3.7: The meltwater stream emerging from the snout of Leverett Glacier. This single portal grows in size over the course of a melt season and is the outlet for a large subglacial channel and carries virtually all the water that drains from the glacier.

and Raymond, 1994). Theoretical analysis suggests that the hydraulic efficiency of subglacial drainage is likely to be a critical control on basal sediment evacuation because it controls flow competence and capacity (*Alley et al.*, 1997). Distributed drainage systems are likely to access a large area of the glacier bed, but their hydraulic inefficiency limits the mobilisation and transport of basal sediments (*Alley et al.*, 1997). In a channelised drainage system, however, higher energy flow allows greater entrainment of sediment and evacuations rates increase rapidly as a nonlinear function of flow velocity and discharge (*Alley et al.*, 1997).

Electrical conductivity of meltwater can also be used to crudely differentiate runoff components and hydrological pathways through a glacial catchment (*Collins*, 1979). Electrical conductivity of meltwater is an indicator of its ionic concentration. When water is transported efficiently through the subglacial drainage system water-rock contact times are short, and water:rock ratios are low, which limits the potential for solute acquisition (*Collins*, 1979; *Fenn*, 1987). Under these circumstances, weathering is limited to fast surface exchange reactions (*Tranter et al.*, 1993). Conversely, the

Figure 3.8: River cross-section where hydrological measurements were made (dates in the photographs are from 2009). At the start of the melt season the river bed is empty and discharge grows to several hundred $m^3\ s^{-1}$ by late summer. The cross-section is located at the top of a large waterfall approximately 2 km from the glacier snout (see Figure 3.3).

distributed system transports meltwaters relatively slowly at the ice-bed interface, allowing longer for meltwater to interact with the products of subglacial erosion, hence weathering may include slower dissolution and the potential for solute acquisition is high (*Tranter et al.*, 1993). In Alpine and High Arctic glacier systems a basic pattern of decline from high to low solute concentration is typical as the drainage system becomes more efficient and a greater proportion of water is transported rapidly through the glacier over the course of a melt season (e.g. *Collins*, 1979; *Skidmore and Sharp*, 1999).

It is recognised that these hydrological parameters are somewhat crude indicators of subglacial drainage system behaviour and we rely on inference about the spatial extent of each of two drainage system types and the partitioning of water between them (e.g. *Hubbard and Nienow*, 1997; *Brown*, 2002). In light of this, we are careful only to draw conclusions which are clearly supported within the limits of the data. One significant advantage, however, is that these are simple data to collect using commercially available sensors. This allows us to collect continuous records at high temporal resolution throughout the entire melt season which can be compared with the detailed records of ice velocity and meltwater production.

The monitoring station was located in a single channel close to the ice margin that did not overflow at peak discharge. During a 2 week period simultaneous measurements of EC and turbidity were taken within 50 m of the glacier snout, and showed that the

Figure 3.9: Hydrogical monitoring station in the proglacial stream. Pressure transducers, turbidity meters and an electrical conductivity meter are mounted on a support structure which is fixed to bedrock and are submerged at a fixed height. A UDG is also suspended above to channel to provide a secondary record of river stage.

hydrological parameters we measured did not change significantly following emergence of the meltwaters from the glacier terminus (*Cowton et al.*, in review). As a result, our analysis is not greatly complicated by riverine or subaerial processes allowing us to make direct inference about the drainage system under this section of the GrIS margin (*Clifford et al.*, 1995a).

Measurements of stage were made using a pressure transducer submerged at a fixed level in the proglacial stream and a sonic-ranging device suspended above the water surface (Figure 3.9). As stage was monitored at a bedrock cross-section, the relationship between water stage and discharge is temporally stable. Stage was converted into discharge using a rating curve derived from repeat dye-dilution gauging tests (*Kilpatrick and Cobb*, 1984) conducted in the proglacial stream across the full range of discharges. Use of the dye-dilution method was necessitated by high discharges which made standard gauging techniques, such as the velocity-area method, impracticable.

Measurements of turbidity were made using a Partech IR40C active-head turbidity

meter (*Clifford et al.*, 1995b), which measures attenuation of a pulse of infrared light across a fixed gap to determine the opacity of meltwater. A relationship between turbidity and suspended sediment concentration was derived by calibration against manual samples of sediment. Depth integrated samples of suspended sediment concentration were obtained using a USDH-48 sampler which was lowered through the water column near the stream edge. These samples were filtered and the remaining sediment was weighed to determine the sediment concentration.

Electrical conductivity was measured using a Campbell CS547A Conductivity meter and the data were recorded using a Campbell CR1000 datalogger. The sensors were mounted on a support structure that was placed in the proglacial stream for the course of the melt season (Figure 3.9). Given the large size of the cross-section and high discharge in late summer (Figure 3.8) the sensors had to be moved regularly through the melt season to avoid being washed away. Continuity in the stage record was maintained, however, by using two sensors which were not moved at the same time. The hydrological data are presented in chapter 5 which includes discussion of the dye-dilution method and uncertainties in the discharge and suspended sediment data.

3.2.4 Satellite data

In addition to the field observations, we used freely-available satellite data to provide information about ice sheet surface conditions inland from the Leverett Glacier tongue in 2009. Observations from the Moderate-resolution Imaging Spectrometer (MODIS) allow us to study the development of supraglacial lakes within the region of our GPS transect (*Sundal et al.*, 2009). In addition, we used the MYD10A1 1-day albedo product, part of the MODIS Aqua snow cover daily L3 global 500 m gridded product (*Hall and Salomonson*, 2009; *Hall et al.*, 2009), to map changes in the albedo of the ice sheet surface in this region of the GrIS through the survey period. By using repeat imagery we used these data to build timeseries of lake development and drainage (Chapters 5 & 6; *Sundal et al.*, 2009) and to quantify the lowering of surface albedo associated with meltwater generation and retreat of the seasonal snowline (Chapter 6). Aside from days where cloud cover obscures satellite images, the timeseries cover the whole melt season, from before the onset of melt at the ice sheet margin in spring, to the period of

refreezing and snowfall in the autumn. These data are presented in chapters 5 and 6.

CHAPTER 4

Seasonal evolution of subglacial drainage and acceleration in a Greenland outlet glacier

Published in **Nature Geoscience**, June 2010.

Authors: Ian Bartholomew[1], Peter Nienow[1], Douglas Mair[2], Alun Hubbard[3], Matt A King[4] & Andrew Sole[5*]

1. School of Geosciences, University of Edinburgh, Drummond Street, Edinburgh, EH8 9XP, UK

2. School of Geosciences, University of Aberdeen, Aberdeen, AB24 3UF, UK

3. Institute of Geography and Earth Sciences, Aberystwyth University, Penglais Campus, Aberystwyth, SY23 3DB, UK

4. School of Civil Engineering and Geosciences, Newcastle University, Newcastle upon Tyne, NE1 7RU, UK

5. School of Geographical Sciences, University of Bristol, University Road, Bristol, BS8 1SS, UK

*now at (1).

Citation: Bartholomew, I., P. Nienow, D. Mair, A. Hubbard, M. King, and A. Sole (2010), Seasonal evolution of subglacial drainage and acceleration in a Greenland outlet glacier, *Nature Geoscience*, *3*, 408-411.

Author contributions: IB, PN, DM and AS collected the data. MAK processed the GPS data for sites 2 - 4 and IB processed the GPS data for site 1. IB analysed the data and wrote the manuscript. AS prepared Figure 4.1. All authors contributed to discussions of the paper during the writing process.

Abstract

The Greenland Ice Sheet contains 7m equivalent sea level rise yet its present mass and future contribution to sea level is poorly understood (*IPCC*, 2007). Recent observations indicate that mass loss near the margin is accelerating, partly the result of increases in ice motion (*Krabill et al.*, 2004; *Rignot and Kanagaratnam*, 2006; *Joughin et al.*, 2008a). Surface meltwaters are known to access the ice sheet base and affect ice motion through the enhancement of basal motion (*Das et al.*, 2008; *Zwally et al.*, 2002). However, the ice-motion response to seasonal variations in meltwater inputs remains poorly constrained both spatially and temporally. Here, we present ice motion data from global positioning system receivers located along a ∼35 km transect at the western margin of the Greenland Ice Sheet throughout a summer melt-season. Our measurements reveal substantial increases in summer motion, up to 220% above the winter background. These speed-up events display an upglacier evolution over the course of the summer. The relationship between melt and ice motion varies both at a site and between sites during the melt-season and can be explained by seasonal evolution in the subglacial drainage system similar to hydraulic-ice dynamic forcing mechanisms observed at smaller valley glaciers.

Recent studies have focused on the role that seasonal changes in hydrological forcing have on ice motion of the Greenland Ice Sheet (GrIS; *Rignot and Kanagaratnam*, 2006; *Joughin et al.*, 2008a; *Das et al.*, 2008; *Parizek and Alley*, 2004; *Van de Wal et al.*, 2008) and suggest that surface melting generates large enough volumes of meltwater to lubricate basal flow should it reach the bed (*Shepherd et al.*, 2009). This process has the potential to create a positive feedback between climate warming and ice velocity that has not been considered in ice sheet models that predict sea-level rise (*IPCC*, 2007). A theoretical mechanism of hydro-fracture (*Van der Veen*, 2007; *Alley et al.*, 2005b) proposes how surface meltwater can penetrate to the bed through cold ice >1000m thick and has been invoked to explain changes in vertical and horizontal components of ice motion in response to a lake drainage event (*Das et al.*, 2008). Simultaneous measurements of ice velocity and air temperature have established, over short-time

scales, a correlation between local surface melting and velocity fluctuations over a widespread area (*Joughin et al.*, 2008a; *Van de Wal et al.*, 2008; *Shepherd et al.*, 2009). However, it has been shown that higher annual ablation does not necessarily lead to increased annual ice velocities (*Van de Wal et al.*, 2008) and the importance of this relationship for large-scale dynamic behaviour of the GrIS remains equivocal. *Shepherd et al.* (2009) suggest that Alpine glaciers may provide an appropriate analogue for the evolution of the GrIS in a warming climate. In Alpine and High Arctic polythermal valley glaciers ice motion depends on variations in the structure, hydraulic-capacity and efficiency of the subglacial drainage system (*Iken et al.*, 1983), each of which evolve spatially and temporally on a seasonal basis (*Kamb*, 1987; *Bingham et al.*, 2003; *Anderson et al.*, 2004; *Kessler and Anderson*, 2004; *Mair et al.*, 2002b). Until now, limited datasets have been unable to confirm this hypothesis for the GrIS.

We used global positioning system (GPS) observations to provide continuous ice velocity measurements, from May 7th, during the 2008 melt-season and subsequent winter at four sites along a land-terminating transect in the ablation zone of the western margin of the GrIS at ∼67.10°N (Figure 4.1). Simultaneous measurements of air temperature were made at each site.

The GPS observations show that each site experienced changes in daily ice velocity that were >110% above winter motion over the course of our survey (Figure 4.2). This variability is consistent with, but much stronger than, previously reported observations (*Zwally et al.*, 2002; *Parizek and Alley*, 2004; *Shepherd et al.*, 2009). When our survey began, melt had commenced near the ice margin and site 1 was already experiencing motion above winter background level. At sites 2, 3 and 4 a common pattern of seasonal ice velocity variation is characterised by an initial period of slow-flow at winter levels, followed by a 70 - 100% increase in horizontal velocity, following the onset of melt, that marks a change in the dynamic regime to higher mean velocities. These sites gradually return to velocities below their winter values by the end of the summer, although individual high velocity events occur throughout the summer. Average rates of ice motion at sites 1, 3, and 4, following the seasonal increase in horizontal velocity, were 114, 132, and 142 m yr^{-1} respectively. The net increases in ice motion above winter background motion, due to these summer variations, are 19%, 40% and 17% equating

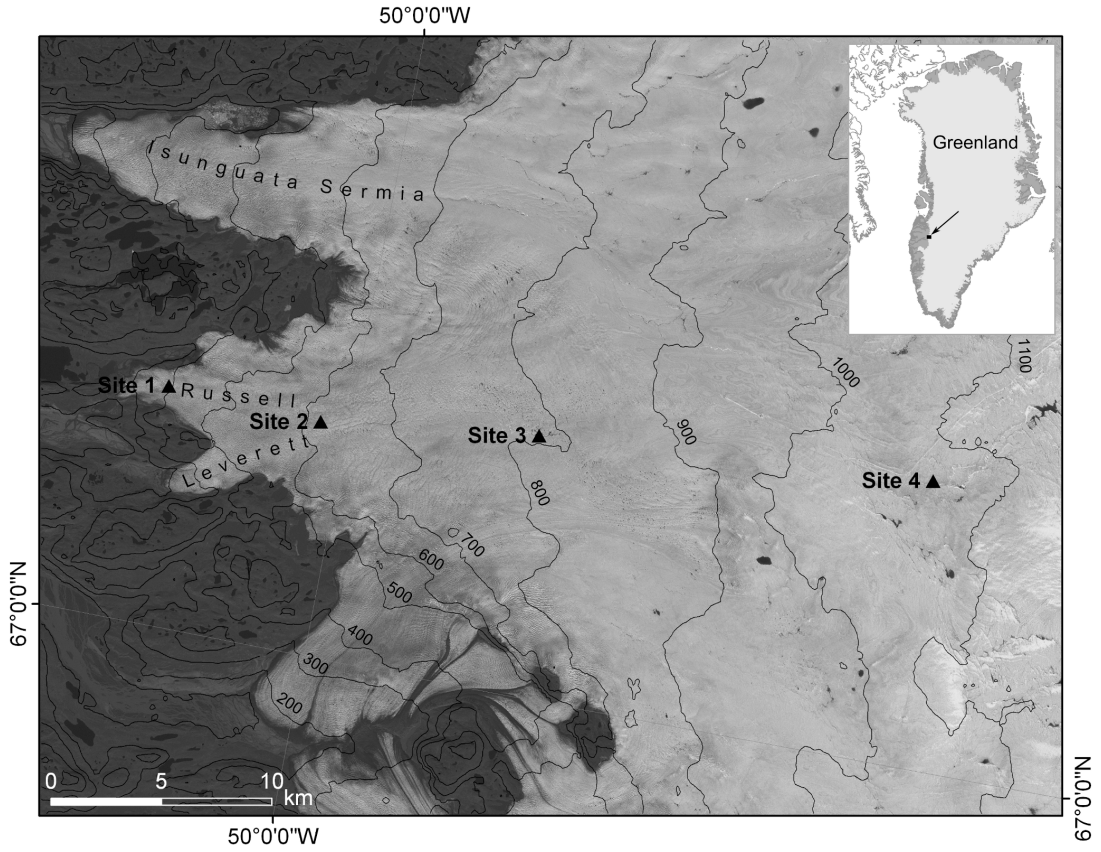

Figure 4.1: Location of the GPS transect on the western margin of the Greenland Ice Sheet. The four GPS sites are located in the ablation zone of the GrIS across an altitudinal range of 395 - 1060 m a.s.l., where ice thickness ranges from 270-920 m (*Bamber et al.*, 2001) and are located along a flowline from the ice sheet interior as determined by interferometric synthetic aperture radar (InSAR) observations (*Palmer et al.*, 2008). Simultaneous measurements of air temperature were made at each site to constrain surface melt-rates.

to an increase in annual ice flux of 8%, 14% and 6%. In addition, the data reveal an up-glacier evolution in the onset of horizontal acceleration, and in the subsequent slowdown. Site 2 began to speed up on May 15th and sites 3 and 4 followed on May 27th and June 11th respectively.

At all sites, the highest horizontal velocities coincide with uplift of the ice sheet surface, up to 12 cm in a single event, and reductions in velocity occur when the surface is lowering or stable. The highest daily horizontal velocities occur during periods of rapid uplift, rather than at peak elevation. Clear longer-term seasonal changes in surface elevation are associated with variations in the horizontal flow regime, particularly at sites 3 and 4, and can be categorised into three phases. Phase 1 is characterised by no enhanced surface uplift and low horizontal velocities (May 7 - 30 at site 3; May 7 - June

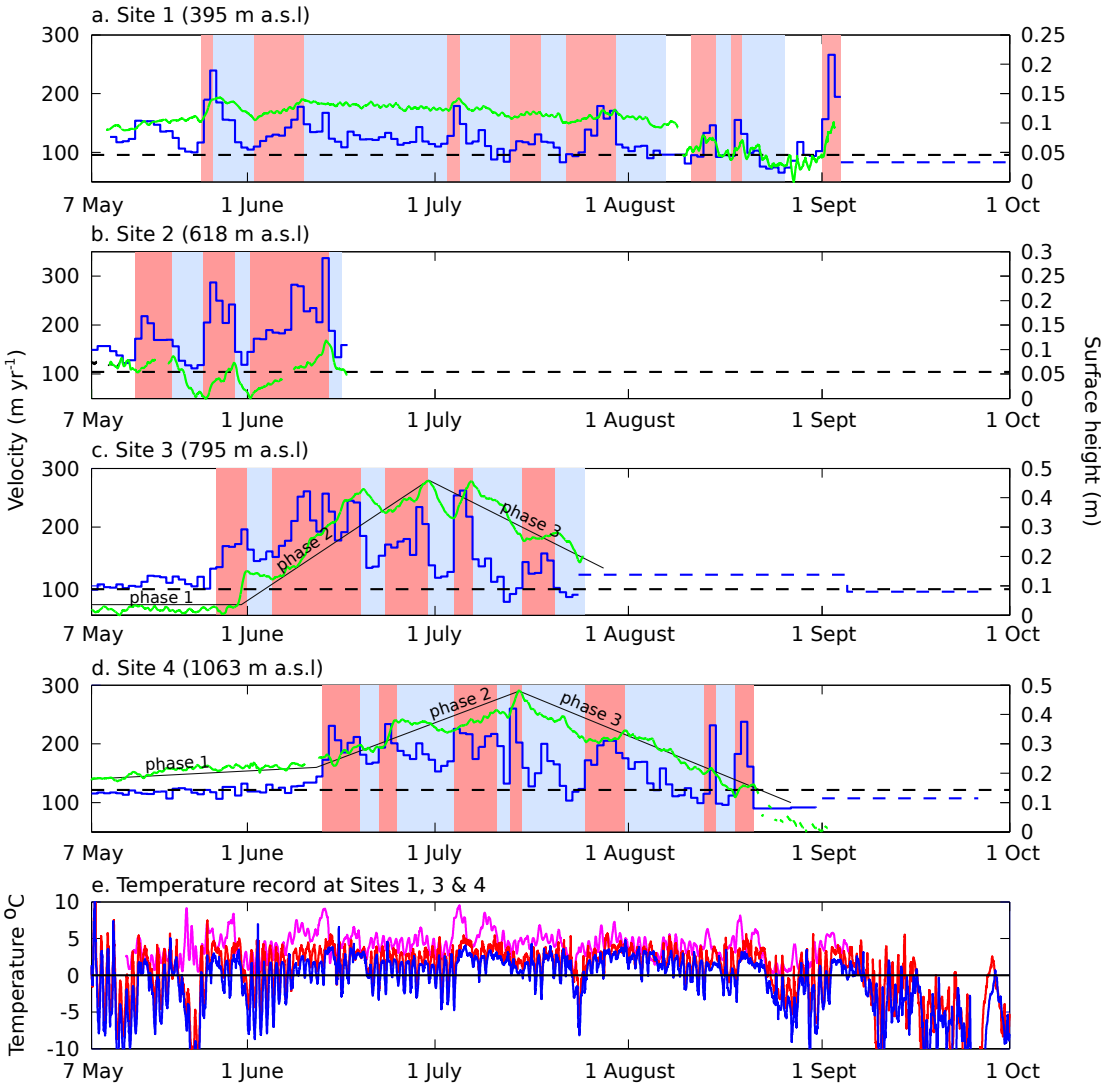

Figure 4.2: Seasonal development of melt-induced ice velocity variations. a-d, 24-hour horizontal velocity (blue) and surface height (green) at each GPS site. Surface height is displayed relative to an arbitrary datum with a linear, surface-parallel, slope removed. Dashed lines show winter background velocity (black) and velocities from periods with sparse data (blue). Shaded sections identify periods of ice acceleration associated with ice-surface uplift (red), and slower ice motion associated with a decrease in surface height (blue). Solid lines indicate different phases of longer-term ice velocity vs. surface uplift relationship. e. Temperature record from sites 1 (magenta), 3 (red) and 4 (blue).

10 at site 4) and, the slow flowing inland ice (sites 3 and 4) appears to be unaffected by the faster ice downstream (sites 1 and 2). During phase 2 the rate of uplift increases as do the horizontal velocities (May 31 - June 19, at site 3; June 11 - July 14 at site 4) and in phase 3, surface elevations gradually decrease towards (site 3) and below (site 4) their early season levels (June 20 - July 21 at site 3; July 15 - August 29 at site 4) but can fluctuate by $\sim$0.05 m day^{-1}.

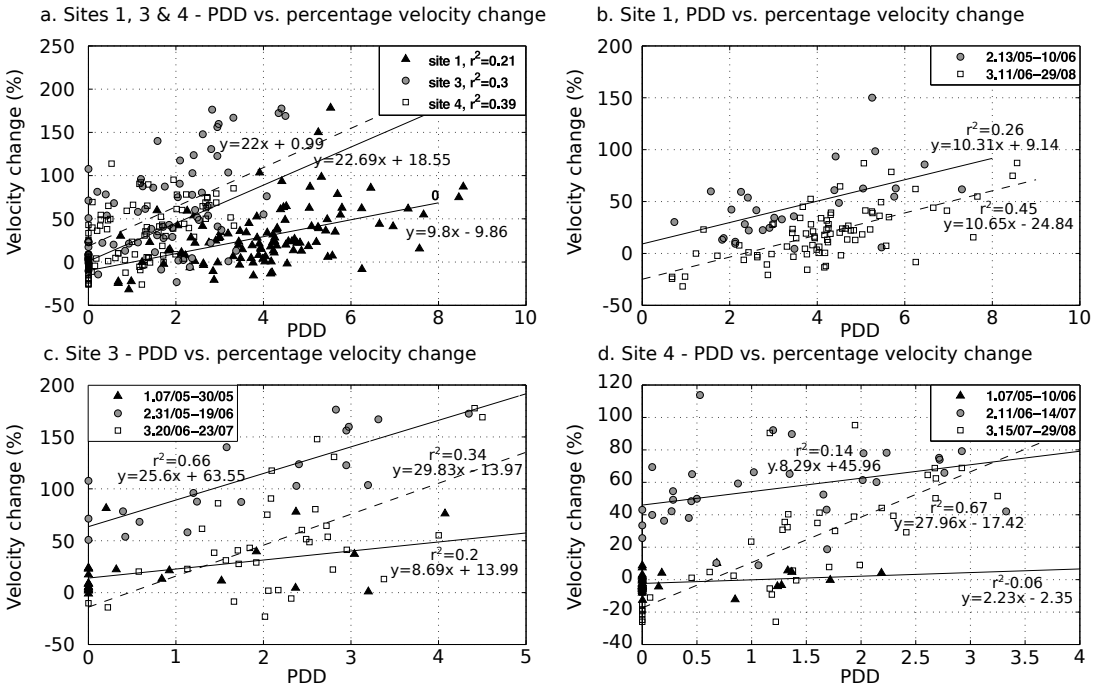

Figure 4.3: Intra-seasonal changes in surface melting vs. ice velocity relationships. a, Positive Degree Day (PDD) vs. velocity change at sites 1, 3 & 4 for whole season. 24-hour velocities are shown as percentage change relative to winter background. b-d, PDD vs. velocity for different phases of ice-velocity vs. uplift relationship 1. 'pre-melt', 2. 'enhanced surface uplift', and 3. 'surface lowering' at GPS sites 1, 3 & 4 respectively.

We used air temperature data to derive positive degree days (PDD) at each site to investigate relationships between surface melt (as inferred from PDDs) and ice velocity. For the melt-season as a whole there was a weak but significant correlation between PDD and daily ice velocity at each site but there is no link between the intensity of seasonal melting and the mean horizontal velocity increase (Figure 4.3a).

Studies of hydro-mechanical coupling at alpine and sub-polar glaciers reveal that intra-seasonal changes in the hydraulic efficiency of the subglacial drainage system are a major control on the sensitivity of ice motion to meltwater inputs (*Kamb*, 1987; *Bingham et al.*, 2003; *Anderson et al.*, 2004; *Kessler and Anderson*, 2004; *Mair et al.*, 2002b). Our data show that: i) phase 1 (pre-melt) velocities are low and show no relationship to PDD (Figure 4.3c,d); ii) phase 2 (enhanced surface uplift) mean velocities are high (>50% above winter background) and positively correlated with PDD (Figure 4.3b-d); and iii) during phase 3 (surface lowering) the sensitivity of the relationship between PDD and velocity changes such that only periods of most intense melting (i.e.

high PDDs; Figure 4.3b-d) are associated with substantial enhanced surface velocity (>50% above winter background). This accounts for the gradual decline in ice velocities, but explains the sporadic high velocity events.

From the association between the onset of surface melting, surface uplift and enhanced horizontal velocities we infer rapid delivery of surface meltwater to the ice sheet bed following the establishment of a hydraulic connection (*Das et al.*, 2008; *Zwally et al.*, 2002; *Van de Wal et al.*, 2008; *Shepherd et al.*, 2009). This meltwater increases basal sliding by reducing friction between overlying ice and its bed, likely through hydraulic jacking or cavitation (*Anderson et al.*, 2004; *Iken*, 1981). Although changes in surface elevation can also result from changes in bedrock topography and strain rates (*Gudmundsson*, 2003), the patterns we observe cannot be attributed to these effects alone. We would expect acceleration of downstream ice to cause thinning upstream, yet observe the opposite, and would not expect bedrock obstacles to be expressed at the ice sheet surface on the length scales of the changes in our data. The coincidence of highest velocities with rate of uplift, rather than peak elevation, suggests 'stick-slip' behaviour similar to that observed in an Alpine type glacier (*Anderson et al.*, 2004; *Iken*, 1981; *Fischer and Clarke*, 1997), whereby separation of the ice and bed allows the immediate release of built-up stresses in the overlying ice.

Our observations of temperature and the pattern of changes in horizontal and vertical motion at each site, suggest a local, temperature-related, forcing mechanism for the seasonal changes in ice-motion. As also observed at Alpine and High Arctic polythermal glaciers (*Anderson et al.*, 2004; *Kessler and Anderson*, 2004; *Mair et al.*, 2002b), the initiation of summer velocity changes is dependent on the establishment of a hydraulic connection between the ice surface and bed, which occurs first in the lowest parts of the ablation zone, through thinner ice, and migrates progressively up-glacier (Figure 4.2). However, our results from Greenland suggest that a temporally consistent relationship between surface melt and ice velocity does not exist once a hydraulic connection has been made. Instead, the relationship evolves both at a point and develops upglacier. When melt first accesses the bed, the onset of high surface velocities and uplift (phase 2; Figure 4.3) is indicative of an inefficient basal hydraulic system in which basal water pressures are highly sensitive to relatively small inputs of water (*Kamb*, 1987).

During the latter part of the melt-season (phase 3), the gradual surface lowering and ice slow-down indicates a more efficient channelised system in which basal water pressures are generally lower (*Kamb*, 1987). Only during very high meltwater inputs are basal water pressures raised enough to reduce basal friction significantly and enhance surface velocity (*Iken and Bindschadler*, 1986). This categorisation is complicated by a small number of examples of high horizontal velocity in our data in the absence of high temperatures (e.g. site 4 on Aug 14th (Figure 4.2)), which may be caused by rapid drainage of surface lakes to the ice sheet bed (*Das et al.*, 2008; *Zwally et al.*, 2002).

Sites 3 and 4 do not show velocity increases to above winter values even when sites downstream have started accelerating (Figure 4.2) suggesting that longitudinal coupling is not effective over >10 km at these locations. Whilst numerical studies have suggested that it may be possible for seasonal acceleration of inland ice to be explained through longitudinal coupling to marginal ice (*Price et al.*, 2008), and our data do not preclude its effectiveness in other parts of the GrIS, we do not observe that process here at length-scales of >10 km. Therefore, enhanced surface velocity is primarily a consequence of local hydrological forcing at each site and the efficiency of the hydrological system.

Thus the ice sheet exhibits a transient dynamic response to seasonal melting at each site (*Rignot and Kanagaratnam*, 2006; *Joughin et al.*, 2008a; *Iken*, 1981). We find that, in addition to surface melt-rates, a key control on the magnitude and location of enhanced basal sliding is the structure and efficiency of the subglacial drainage system which evolves seasonally, in a similar manner to Alpine glaciers (*Anderson et al.*, 2004; *Iken*, 1981; *Nienow et al.*, 1998). The seasonal and spatial increase in subglacial hydraulic efficiency is likely responsible for the lack of correlation between seasonal ablation rates and velocity changes that has caused previous authors to question the existence of positive feedback between climate warming and annual ice velocity of the GrIS (*Van de Wal et al.*, 2008; *Truffer et al.*, 2005). Using a more extensive dataset, we find that the relationship between melt-rate and ice motion evolves through time at each site and with distance up-glacier, suggesting that its significance lies at higher elevations. Although our data only extend up to 1000 m altitude, additional ground-based observations have also detected ice-motion variations during late summer

that are strongly associated with changes in surface hydrology, at elevations above 1400 m in the same region (*Shepherd et al.*, 2009).

In a warming climate, with longer and more intense summer melt-seasons, we would expect that water will reach the bed farther inland (*Hanna et al.*, 2008) and a larger portion of the ice sheet will experience summer velocity changes. Modelling studies have suggested that the enhancement of summer ice motion is critical in drawing down ice from the accumulation zone thereby reducing the surface elevation of the ice sheet, exposing more of the ice sheet to surface ablation (*Parizek and Alley*, 2004). Additionally, the low gradient of the GrIS interior ensures that a small rise in temperature will induce melt across a spatially extensive area and substantial melt at elevations above 1600 m is already evident in the presence of supraglacial lakes (*Sundal et al.*, 2009). Our findings emphasise the importance of both surface melting and seasonal evolution of the subglacial drainage system on ice motion in marginal regions of the GrIS and will help parameterise numerical models that predict the future evolution of the GrIS.

4.1 Supplementary methods

Each GPS antenna was mounted on a support pole drilled several metres into the ice, which froze in subsequently, providing measurements of ice motion that are independent of ablation. The GPS receivers collected data that were processed kinematically using a Precise Point Positioning approach (sites 2, 3 & 4 at 300s intervals), and relative to a local (<2.5 km, 10s intervals) base station for site 1 (*King*, 2004). Estimates of the uncertainty associated with positioning are ± 1.5 cm in the horizontal and ± 2.5 cm in the vertical. The precision and resolution of the dataset is therefore sufficient to study changes along the flowline on seasonal and shorter (<1 day) timescales. Daily horizontal velocities reported in this paper are calculated by differencing 1-hour mean positions every 24 hours. Vertical profiles are generated by filtering the whole data set to suppress noise without over-smoothing the time series.

The GPS units were powered by solar panels. The GPS receiver at site 2 lost power on June 16th and our analysis is focused mainly on the three remaining sites. The receiver at site 1 was installed 3 days later than the others on June 10th. We also

experienced power problems later in the season at site 3 and data from the beginning of September onwards is sporadic. This means that the detail of the ice motion record is unavailable at the very end of the melt-season and through the subsequent winter. However, using occasional GPS positions (Figure 4.2 a-d, dashed blue lines), horizontal ice motion can still be calculated over longer periods, allowing us to assess the net velocity increase in summer compared with winter. The values for net summer velocity over winter background reported in this paper are calculated on the basis of ice motion from the onset of speed-up (the beginning of the survey period in the case of site 1) until the end of summer, when melting has finished at all sites and the effect of 'slower than winter' motion that we observe in late summer has been incorporated - as such they may be considered minimum estimates of summer velocity.

The values for background velocities are derived from the displacement of each site over the subsequent winter, following the end of the summer melting period (between 11 October - 27 February at Site 1, 26 September - 2 May at site 2, 26 September - 8 May at site 3, and 11 October - 8 May at site 4). The reported contribution to annual ice flux from the hydrologically-forced summer ice velocity variations is the percentage by which the observed displacement exceeds that which would occur if the ice flowed at calculated winter rates all year round. At sites 3 & 4, the pre-speed up velocities bear close agreement with over-winter velocities, however, are not included in the calculations in order to retain consistency between the approach adopted for each site.

Measurements of air temperature were made using shielded HOBO air temperature sensors. PDDs, used as a proxy for rates of surface melting, are derived using mean daily air temperature. Lack of ablation data meant that it was not possible to obtain Degree-Day Factors, which vary for ice and snow. However, accumulation rates are low in this part of Greenland and snow depths when the GPS were deployed at the beginning of May were less than 20 cm.

CHAPTER 5

Supraglacial forcing of subglacial drainage in the ablation zone of the Greenland Ice Sheet

This paper is a study of the seasonal drainage system development at Leverett Glacier in 2009. In the previous chapter we used ice motion data to show that the relationship between surface melting (as parameterised by positive degree-days) and ice velocity in this section of the GrIS margin is not consistent over the course of the summer melt season. It was argued that this is due to development in the structure and efficiency of the subglacial drainage system, which operated at lower pressure for a given discharge as the summer progressed in a manner similar to Alpine Glaciers. There are no direct measurements of seasonal drainage system evolution, however, to confirm this hypothesis for the Greenland Ice Sheet. We use a combination of field and satellite data to investigate development of the drainage system within the Leverett Glacier catchment over the course of a full melt season, from the start of May 18th until September 3rd 2009, in response to inputs of meltwater from the ice sheet surface.

Published in **Geophysical Research Letters**, April 2011.

Authors: Ian Bartholomew[1], Peter Nienow[1], Andrew Sole[2*], Douglas Mair[2], Thomas Cowton[1], Steven Palmer[3] & Jemma Wadham[4]

1. School of Geosciences, University of Edinburgh, Drummond Street, Edinburgh, EH8 9XP, UK

2. School of Geosciences, University of Aberdeen, Aberdeen, AB24 3UF, UK

3. School of Earth and Environment, University of Leeds, Leeds, LS2 9JT, UK

4. School of Geographical Sciences, University of Bristol, University Road, Bristol, BS8 1SS, UK

*now at (1).

Citation: Bartholomew, I., P. Nienow, A. Sole, D. Mair, T. Cowton, S. Palmer, and J. Wadham (2011), Supraglacial forcing of subglacial hydrology in the ablation zone of the Greenland Ice Sheet, *Geophysical Research Letters*, *38*, L08502 doi:10.1029/2011GL047063.

Author contributions: IB, AS, TC, PN, DM and JW collected the field data. TC processed the satellite data to produce the timeseries of supraglacial lake drainage events. SP provided a surface digital elevation model which was used to calculate runoff at different elevations. IB, AS and TC processed the stage and dye-dilution data to produce the discharge record. IB analysed the data and wrote the manuscript. All authors contributed to discussions of the paper during the writing process.

Abstract

We measure hydrological parameters in meltwater draining from an outlet glacier in west Greenland to investigate seasonal changes in the structure and behaviour of the hydrological system of a large catchment in the Greenland Ice Sheet (GrIS). Our data reveal seasonal upglacier expansion and increase in hydraulic efficiency of the subglacial drainage system, across a catchment >600 km^2, to distances >50 km from the ice-sheet margin. This expansion occurs episodically in response to the drainage of surface meltwaters into a hitherto inefficient subglacial drainage system; this system is similar to Alpine glaciers. Combining satellite observations with changes in hydrological parameters reveals that supraglacial lake drainage events play a key role in developing an efficient subglacial drainage system at higher elevations, allowing large volumes of surface generated meltwater to be transported via the ice sheet bed to the margin. These observations provide the first synopsis of seasonal hydrological behaviour in the ablation zone of the GrIS, providing a conceptual model of drainage system development that can be applied to investigations of the role of glacier hydrology in the dynamic response of the GrIS to anticipated climate warming.

5.1 Introduction

In land-terminating sections of the GrIS, meltwater production enhances ice motion through seasonal velocity variations that are initiated when surface meltwaters gain access to the ice-bed interface (*Zwally et al.*, 2002). It has been hypothesised that a feedback between surface melting and ice velocities will accelerate mass loss from the GrIS in a warmer climate (*Zwally et al.*, 2002; *Parizek and Alley*, 2004; *Shepherd et al.*, 2009). On the basis of correlations between ice motion and surface melting, however, it has been shown that a key control on the relationship between surface melting and ice velocity variations is the structure and hydraulic efficiency of the subglacial drainage system, which develops spatially and temporally on a seasonal basis (*Bartholomew et al.*, 2010). A more efficient subglacial drainage system can evacuate large volumes of water in discrete channels which operate at a lower steady-state water pressure, thereby reducing the basal lubrication effect of external meltwater inputs (*Kamb*, 1987; *Pimentel*

and Flowers, 2011).

Despite the clear link between rates of ice motion and the structure of the subglacial drainage system, predictions about the future extent and magnitude of hydrologically-forced ice velocity changes in the GrIS remain uncertain (*Van de Wal et al.*, 2008). To address this, we need to understand how spatial and temporal changes in surface melting of the GrIS force development of an efficient subglacial drainage system on a seasonal basis (*Pimentel and Flowers*, 2011). Here we present observations from Leverett Glacier, a land-terminating outlet glacier at ∼67°N in west Greenland (Figure 5.1) in 2009, that are used to elucidate seasonal development of the hydrological system of a large catchment in the ablation zone of the GrIS.

5.2 Data and methods

Drainage from Leverett Glacier occurs through one large portal on the North side of the glacier snout, which grows in size over the season and is the outlet for runoff from a large subglacial conduit. Water stage, electrical conductivity (EC) and turbidity were monitored continuously in the proglacial stream at a stable bedrock section ∼2 km downstream from the glacier terminus from May 18th 2009, before melting had started, until September 3rd. Stage was converted into discharge (Q) using a rating curve (r^2=0.85) derived from 29 repeat dye-dilution gauging tests (*Kilpatrick and Cobb*, 1984) conducted in the proglacial stream across the full range of discharges. Uncertainty in the discharge record is the result of measurement error and application of a rating curve, and is estimated to be ± 14.5%. A relationship between turbidity and suspended sediment concentration (SSC) was derived by calibration against 49 manual gulp sediment samples (r^2=0.82). Uncertainties in the SSC and EC record are estimated to be ± 6.6% and ± 10% respectively. Our monitoring station was located in a single channel close to the ice margin that did not overflow at peak discharge. During a 2 week period, simultaneous measurements of SSC and EC taken within 50 m of the glacier snout show that the hydrological parameters we measured were not substantially modulated following emergence of the meltwaters from beneath the glacier terminus.

A surface digital elevation model (*Palmer et al.*, 2008) was used to derive a first

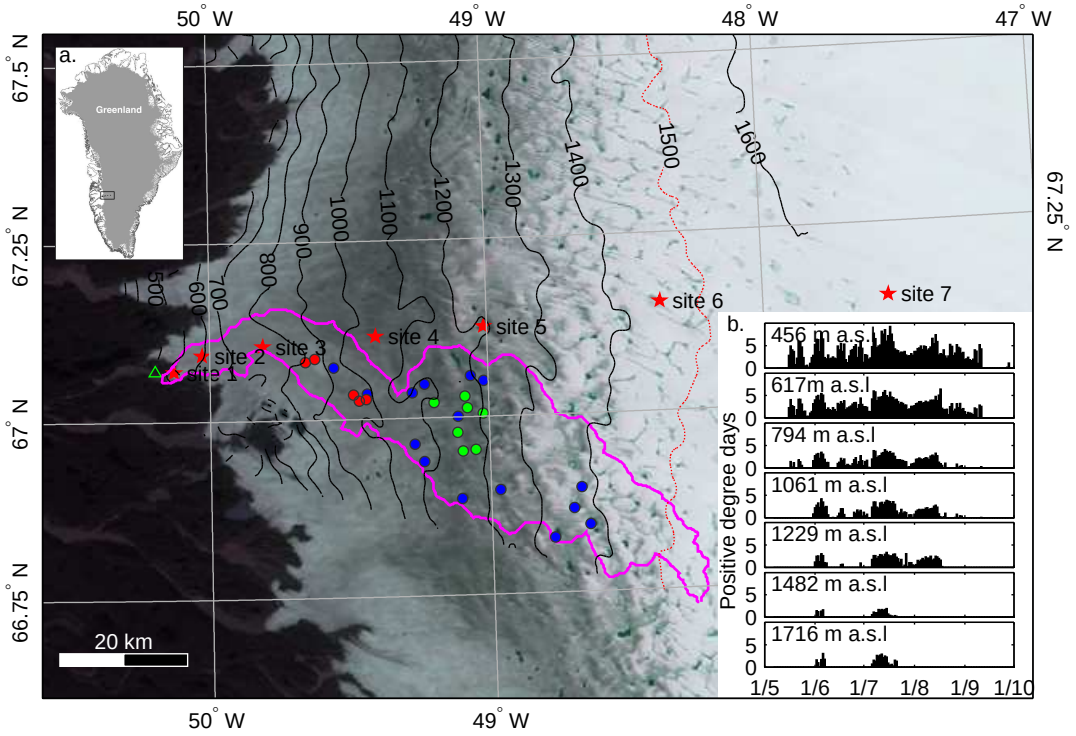

Figure 5.1: a. Map showing the location of Leverett Glacier, a catchment derived from the surface DEM (purple), and locations of temperature measurements (red stars). Lakes that drain during the survey period are denoted by circles, colour-coded to show drainage events that coincide with meltwater pulses P2 (red) and P4 (green). Lakes which drain during the survey period but are not clearly associated with pulses in the discharge record are coloured blue. Contours are at 100 m intervals and the equilibrium line is identified in red (*Van de Wal et al.*, 2005). The location of the bedrock section where stage, EC and turbidity were measured is shown by the green triangle. b. Positive degree-days at each of the temperature measurement locations.

approximation of the Leverett Glacier hydrological catchment (Figure 5.1), which is less than 10 km wide below 800 m and widens to 30 - 40 km at higher elevations. Although there is uncertainty in such an approach, lack of appropriate bed elevation data prevents an estimate of catchment geometry based on calculations of subglacial hydraulic potential (*Shreve*, 1972). We used satellite observations from the Moderate-resolution Imaging Spectroradiometer (MODIS) to study the development and drainage of supraglacial lakes within the Leverett catchment (*Sundal et al.*, 2009; *Box and Ski*, 2007). 40 MODIS images were used spanning the period 31st May to 18th August, representing all days when lake identification was not impeded by cloud cover. There is significant uncertainty in applying a depth-retrieval algorithm based on surface reflectance to find the depth of GrIS supraglacial lakes shallower than 2.5 m (*Box and*

Ski, 2007). Therefore, we used an estimate (*McMillan et al.*, 2007) of the average depth of supraglacial lakes obtained within this region to estimate volumes of lakes that drain from the ice sheet surface. Continuous measurements of air temperature were made at seven sites, from 450 -1700 m altitude (Figure 5.1). Ablation rates were also monitored in order to constrain a temperature-melt index model (*Hock*, 2003) which we used to predict volumes of runoff generated from the catchment during our survey period.

5.3 Hydrological observations

The proglacial runoff hydrograph (Figure 5.2a) shows that prior to June 1st discharge was <6 m^3 s^{-1}, during a period of ∼20 days of above-zero temperatures, extending up to 1400 m altitude before this date (Figure 5.2d). Discharge then increased rapidly over 3 days to 46 m^3 s^{-1} on June 4th and continued to grow episodically before rising dramatically, by 220 m^3 s^{-1} in 10 days, to a peak of 317 m^3 s^{-1} on July 16th. Following this peak, discharge declined gradually but remained 3-4 times greater than early-season levels until late August. Proglacial runoff showed clear diurnal cycles which had greatest amplitude (∼25 m^3 s^{-1}) later in the season, after July 16th, and were more subdued (∼6 m^3 s^{-1}) earlier in the summer.

The rising limb of the seasonal hydrograph is also marked by four distinct pulses of water, superimposed on the general pattern of runoff growth. These pulses each last a few days, and contribute between 4.9 - 11.8 x 10^6 m^3 of water to the total runoff. These pulses are also defined by coincident spikes in the EC and SSC records (Figure 5.2a-c). The first pulse of water (P1 on June 3rd) marks the start of significant runoff growth. It was followed by further pulses (P2-P4) starting on June 7th, June 17th and July 3rd (Figure 5.2a).

Maximum EC (69.9 μS cm^{-1}) occured while discharge was still low at the beginning of the season and declined in a stepwise fashion to a minimum of 9.9 μS cm^{-1} on July 3rd, immediately prior to P4 (Figure 5.2b). There is a negative relationship between EC and discharge over the whole melt season (r^2=0.27). Following P4 EC remains low (<20 μS cm^{-1}) and the daily cycles of Q and EC develop a characteristic inverse relationship (*Fenn*, 1987) with clear stable hysteresis where EC is highest on the rising

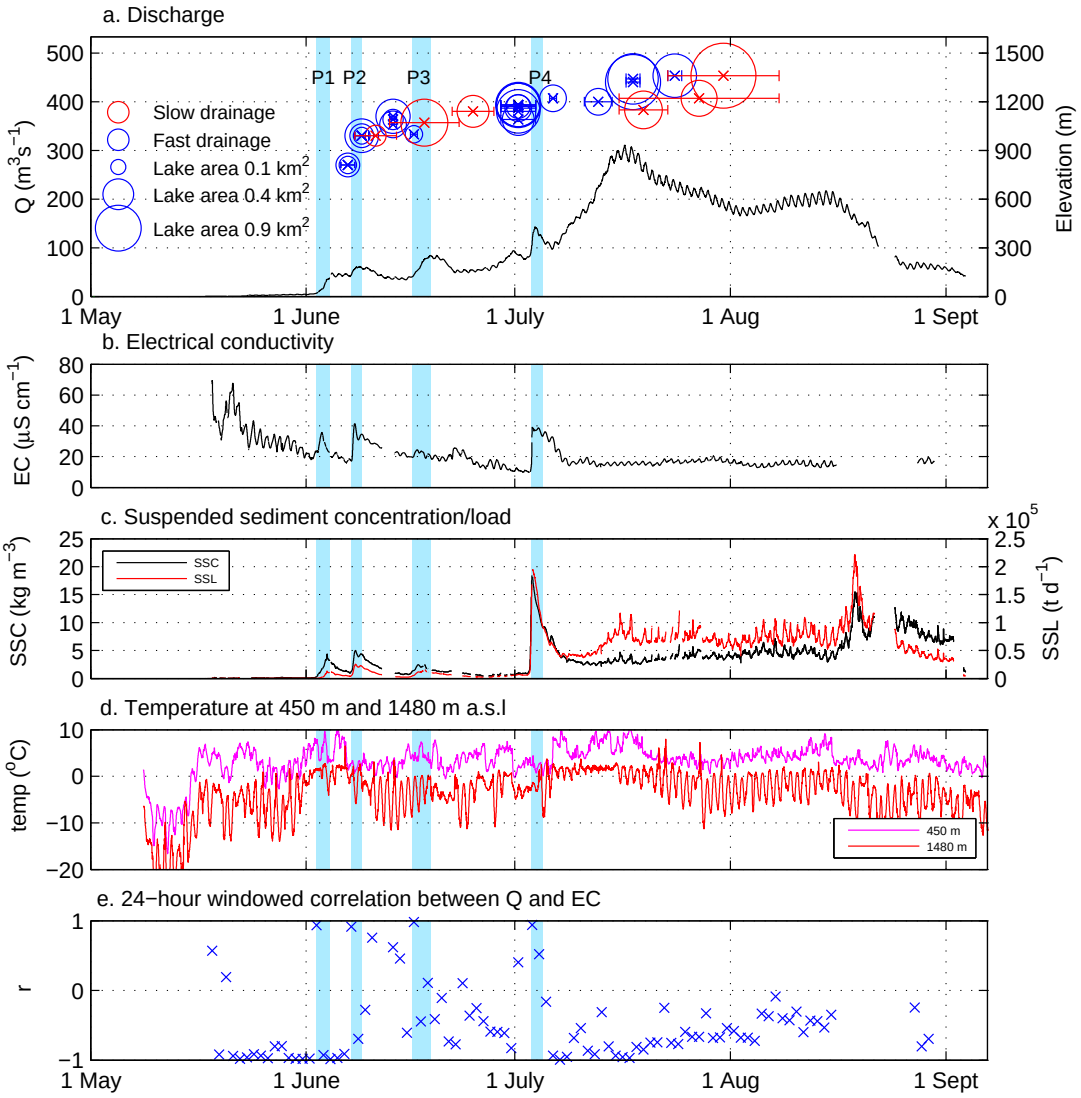

Figure 5.2: a. Proglacial meltwater stream discharge (m^3 s^{-1}; blue line). Timing, area and elevation of lake drainage events. Each circle represents a single lake drainage event, based on change in surface area on MODIS images. Horizontal bars represent the time period in which drainage took place. Red circles are lakes that drained slowly over several images while blue circles drained in a discrete event between two images. b. Electrical conductivity (μS cm^{-1}). c. suspended sediment concentration (kg m^{-3}; left-axis, black) and suspended sediment load (t d^{-1}; right-axis, red). d. Temperature measurements from 450 m and 1480 m elevation. e. 24-hour windowed correlation coefficient between EC and Q.

limb of the diurnal hydrograph (Figure 5.3). However, the relationship is not consistent throughout the survey period (Figure 5.2e), and early in the season can fluctuate between a strong positive relationship and a strong negative one over short time-scales (<1 week). In particular, the pulses of water P1, P2 and P4 are characterized by pronounced conductivity peaks (Figure 5.2b) that show a strong positive relationship

with increasing Q on their rising limbs. During P2, EC increases from 17 - 42 μS cm^{-1} in 9 hours as Q increases from 40 - 59 m^3 s^{-1} and during P4, EC increases from 10 - 40 μS cm^{-1} in 6 hours as Q increases from 74 - 140 m^3 s^{-1}. In these pulses, an EC peak shortly precedes maximum discharge, and EC returns to pre-pulse levels within a few days (Figure 5.2b). By contrast, there is no large peak in EC associated with P3.

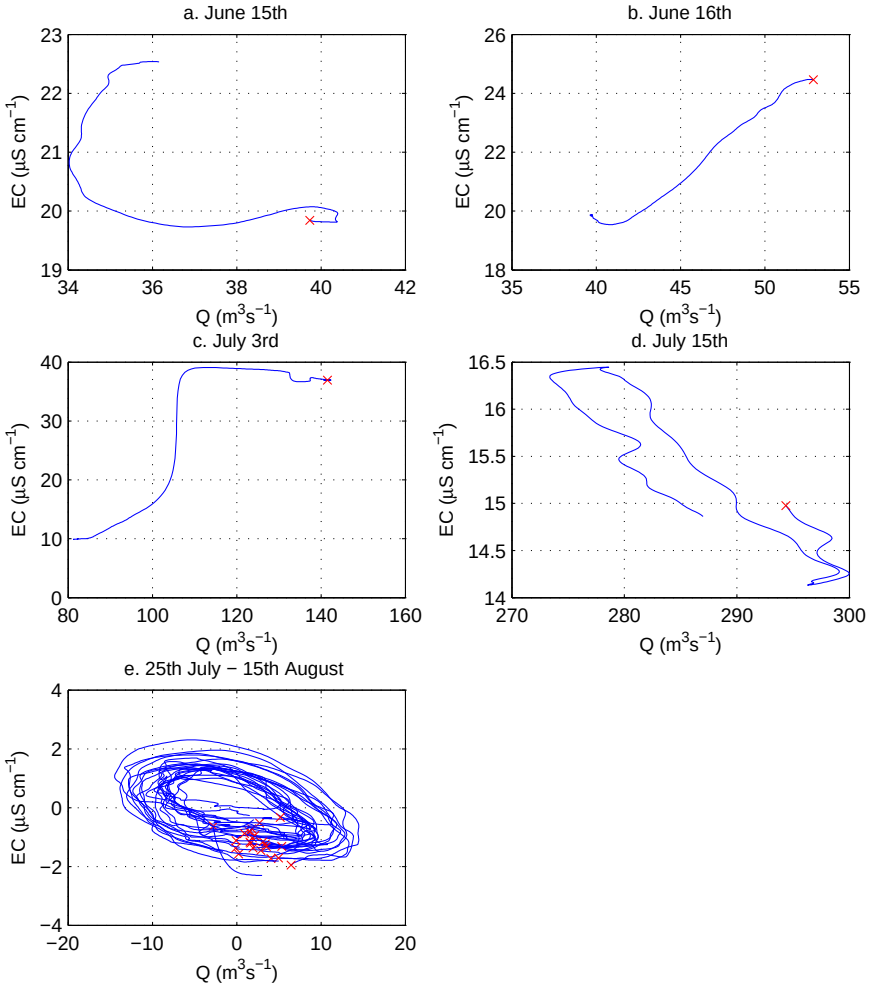

Figure 5.3: a-d. Diurnal variability in the relationship between EC and Q early in the melt-season. 24 hours of data are shown in each window and crosses mark the last measurement at 2400h. The relationship is unstable and often reverses over short timescales. We note that b & c are on the rising limb of P2 & P4 respectively and show a strong positive relationship, this is in contrast to the more typical negative relationship shown in a & d. e. 22 consecutive days of data (25th July - 15th August) show the stable hysteresis pattern that develops on the falling limb of the seasonal hydrograph. The data are split into 24-hour windows and normalised about their midpoint.

Suspended sediment concentration ranged from less than 0.2 kg m^{-3} to greater than 18 kg m^{-3}, beyond the range of our sensor, and increased gradually but episodically

throughout the season (Figure 5.2c). In common with the pattern in electrical conductivity and discharge, there are large spikes in SSC at P1, P2 and P4, and to a lesser extent at P3. These spikes precede the local discharge peaks and are characterised by a steep rise followed by a more gradual return to lower values. The SSC peak at P4 is the most dramatic and shows a jump from 2 - >18 kg m^{-3} within 6 hours. The suspended sediment load (SSL) also grows throughout the season, and is significantly greater in the latter part of the season (Figure 5.2c). Prior to P4, SSL ranges from 0 - 4 x 10^4 t d^{-1}, and following P4 ranges from 4 - 20 x 10^4 t d^{-1}. The total suspended sediment flux for the survey period is $\sim$4.7 $\pm$ 0.74 x 10^6 t.

5.4 Discussion

The delay in the onset of significant runoff, following $\sim$20 days with high temperatures, can be explained by refreezing of an initial fraction of the surface melt in cold snow until the firn becomes isothermal (*Pfeffer et al.*, 1991; *Van den Broeke et al.*, 2008) and observed ponding of surface meltwater prior to accessing the subglacial drainage system. Prior to P1, low runoff volume and high EC indicate that water in the proglacial stream was derived substantially from leakage of basal meltwater from an inefficient winter drainage system beneath Leverett Glacier (*Collins*, 1979; *Skidmore and Sharp*, 1999).

Comparison with a temperature-melt index model (*Hock*, 2003) shows that the seasonal discharge volumes we observe cannot be explained by an increase in melt intensity within a stable catchment area, indicating delivery of surface-generated meltwater from a progressively larger area of the ice sheet as the melt season develops (Figure 5.4). The required development and expansion of the contributing hydrological catchment, up to 800 m elevation by June 6th, and to 1000 m by July 9th, eventually delivers surface meltwater from an area of over 600 km^2 that extends higher than 1200 m elevation and to a distance of >50 km from the ice margin by July 21st. The dramatic rise in runoff observed in the first half of July is driven, therefore, by a combination of high temperatures (Figure 5.2d) and recent expansion of the area of the ice sheet which delivers water to the ice margin via Leverett Glacier.

The EC of meltwater can be used crudely to differentiate runoff components and

hydrological pathways through a glacial catchment (*Collins*, 1979). The basic pattern of decline from high to low solute concentration that we observe is typical of Alpine and High Arctic glaciers (*Collins*, 1979; *Skidmore and Sharp*, 1999) as the hydrological system becomes more efficient and a greater proportion of water is transported rapidly through the hydrological system, limiting the potential for solute acquisition. Therefore, along with the upglacier expansion of the hydrological catchment in response to surface melt inputs, our data suggest a concomitant increase in its hydraulic efficiency throughout the melt-season.

High suspended sediment concentrations indicate that meltwater emerging from Leverett Glacier has been routed from the ice sheet surface, where it was generated, via the ice sheet bed. Rates of basal sediment evacuation are controlled by the hydraulic efficiency of the subglacial drainage system, but can be limited by the availability of source material (*Alley et al.*, 1997; *Swift et al.*, 2002). A sustained increase in subglacial hydraulic efficiency, and ongoing expansion of the subglacial drainage system, is consistent with the continued increase in SSC, even while runoff diminishes following peak discharge on July 17th (*Alley et al.*, 1997). In addition, SSC shows no sign of supply exhaustion suggesting that expansion of the efficient basal hydraulic system provides continual access to an extensive reservoir of basal sediment (*Swift et al.*, 2002).

Spatial expansion of efficient subglacial drainage at the expense of a hydraulically inefficient distributed system explains temporal instability in the correlation between EC and Q on the rising limb of the seasonal discharge hydrograph. Upglacier expansion of supraglacial melt extent results in the headward expansion of the efficient subglacial drainage system through the contribution of surface meltwater to the subglacial hydraulic system (*Nienow et al.*, 1998). These surface waters drain initially into a hydraulically inefficient drainage system causing channel sections to grow in a downglacier direction until they connect with existing channels further downstream. Reduction of mean water pressure in the channels, relative to the distributed drainage system, is probably responsible for drawing out stored basal waters. Temporal and spatial evolution of the efficiency of the hydrological system therefore complicates the relationship between surface melting and proglacial runoff characteristics during its seasonal growth phase. The stable hysteresis pattern that develops with EC peaking on the rising limb of the

diurnal flow hydrograph, and the constant inverse relationship between EC and Q (Figure 5.2e), demonstrates that the hydrological system has reached a more stable and uniform configuration by July 21st.

Observations on the GrIS have shown that moulins essentially comprise vertical conduits which transport water from the ice sheet surface to its bed (*Das et al.*, 2008; *Catania and Neumann*, 2010). While there may be some lateral transport of water via englacial channels, in order to explain the trends in Q, EC and SSC we argue that opening of moulins at progressively higher elevations allows surface generated meltwater to be delivered to the ice sheet bed further inland through the melt season. Growth of the efficient subglacial system therefore follows upglacier development of supraglacial drainage and proceeds in a stepwise fashion as new input points become active (*Nienow et al.*, 1998), transporting water to the ice sheet margin via the subglacial hydrological system. This proposed model is analogous to Alpine glacier systems. It is notable, therefore, that the channelised subglacial drainage system is sustained in the GrIS where ice thicknesses are much greater. This implies that the high volumes of meltwater input are sufficient to offset increased channel closure potential by deformation of thicker ice.

5.5 Supraglacial lake drainage

Two pulses of water (P2 & P4) that are superimposed on the rising limb of the seasonal hydrograph (Figure 5.2a) are not explained by trends in surface melting. Dramatic rises in EC associated with P2 and P4 suggest that a significant component of these flood-waters is of subglacial provenance and indicates the displacement of large volumes of solute-rich stored water from an inefficient hydrological system (*Skidmore and Sharp*, 1999). Large sediment flushes (Figure 5.2c) also confirm interaction of meltwaters with the basal environment. They indicate sudden access of water to areas of stored subglacial sediments and a dramatic increase in hydraulic efficiency to evacuate them (*Raymond et al.*, 1995; *Swift et al.*, 2002).

We used MODIS satellite imagery to investigate possible supraglacial sources for the pulses of meltwater and identify a number of lakes that develop and subsequently drain from the ice sheet surface during the survey period (Figure 5.1). The timing of

their drainage, their size and elevation (Figure 5.2a), and location within the proposed catchment of Leverett Glacier, suggests that they are likely candidates for the source of the pulses of water that we observe on the rising limb of the runoff hydrograph. In particular, P2 is associated with the drainage of five lakes between 800 - 1000 m, and P4 coincides with seven drainage events between 1100 - 1200 m.

We note that there are also spikes in SSC and EC at P1, which indicate a similar process of change in hydraulic efficiency, but that it precedes any lake drainage events observable on MODIS imagery. The rise in EC is less dramatic than at P2 and P4, and we suggest that P1 is the result of initial access of meltwater to the subglacial drainage system through moulins crevasses low down on the glacier following the onset of spring melting. This is supported by observations of meltwater ponded in crevasses and supraglacial channels prior to P1. P3 is not accompanied by a rise in EC and therefore does not appear to be driven by a rapid lake drainage event but by changes in temperature-driven runoff feeding into the existing drainage system.

Estimation of lake area (Figure 5.2a), based on manual pixel counting of classified images (*Sundal et al.*, 2009), indicates that the lakes that drain at P2 have areas between 0.13 and 0.49 km^2 and those that drain at P4 are between 0.25 and 0.88 km^2. Using an average lake depth of 2.7 m (a value determined (*McMillan et al.*, 2007; *Shepherd et al.*, 2009) for ∼150 lakes in this region in summer 2001), we find that the volume of water in each pulse (4.9 and 7.2 x 10^6 m^3 respectively) is accounted for by the drainage of multiple lakes in a single event. Previous studies have found that MODIS classification of GrIS supraglacial lakes is robust when compared with higher resolution satellite data (*Sundal et al.*, 2009) and has approximate error of 0.22 km^2. Since there is also uncertainty about the depth of individual lakes we are unable to determine precisely which, or how many, of the lakes contribute to each meltwater pulse. It is clear, however, that the pulses at P2 and P4 are caused by drainage of a cluster of lakes within close proximity to one another (Figure 5.1), rather than drainage of an individual lake.

Rapid transfer of these pulses to the ice margin implies that the hydraulic system further downglacier already has the capacity to transport water efficiently. Combined with the hydrological signature of the pulses, our data indicate that these events

represent the emergence at the ice sheet margin of large volumes of meltwater which had been stored at the ice surface and subsequently drained to its bed on the establishment of a hydraulic connection between the two (*Das et al.*, 2008). These surface waters mix with and flush out long-term subglacially stored water, hence the large rise in EC values, and effect a stepwise expansion of the efficient subglacial hydrological system, progressively further inland.

Our observations suggest that a key role of lake drainage in GrIS hydrology is contribution to the expansion of the subglacial area that is subject to inputs of surface meltwater, and therefore undergoes hydraulic reorganisation, on a seasonal basis. Supraglacial lake drainage may be particularly important at high elevations for two reasons. Firstly, by providing a mechanism for water to penetrate through thick, cold ice. Secondly, concentration of surface meltwater into lakes may be critical to provide the volumes of water required to force evolution of a channelised drainage system beneath thicker ice where overburden pressure is greater. Under warmer climatic conditions we expect lakes to form and drain from backslopes which occur at higher elevations on the GrIS (*Sundal et al.*, 2009). Previous studies have shown that the immediate effect of lake drainage to the ice sheet bed is a short-term increase in horizontal and vertical ice velocities (*Das et al.*, 2008). A recent study (*Bartholomew et al.*, 2010) indicates further that the net effect of meltwater delivery to the ice-bed interface of the GrIS is an increase in annual ice velocity compared with winter background rates. Drainage of supraglacial lakes has the potential, therefore, to create a positive relationship between GrIS dynamic mass loss and surface melting, albeit one that is moderated by resultant variations in the structure of the drainage system (*Pimentel and Flowers*, 2011; *Truffer et al.*, 2005).

5.6 Conclusions

Our observations provide the first synopsis of the seasonal hydrological behaviour from a large (>600 km^2) catchment in the ablation zone of the GrIS, showing how surface meltwater production drives spatial and temporal changes in the subglacial drainage system. They attest to the development and expansion of a hydrological system that

delivers water from the ice surface, via the ice-sheet bed, to the margin. This system expands progressively throughout the ablation season to >50 km from the ice margin. We propose that the model is similar to Alpine systems where the drainage system becomes increasingly efficient as hydraulic connections between the surface and bed are established further inland, evacuating large volumes of meltwater and sediment. Supraglacial lake drainage events appear to play a key role in establishing hydraulic connections between the ice sheet surface and bed, helping to drive evolution of the subglacial drainage system. Lake drainage events may be especially important at higher elevations where stronger forcing is required to overcome greater overburden pressures associated with thicker ice.

5.7 Supplementary material

5.7.1 Degree-day melt model

We used a temperature-melt index model (*Hock*, 2003) to predict volumes of meltwater generated at the ice-sheet surface within an estimated catchment that drains from Leverett glacier. The catchment was derived from a surface digital elevation model with a spatial resolution of 100 m (Figure 5.1).

Air temperatures were measured continuously at 7 sites throughout the survey period (Figure 5.1). We used Campbell T107 temperature sensors, which were mounted in radiation shields and connected to a Campbell CR800 datalogger at 4 sites and Onset HOBO U21-004 temperature sensors at the remaining three. Degree-day factors (DDFs) for snow and ice were then derived at 2 sites using continuous measurements of ablation from a sonic ranging device. At the five additional sites, seasonal ablation was measured against stakes, producing DDFs for both snow and ice across a range of elevations.

We estimated an elevation-dependent initial snow depth based on measurements made at each temperature recording site just prior to the onset of the melt season. The model was then run using an hourly timestep to calculate the surface melt rate by elevation band using the temperature data as a forcing signal. This melt was multiplied by the area of the catchment within each elevation band to estimate total runoff volume at each timestep.

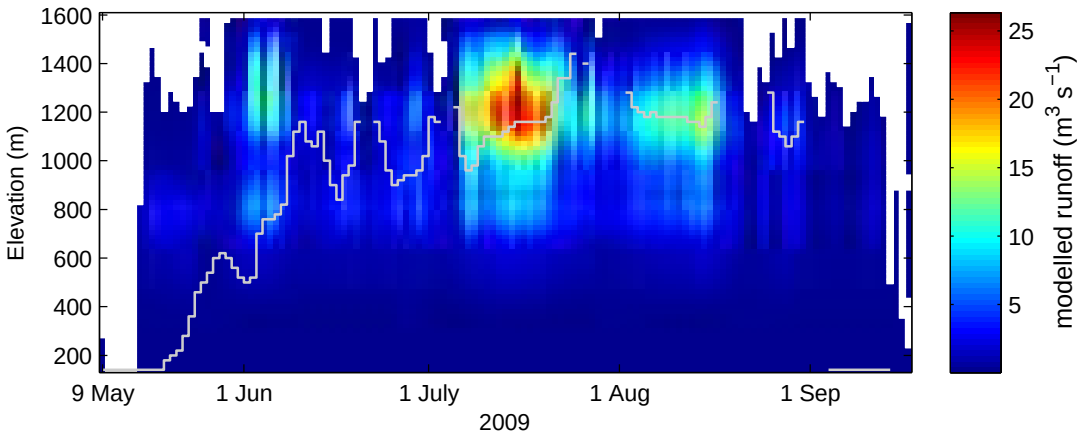

Figure 5.4: Predicted runoff volume by elevation (at 20 m intervals) for each day of the survey period using a simple temperature-index model (i.e. the melt rate (m s^{-1}) multiplied by the catchment area (m^2) at that elevation). White sections did not experience melting. The runoff rate for the whole catchment can be calculated by integration of each column of the plot. The white line indicates the elevation below which the modelled runoff produced is equal to the discharge observed at Leverett Glacier. The lags caused by sharp drops in air temperature and the resulting drop in discharge at Leverett Glacier are not captured by the simple model and cause short-term increases in the apparent catchment extent to unrealistic elevations and these values have been removed from the figure.

Figure 5.4 shows modelled runoff volume by elevation for each day of the survey period (i.e. the melt rate (m s^{-1}) multiplied by the catchment area (m^2) at that elevation). White sections did not experience melting. The runoff rate for the whole catchment can then be calculated by integration of each column of the plot. The white line indicates the elevation below which the modelled runoff produced is equal to the observed discharge record (Figure 5.2). It is clear from Figure 5.4 that we are unable to account for the discharge observed at Leverett glacier without progressive upglacier expansion of the catchment to include runoff from higher elevations through the melt season.

This analysis rests on the assumption that discrepancy between modelled melt values and the observed discharge at each timestep indicates the size of the catchment that drains through Leverett Glacier. Interpretation of the model results is complicated, however, by a number of factors. Firstly, very little of the initially predicted runoff (e.g. May and early June) emerges from the glacier immediately following melt. This result suggests that early in the season meltwater percolates and refreezes in the cold snowpack and actual runoff of meltwater from a particular site will only start once

the whole of the snowpack is isothermal (*Pfeffer et al.*, 1991). Secondly, we assume that there is zero delay between runoff production and meltwaters emerging from the glacier snout. In reality there is a lag due to supraglacial, englacial and subglacial travel times (which are likely to reduce over the season) as well as supraglacial storage of meltwater in crevasses and lakes. This is particularly clear when runoff exceeds total melt due to lake drainage event (Figure 5.2), or continued release of water after sudden cooling. Smaller errors may be introduced, however, when the discrepancy is less striking. Thirdly, the lateral boundaries of the catchment are derived from surface elevation data (*Palmer et al.*, 2008, 2011), while the direction of meltwater flow within a glacier is also governed by bed topography (*Shreve*, 1972).

Discrepancies between modelled runoff and observed discharge have the potential to provide important information about development of the subglacial drainage system. For example, a reduced lag between peak discharge and diurnal peaks in temperature would be indicative of more efficient transport of meltwater. Unfortunately, although the degree-day method has often been shown to be effective on catchment scales (e.g. *Hock*, 2003) its performance deteriorates with increasing temporal resolution. In addition, our crude method of distributing runoff by elevation band is unlikely to be accurate in representing spatial variability in melt rates, which may vary substantially due to topographic effects such as shading, slope and aspect (*Hock*, 2003).

In light of these uncertainties, defining the exact catchment area at any one time is approximate, and we cannot verify a precise figure. The value of 600 km^2 as the maximum summer extent represents our best estimate from the available data. The results are useful, however, in support of observations from the hydrological and satellite data which demonstrate upglacier expansion of the contributing catchment through the melt season as water reaches the bed further inland.

5.7.2 Discussion of errors

Discharge

The discharge record was constructed using continuous measurements of stage in the proglacial stream which were calibrated against discrete measurements of river discharge

obtained using the dye-dilution method (*Kilpatrick and Cobb*, 1984). Uncertainty in the estimates of river discharge results from error in the discharge measurements themselves and error introduced by the rating curve between the discharge measurements and water stage in the bedrock cross-section.

A nonlinear rating curve is widely used for stage-discharge relationships, and is justified by the shape of the cross section where the filled area grows in a nonlinear fashion as water depth increases (Figure 5.5). Since depth integrated flow velocity is also expected to become greater with water depth (*Richards*, 1982), a nonlinear rating curve performs significantly better than a linear one. Investigations of uncertainty in river discharge observations (e.g. *Di Baldassarre and Montanari*, 2009), indicate that appropriate rating curves can be found using power law or exponential relationships. Both these performed better than other types that we tested (e.g. linear or polynomial) and when applied, the power law fit provided the best option for our data (r^2=0.85, compared with r^2=0.79 for an exponential fit, n=29; Figure 5.6).

Uncertainty induced in the calculated discharge record by application of the rating curve is due to: interpolation and extrapolation of the modeled values, unsteady flow conditions, and changes in river roughness throughout the survey period (*Di Baldassarre and Montanari*, 2009). Given the lack of vegetation and the use of a bedrock cross-section, changes in roughness during the season are likely small (*Richards*, 1982) and this uncertainty is therefore negligible. In addition, discharge was measured across the full range of observed stage meaning that we have no need to extrapolate discharge values. Measurements of stage were made using a Druck pressure tranducer connected to a Campbell CR1000 datalogger and the errors in these measurements are small (±1-2 cm on a stage depth ranging up to 6 m). Therefore, uncertainties due to application of the rating curve are primarily due to a combination of interpolation errors and the effect of unsteady flow conditions.

Calculation of the different components of error induced by application of the rating curve would require use of a hydrological model and is beyond the realistic scope of this investigation. A crude estimate of the error is therefore achieved by calculating the root mean square difference (rmsd) between the observed and fitted discharge estimates. This effectively lumps the components discussed in the previous paragraph

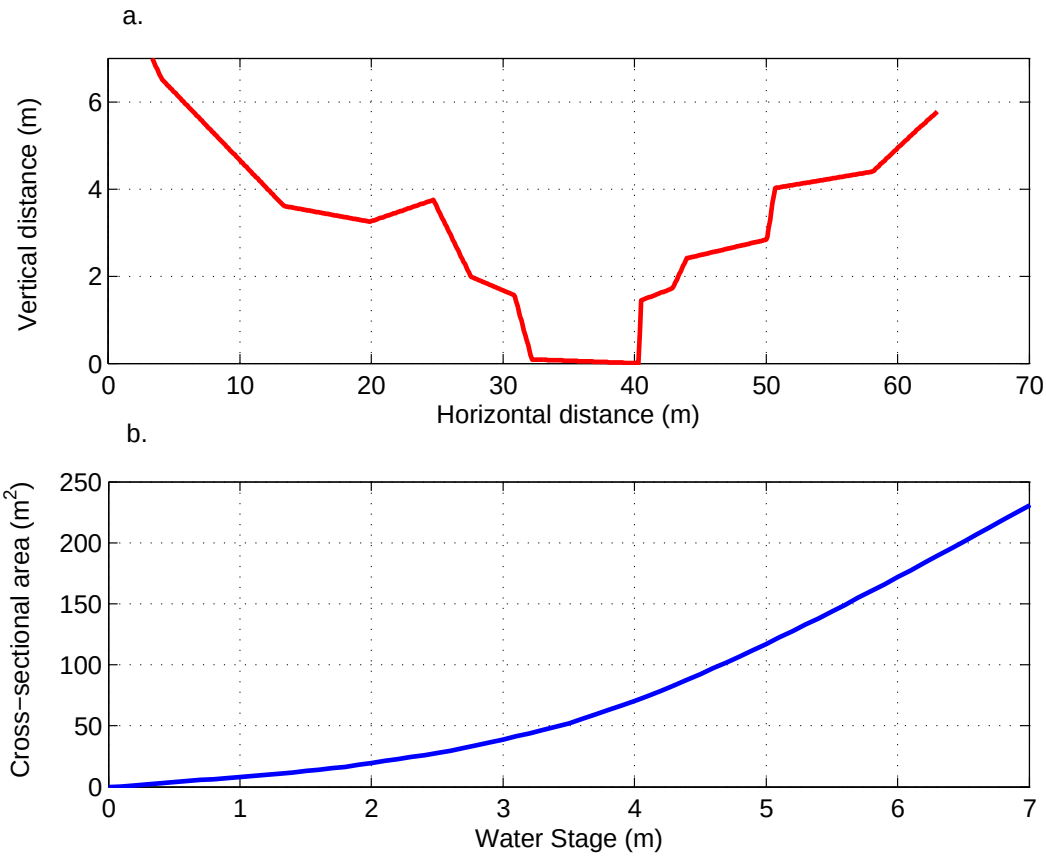

Figure 5.5: a. River cross-section at gauging site. b. Filled cross-sectional area vs. water depth for the cross-section

into a single term. We express this uncertainty as a normalised root mean square difference (nrmsd) between the modelled and measured discharge. The rmsd between the discharge measurements and the power law rating curve is 40.1 m^3s^{-1} (as opposed to 48.6 m^3s^{-1} for the exponential fit), and the nrmsd (expressed as a percentage) is 10.4%.

Discharge estimates were made using the dye-dilution method (e.g. *Kilpatrick and Cobb*, 1984; *Rantz*, 1982; *Hubbard and Glasser*, 2005). A known quantity of fluorescent Rhodamine dye was manually injected into the stream in a single pulse. Dye concentration was then measured at a downstream location using a Turner Designs CYCLOPS-7 Submersible Fluorometer attached to a Campbell CR800 datalogger and used to estimate discharge according to the conservation of mass.

The main sources of error in dye dilution gauging are due to:

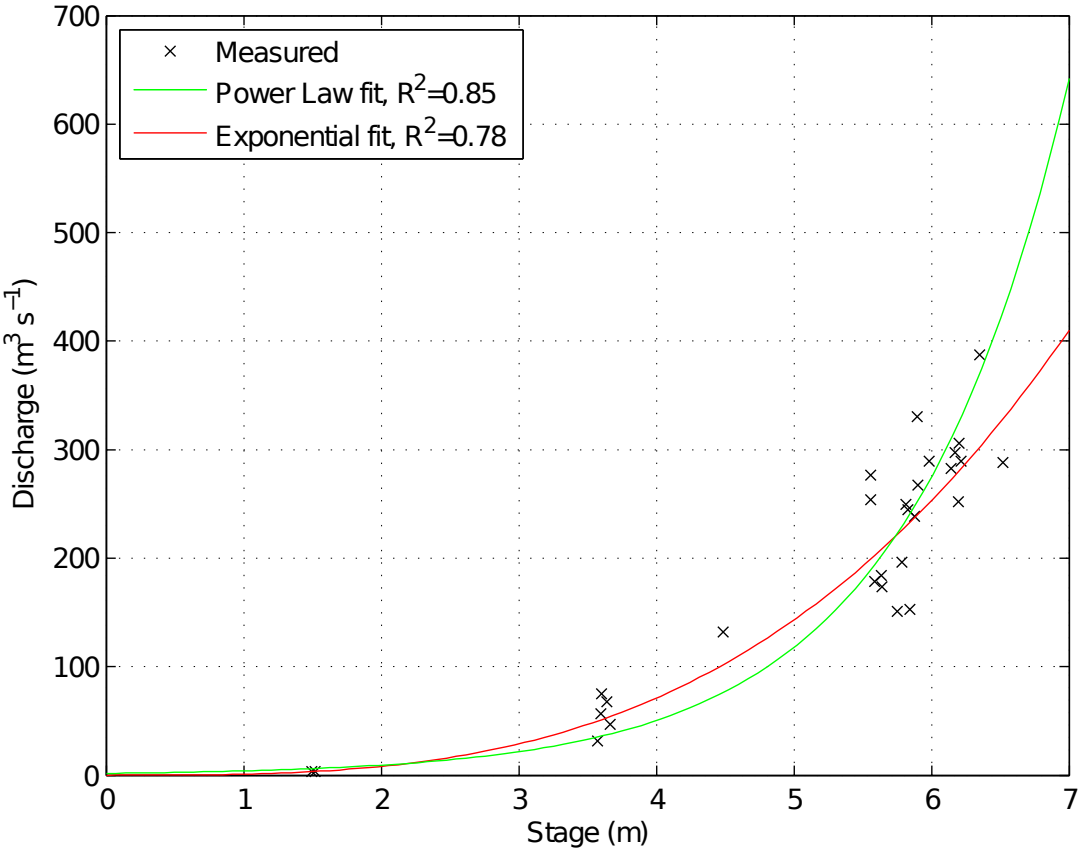

Figure 5.6: Stage-discharge rating curve

i. Assumption of complete mixing of dye within the channel. The tests were made in a reach with a single turbulent channel of approximately 1 km. Dye was injected above, and sampled below, a waterfall to ensure complete mixing. This was confirmed by a test where dye was injected from each side of the channel within a short time period, which produced the same dye concentrations (and 'area under the curve') at the sample site.

ii. Fluorescence of suspended sediment at a similar wavelength to the dye. This resulted in background fluorescence for each tracer test which was related to turbidity. This was removed by recording for 10 minutes before and after each dye test in order to measure the background fluorescence, which was removed in subsequent processing. Repeat calibrations of river water with known concentrations of dye but on different days (and therefore with different sediment concentrations) showed that the calibration slope was not affected by turbidity

and that an offset is effective in minimising this background signal.

iii. Loss of dye along the reach. Tracer losses are primarily due to sorption and chemical reaction between the tracer and one or more of the following: streambed material, suspended sediments, dissolved material in the river water, plants, and other organisms. These errors were minimised by use of Rhodamine WT, which is known to adsorb onto suspended sediment less than other fluorescent dyes (Smart and Laidlaw, 1977). We note that significant loss of tracer would cause measured dye concentrations to be reduced, resulting in an overestimate of discharge.

Other sources of error include measurement of the volume of tracer used and calibration and resolution of the fluorometer (which was repeated at intervals throughout the season using water from the river with standards of known concentration). Although dye-dilution gauging is an established technique for measuring streamflow, there are very few estimates for its accuracy in the literature. *Herschy* (1995) suggests a figure of ± 5 % while information from the fluorometer manufacturer suggests that uncertainties are ± 2 % (*Turner Designs Inc.*, 2011).

Without an independent measure of discharge we are unable to verify the accuracy of our discharge measurements. However, based on repeatability of traces which were done within a short time of each other (less than an hour) at high rates of discharge, a conservative estimate is ± 10%.

We assume that the error due to uncertainty in the discharge measurements and from the rating curve are independent (Di Baldassare & Montanari, 2009) and compute the total error in the discharge from the quadratic sum as follows:

$$\begin{aligned}\text{Discharge error} &= \sqrt{(\text{rating curve error})^2 + (\text{discharge measurement error})^2} \\ &= \sqrt{10.4^2 + 10^2} \\ &= \pm 14.5\%\end{aligned}$$

Suspended sediment

Turbidity was measured continuously in the proglacial stream using a Partech IR15C turbidity meter connected to a Campbell CR1000 datalogger (*Clifford et al.*, 1995b).

Suspended sediment samples were collected manually on 50 occasions from the vicinity of the turbidity probe using a USDH-48 depth-integrating suspended sediment sampler. The samples were filtered in the field with 0.2 m filter papers following the procedure laid out by *Hubbard and Glasser* (2005), and the volume of filtrate was measured in a measuring cylinder. The samples were stored and returned to a lab for drying and weighing in order to calculate suspended sediment concentration.

Given the high precision and accuracy of a mass balance and the routine nature of the field sampling, errors in the suspended sediment sampling are likely to be small (taken here to be less than 2%).

The greatest error is that induced by application of a relationship between measured turbidity and suspended sediment concentration. Uncertainty is minimised by calibration of the turbidity record with field samples rather than in a laboratory. Following a similar procedure that that for the discharge rating curve, the rmsd in the ssc vs turbidity record is 1.07 kg m^{-3}, and the nrmsd is 6.2 %.

$$\begin{aligned}\text{SSC error} &= \sqrt{(\text{SSC vs. turbidity relationship error})^2 + (\text{SSC measurement error})^2} \\ &= \sqrt{6.2^2 + 2^2} \\ &= \pm 6.5\%\end{aligned}$$

Uncertainty in suspended sediment load (SSL) is due to error in both discharge and suspended sediment concentration. We therefore compute this error as follows:

$$\begin{aligned}\text{SSL error} &= \sqrt{(\text{SSC error})^2 + (\text{discharge error})^2} \\ &= \sqrt{6.5^2 + 14.5^2} \\ &= \pm 15.9\%\end{aligned}$$

Measurements of turbidity in glacial meltwater streams are subject to significant variation across a range of timescales (*Clifford et al.*, 1995a). Over a diurnal cycle, SSC is partly controlled by rates of glacier melting and daily peaks in discharge are associated with increased sediment concentration (*Richards*, 1984; *Clifford et al.*, 1995a). In our dataset this is particularly the case when the subglacial system is well developed (Figure 5.2; *Swift et al.*, 2005). Daily cycles of suspended sediment concentration also contain short-term, pseudo-periodic fluctuations that are not directly related to discharge. *Clifford et al.* (1995a) argue that fluctuations over timescales of 10 - 30 minutes may be associated with channel bank collapse or migration of the proglacial stream, contributing 5 - 30 % of the total daily range in an Alpine glacier setting. On even shorter timescales, variability in SSC is caused by turbulent velocity fluctuations, which may be on the order of $\sim$0.1 kg m^{-3} (*Clifford et al.*, 1995a).

In order to minimise the impact of short-term variability on our record of SSC, measurements were made continuously at 30s intervals over the entire survey period. This allowed us to reliably capture diurnal variability in SSC and the seasonal signal, as well as sudden short-term fluctuations such as those associated with large meltwater pulses (Figure 5.2).

The major impact of short-term fluctuations in SSC on our dataset is most likely in the uncertainty added to calibration of the turbidity record against manual sediment samples. In addition to temporal variability, there is also likely to be significant lateral and vertical variation in SSC within the proglacial stream. We collected depth-integrated meltwater samples using a USDH-48 sediment sampler which was lowered through the water column. While this helps capture vertical variation in the sediment sample, turbidity was measured at a fixed height. This discrepancy is incorporated in the uncertainty estimates described above, however, lateral variability in SSC across the river section cannot be captured as the exceptionally high discharges made sampling further out into the channel impracticable.

A second turbidity sensor, placed within 50 m of the glacier snout between 11th July and 16th August to test the reliability of the downstream sampling site, generated the same pattern of SSC as at the cross-section with values that were $\sim$4% lower on average (r = 0.98, *Cowton et al.*, in review). This observation indicates, therefore, that the SSC

record we have derived is representative of the patterns in sediment transport from beneath Leverett Glacier on the relevant timescales within reasonable error estimates.

CHAPTER 6

Seasonal variations in Greenland Ice Sheet motion: inland extent and behaviour at higher elevations

The data in chapters 4 and 5 showed that the subglacial drainage system of Leverett Glacier develops to become more efficient over the course of a summer melt season, limiting the impact of summer velocity variations on ice motion at sites up to ∼35 km from the ice sheet margin. These and similar findings lead some authors to suggest that ice in Greenland might flow more slowly in a warmer climate (e.g. *Van de Wal et al.*, 2008; *Schoof*, 2010; *Pimentel and Flowers*, 2011; *Sundal et al.*, 2011). Their hypothesis suggests that higher rates of meltwater input to the ice sheet bed will cause the drainage system to become channelised more rapidly and that ice velocity will therefore be reduced earlier in the summer, leading to lower seasonal mean ice velocity. However, such an argument ignores the spatial aspect of this problem. Firstly, in a warmer climate a larger area of the ice sheet will experience summer melting and we

would expect changes in ice velocity to occur further inland. Secondly, it is not clear that patterns in hydrologically-forced dynamic behaviour observed near the ice sheet margin are replicated at higher elevations where the ice sheet is both thicker and colder.

In this chapter we present ice velocity data from the GPS transect in 2009, which had been extended up to ∼115 km from the ice sheet margin. These data capture, for the first time over a full melt season, the full inland extent of summer ice velocity variations in a land-terminating section of the Greenland Ice Sheet. This allows us to investigate the full impact of summer velocity changes on rates of mass loss from this part of the ice sheet. In addition, by comparing the GPS velocity records with observations of air temperature, proglacial discharge and lake drainage events, we can examine the controls on hydrological forcing of ice motion at higher elevation sites.

Published in **Earth and Planetary Science Letters**, July 2011.

Authors: Ian Bartholomew[1], Peter Nienow[1], Andrew Sole[1], Douglas Mair[2], Thomas Cowton[1], Matt A King[3] & Steven Palmer[4*]

1. School of Geosciences, University of Edinburgh, Drummond Street, Edinburgh, EH8 9XP, UK
2. School of Geosciences, University of Aberdeen, Aberdeen, AB24 3UF, UK
3. School of Civil Engineering and Geosciences, Newcastle University, Newcastle upon Tyne, NE1 7RU, UK
4. School of Earth and Environment, University of Leeds, Leeds, LS2 9JT, UK

*now at Scott Polar Research Institute, University of Cambridge, Cambridge, CB2 1ER, UK

Citation: Bartholomew, I., P. Nienow, A. Sole, D. Mair, T. Cowton, S. Palmer, and M. King (2011), Seasonal variations in Greenland Ice Sheet motion: inland extent and behaviour at higher elevations, *Earth and Planetary Science Letters*, *307*, 271-278, doi:10.1016/j.epsl.2011.04.014.

Author contributions: IB, AS, PN, DM, and TC collected the data. IB processed

the GPS data for sites 1 - 6 and MAK processed the GPS data for site 7. IB analysed the data and wrote the manuscript. SP provided the surface digital elevation model used to determine snowline and lake drainage event elevations. All authors contributed to discussions of the paper during the writing process.

Abstract

We present global positioning system observations that capture the full inland extent of ice motion variations in 2009 along a transect in the west Greenland Ice Sheet margin. *In situ* measurements of air temperature and surface ablation, and satellite monitoring of ice surface albedo and supraglacial lake drainage are used to investigate hydrological controls on ice velocity changes. We find a strong positive correlation between rates of annual ablation and changes in annual ice motion along the transect, with sites nearest the ice sheet margin experiencing greater annual variations in ice motion (15 - 18 %) than those above 1000 m elevation (3 - 8 %). Patterns in the timing and rate of meltwater delivery to the ice-bed interface provide key controls on the magnitude of hydrologically-forced velocity variations at each site. In the lower ablation zone, the overall contribution of variations in ice motion to annual flow rates is limited by evolution in the structure of the subglacial drainage system. At sites in the upper ablation zone, a shorter period of summer melting and delayed establishment of a hydraulic connection between the ice sheet surface and its bed limit the timeframe for velocity variations to occur. Our data suggest that land-terminating sections of the Greenland Ice Sheet will experience increased dynamic mass loss in a warmer climate, as the behaviour that we observe in the lower ablation zone propagates further inland. Findings from this study provide a conceptual framework to understand the impact of hydrologically-forced velocity variations on the future mass balance of land-terminating sections of the Greenland Ice Sheet.

6.1 Introduction

Our ability to make robust predictions about the future mass balance of the Greenland Ice Sheet (GrIS), and therefore its contribution to sea-level change, is limited by uncertainty about how the dynamic component of mass loss (i.e. due to changes in ice motion) will respond to anticipated changes in atmospheric temperature (*IPCC*, 2007; *Pritchard et al.*, 2009). In land-terminating sections of the GrIS, variations in ice velocity are initiated when surface meltwater gains access to the ice-bed interface, lubricating basal motion (*Zwally et al.*, 2002; *Van de Wal et al.*, 2008; *Joughin et al.*,

2008a; *Shepherd et al.*, 2009; *Bartholomew et al.*, 2010). This effect is both widespread (*Joughin et al.*, 2008a; *Sundal et al.*, 2011) and persistent each summer (*Van de Wal et al.*, 2008; *Sundal et al.*, 2011; *Zwally et al.*, 2002) near the ice sheet margin. Initial observations show that summer velocities in land-terminating sections of the GrIS can be 50% faster than in winter (*Van de Wal et al.*, 2008; *Joughin et al.*, 2008a), and that summer velocity variations increase annual ice motion by 6 - 14 % in the lower ablation zone (*Bartholomew et al.*, 2010). A direct positive relationship between rates of surface melting and basal motion would create a mechanism to significantly increase rates of mass loss from the GrIS in a warming climate by drawing more ice to lower elevations where ablation rates are higher (*Parizek and Alley*, 2004). This process allows the dynamic component of the GrIS mass balance to respond to climatic variability within decades or less, yet is not considered in current sea-level projections made by the Intergovernmental Panel on Climate Change (IPCC).

Recent observations (*Bartholomew et al.*, 2010; *Sundal et al.*, 2011) and theoretical work (*Pimentel and Flowers*, 2011; *Schoof*, 2010) suggest, however, that the contribution of seasonal velocity variations to annual rates of ice motion at a particular site is limited by evolution in the structure of the subglacial drainage system. Each summer in the lower ablation zone, sustained inputs of meltwater from the ice sheet surface transform the subglacial hydrological system into an efficient network of channels that can evacuate large quantities of water rapidly (*Bartholomew et al.*, 2011a). This moderates the lubricating effect of meltwater on ice velocities by reducing the pressure within the hydrological system for a given volume of water (*Kamb*, 1987; *Van de Wal et al.*, 2008). It has been observed that late summer velocities near the GrIS margin are lower for a given intensity of surface melting than earlier in the season (*Bartholomew et al.*, 2010; *Sundal et al.*, 2011). As a result, it is not expected that increased annual ablation rates at a specific location will necessarily stimulate faster ice flow than at present; in this respect the process could be seen as self-limiting (*Van de Wal et al.*, 2008). By extension, it has been argued that summer, and therefore annual mean ice velocities at a given site on the GrIS could be *lower* in high ablation years than in low ablation years because channelisation of the subglacial hydrological system occurs more quickly (*Truffer et al.*, 2005; *Pimentel and Flowers*, 2011; *Sundal et al.*, 2011).

A key feature of hydrologically-forced velocity variations in the GrIS is also that they propagate inland from the ice sheet margin on a seasonal basis, in response to the onset of surface melting at successively higher elevations (*Bartholomew et al.*, 2010). The initiation of hydrologically-forced ice velocity variations is dependent on the development of a conduit from the ice sheet surface to allow surface meltwater to access the ice-bed interface. In a warmer climate we expect summer melting of the GrIS to be more intense, affecting a wider area for a longer time period than is currently the case (*Hanna et al.*, 2008), providing greater volumes of surface meltwater. The melt regime will be amplified because the hypsometry of the GrIS, which flattens inland, gives a non-linear expansion of the area of the GrIS experiencing melt in response to a rise in the equilibrium-line altitude (ELA). It is therefore possible that seasonal velocity variations in the GrIS will propagate further inland in response to climate warming. One mechanism to allow this is drainage of supraglacial lakes, which have the potential to concentrate surface meltwaters into large enough reservoirs to propagate fractures through ice that is >1000 m thick (*Alley et al.*, 2005b; *Das et al.*, 2008; *Krawczynski et al.*, 2009).

Current debates over whether increased melt rates across the GrIS will induce greater dynamic mass loss can therefore be reduced to whether increased mass loss due to inland propagation of velocity variations in warmer years will more than offset any potential reduction in mass loss due to earlier onset of channelisation in the lower ablation zone. However, uncertainty remains over the effect of increased meltwater production on dynamic behaviour in the lower ablation zone - observations to date do not show conclusively whether annual mean ice velocities will increase or decrease in a warmer climate (*Van de Wal et al.*, 2008; *Joughin et al.*, 2008a; *Bartholomew et al.*, 2010; *Sundal et al.*, 2011) and a more detailed understanding of the response of the subglacial drainage structure to large inputs of surface meltwater is required. In addition, while diurnal ice velocity variations have been observed up to 72 km from the GrIS margin in a short-term study (*Shepherd et al.*, 2009), it is not clear that patterns in hydrologically-forced dynamic behaviour observed near the ice sheet margin are replicated at higher elevations. While singular lake drainage events have been described in detail (*Das et al.*, 2008), it has not been shown that the integrated effect of

widespread meltwater generation and lake drainage (*McMillan et al.*, 2007; *Box and Ski*, 2007; *Sundal et al.*, 2009) is a significant and sustained increase in glacier flow speed at higher elevations.

A secondary effect of meltwater inputs to the glacier system on ice dynamics is 'cryo-hydrologic warming', whereby heat conduction from water within the englacial system causes ice temperatures to be raised (*Phillips et al.*, 2010). Increased temperatures will reduce ice viscosity and thus contribute to faster ice flow. It has been suggested that, in a warmer climate, drainage of meltwater into the ice sheet across a wider area will also cause a rapid thermal response in deep layers of the GrIS, compounding the effect of meltwater drainage on ice velocities (*Phillips et al.*, 2010).

The aim of this study is to provide a clearer understanding of the mechanisms which control the magnitude and extent of hydrologically-forced dynamic behaviour at elevations up to and beyond the current ELA *on a seasonal basis*. This is motivated by the need to incorporate these processes in numerical models which predict the future evolution of the GrIS and the current lack of comprehensive empirical data with which to inform them (*Parizek*, 2010). The thermal effect of meltwater, which affects ice deformation rates rather than basal motion, does not have a significant seasonal signal (*Phillips et al.*, 2010) and is not considered here.

We present continuous ice velocity measurements, derived from global position system (GPS) observations, that capture the full inland extent of seasonal velocity variations along a land-terminating transect at ∼67°N in western Greenland during the 2009 melt season (Figure 6.1). Measurements were made at seven sites up to 1716 m elevation, which is ∼115 km inland from the GrIS margin. The ice motion record is compared with *in situ* and satellite observations of air temperatures, surface melt characteristics and supraglacial lake evolution within the region of study, as well as with proglacial hydrological data (*Bartholomew et al.*, 2011a).

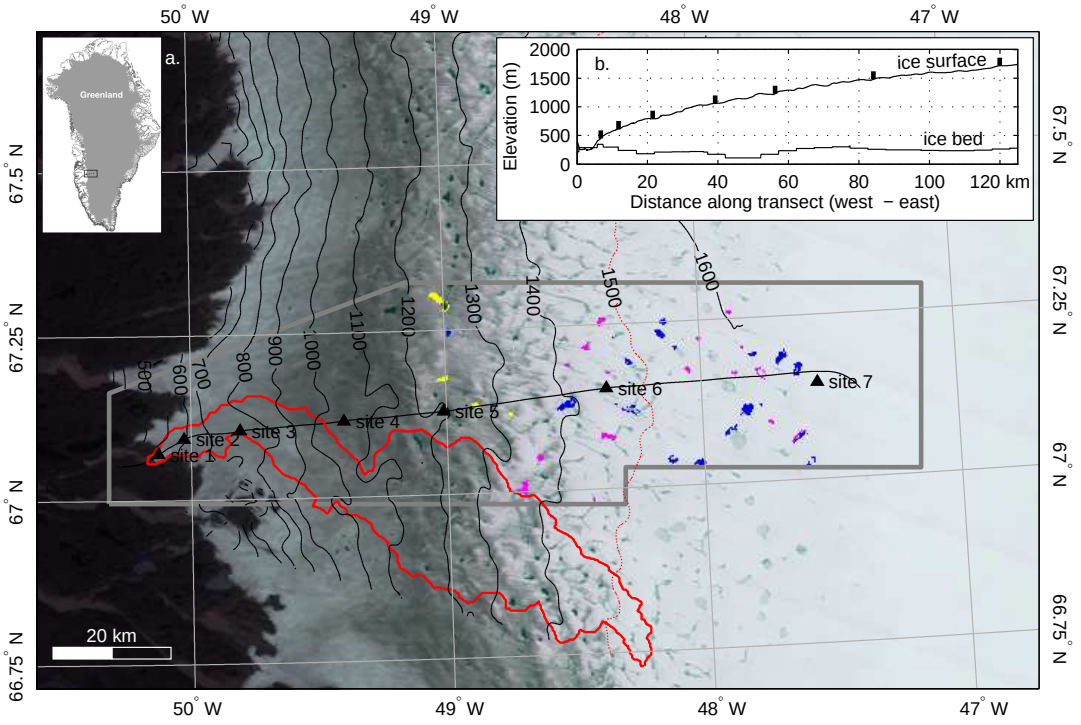

Figure 6.1: a. Location of the study region on the western margin of the GrIS. The GPS sites are located along a transect across an altitudinal range of 450 - 1700 m a.s.l. Simultaneous measurements of air temperature and seasonal measurements of ablation were made at each site. The ELA in this region is at 1500 m (*Van de Wal et al.*, 2005). Contours are produced from a digital elevation model derived from InSAR (*Palmer et al.*, 2011) at 100 m intervals. Lakes which drain in the interval between sequential MODIS satellite images during the survey period are denoted by coloured patches which represent their surface area immediately prior to drainage (yellow: July 11th-15th; red: July 19th-23rd; blue: July 26th-29th). The region in which lake drainage events were monitored is enclosed by the grey box and the catchment of the river which drains through Leverett glacier and which was also monitored in 2009 is shown in red (*Bartholomew et al.*, 2011a). b. Ice surface (*Krabill*, 2010) and bed elevation (*Bamber et al.*, 2001) profiles along the transect (black line, main figure). The locations of the GPS sites are shown by black vertical marks.

6.2 Data and methods

6.2.1 GPS data

We used dual-frequency Leica 500 and 1200 series GPS receivers to collect the season long records of ice motion at each site. Each GPS antenna was mounted on a pole drilled several metres into the ice, which froze in subsequently, providing measurements of ice motion that were independent of ablation. The GPS receivers collected data at 30 second intervals that were processed using a kinematic approach relative to an off-ice base station (*King*, 2004) using the Track 1.21 software (*Chen*, 1999; *King and*

Bock, 2006). Conservative estimates of the uncertainty associated with positioning at each epoch are approximately ± 1 cm in the horizontal direction and ± 2 cm in the vertical direction. The data were smoothed using a Gaussian low-pass filter to suppress high-frequency noise without distorting the long-term signal. Daily horizontal velocities reported in this paper (Figure 6.2a-g) are calculated by differencing the filtered positions every 24 hours. Shorter-term variations in ice velocity were derived by differencing positions across a 6 hour sliding window, applied to the whole timeseries of filtered positions for each site. This window length was chosen in order to highlight short-term variations in the velocity records while retaining a high signal to noise ratio. Estimates of the magnitude of daily cylces in horizontal velocity are therefore minimum estimates. Unfortunately, the quality of the GPS data at site 1 was compromised by technical problems, and we are unable to resolve short-term variations in horizontal velocity at this site.

Uncertainties associated with the filtered positions are <0.5 cm in the horizontal and <1 cm in the vertical directions, corresponding to annual horizontal velocity uncertainties of <3.7 m yr^{-1} and <14.6 m yr^{-1} for the 24 hour and 6 hour velocity measurements respectively. We used the standard deviation of 24 hour and 6 hour sliding window velocities from site 7, which has the longest processing baseline and experienced negligible velocity variations, to estimate the noise floor in the GPS velocity records. The standard deviations for 24 hour and 6 hour velocities at site 7 are 5.6 m yr^{-1} and 19.5 m yr^{-1} respectively. These values compare well with the calculated uncertainties and represent conservative error estimates for our dataset.

The values for winter background ice-velocities are derived from the displacement of each GPS receiver between the end of the summer melt season and the following spring (*Bartholomew et al.*, 2010). The reported contribution to annual ice flux from the hydrologically-forced summer ice velocity variations is the percentage by which the observed annual displacement exceeds that which would occur if the ice moved at winter rates all year round.

6.2.2 Air temperate and surface ablation

Simultaneous measurements of air temperature were made at each GPS site to constrain melt rates, and show that the velocity data cover the whole seasonal melt cycle. Measurements of air temperature were made using shielded Campbell Scientific T107 temperature sensors connected to Campbell Scientific CR800 dataloggers (sites 1, 3 and 6) and shielded HOBO U21-004 temperature sensors (sites 2, 4, 5 and 7) at 15 minute intervals throughout the survey period. Seasonal melt totals were also measured using ablation stakes at each GPS site.

6.2.3 Proglacial discharge

We made continuous measurements of water stage in the proglacial stream that emerges from the terminus of Leverett Glacier. Proglacial discharge was derived from a continuous stage-discharge rating curve calibrated with repeat dye dilution gauging experiments throughout the melt-season as described in detail in *Bartholomew et al.* (2011a).

6.2.4 Supraglacial lake evolution

We used satellite observations from the Moderate-resolution Imaging Spectroradiometer (MODIS) to study the development of supraglacial lakes within the region of our GPS transect (Figure 6.1; delimited by the grey line). 20 MODIS images, spanning the period 31st May to 18th August 2009, were used, representing all the days when lake identification was not impeded by cloud cover. MODIS level 1B Calibrated Radiances (MOD02) were processed and projected as 250 m resolution true colour images in conjunction with the MODIS Geolocation product (MOD03), according to the methodology laid out by *Gumley et al.* (2003); see also *Box and Ski* (2007), and *Sundal et al.* (2009). Lakes were digitised manually in order to allow classification even on days of partial or thin cloud cover, producing a dataset with slightly higher temporal resolution than fully automated classification (*Sundal et al.*, 2009). Drainage events were identified as occasions on which the area of a lake decreased to zero (or a very small fraction of its former size) without an intermediate period of refilling. Previous studies have found that MODIS classification of GrIS supraglacial lakes is robust when

compared with higher resolution satellite data (*Sundal et al.*, 2009) and has approximate error of 0.22 km^2 per lake. However, since the lakes within this region are relatively small (typically <1 km^2) and there is considerable uncertainty in using a depth-retrieval algorithm to determine the depth of individual lakes (*Box and Ski*, 2007) we do not estimate individual lake volume. We note, however, that on the basis of a recent theoretical study of supraglacial lake drainage in the western GrIS (*Krawczynski et al.*, 2009), any lake which is large enough to be resolved on MODIS images (theoretically one 250m x 250m pixel (0.0625 km^2)) will contain enough water to drive a water-filled crack through 1 km of ice.

6.2.5 Ice sheet surface characteristics

We used the MYD10A1 1-day albedo product, part of the MODIS Aqua snow cover daily L3 global 500 m gridded product (*Hall and Salomonson*, 2009; *Hall et al.*, 2009), to map changes in the albedo of the ice sheet surface in this region of the GrIS through the survey period. These data are used to quantify the lowering of surface albedo associated with meltwater generation and retreat of the seasonal snowline through the survey period. This product provides albedo values for pixels identified as cloud free and snow-covered on a 500m grid derived from a snapshot taken once per day (*Stroeve et al.*, 2006). We used 70 days of data, from April 22nd to September 20th, representing all the days on which the image was not obscured by cloud cover. This time period covers the whole melt season, from before the onset of melt at the ice sheet margin in spring, to the period of refreezing and snowfall in the autumn. In order to integrate the albedo characteristics across the region surrounding the transect, mean albedo was calculated by 50 m elevation bands in the study region using a surface digital elevation model (*Palmer et al.*, 2011). Albedo thresholds for snow (<0.45) and bare ice (>0.66) surfaces were used to classify pixels on the basis of field observations along the nearby K-transect (*Knap and Oerlemans*, 1996). A resulting transitional band between the two zones is assumed to comprise a mixture of snow, ice with surface water and slush surfaces and broadly delimits the transient snowline (*Knap and Oerlemans*, 1996).

6.3 Hydrological forcing of velocity variations

Sites 1 - 6 all experience velocity peaks that are over 100 % higher than their winter background values (Figure 6.2a-f). These variations begin nearest the margin on May 22nd, and propagate inland following the onset of surface melting up to a distance of 80 km from the GrIS margin in late July, at 1482 m elevation. Initial uplift of the ice sheet surface at each of these sites is interpreted to signal the establishment of a local hydraulic connection to the ice sheet bed (*Iken et al.*, 1983; *Zwally et al.*, 2002; *Das et al.*, 2008; *Anderson et al.*, 2004; *Bartholomew et al.*, 2010). A high-velocity 'spring-event', accompanied by uplift of the ice sheet surface, characterises the start of locally-forced velocity variations at each of these sites in a manner similar to Alpine and High Arctic glaciers (*Iken et al.*, 1983; *Iken and Bindschadler*, 1986; *Mair et al.*, 2001; *Bingham et al.*, 2008). This behaviour is consistent with inputs of meltwater to a subglacial hydrological system which is incapable of accommodating them without a great increase in pressure (*Röthlisberger and Lang*, 1987; *Iken et al.*, 1983; *Iken and Bindschadler*, 1986; *Hooke et al.*, 1989; *Mair et al.*, 2001).

Although a small component of the coincident vertical and horizontal velocity changes is due to thickness changes resulting from longitudinal strain-rate or stress-gradient coupling, the signals we observe cannot be attributed to these effects alone. Based on motion of adjacent sites and ice thickness data (Figure 6.1b; *Bamber et al.*, 2001; *Krabill*, 2010), we calculate that the thickness changes originating due to longitudinal coupling are approximately an order of magnitude smaller than the elevation changes we have recorded. They also typically operate in the opposite direction as acceleration of downstream sites causes extension and thinning of ice upstream as opposed to the uplift observed. Throughout the summer, further speed-up events which are coincident with ice surface uplift confirm the role of surface generated meltwater in forcing seasonal changes in ice motion for this section of the GrIS. We also note that the evidence for hydraulically-forced enhanced basal motion implies that basal temperatures along this transect are at the pressure melting point.

Immediately prior to the spring events most sites also experience a short period of increased velocity in the absence of uplift of the ice surface, which we attribute to

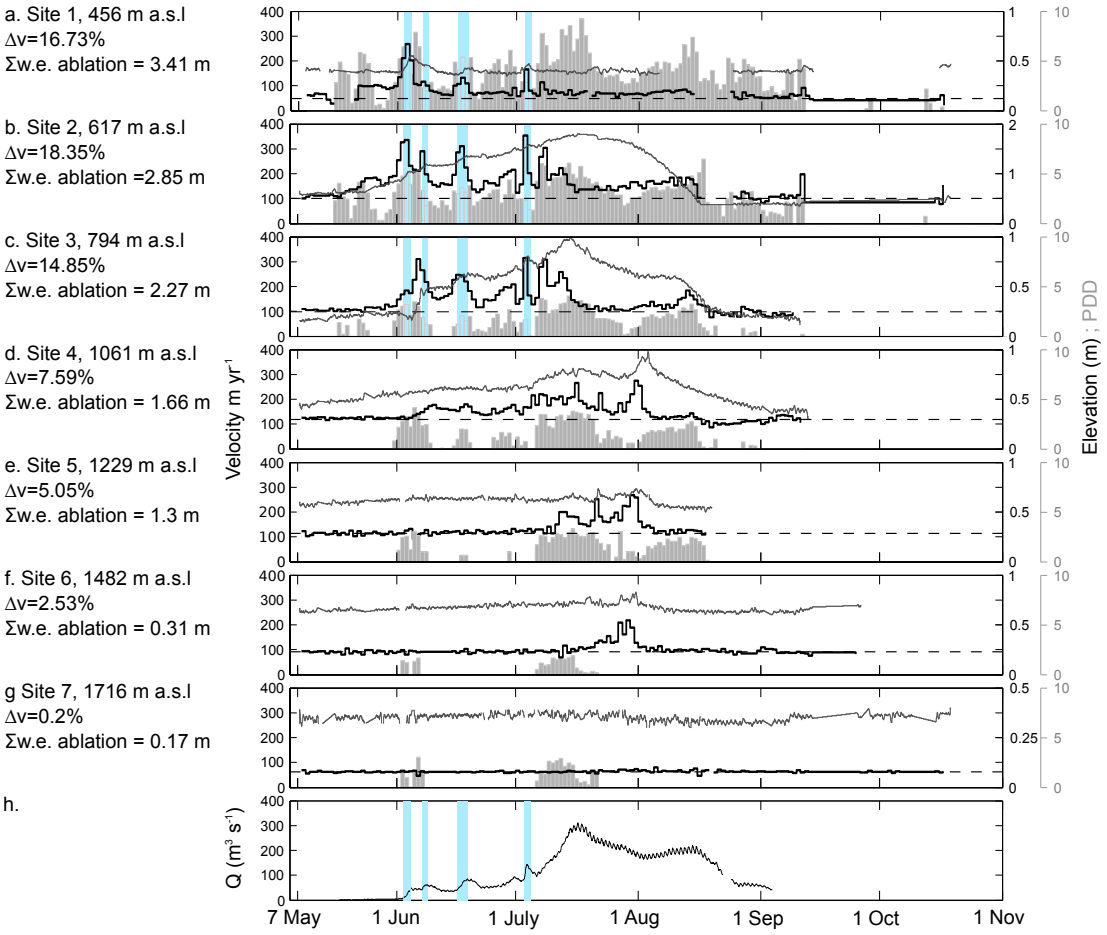

Figure 6.2: a-g. 24-h horizontal velocity (black stairs), surface height (grey line) and positive-degree days (grey bars) at sites 1-7 for the survey period. The surface height is shown relative to an arbitrary datum, with a linear, surface-parallel, slope removed. Winter background velocity (black dashes) is determined by bulk movement of each GPS site over the subsequent winter. Text to the left of each panel shows the elevation, percentage annual velocity change due to summer velocity variations compared with values if the ice moved at winter rates all year and the total surface ablation in water equivalence at each site for the whole survey period. h. Discharge hydrograph (black; m^3s^{-1}) from Leverett Glacier in 2009. The estimated catchment for this outflow channel (*Bartholomew et al.*, 2011a) is shown on Figure 6.1 and contains GPS sites 1, 2 and 3. The blue shaded sections identify pulses of meltwater which are associated with dramatic reorganisation and expansion of the subglacial drainage system within the catchment.

mechanical coupling to ice downglacier that is already moving more quickly (*Price et al.*, 2008). At site 7, which is located at 1716 m elevation, 115 km from the margin, there is no surface uplift or significant ice acceleration indicating that surface generated meltwater did not penetrate to the bed this far inland (Figure 6.2g). Site 7 does display a small, but clear, change in horizontal velocity (Figure 6.3), however, which can likely be attributed to coupling to ice downstream. Since the magnitude of these changes is insignificant in terms of annual ice flux, site 7 delimits the inland extent of hydrologically

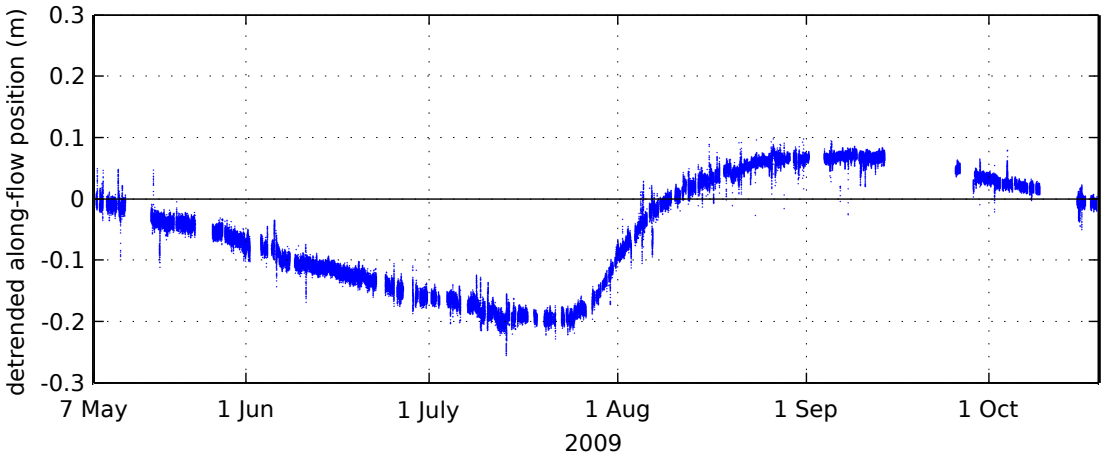

Figure 6.3: Detrended along-flow position for the GPS at site 7. The residual value indicates the observed distance in metres of the GPS from the expected position if it flowed at its mean rate for the whole survey period. Negative slopes therefore occur when the velocity is slower than the survey period average and *vice versa*.

forced velocity variations in 2009 for this transect.

6.3.1 Behaviour in the lower ablation zone

At sites 1 - 3, which are low in the ablation zone and experience the greatest acceleration, spring-events occur early in the melt-season, near the beginning of June, and ice velocity become less sensitive to air temperature variations as the melt season progresses (Figure 6.2). This behaviour is explained by evolution in the structure of the subglacial drainage system in response to sustained inputs of meltwater from the ice sheet surface, consistent with previous observations and predictions of dynamic behaviour in this section of the GrIS (*Bartholomew et al.*, 2010; *Pimentel and Flowers*, 2011).

A recent hydrological study (*Bartholomew et al.*, 2011a) supports the conclusion that evolution in the structure of the subglacial drainage system is responsible for limiting the magnitude of hydrologically-forced velocity variations at sites 1 - 3 later in the melt season. Observations of hydrological parameters from a catchment that drains through Leverett Glacier show that an efficient subglacial drainage system expands upglacier at the expense of an inefficient one as the summer progresses, a process that has been observed previously on Alpine glaciers (*Nienow et al.*, 1998). Episodic increases in the runoff hydrograph (Figure 6.2h), which are interpreted as evidence for dramatic re-organisation and expansion of the subglacial drainage system in response to new

inputs of meltwater from the ice sheet surface, have a clear short-lived effect on the velocity records at sites 1, 2 and 3 (Figure 6.2a-c,h). These events indicate, firstly, that sites 1 - 3 are within the hydrological catchment of the river and, secondly, that changes in the subglacial drainage system have a direct impact on ice velocity downglacier from where they initially occur. The large volumes of water exceed the capacity of the subglacial drainage system, causing pressurisation, and a concomitant reduction in basal drag (*Iken and Bindschadler*, 1986), as the water is transported to the ice sheet margin.

Clear daily-cycles in horizontal velocity occur at sites 2 and 3 following the spring events, and persist until mid-August. The magnitude of these cycles is typically between 100 and 150 % of the mean daily velocity, and can be over 200 % of winter background velocity during periods of significantly enhanced motion (Figure 6.4). Their existence indicates that over-pressurisation of the subglacial drainage system also happens regularly on diurnal timescales. The daily cycles in ice velocity appear to be closely related to variations in air temperature, with a typical lag between peak temperature and peak velocity of less than 3 hours, suggesting that they occur in direct response to diurnal variations in meltwater production at the ice sheet surface and that surface and englacial transit times are short (*Shepherd et al.*, 2009).

In addition to these short-lived events, ice velocities at sites 1, 2 and 3 are higher on the rising limb of the seasonal runoff hydrograph for Leverett Glacier, subdued following peak discharge on July 21st, and display a return to winter background rates in late August, when runoff is diminishing (Figure 6.2a-c,h). 'Slower than winter' ice velocities are also observed for a short period at some sites once the summer melt has stopped, however this signal is not large enough to have a significant impact on rates of annual ice motion.

These findings from the lower ablation zone can be explained in physical terms. Although increased efficiency of the subglacial hydrological system reduces the dynamic response to absolute water input volume (*Bartholomew et al.*, 2010), lake drainage and other singular high velocity events, as well as diurnal fluctuations in horizontal velocity testify that the system can still be overfilled by a large enough increase in meltwater input, causing an increase in subglacial water pressure (*Das et al.*, 2008; *Shepherd et al.*,

Figure 6.4: a. Daily cycles in horizontal ice velocities at sites 2 (blue) and 3 (magenta) for $\sim$ 3 weeks in late-July/early-August. 24-hour mean velocities are shown by black stairs and coloured lines indicate winter background velocities. b. Temperature record for sites 2 (blue) and 3 (magenta) for the same period.

2009; *Pimentel and Flowers*, 2011; *Schoof*, 2010). Production of surface meltwater, and its delivery to the ice-bed interface, is inherently variable on timescales of hours, days, weeks and months. Since the capacity of the subglacial hydrological system reflects the balance between channel opening by melting of the channel walls, and closure due to deformation of the surrounding ice, and adjusts relatively slowly to changes in water flux (*Röthlisberger*, 1972; *Schoof*, 2010), the system never reaches steady-state. We argue, therefore, that once a conduit has been established to deliver surface meltwater to the glacier bed, large changes in the rate of meltwater delivery to the subglacial hydrological system will continue to force velocity variations.

This analysis explains why high-velocity events at sites 1, 2 and 3 occur on the rising limb of the discharge hydrograph, when the system is continuously challenged to evacuate larger and larger volumes of water. Later in the season, when a channelised

drainage system has been established, and volumes of meltwater are diminishing, the drainage system is better able to evacuate meltwater without overfilling, explaining the reduction in magnitude of hydrologically-forced variations in ice motion. While ice velocities are subdued on the falling limb of the runoff hydrograph, velocities at sites 1 - 3 still exceed winter flow rates until mid-August. This appears to be the result of continued diurnal fluctuations in ice velocity (Figure 6.4), which occur until there is a dramatic reduction in runoff volumes at Leverett glacier after August 15th (*Bartholomew et al.*, 2011a).

6.3.2 Behaviour in the upper ablation zone

At sites 4 - 6, which are higher in the ablation zone (>1000 m), the relationship between changes in the rate of horizontal motion and the rate of uplift of the ice sheet surfaces indicates that the forcing mechanism is the same as in the lower ablation zone. Mapping of surface albedo using satellite data shows that the observed spring-events at these sites follow the onset of surface melting above their respective elevations (Figure 6.5), although both satellite and *in situ* observations showed that the snowpack was not fully removed at sites 5 and 6 by the end of the summer.

A key difference from the lower ablation zone is that the spring events occur later in the melt season (Figure 6.2a-g). There is also a significant time lag between the onset of surface melting, as inferred from both positive degree days (PDD's) and MODIS-derived albedo values, and the establishment of a hydraulic connection between the ice sheet surface and its bed as inferred from uplift of the ice surface. This means that significant velocity enhancement occurs for a much shorter time period than at lower elevations. At site 4, surface melting begins in early June, while coincident surface uplift and horizontal acceleration, which are diagnostic of local hydrological-forcing, are delayed until July 5th (Figure 6.2d). Increased velocities prior to this date, which occur without accompanying surface uplift, are explained by coupling to downglacier ice and are not as large as those induced by local forcing at the sites nearer the margin. *In situ* measurements of air temperature and satellite observations of surface albedo show that sites 5 and 6 both experience prolonged surface melting from July 6th onwards, and experience locally-forced velocity variations from July 12th and July 27th respectively

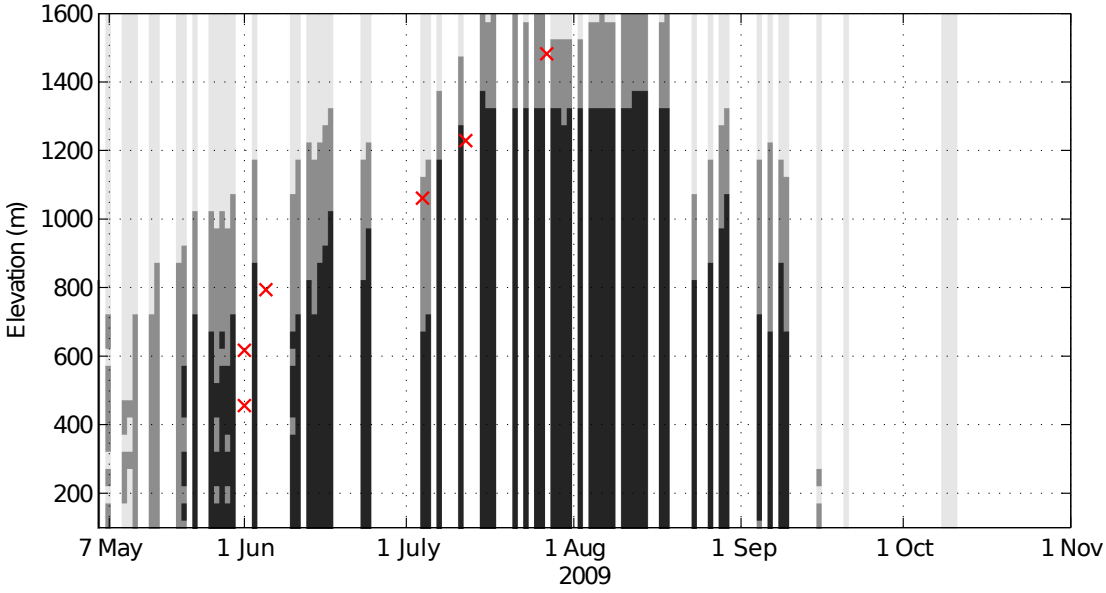

Figure 6.5: Ice sheet surface conditions inferred using the MODIS MYD10A1 1-day albedo product. Thresholds for bare ice (<0.45; black) and snow (>0.66; light grey) are used to delimit zones across the study region by elevation (y-axis) throughout the survey period (x-axis). A transitional zone (dark grey) is assumed to comprise a mixture of snow, slush, surface water and bare ice surfaces and broadly delimits the altitudinal extent of surface albedo changes caused by melting of the ice sheet surface (*Knap and Oerlemans*, 1996). The timing and elevation of the onset of hydrologically forced velocity variations, which occur at sites 1 - 6 successively, is denoted by red crosses.

(Figure 6.2e,f). Later spring events and the delay between the onset of surface melting and hydraulic connection between the ice surface and its bed are due in part to lower rates of surface melting. In addition greater volumes of water are required to propagate fractures through thicker ice (*Alley et al.*, 2005b; *Van der Veen*, 2007). These factors both increase the time required for the accumulation of sufficient volumes of meltwater to penetrate to the ice sheet bed.

Sites 4, 5 and 6 all experienced their highest velocities during a period of cooler temperatures from July 22nd to August 2nd (Figure 6.2d-f), suggesting that drainage of stored surface water was a key factor in these hydrologically-forced events. Satellite images show surface meltwater accumulation in supraglacial lakes in this region from mid-June at elevations between 1000 - 1200 m, and from 1200 m to >1600 m from early July. This storage of surface meltwater is made possible by relatively low surface gradients, which reduce the tendency for water to runoff to lower elevations (*Nienow and Hubbard*, 2006), and allows concentration of the large volumes of water required to

propagate fractures to the ice sheet bed through thick ice (*Das et al.*, 2008; *Box and Ski*, 2007; *McMillan et al.*, 2007; *Sundal et al.*, 2009).

Using MODIS imagery, we identify a number of events where changes in horizontal and vertical movement at one or more of our GPS sites is coincident with the disappearance of supraglacial lakes from the ice sheet surface. In particular, the spring event at site 5 on July 12th is coincident with disappearance of three supraglacial lakes from between 1200 - 1350 m elevation (Figure 6.1, yellow). Widespread drainage of supraglacial lakes at elevations up to 1500 m between July 19th - 23rd (Figure 6.1, red) corresponds with increases in ice velocity at sites 4 and 5 of up to 100 m y^{-1} on July 21st and 22nd respectively. The peak in horizontal velocities at sites 4, 5 and 6 at the end of July also coincides with drainage of a lake at $\sim$ 1400 m elevation and a number of lakes above $\sim$1500 m between July 26th and July 29th (Figure 6.1, blue). It is not possible to be certain, using optical imagery, that all lakes which disappear from the ice sheet surface drain directly into englacial conduits. For example, some lakes may drain superficially either into other lakes or to join with water input points that are already open further downglacier. However, the repeated coincidence of lake disappearance from the ice sheet surface with changes in ice velocities suggests strongly that a large number of these lakes drain to the ice-bed interface locally. Uplift of the ice surface indicates that this water is delivered to a subglacial drainage system which is unable to evacuate it without a large increase in water pressure, leading to the enhanced basal motion (*Das et al.*, 2008).

Drainage of supraglacial lakes therefore appears to be responsible for the initiation of hydrologically forced velocity variations at both sites 5 and 6. It is not clear that the spring event at site 4, on July 5th, is caused directly by drainage of supraglacial lakes. This site is located by a large moulin which becomes active each year (*Catania and Neumann*, 2010), and it is likely that the spring event is associated with the re-opening of this moulin. A common factor in the upper ablation zone, however, is that by the time a hydraulic connection has been established between the ice sheet surface and its bed, facilitating hydrologically-forced velocity variations, air temperatures and proglacial runoff are already decreasing. Lake drainage events are known to be rapid, delivering large enough volumes of water to quickly transform the subglacial hydrological system

into an efficient channellised network (*Das et al.*, 2008). Under these circumstances, it is unlikely that the volumes of water generated at the ice sheet surface at these elevations following lake drainage events will be sufficient to sustain large velocity variations (*Pimentel and Flowers*, 2011). Accordingly, even though the temperature data show considerable melting occurs at sites 4 and 5 until mid-August, we do not observe any changes in ice velocity at sites above 1000 m elevation beyond August 2nd.

6.4 Changes in annual motion

Annual mean ice velocities at sites 1 - 7 respectively are 16.7 %, 18.4 %, 14.8 %, 7.6 %, 5.1 %, 2.5 % and 0.2 % greater than they would be if the ice flowed at winter rates all year round. We find a strong correlation between the magnitude of local ablation and the percentage changes in annual ice motion due to hydrologically-forced velocity variations at each GPS site (Figure 6.6). Sites 1, 2 and 3, which are nearest the margin and below 800 m elevation, experience the most surface melting and show significantly greater annual acceleration than those at higher elevations, with the effect attenuating inland. Data from 2008 also show increases in mean annual ice velocity of 13.5 % and 5.6 % at sites 3 and 4 respectively due to summer velocity variations (*Bartholomew et al.*, 2010), indicating that the velocity changes that we observe in 2009 are a persistent feature of the dynamic behaviour of this part of the GrIS.

The relationship between rates of annual ablation and the amplitude of hydrologically-forced velocity change is not intuitive on the basis of previous theoretical work (*Pimentel and Flowers*, 2011) and observations (*Van de Wal et al.*, 2008), which have suggested that higher volumes of surface meltwater production will ultimately reduce the impact of hydrological forcing on GrIS motion. Implicit in these arguments is a concept of 'optimum melt': too much meltwater and the hydrological system will become channelised earlier in the summer, making ice velocities less sensitive to the volumes of meltwater reaching the bed more quickly, reducing the impact of seasonal velocity variations on the annual displacement of the ice. However, it is important to consider that the hydrological forcing at each site is a product of both local melting *and* meltwater delivered through the subglacial drainage system from further upglacier. As a result,

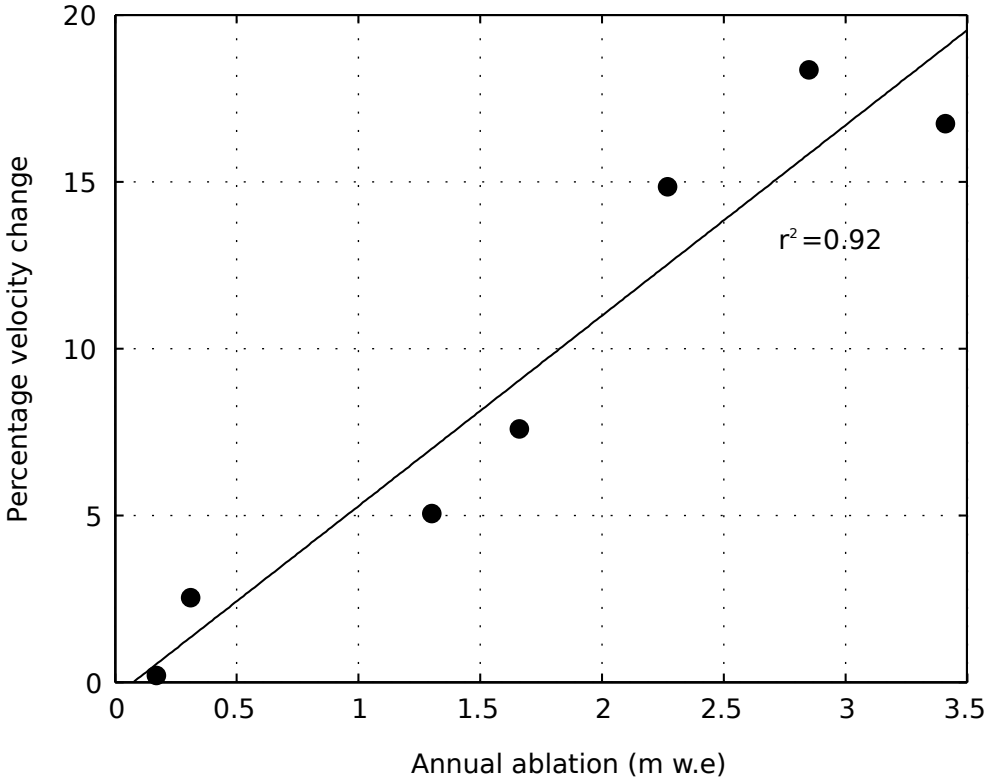

Figure 6.6: Percentage change in mean annual ice velocity vs. total surface ablation (m w.e.) at the GPS sites. The increase in annual ice velocity is calculated as the percentage by which the observed annual displacement exceeds that which would occur if the ice moved at winter rates all year round.

sites nearest the margin will receive disproportionately more meltwater per unit of local melting than those at higher elevations. Following this logic, previous theoretical work (*Pimentel and Flowers*, 2011) and observations (*Van de Wal et al.*, 2008) expect sites nearest the margin, where the total flux of meltwater through the subglacial drainage system will be greatest, to show smaller overall velocity changes than sites further inland. However, despite significant differences in the local volume of meltwater delivered to the ice-bed interface, we see similar increases in annual ice motion at sites 1 - 3 (14.8 - 18.4 %).

Our findings from the lower ablation zone are consistent with the numerical model of subglacial drainage proposed recently by *Schoof* (2010) and suggest that hydrologically-forced ice velocity variations are controlled more strongly by variations in the rate, rather than the absolute volume, of meltwater production and delivery to the ice-bed

interface. In particular, this reflects a temporary imbalance between the volume of water within the subglacial drainage system, and its inability to evacuate this water without an increase in pressure over a wide enough area to significantly affect basal motion (*Kamb et al.*, 1994). We argue that in a warmer climate, where greater volumes of surface meltwater are produced in the lower ablation zone, the seasonal rising limb and shorter-term variations in water delivery to the subglacial drainage system will continue to cause significant increases in annual ice motion despite the potential for an earlier 'switch' from a distributed to a channelised subglacial drainage system (*Schoof*, 2010). However, the overall magnitude of velocity variations will continue to be limited by evolution in the structure of the subglacial drainage system, which responds to inputs of surface meltwater over a longer period (*Mair et al.*, 2002a; *Anderson et al.*, 2004; *Bartholomew et al.*, 2010; *Schoof*, 2010).

While development in the efficiency of the subglacial drainage system also exerts some control on hydro-dynamic behaviour at higher elevations, the dominant limiting factor on the contribution of velocity variations to annual ice motion at sites in the upper ablation zone is the shorter duration and later establishment of the hydraulic connection between the ice sheet surface and its bed. The expectation that surface melting will be more intense, and spatially extensive, in a warmer climate (*Hanna et al.*, 2008), leads us to suggest that, in future, sites at higher elevations are likely to experience velocity variations for a longer period of time, allowing a greater annual change in ice velocity. In particular, higher rates of meltwater production would allow lakes that fill and subsequently drain to reach the volume required to propagate cracks through thick, cold ice earlier in the summer season (*Krawczynski et al.*, 2009). We therefore expect that the behaviour observed at sites 1 - 3 would be extended to higher elevations, creating a positive relationship between atmospheric warming and dynamic mass loss in land-terminating sections of the GrIS, albeit one that is modified by development in the structure of the subglacial drainage system.

We do not infer direct cause and effect between bulk volumes of surface ablation and changes in ice motion on the basis of the relationship shown in Figure 6.6. Instead, our data show contrasting regimes in hydrologically-forced dynamic behaviour of the GrIS at different elevations within the ablation zone, which provide a compelling explanation

for the relationship between total surface ablation and changes in annual ice motion. We therefore believe that our data provide a realistic basis for parameterisation of ice flow models that are used to predict the future evolution of the GrIS (*Parizek and Alley*, 2004).

6.5 Conclusions

Our data show that seasonal changes in horizontal ice velocity along a ∼115 km transect in a land-terminating section of the western GrIS are forced by the generation of surface meltwater which is able to reach the ice-bed interface. These velocity variations propagate inland from the ice sheet margin to progressively higher elevations in response to the onset of surface melting, and the creation of a hydraulic connection between the ice sheet surface and its bed. We find a positive relationship between rates of annual ablation and percentage changes in annual ice motion along the transect, with sites nearest the ice sheet margin experiencing greater annual variations in ice motion (15 -18 %) than those above 1000 m elevation (3 - 8 %).

Patterns in the timing and rate of meltwater delivery to the ice-bed interface are key controls on the magnitude of hydrologically-forced velocity variations at each site. In the lower ablation zone (<800 m elevation), 'spring events' occur early in the melt season and the overall contribution of variations in ice motion to annual flow rates is limited by evolution in the structure of the subglacial drainage system (*Bartholomew et al.*, 2010). At these sites, hydrologically-forced ice acceleration is greatest on the rising limb of the seasonal runoff hydrograph, when the hydraulic capacity of the subglacial drainage systems is consistently exceeded. However, we find that this behaviour is not replicated at sites in the upper ablation zone (>1000 m), where the period of summer melting is shorter, and the establishment of a hydraulic connection between the ice sheet surface and its bed is delayed, limiting the timeframe for velocity variations to occur.

In a warmer climate we expect seasonal melting of the GrIS surface to extend over a wider area, and to be more prolonged (*Hanna et al.*, 2008). This makes it likely that volumes of meltwater sufficient to reach the ice-bed interface will accumulate further from the ice sheet margin and that the timing of meltwater input will occur earlier each

summer (*Sundal et al.*, 2009; *Krawczynski et al.*, 2009). Our data therefore support the hypothesis that inland propagation of hydrologically-forced velocity variations will induce greater dynamic mass loss in land-terminating sections of the GrIS in a warmer climate, as patterns of hydro-dynamic behaviour observed in the lower ablation zone extend upglacier. These considerations provide a conceptual framework to understand the positive relationship between annual rates of surface ablation and percentage variations in annual ice velocity, and can be used to improve numerical simulations used for predicting the impact of hydrologically-forced variations in ice velocity on the future mass balance of the GrIS (*Parizek*, 2010).

CHAPTER 7

Acceleration of a land-terminating margin of the Greenland Ice Sheet in contrasting melt years

In chapter 6 we compared hydrological forcing of ice acceleration at different elevations along the GPS transect in 2009. At sites above 1000 m, where the ice is thicker and melt rates are lower, timing of drainage of meltwater to the ice-bed interface appears to be the main control on the the overall magnitude of summer acceleration. Although evolution in the structure of the drainage system limited late summer ice velocities at the lower elevation sites (confirming observations made in chapter 4), we still found a positive relationship between rates of annual ablation and percentage changes in annual ice motion along the whole transect. On the basis of comparison with the hydrograph we suggest that variability in the rate of meltwater input is important in sustaining raised ice velocities at sites near the ice sheet margin, even once a transition to an efficient drainage system has occurred.

The results presented in chapter 6 lead us to hypothesise that overall rates of mass loss will increase along the transect in warmer years because meltwater will drain to the bed earlier and over a greater part of the ice sheet, while acceleration is sustained at sites near the ice sheet margin. Regional scale data showed that summer temperatures near to the transect were approximately the same in 2009 as the 1960 - 2010 average, while 2010 was ∼2.5°C warmer. In this chapter we compare GPS records from the whole transect in 2009 and 2010 to test the hypothesis proposed in chapter 6 and to further investigate controls on inter-annual variability in hydrologically-forced ice acceleration in Leverett Glacier.

Authors: Ian Bartholomew[1], Peter Nienow[1], Andrew Sole[1], Douglas Mair[2], Thomas Cowton[1] & Matt A King[3]

1. School of Geosciences, University of Edinburgh, Drummond Street, Edinburgh, EH8 9XP, UK
2. School of Geosciences, University of Aberdeen, Aberdeen, AB24 3UF, UK
3. School of Civil Engineering and Geosciences, Newcastle University, Newcastle upon Tyne, NE1 7RU, UK

Author contributions: IB, AS, TC, PN and DM collected the data. IB processed the GPS data for sites 1 - 6 and MAK processed the GPS data for site 7 from 2009. IB and AS processed the GPS data from 2010 IB analysed the data and wrote the manuscript. AS prepared the figures. All authors contributed to discussions of the paper during the writing process.

Abstract

Coupling between surface melting of the Greenland Ice Sheet and accelerated ice flow, through lubrication of the ice-bed interface, is controlled strongly by behaviour of the subglacial drainage system. It is not agreed, however, whether higher melt rates will increase or decrease dynamic mass loss from the ice sheet in a warmer climate. To address this we present data from a land-terminating transect on the western ice sheet margin in two years with contrasting melt regimes. Near the ice sheet margin high summer acceleration is sustained in both years by non-steady behaviour of the channelised subglacial drainage system. At higher elevations the change in summer acceleration was greater in response to higher temperatures as meltwater accessed the ice-bed interface earlier in the season, prolonging summer acceleration. Overall, mean annual ice velocities were higher in the warmer year due to the increase in summer acceleration, suggesting that hydro-dynamic coupling will increase mass loss from the ice sheet in response to climate warming.

Each summer, meltwater generated at the Greenland Ice Sheet (GrIS) surface drains through the ice sheet into the subglacial hydraulic system. These external inputs of meltwater raise subglacial water pressure and reduce the resistance to basal sliding (*Iken*, 1981), facilitating faster ice motion (*Iken and Bindschadler*, 1986). As a result, rates of ice flow in marginal areas of the GrIS are greater in summer than in winter (*Zwally et al.*, 2002; *Joughin et al.*, 2008a; *Van de Wal et al.*, 2008; *Bartholomew et al.*, 2010; *Sundal et al.*, 2011), which can increase annual ice flux by 6 - 14 % compared with if the ice flowed at winter rates all year round (*Bartholomew et al.*, 2010). If the relationship between meltwater production and ice motion is positive (*Zwally et al.*, 2002), this mechanism has the potential to significantly increase rates of mass loss from the GrIS in response to anticipated climate warming by amplifying the seasonal velocity change signal (*Parizek and Alley*, 2004).

In response to inputs of surface meltwater, however, the subglacial drainage system increases in capacity, developing from a hydraulically inefficient structure into a network of efficient channels, which operate at lower mean pressures for a given discharge (*Kamb*,

1987; *Röthlisberger*, 1972; *Schoof*, 2010), reducing the lubrication effect of external meltwater inputs to the ice sheet bed (*Bartholomew et al.*, 2010; *Sundal et al.*, 2011; *Bartholomew et al.*, 2011b). This reasoning, underpinned by steady-state theory of water flow through subglacial channels (*Röthlisberger*, 1972; *Schoof*, 2010), has been invoked to explain observations that ice velocities in the GrIS in late summer are lower than those in early summer (*Bartholomew et al.*, 2010; *Sundal et al.*, 2011). In a number of recent studies it has been proposed that ice in marginal areas will flow *more slowly* in years with higher melt since channelisation of the subglacial drainage system will occur more quickly in response to greater volumes of water, reducing the dynamic sensitivity of the GrIS to climate warming (*Van de Wal et al.*, 2008; *Pimentel and Flowers*, 2010; *Schoof*, 2010; *Sundal et al.*, 2011).

A key feature of hydrologically-forced velocity variations in the GrIS is that they propagate inland from the ice sheet margin over the course of each summer following the onset of surface melting at successively higher elevations (*Bartholomew et al.*, 2010; *Sundal et al.*, 2011). Summer velocity increases have been observed to occur at elevations above 1500 m (*Palmer et al.*, 2011; *Bartholomew et al.*, 2011b). However, evidence for seasonal development of the subglacial drainage system and its effect on the relationship between surface melting and ice velocities has come mostly from the lower ablation zone (*Bartholomew et al.*, 2010; *Sundal et al.*, 2011), at elevations below 1000 m. Further, much analysis has focused on the implications of dynamic behaviour at a point or within a specific elevation band in the ablation zone (*Van de Wal et al.*, 2008; *Shepherd et al.*, 2009; *Sundal et al.*, 2011).

Two major uncertainties in the question of whether increased surface melting across the GrIS will cause an increase in the rate of mass loss from the ice sheet in a warmer climate therefore remain unaddressed. Firstly, the behaviour observed at sites below 1000 m is not necessarily replicated upglacier where the ice sheet is thicker and the melt season is currently much shorter (*Bartholomew et al.*, 2011b). Secondly, in a warmer year meltwater is likely to penetrate to the bed further inland, increasing the area of the GrIS which is subject to hydrologically-forced velocity variations.

Greenland climate in 2010 was marked by record-setting high air temperatures and ice loss by melting (*Box et al.*, 2010). Summer seasonal average (June-August)

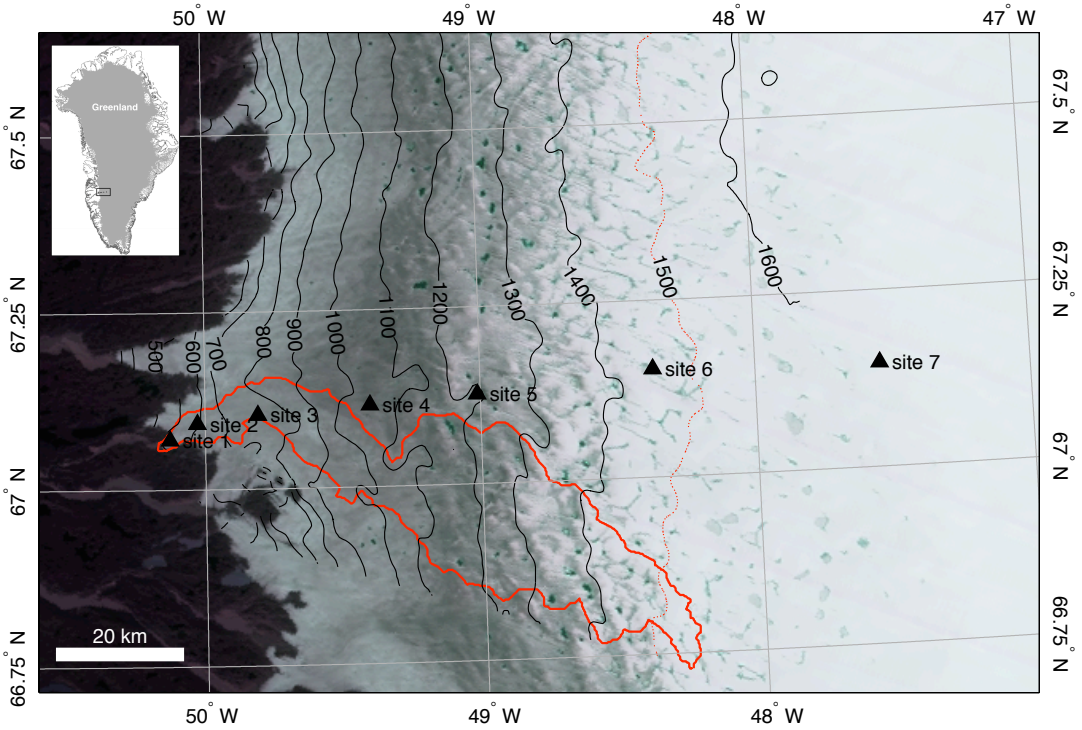

Figure 7.1: Location of the study region on the western margin of the GrIS. Contours (100 m intervals) are produced from a digital elevation model derived from InSAR (*Palmer et al.*, 2011). The catchment of the river which drains through Leverett glacier is shown in red (*Bartholomew et al.*, 2011a).

air temperatures around Greenland were 0.6 to 2.4°C above the 1971-2000 baseline and were highest in the west (*Box et al.*, 2010). As a result, bare ice was exposed at the GrIS surface earlier than in previous years and for longer (*Tedesco et al.*, 2011). NCEP/NCAR reanalysis data shows that the June-August 700 mb temperature anomaly in west Greenland near to Kangerlussuaq was +2.5°C relative to the 1960 - 2010 mean (*Kalnay et al.*, 1996). In contrast, this anomaly was approximately 0°C in 2009. The regional temperature characteristics of these years provide an opportunity to evaluate the effect that an increase in summer temperatures, commensurate with predictions for climate warming over the next century (*Meehl et al.*, 2007), will have on hydrologically-forced ice dynamic behaviour compared with the late 20th century.

We present data from 7 sites along a land-terminating transect in west Greenland at approximately 70° N that extends to 115 km from the margin, up to 1715 m elevation (Figure 7.1), from both 2009 and 2010. At each site we made continuous measurements of ice velocity, air temperature and seasonal measurements of surface ablation. In addition

we measured discharge from a portal at Leverett glacier which drains runoff from a catchment of approximately 1200 km^2 (*Bartholomew et al.*, 2011a), incorporating our lowest three sites (Figure 7.1). Displacement of each GPS antenna over the intervening winter was used to calculate mean winter ice velocities. In the following analysis these are used as baseline values when calculating increases in ice velocity due to summer velocity variations. When calculating annual velocities we assume that the ice flowed at winter rates for all days of the year for which we do not have measurements.

The regional temperature difference between 2009 and 2010 is reflected in the local measurements of air temperature at our sites, where the average difference in May-August mean temperature is 2.1°C. Local measurements of surfacing lowering at each GPS site show that total summer ablation was 22 - 220% greater in 2010 than 2009, while the runoff observations from Leverett Glacier glacier show that cumulative bulk discharge was approximately twice as great in 2010 compared with 2009 (Figure 7.2h).

We measured summer velocity variations of up to 300 % greater than winter background rates along the transect in both 2009 and 2010, following the onset of surface melting. Velocity variations occurred first near the ice sheet margin and at progressively higher elevations as the melt season progressed in a pattern which was repeated over the two years (Figure 7.2a-g). This broad relationship with patterns of surface melting is consistent with previous studies in this region (*Bartholomew et al.*, 2010, 2011b; *Sundal et al.*, 2011) and indicates that the velocity variations were driven by inputs of surface meltwater to the subglacial drainage system once a hydraulic connection had been established between the ice surface and bed.

Sites nearest the ice sheet margin, which are at lower elevations and experienced the highest rates of surface melting, showed the greatest summer acceleration over winter background motion and the effect attenuated inland (Figure 7.2a-g). Sites 1 - 3, below 1000 m elevation, all experienced an increase in mean annual velocity of greater than 14.8 % due to the summer acceleration, while sites 5 - 7, which are above 1200 m elevation, showed increases in annual velocity of 8.2 % or less (Figure 7.3a, Table 7.1).

Ice acceleration at site 1, nearest the ice sheet margin, started 15 days earlier in 2010 (2nd May) than in 2009 (22nd May). We infer that the earlier onset of above zero temperatures produced enough water at the ice surface to force a hydraulic connection

with the subglacial drainage system at an earlier date (Figure 7.2a,h). This pattern was repeated at the sites upglacier, where earlier onset of melting in 2010 induced ice acceleration earlier than in 2009 by an average of 25 days.

Significantly, comparison of annual motion data from 2009 and 2010 shows, with the exception of site 2, that annual mean velocities along the transect were greater in 2010 than in 2009. On average, velocity variations in 2010 contributed an extra 2 % increase in annual motion on top of winter background rates compared with 2009 (Figure 7.3a).

In 2009 site 7 did not speed-up appreciably and broadly delimited the inland extent of hydrologically forced velocity variations along the transect for that year. A small and short-lived acceleration, in the absence of surface uplift, was likely due to mechanical coupling of faster moving ice downglacier (*Bartholomew et al.*, 2011b) and is the cause of the 0.2 % increase in annual motion (Table 7.1; *Bartholomew et al.*, 2011b). In 2010, when the May-August mean temperature at site 7 was 2.8°C warmer than in 2009, the increase in mean annual ice velocity was 1.9 %. Our data suggest, therefore, that ice velocity variations also propagated further into the ice sheet in the warmer year of 2010 (Figure 7.3a,b).

In order to explain these findings we used the detailed records of ice motion, air temperature, and runoff to investigate factors which control temporal and spatial

Site	Winter velocity (m yr^{-1})	% change 2009			% change 2010		
		early	late	annual	early	late	annual
1	49.5	62.8	23.0	16.7	76.4	22.6	20.5
2	100.9	65.8	26.0	18.4	75.5	9.9	17.7
3	97.2	53.8	18.2	14.8	67.1	10.8	16.1
4	119.5	19.3	17.7	7.6	-	-	10.2
5	113.1	3.3	21.7	5.1	26.2	13.6	8.2
6	91.8	-0.1	13.0	2.5	14.9	19.1	7.0
7	62.7	-1.0	2.4	0.2	1.4	7.8	1.9
Average 1-3	-	60.8	22.7	16.6	73.0	14.5	18.1
Average 5-7	-	0.7	12.3	2.6	14.2	13.5	5.7

Table 7.1: Percentage speed-up relative to winter background rates during 2009 and 2010. Early summer is defined as April 26th to July 9th and late summer is defined as July 10th to August 23rd. Annual percentage speed-up is the percentage by which annual mean velocity exceeds that which would occur if the ice flowed at winter rates all year round.

changes in the relationship between surface melting and ice acceleration in both years. In the following analysis we define the summer period from April 26th to August 23rd, which is further divided into early and late summer by the mid-point on July 10th. This period covers the full extent of accelerated ice flow in both years and allows direct comparison of our results with other recent studies in the same region (*Sundal et al.*, 2011).

Further down in the ablation zone, at sites 1 - 3, ice velocities were lower in late summer than early summer in both 2009 and 2010 even though air temperatures and runoff remained high (Table 7.1, Figure 7.2a-c,h). This phenomenon has been observed before and indicates that, by late summer, the subglacial drainage system has developed to evacuate large volumes of water at lower pressure than earlier in the summer (*Iken and Bindschadler*, 1986; *Bartholomew et al.*, 2010; *Sundal et al.*, 2011; *Bartholomew et al.*, 2011b). We confirm, therefore, that seasonal development in the structure of the subglacial drainage system acts to limit the overall impact of meltwater-forced ice acceleration on mean annual ice velocity (*Van de Wal et al.*, 2008; *Bartholomew et al.*, 2010; *Sundal et al.*, 2011; *Schoof*, 2010).

Late summer velocities at sites 1 - 3 are also lower in 2010 than in 2009. This difference appears because ice velocities in 2010 begin to decline, following early season acceleration, at an earlier date than in 2009. In our dataset, however, the earlier decline in velocities is offset by an earlier spring event and, integrating the velocity signal over the whole season, we find that it does not necessarily equate to an overall reduction in annual ice motion (Table 7.1; *Sundal et al.*, 2011). Mean temperatures for the summer period (April 26th - August 23rd) at sites 1 - 3 were 1.5, 1.2 and 2.7 °C greater in 2010 than 2009 respectively. For the same period, site 1 and site 3 experienced increases in acceleration from 16.7% to 20.5 % and 14.8 % to 16.1 % respectively, while at site 2 acceleration decreased from 18.4 % to 17.7 %.

In contrast with recent suggestions (*Truffer et al.*, 2005; *Van de Wal et al.*, 2008; *Pimentel and Flowers*, 2010; *Schoof*, 2010; *Sundal et al.*, 2011), therefore, we do not agree that the timing of the transition from a distributed to channelised subglacial drainage system, presumed to occur more quickly in a warmer year, is the main control on inter-annual variations in ice velocity. Should that be the case, we would expect that

the effect of higher amounts of meltwater produced in 2010, which is assumed to have effected the development of an efficient drainage system earlier in the summer than in 2009, to subdue the transient early-summer acceleration more quickly, thereby reducing mean summer ice velocity. Although the increases in summer ice velocity observed at sites 1 and 3 between 2009 and 2010 are relatively small, the fact that they are at least sustained, and not dramatically reduced, is therefore significant. If we accept the logic that higher melt will cause quicker development of an efficient drainage system at any one site, then we must conclude that more rapid development of an efficient drainage system is not sufficient, on its own, to reduce mean summer ice velocities.

An alternative characterisation of early and late summer is offered by the Leverett Glacier hydrograph in both 2009 and 2010. At sites 1 - 3, velocities are greatest on its rising limb (Figure 7.2h), and are subdued once discharge has stabilised or is declining; after July 16th in 2009 and July 1st in 2010 (Figure 7.2a-c). Although theoretical analyses (*Röthlisberger*, 1972; *Schoof*, 2010) show that larger subglacial meltwater channels operate at lower mean pressure under steady-state conditions, or in response to gradually changing inputs of meltwater, discrepancy between changes in the rate that water is delivered to a drainage system and how quickly it can adjust to accommodate this water leads to short-term excursions in water pressure (*Röthlisberger*, 1972; *Schoof*, 2010). While meltwater inputs are consistently rising, steady-state conditions are unlikely to be met, even when the subglacial drainage system has become channelised (*Röthlisberger*, 1972). Our data suggest that the rising limb of seasonal runoff is able to sustain raised subglacial water pressures, and therefore ice velocities, by constantly challenging the drainage system to accommodate larger volumes of water. As the discharge stabilises and/or decreases in late summer the pressure and ice velocities fall because closure of the ice walled conduits lags behind the reduced flux of water (*Röthlisberger*, 1972).

At our higher elevation sites, while summer ice acceleration is also forced by melting at the ice sheet surface, the behaviour in relation to patterns of surface melting is different from lower in the ablation zone. The velocity variations at sites 5 - 7 also cause smaller increases in annual ice motion (0.2 - 8.2 %) than in the lower ablation zone (Table 7.1). Initial acceleration is delayed relative to the onset of above-zero

temperatures (particularly in 2009) and occurs later in the melt season. The initiation of meltwater-forced ice acceleration is critically dependent on the development of a hydraulic connection between the ice surface and its bed. The delay is presumably due to lower melt rates which mean that it takes longer to accumulate enough water to penetrate to the ice sheet bed, in particular since more water is required to propagate cracks via hydrofracture through thicker, cold ice (*Van der Veen*, 2007; *Krawczynski et al.*, 2009). Periodic drainage of supraglacial lakes is likely to play an important role in this process, especially at the highest elevations, by concentrating surface meltwater from wide areas into large reservoirs (*Das et al.*, 2008; *Bartholomew et al.*, 2011b).

Comparison between sites and across both years suggests that this delay in the onset of acceleration exerts primary control on the magnitude of summer acceleration by limiting the time frame for velocity variations to occur. For example, in 2009, accelerated ice motion began at sites 4, 5 and 6 on June 5th, July 11th and July 21st respectively and lasted until approximately the end of August, leading to increases in annual ice velocity of 7.6 %, 5.1 % and 2.5 %. In 2010 site 5 accelerated on June 6th, 31 days earlier than in 2009, and site 6 accelerated on June 25th, 24 days earlier, leading to accelerations of 8.2 % and 7.0 % respectively - an increase of over 3 % on 2009.

Combining both years data we find that there is a positive relationship (r=0.92) between the amount of local ablation and the percentage increase in annual motion due to the summer velocity variations at each site (Figure 7.3c). The relative enhancement of annual velocity in 2010 compared with 2009 is greater at higher elevations: while the average percentage increase in acceleration across all sites was 2 %, at sites 5, 6 and 7 this amounted to 1.6 and 2.8 times the acceleration compared with 2009 at sites 5 and 6. Site 7 experienced 9.6 times the acceleration in 2010 compared with 2009, however, given the very small acceleration in 2009 (0.2 %) the exact figure is not that meaningful (Figure 7.3d, Table 7.1).

The strong relationship between local surface ablation and the increase in velocity seen in our data is explained by the competing influence of different mechanisms at different elevations. In a warmer climate we would expect to see increased rates of ice motion above 1000 m elevation because meltwater will reach the ice-bed interface earlier in the summer. The 'time-limited' behaviour at our upper sites will also extend further

inland, increasing the proportion of the ice sheet that is subject to summer velocity variations; particularly because the hypsometry of the GrIS, which flattens inland, gives a non-linear expansion of the area producing runoff in response to rising temperatures.

We find no evidence to support the recent hypothesis (*Van de Wal et al.*, 2008; *Pimentel and Flowers*, 2010; *Sundal et al.*, 2011) that higher rates of surface melting near the margin of the GrIS will reduce the overall magnitude of summer velocity variations due to earlier channelisation of the subglacial drainage system. This finding highlights the importance of non-steady behaviour of the channelised subglacial drainage system, where raised water pressures can still result from short-term imbalance between inputs of meltwater to the channelised subglacial drainage system and its capacity to accommodate them (*Röthlisberger*, 1972; *Schoof*, 2010). This process appears able to sustain ice velocity variations while runoff is increasing. The length of time between the onset of seasonal runoff and its peak at sites in the lower ablation zone is not expected to change in response to climate warming. We suggest, therefore, that the current level of summer acceleration at sites nearest the ice sheet margin will remain high in response to climate warming, maintained by short-term variability in meltwater supply on the rising limb of seasonal runoff. Overall our data show that rates of mass loss from land-terminating sections of the GrIS will be *enhanced* in a warmer climate by the dynamic effect of increased surface melting. In order to capture this behaviour, numerical simulations of GrIS dynamics in a warmer climate should be able to account for both longer-term evolution of the subglacial drainage system and short-term variations in subglacial water pressure, as well as behaviour at higher elevations where melt rates are lower and ice is thicker.

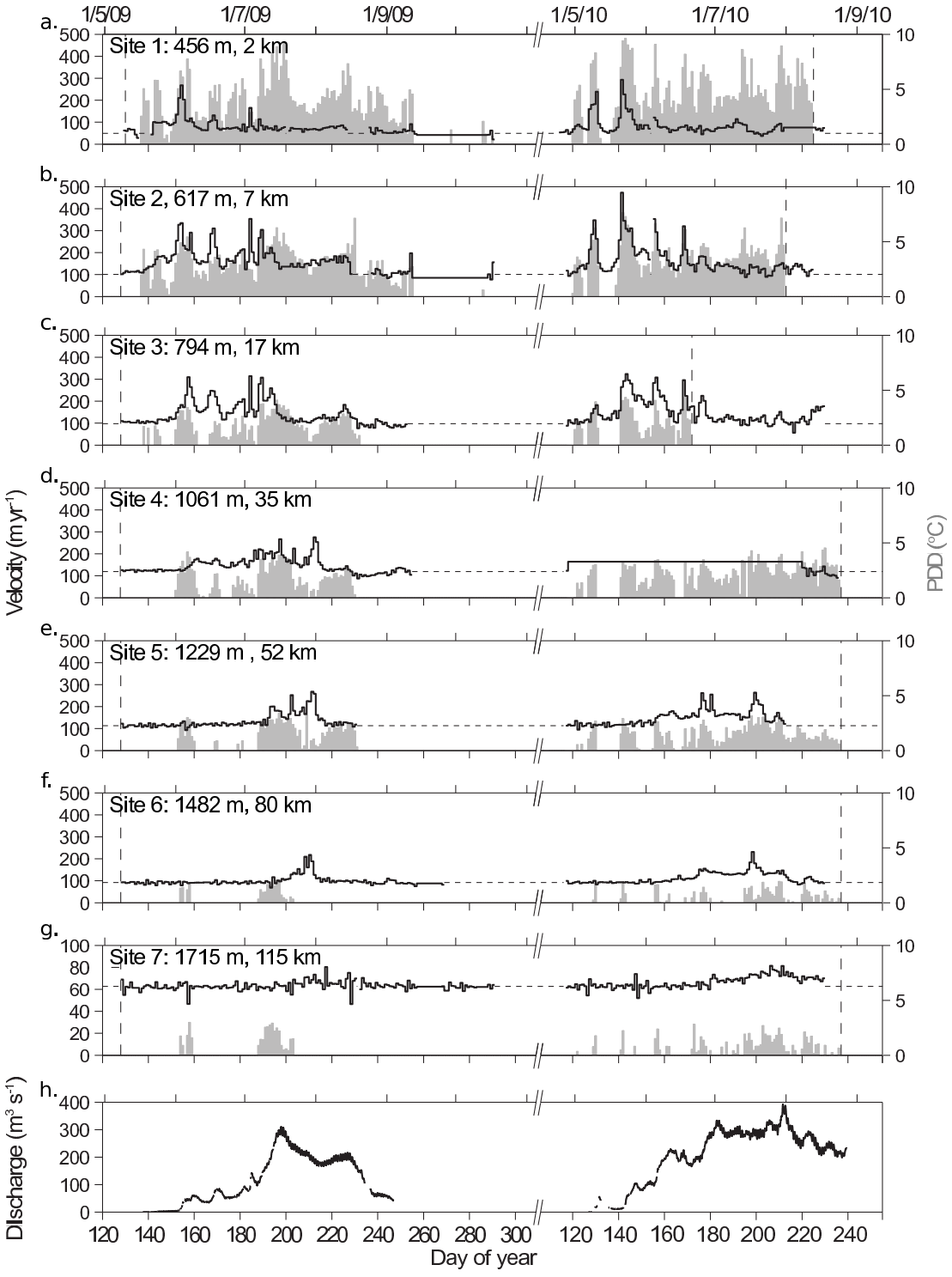

Figure 7.2: a-g. 24-h horizontal velocity (black stairs) and positive-degree days (grey bars) at sites 1-7 for the survey period in 2009 and 2010. Winter background velocity (black dashes) is determined by bulk movement of each GPS site over the intervening winter. Vertical dashed lines indicate the end of temperature data used to calculate PDD's. At site 4, power was lost in early May in the GPS unit, and was only recovered in August. As a result, the detail of the ice velocity record was lost, although we were able to calculate mean summer velocity from the bulk displacement. h. Discharge hydrograph (m^3 s^{-1}) from Leverett Glacier. The estimated catchment for this outflow channel (*Bartholomew et al.*, 2011a) is shown on Figure 1 and contains GPS sites 1, 2 and 3.

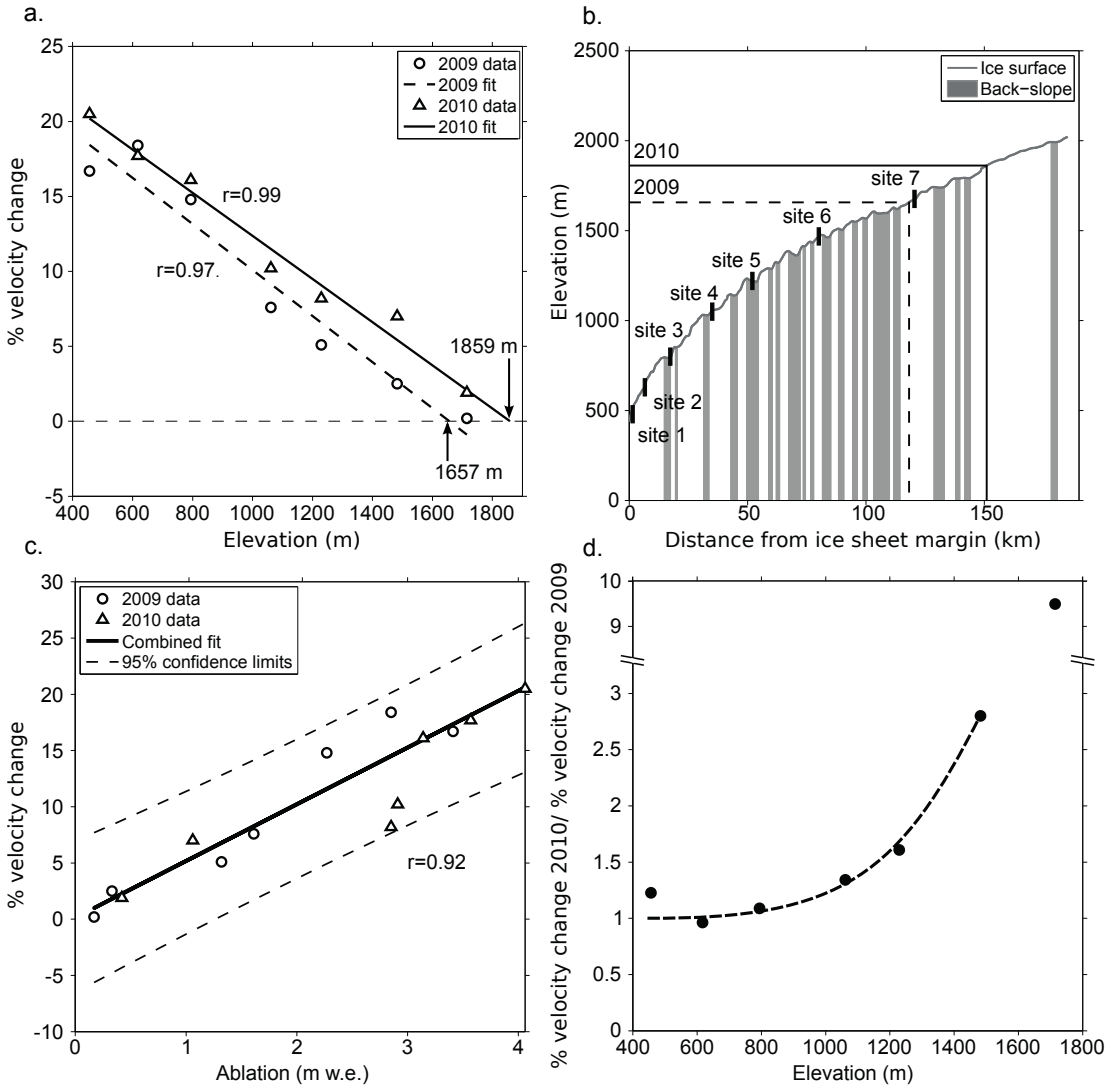

Figure 7.3: a. Percentage change in annual velocity due to the summer acceleration vs. elevation for GPS sites in 2009 and 2010. b. Surface elevation profile of the transect showing the extent of summer velocity variations in 2009 and 2010. Backslopes on the ice sheet surface where meltwater can accumulate are shown in grey. c. Percentage change in annual velocity vs. local ablation for each GPS site. d. Ratio of percentage change in annual motion in 2010 compared with 2009 vs. elevation for each GPS site along the transect.

CHAPTER 8

Short-term variability in Greenland Ice Sheet motion forced by time-varying meltwater inputs: implications for the relationship between subglacial drainage system behaviour and ice velocity

In chapters 6 and 7 we found a positive relationship between seasonal rates of ablation and percentage changes in ice acceleration at all elevations across our transect. At higher elevation sites (>1000 m) this is explained by earlier drainage of meltwater to the ice-bed interface in the warmer year. At sites nearer the ice sheet margin, however, where meltwater drains more easily to the ice-bed interface, this finding has important implications for the behaviour of the subglacial drainage system. Many authors have suggested, on the basis of steady-state analysis, that channelisation of the drainage system is the primary control on the late summer reduction in ice velocities.

Therefore, increased rates of surface melting will cause more rapid channelisation of the drainage system and earlier slowdown, leading to lower annual mean velocities. The results presented in chapter 6 show, however, that short-term variability in the *rate* of meltwater input to the subglacial drainage system can result in high ice velocities at sites near the ice sheet margin (<1000 m elevation) even once the drainage system has become channelised. In light of the failure of steady-state considerations to explain inter-annual variation in summer acceleration we suggest that this may have greater control over the pattern of seasonal ice acceleration than has previously been acknowledged.

In this chapter we use high temporal resolution records of ice velocity, derived from our GPS data, to investigate the short-term structure of summer ice velocity variations on Leverett Glacier and the relationship with air temperature and runoff. In the second part of the paper, we use a simple model of the behaviour of a subglacial conduit to assess whether the features of the ice acceleration signal can be explained as a response of subglacial water pressure to time-varying water input.

Authors: Ian Bartholomew[1], Peter Nienow[1], Andrew Sole[1], Douglas Mair[2], Thomas Cowton[1] & Matt A King[3]

1. School of Geosciences, University of Edinburgh, Drummond Street, Edinburgh, EH8 9XP, UK
2. School of Geosciences, University of Aberdeen, Aberdeen, AB24 3UF, UK
3. School of Civil Engineering and Geosciences, Newcastle University, Newcastle upon Tyne, NE1 7RU, UK

Author contributions: IB, AS, TC, PN and DM, collected the data. IB processed the GPS data for sites 1 - 6 and MAK processed the GPS data for site 7 from 2009. IB and AS processed the GPS data from 2010 IB analysed the data and wrote the manuscript. All authors contributed to discussions of the paper during the writing process.

Abstract

High resolution measurements of ice motion along a ∼120 km transect in a land-terminating section of the GrIS reveal short-term velocity variations (<1 day), which are forced by rapid variations in meltwater input to the subglacial drainage system from the ice sheet surface. The seasonal acceleration signal at low elevations (<1000 m) is dominated by events lasting from 1 day to 1 week, although daily cycles are largely absent at higher elevations, reflecting different patterns of meltwater input. Using a simple model of subglacial conduit behaviour we show that the seasonal record of ice velocity is best understood in terms of a time-varying water input to a channelised subglacial drainage system. Our investigation substantiates arguments that variability in the *duration* and *rate*, rather than absolute volume, of meltwater delivery to the subglacial drainage system is an important control on seasonal patterns of subglacial water pressure, and therefore ice velocity. Our results challenge predictions, based on analysis of subglacial conduit behaviour in response to gradually varying meltwater input, that development in the structure of the subglacial drainage system will exert primary control on inter-annual variations in summer acceleration in this part of the GrIS margin.

8.1 Introduction

Mass loss from the Greenland Ice Sheet (GrIS) is one of the largest unknown components in predictions of future sea-level change (*Meehl et al.*, 2007). The ice sheet loses mass primarily through melting at its surface, which runs off, and discharge of icebergs to the ocean where glaciers meet the sea. Where the ice sheet terminates on land, ice flow velocities are enhanced each summer by meltwater which drains to the ice-bed interface, lubricating basal motion (*Zwally et al.*, 2002; *Van de Wal et al.*, 2008; *Joughin et al.*, 2008a; *Bartholomew et al.*, 2010, 2011b; *Sundal et al.*, 2011). Should there be a direct and positive relationship between the amount of meltwater produced and the magnitude of the seasonal acceleration signal (*Zwally et al.*, 2002), this process has the potential to increase the rate of mass loss from the GrIS significantly in response to anticipated climate warming, by drawing ice to lower elevations where temperatures are warmer

(*Parizek and Alley*, 2004). While the impact of meltwater on fluctuations in ice flow has been a research focus for glaciologists studying Alpine and Arctic glaciers for decades (e.g. *Iken*, 1981; *Iken et al.*, 1983; *Iken and Bindschadler*, 1986; *Hooke et al.*, 1989; *Kamb et al.*, 1985; *Kamb*, 1987; *Mair et al.*, 2001; *Anderson et al.*, 2004; *Bartholomaus et al.*, 2007; *Bingham et al.*, 2008), the problem is now receiving renewed attention in the context of large ice sheet systems (*Zwally et al.*, 2002; *Van de Wal et al.*, 2008; *Joughin et al.*, 2008a; *Das et al.*, 2008; *Shepherd et al.*, 2009; *Bartholomew et al.*, 2010; *Schoof*, 2010; *Pimentel and Flowers*, 2010; *Bartholomew et al.*, 2011a,b; *Sundal et al.*, 2011), with the ultimate aim of reducing uncertainty in ice sheet models that are used to predict sea-level change (*Parizek*, 2010).

Effective pressure at the ice-bed interface, defined as ice overburden minus subglacial water pressure, strongly influences rates of basal motion; lower effective pressure (higher water pressure) favours faster sliding if it occurs over a wide enough area, as it reduces drag between ice and the bed (*Iken and Bindschadler*, 1986). In classical theories of sliding over a hard bed, higher basal water pressure encourages the growth of subglacial cavities in the lee of bedrock undulations (*Lliboutry*, 1968; *Iken*, 1981; *Fowler*, 1986; *Schoof*, 2005). Growth of subglacial cavities leads to local separation of the ice and its bed, causing a reduction in basal drag thus allowing higher sliding velocities (*Bindschadler*, 1983). Where the glacier bed is comprised of sediments, higher water pressures are also associated with faster rates of basal motion. Basal motion of an ice mass over a sedimentary bed can arise from pervasive deformation of the bed, shearing across discrete planes in the bed or ploughing of clasts through the upper layer of the bed (*Alley et al.*, 1989) as well as sliding of the ice over its bed (*Iverson et al.*, 1995). High basal water pressures promote glacier sliding by weakening coupling between the ice and its bed, and also has the potential to weaken basal sediments allowing the bed to deform (*Fischer and Clarke*, 2001).

One of the major controls on subglacial water pressure is the structure of the drainage system (*Röthlisberger*, 1972; *Walder*, 1986; *Röthlisberger and Lang*, 1987; *Schoof*, 2010), which, in turn, reflects the recent water flux (*Nienow et al.*, 1998). Overall, the size of subglacial conduits is determined by the balance between the tendency for conduit closure by collapse under the weight of overlying ice, and opening due to frictional

melting of the walls by water, horizontal flow of the ice past bedrock obstacles and the pressure of water within the conduits (*Röthlisberger*, 1972; *Walder*, 1986; *Schoof*, 2010). Larger water flux therefore leads to faster rates of conduit opening and a drainage system dominated by larger conduits, and vice versa.

The relationship between drainage system structure and its pressure-discharge characteristics is generally understood in terms of the steady-state behaviour of subglacial conduits (*Röthlisberger*, 1972; *Walder*, 1986; *Schoof*, 2010). In small conduits, opening by frictional melting is small due to the low water flux and conduit size is maintained largely by flow of ice past bedrock obstacles. In conduits of this type, generally described as 'cavities', the tendency for creep closure is balanced by an increase in water pressure to maintain equilibrium (*Walder*, 1986; *Schoof*, 2010). In a drainage system which is dominated by cavity-type drainage there is positive relationship between conduit size, subglacial discharge and water pressure.

In larger conduits where the water flux is much greater (known as 'R-channels'), closure is principally offset by higher rates of wall melting, which is controlled by the conduit discharge (*Röthlisberger*, 1972). The largest channels have the highest closure rates (greatest effective pressure) and therefore require the highest discharge to maintain conduit size by melting. Effectively, the melting of walls relieves water pressure as a channel grows in a way that is not possible in cavities where flux is low. As a result, in a predominantly channelised subglacial drainage system in steady-state, there is an inverse relationship between drainage system discharge and mean subglacial water pressure (*Röthlisberger*, 1972; *Schoof*, 2010).

In a drainage system where R-channels predominate, the largest channels, which operate at lower mean pressure, will tend to capture water from smaller channels, leading to concentration of flow into fewer channels and development of a dendritic drainage pattern (*Röthlisberger*, 1972; *Shreve*, 1972). Conversely, in a system where there is a positive relationship between conduit discharge and water pressure there is no tendency for one conduit to outgrow others by capturing water across a hydraulic gradient. As a result, cavity-type drainage systems with low water flux are spatially distributed across the glacier bed (*Walder*, 1986). Since a channelised drainage system occupies a small portion of the bed, however, the two drainage configurations may

co-exist once a channelised drainage system has developed, with a distributed system filling the space between channels (*Fountain*, 1994; *Hubbard et al.*, 1995; *Hubbard and Nienow*, 1997). Under these circumstances the two types of drainage system do not operate in isolation. Over-pressurisation of a subglacial conduit can set up lateral pressure gradients, driving water away from the conduit and increasing water pressure in the surrounding drainage system (*Hubbard et al.*, 1995; *Hubbard and Nienow*, 1997). Since the volume of meltwater produced at the ice sheet surface is more than an order of magnitude greater than is generated at the ice-bed interface, the behaviour of these conduits is likely to force, rather than respond to, behaviour in the remainder of the system. Large R-channels can therefore interact with the surrounding distributed system to alter water pressure, and ice velocity, over a wider area (*Hubbard et al.*, 1995; *Nienow et al.*, 2005; *Bartholomaus et al.*, 2007).

It is acknowledged that cavities in the lee of bedrock protrusions may not occur if the glacier bed is comprised of a sediment layer. In this case it is likely that inefficient subglacial drainage may occur by Darcian porewater flow (e.g. *Alley*, 1989; *Flowers and Clarke*, 2002). When subglacial water flux is higher, however, R-channels can still occur and the pressure-discharge characteristics of drainage when the bed is comprised of subglacial sediments is likely to be qualitatively similar to that when the substrate is bedrock (*Walder*, 1986; *Flowers and Clarke*, 2002).

The consequence of steady-state analysis is a binary classification of the subglacial drainage system. Where the overall flux is low, a spatially distributed system with cavity-type behaviour predominates (*Schoof*, 2010). In such a system any increase in water flux leads to raised water pressures and increased basal sliding. These systems are often described as 'inefficient'. When the water flux is raised above a critical level, conduits are enlarged to the point that their behaviour becomes that of R-channels. Larger channels with more water operate at lower pressure and are described as 'efficient' - increasing the water flux will increase effective pressure (reduce water pressure) and reduce basal sliding.

As in Alpine systems, the drainage system in the ablation zone of the GrIS develops over the course of a melt season from a spatially distributed inefficient system to a discrete network of efficient channels, in response to meltwater inputs from the ice

sheet surface (*Nienow et al.*, 1998; *Bartholomew et al.*, 2011a). Over the winter, the only sources of meltwater are generated subglacially, through frictional and geothermal heating; water fluxes are low and an inefficient system predominates. Channelisation of the drainage system occurs in response to inputs of meltwater from the ice sheet surface and this process occurs further from the ice sheet margin as the melt season progresses (*Bartholomew et al.*, 2011a). The development of a network of channels which cover only a small portion of the ice sheet bed is favoured by input of meltwater through moulins which deliver water to discrete locations, rather than evenly across the bed (*Nienow and Hubbard*, 2006).

As a result of development in its structure the drainage system operates at a lower mean pressure for a given discharge later in the summer. Late summer ice velocities in marginal areas of the GrIS have been observed to be lower than in early summer, indicating that drainage evolution acts to limit the overall magnitude of the summer acceleration signal (*Bartholomew et al.*, 2010; *Sundal et al.*, 2011; *Bartholomew et al.*, 2011b; *Palmer et al.*, 2011; *Nienow et al.*, submitted; *Chapter 7*). Consideration of steady-state theory of subglacial drainage, coupled with such observations from Greenland, have lead a number of authors to suggest further that increased surface melting will lead to a *reduction* in summer acceleration as the transition from an inefficient distributed drainage system to an efficient channelised one occurs more quickly, limiting the time frame for large spikes in water pressure (and therefore ice velocity) to occur (*Joughin et al.*, 2008a; *Van de Wal et al.*, 2008; *Schoof*, 2010; *Pimentel and Flowers*, 2010; *Sundal et al.*, 2011).

Recently, however, we have had the opportunity to compare ice velocities along a land-terminating transect in west Greenland in years with contrasting melt seasons. Summer temperatures in 2009 were approximately the same as the 1960-2010 average, while in 2010 they were approximately 2.5°C warmer. At the Leverett Glacier catchment this resulted in twice the runoff in 2010 compared with 2009 (*Nienow et al.*, submitted; *Chapter 7*). Significantly, at sites nearest the margin where meltwater reaches the ice-bed interface abundantly, the summer acceleration signal was not reduced - rather it increased slightly. Further inland, where ice is thicker and melt rates lower, the acceleration was proportionally much greater in 2010 over 2009 compared to marginal sites. These

findings suggest very strongly that the timing of a transition from predominantly distributed to channelised drainage does not necessarily control inter-annual variations in ice velocity and, therefore, that we should not understand subglacial water pressure in terms of the steady-state behaviour of the subglacial drainage system.

Subglacial conduits adjust in size to accommodate variations in meltwater discharge over timescales of days or more (e.g. *Röthlisberger*, 1972; *Spring*, 1980; *Röthlisberger and Lang*, 1987; *Cutler*, 1998; *Schoof*, 2010), while meltwater delivery can vary significantly over much shorter periods. It is unlikely, therefore, that steady-state conditions ever exist in reality (*Röthlisberger*, 1972). Temporary imbalance between the volume of water delivered to a subglacial drainage system and its ability to evacuate that water are accommodated by temporary spikes in subglacial water pressure *even once the drainage system has become channelised* (*Röthlisberger and Lang*, 1987; *Schoof*, 2010).

This raises a possible alternative explanation for ice acceleration in land-terminating margins of the GrIS: that a large part of the seasonal acceleration signal may result from the aggregation of short-term speed-up events which are caused by overfilling of the drainage system in response to time-varying inputs of meltwater. Using this logic, it has been suggested that the discrepancy between early and late summer ice velocities in the GrIS (*Bartholomew et al.*, 2010; *Sundal et al.*, 2011; *Bartholomew et al.*, 2011b; *Nienow et al.*, submitted; *Chapter 7*) occurs because over-pressurised conditions are common on the rising limb of seasonal meltwater production, regardless of drainage system structure, as the system is constantly challenged to evacuate larger quantities of water than before (*Bartholomew et al.*, 2011b; *Nienow et al.*, submitted; *Chapter 7*). The late summer decline in ice velocities is due, then, to a decline or stabilisation of water input, which allows the subglacial drainage system to adjust to accommodate the water at lower pressures. In this scenario, channelisation of the drainage system would be a prerequisite for the late summer decline in ice velocity, but is not sufficient to cause a drop in subglacial water pressure without a reduction in meltwater input.

The purpose of this paper is to provide a reassessment of the role of drainage system behaviour in mediating the relationship between meltwater and ice velocity in land-terminating section of the GrIS margin. In the first part of the paper, we present high temporal resolution ice velocity measurements, derived from global position system

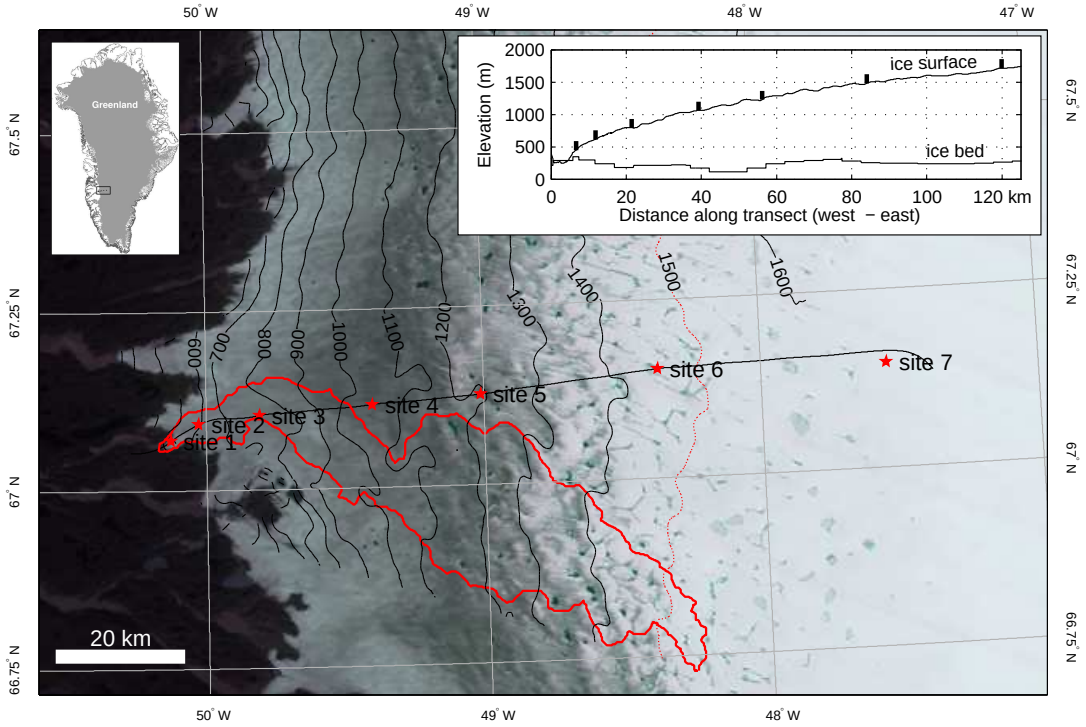

Figure 8.1: Map showing the location of the transect on the western margin of the GrIS. The sites where GPS and temperature measurements were made are indicated by red stars and the hydrological catchment of the proglacial river at Leverett Glacier is delineated in red. Contours are produced from a digital elevation model (DEM) derived from InSAR (*Palmer et al.*, 2011). The long-term ELA in the region is located at around 1500 m (*Van de Wal et al.*, 2005). The ice sheet profile (inset) is derived from surface elevation data collected during an airborne geophysical survey in 2010 (black line; *Krabill*, 2010) and bed elevation data which is sampled from a DEM of the whole ice sheet (*Bamber et al.*, 2001).

(GPS) observations, along a land-terminating transect at ∼67°N in western Greenland during the 2009 and 2010 melt seasons (Figure 8.1). The ice motion record is compared with *in situ* observations of air temperatures, as well as with proglacial hydrological data from the Leverett Glacier catchment which overlaps the lowest three sites (Figure 8.1; *Bartholomew et al.*, 2011a). These data reveal the detailed structure of ice velocity variations which make up the seasonal acceleration signal, allowing us to investigate the relationship between variations in meltwater input and ice velocity on seasonal and shorter-term timescales. In the second part of the paper, we use a simple model of the behaviour of a subglacial conduit to assess whether the features of the ice acceleration signal can be explained as a response of subglacial water pressure to time-varying water input.

8.2 Field site and previous studies

The key features of the seasonal acceleration signal along this transect have been identified in two previous studies using daily ice velocities from the summers of both 2009 and 2010 (*Bartholomew et al.*, 2011b; *Nienow et al.*, submitted; *Chapter 7*). Measurements were made at 7 sites up to 1716 m elevation, which is ∼115 km inland from the GrIS margin (Figure 8.1). The lowest elevation site is located on Leverett Glacier and is approximately 2 km from the glacier terminus. The seasonal development of the drainage system in the part of the ice sheet from which runoff drains through the Leverett Glacier snout (Figure 8.1, red outline) was also investigated in a hydrological study from 2009 (*Bartholomew et al.*, 2011a).

All of the sites along the transect experience summer acceleration, where ice velocities are raised above winter background rates, in both 2009 and 2010. Initial acceleration follows the onset of surface melting at each site, which occurs at progressively higher elevations through the summer (Figures 8.2 - 8.5; *Bartholomew et al.*, 2011b; *Nienow et al.*, submitted; *Chapter 7*). The initiation of locally-forced velocity variations is characterised by rapid horizontal acceleration which is coincident with uplift of the ice sheet surface. This is indicative of initial access of surface meltwaters to the ice-bed interface and is analogous to 'spring-events' widely reported from Alpine and High Arctic glaciers (e.g. *Iken*, 1981; *Mair et al.*, 2001; *Anderson et al.*, 2004; *Bingham et al.*, 2008). At site 7 there was no surface uplift in 2009 and very little in 2010. The minor acceleration at this site is attributed to the effect of coupling to faster ice downglacier (*Bartholomew et al.*, 2011b; *Nienow et al.*, submitted; *Chapter 7*).

The highest velocities, which peaked at site 2 at over 500 m y^{-1}, and greatest overall seasonal acceleration, were achieved at sites nearest the ice sheet margin (*Nienow et al.*, submitted; *Chapter 7*). At lower elevation sites, where melt rates are higher (Figures 8.2 & 8.4) and the ice is less thick (Figure 8.1), initial acceleration closely follows the onset of surface melting. Ice velocities at these sites are higher in early-summer than in late summer (*Nienow et al.*, submitted; *Chapter 7*). This is explained by the development of an efficient subglacial drainage system, in response to abundant meltwater input from the ice sheet surface, which is able to evacuate larger discharge at lower pressures than

earlier in the summer (*Bartholomew et al.*, 2011a,b; *Nienow et al.*, submitted; *Chapter 7*).

At sites further inland, however, there is a greater delay between the onset of melting and ice acceleration as melt rates are lower and it takes longer to accumulate enough meltwater to penetrate through thicker ice to the bed (*Bartholomew et al.*, 2011b). In addition, it is likely that there is significant delay associated with flow through the snowpack to supraglacial streams (e.g. *Campbell et al.*, 2006). This delay between the onset of melting and drainage of water from the ice surface to its bed is responsible for the lower overall acceleration as it limits the time frame for velocity variations to occur (*Bartholomew et al.*, 2011b). Accumulation and drainage of stored water in the form of supraglacial lakes may be particularly important in forcing a hydraulic connection between the ice sheet surface and its bed at higher elevations (*Bartholomew et al.*, 2011a,b).

8.3 Data and methods

8.3.1 GPS data

We used dual-frequency Leica 500 and 1200 series GPS receivers to collect the season long records of ice motion at each site. Each GPS antenna was mounted on a pole drilled several metres into the ice, which subsequently froze in, providing measurements of ice motion that were independent of ablation. The GPS receivers collected data at 30 second intervals in 2009 and the first part of 2010. The data were processed using a kinematic approach (*King*, 2004) relative to an off-ice base station at Kelyville, approximately 40 km west from the snout of Leverett Glacier, using the Track 1.21 software (*Chen*, 1999; *King and Bock*, 2006). In June 2010 we installed a new off-ice reference station less than 2 km from the Leverett Glacier snout, which collected data at 10 second intervals. Conservative estimates of the uncertainty associated with positioning at each epoch are approximately ± 1 cm in the horizontal direction and ± 2 cm in the vertical direction. The data were smoothed using a Gaussian low-pass filter to suppress high-frequency noise without distorting the long-term signal. Short-term variations in ice velocity were derived by differencing positions across a 6 hour sliding window, applied to the

whole timeseries of filtered positions for each site. This window length was chosen in order to highlight short-term variations in the velocity records while retaining a high signal to noise ratio. Estimates of horizontal velocity magnitude are therefore minimum estimates. Unfortunately, the quality of the GPS data at site 1 was compromised by technical problems, making it difficult to resolve short-term variations in horizontal velocity at this site.

Uncertainties associated with the filtered positions are <0.5 cm in the horizontal and <1 cm in the vertical directions, corresponding to annual horizontal velocity uncertainties of <14.6 m yr^{-1} for the 6 hour velocity measurements. We used the standard deviation of the 6 hour sliding window velocities from site 7, which has the longest processing baseline and experienced negligible velocity variations, to estimate the noise floor in the GPS velocity records. The standard deviations for the 6 hour velocities at site 7 are 19.5 m yr^{-1}. These values compare well with the calculated uncertainties and represent conservative error estimates for our dataset. The values for winter background ice-velocities are derived from the displacement of each GPS receiver between the end of the summer melt season and the following spring (*Bartholomew et al.*, 2010). The reported contribution to annual ice flux from the hydrologically-forced summer ice velocity variations is the percentage by which the observed annual displacement exceeds that which would occur if the ice moved at winter rates all year round.

8.3.2 Air temperate and surface ablation

Simultaneous measurements of air temperature were made at each GPS site to constrain melt rates, and show that the velocity data cover the whole seasonal melt cycle. Measurements of air temperature were made using shielded Campbell Scientific T107 temperature sensors connected to Campbell Scientific CR800 dataloggers (sites 1, 3 and 6) and shielded HOBO U21-004 temperature sensors (sites 2, 4, 5 and 7) at 15 minute intervals throughout the survey period. Seasonal melt totals were also measured using ablation stakes at each GPS site.

8.3.3 Proglacial discharge

We made continuous measurements of water stage in the proglacial stream that emerges from the terminus of Leverett Glacier. Proglacial discharge was derived from a continuous stage-discharge rating curve calibrated with repeat dye dilution gauging experiments throughout the melt-season as described in *Bartholomew et al.* (2011a).

8.4 Observations

8.4.1 Hydrological forcing of ice acceleration

The high temporal-resolution GPS data confirm the main findings of previous studies along this transect. The initiation of locally-forced velocity variations is characterised by rapid horizontal acceleration which is coincident with uplift of the ice sheet surface. This is indicative of initial access of surface meltwaters to the ice-bed interface and is analogous to 'spring-events' widely reported from Alpine and High Arctic glaciers (*Iken*, 1981; *Mair et al.*, 2001; *Anderson et al.*, 2004; *Bingham et al.*, 2008).

At the sites nearest the margin, which lie within the Leverett Glacier hydrological catchment, the spring-events are most dramatic and coincide with the outburst of a pulse of meltwater from beneath the glacier (Figures 8.2 & 8.4). For example, at sites 1 and 2, ice velocities in the spring event exceeded 400 - 500 m yr^{-1} in 2010, and was coincident with a rise in proglacial discharge from less than 10 m^3 s^{-1} to 50 m^3 s^{-1} over three days. The spring-events at site 3 in both 2009 and 2010 are also coincident with pulses of meltwater from Leverett Glacier. The hydrological signature of these outbursts shows that the water is both ion-rich and sediment-laden which indicates the flushing out of stored water from an inefficient drainage system (*Bartholomew et al.*, 2011a).

At sites 1 - 3, the spring-event follows a period of warm temperatures and typically lasts a few days (up to a week), building to a sharp peak before velocities return to background levels. The decline in velocities that follows is coincident with levelling-off or a fall in discharge as well as a return to cooler temperatures. Further inland, at the sites which lie outside the Leverett Glacier catchment, the initial locally-forced velocity events are smaller (Figures 8.3 & 8.5). The uplift signal at sites 4 - 6 is more a change

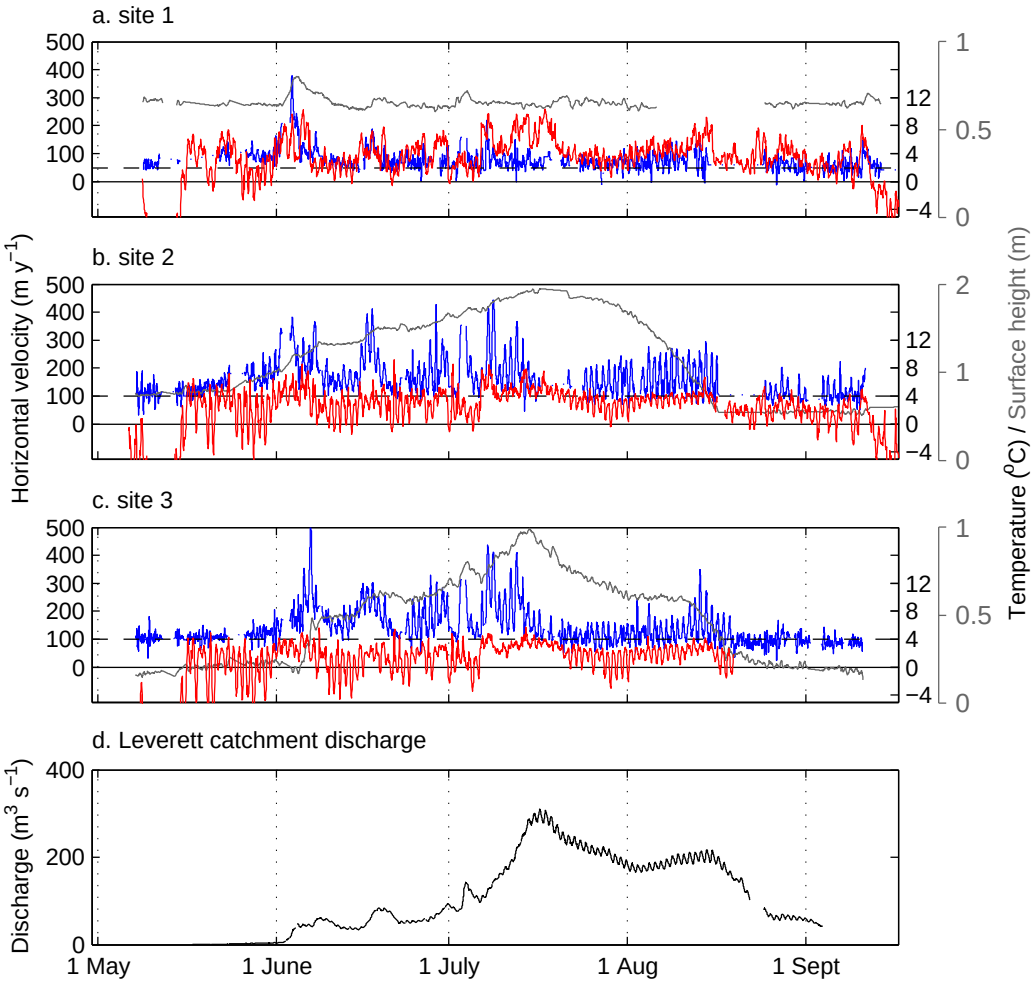

Figure 8.2: a-c. Ice velocity (blue), surface height profile (grey) and air temperature (red) at sites 1 - 3 during the 2009 summer melt season. The surface height profile is shown relative to an arbitrary datum and has a linear, surface parallel, trend removed. Winter background ice velocity (black dashes) is determined from displacement of the GPS sites during winter 2009/2010. d. Discharge from the Leverett Glacier proglacial river during the 2009 summer melt season.

in trajectory than a steep rise, and velocities increase by 50 - 100 % rather than the 300 - 400 % observed at sites 1 - 3 (Figures 8.3 & 8.5). At these sites, the initial acceleration is also sustained for a longer period of time, without the marked drop-off back to winter levels.

Most sites exhibit slight speed-up in the absence of surface uplift prior to the first major speed-up event of the summer. The most obvious example is site 2, which displays a short acceleration in the absence of any surface uplift between approximately May 5th - May 12th in 2010. This feature of the acceleration signal is likely due to coupling

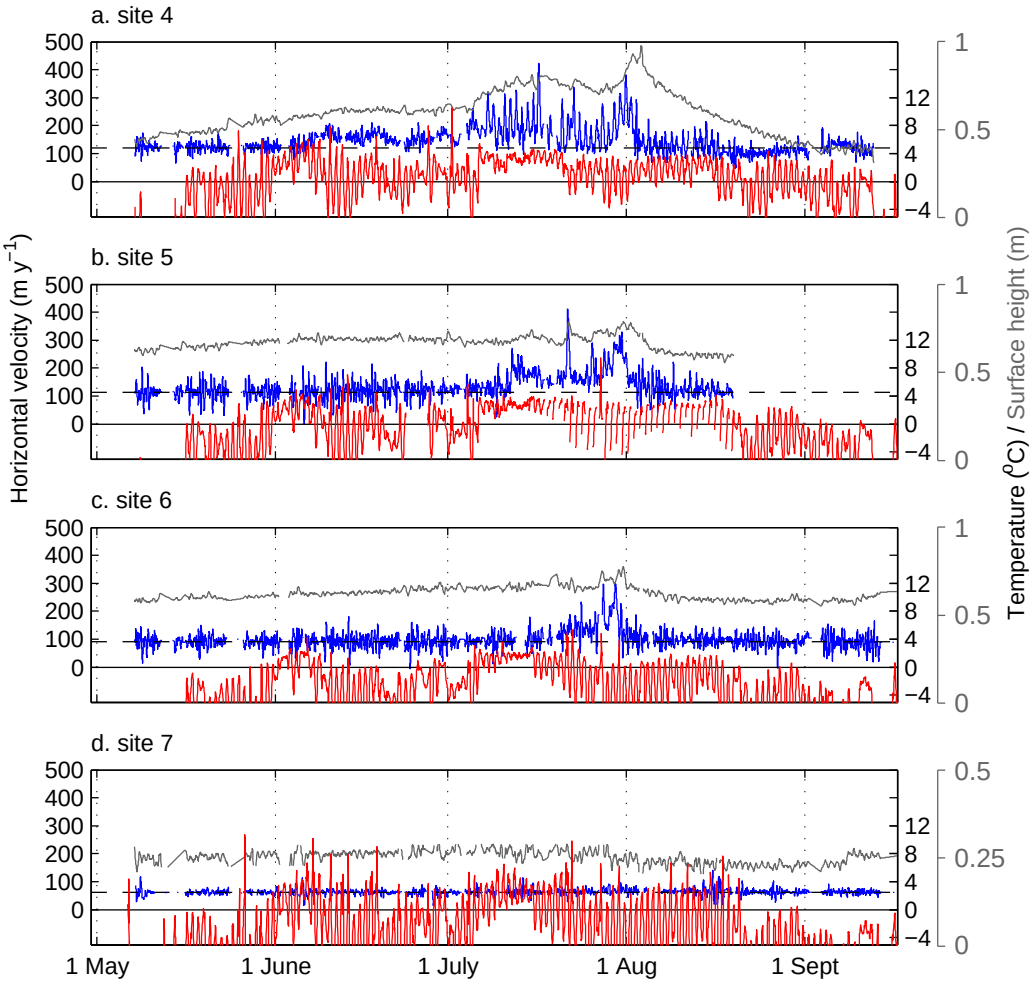

Figure 8.3: a-d. Ice velocity (blue), surface height profile (grey) and air temperature (red) at sites 4 - 7 during the 2009 summer melt season. The surface height profile is shown relative to an arbitrary datum and has a linear, surface parallel, trend removed. Winter background ice velocity (black dashes) is determined from displacement of the GPS sites during winter 2009/2010.

to faster moving ice further downglacier (*Price et al.*, 2008; *Bartholomew et al.*, 2010, 2011b). At the most marginal sites this longitudinal coupling phase lasts only for a matter of days, while at higher sites it can last from a few days up to a number of weeks (Figures 8.2 - 8.5). For example, at site 4 in 2009 ice velocities are raised by approximately 50 % compared with winter background rates for the month of June before uplift of the ice surface occurs on July 5th and velocity is raised to more than 200 m y^{-1}.

Previous studies have found that longitudinal coupling is not effective over length

scales of ∼10 km along this transect on the basis that, in the early season, initial speed-up of the most marginal sites has little effect on ice motion further inland (*Bartholomew et al.*, 2010, 2011b). Similarly, we are unable to account for the horizontal acceleration that precedes initial uplift of the ice surface through longitudinal coupling over length scales determined by the site separation distances in our dataset. We acknowledge, therefore, that some part of the velocity signal at each site is due to non-local forcing. The coupling distance is relatively short (<∼ 10 km), however, and even though the length-scale over which coupling is effective might be increased once water drains to the ice-bed interface, the magnitude of the signal appears to be much smaller than velocity changes which are due to local hydrological forcing. At site 7 there was no surface uplift in 2009 and very little in 2010. The minor acceleration at this site is also attributed to the effect of coupling to faster ice downglacier (*Bartholomew et al.*, 2011b; *Nienow et al.*, submitted; *Chapter 7*).

8.4.2 Short-term variations in ice velocity

Following the spring-events, the ice motion record from sites 1 - 3 is dominated by short-term velocity variations on timescales ranging from a few hours to several days. Multi-day speed-up events, which are characterised by an increase in ice velocities lasting for more than a single day during which ice velocity does not return to background levels, occur at all sites except for site 7 in both 2009 and 2010 (Figures 8.2 - 8.5). Examples of such events occur in 2009 at sites 1 - 3, which all experience velocity increases of more than 100% between June 1st - June 10th. Similar events also occur at these sites in 2010 between May 20th - June 1st, and from June 4th - June 9th at sites 2 and 3. During these multi-day events, ice velocity can increase by more than 200 m yr^{-1} within 24 hours (Figures 8.2 and 8.4) and does not return to background levels for an extended period. Multi-day velocity events also occur at higher elevations in both 2009 and 2010. For example, at sites 4, 5 and 6 between July 23rd - August 1st in 2009, and at sites 5 and 6 from July 18th - 24th in 2010.

Without exception, these speed-ups are accompanied by uplift of the ice sheet surface, pointing to *local* hydrological forcing (*Bartholomew et al.*, 2010) as their cause. The most rapid surface uplift appears in conjunction with the most dramatic horizontal

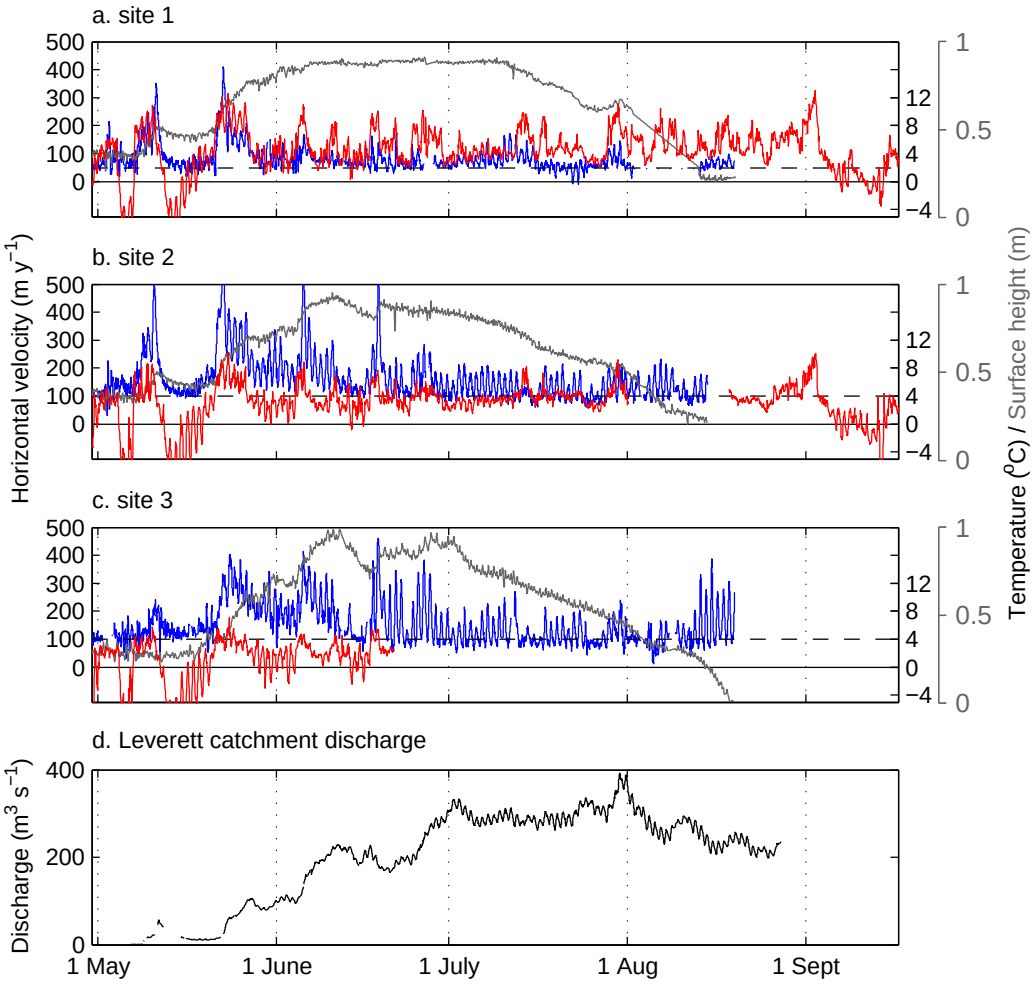

Figure 8.4: a-c. Ice velocity (blue), surface height profile (grey) and air temperature (red) at sites 1 - 3 during the 2010 summer melt season. The surface height profile is shown relative to an arbitrary datum and has a linear, surface parallel, trend removed. Winter background ice velocity (black dashes) is determined from displacement of the GPS sites during winter 2009/2010. d. Discharge from the Leverett Glacier proglacial river during the 2010 summer melt season.

acceleration. At sites 1 - 3 these high velocity events are associated with steep rises in proglacial discharge, linking them to increased water flux through the subglacial drainage system. Strikingly, the surface height profiles of sites 2 and 3 in both 2009 and 2010 mirror the discharge curve measured at Leverett Glacier. The association is less clear at site 1, where the GPS data was of poorer quality, although the largest rises in discharge are still matched with uplift of the ice surface.

The majority of the multi-day events at sites 1 - 3 appear to be forced by periods of raised temperatures which increase the volume of meltwater input to the subglacial

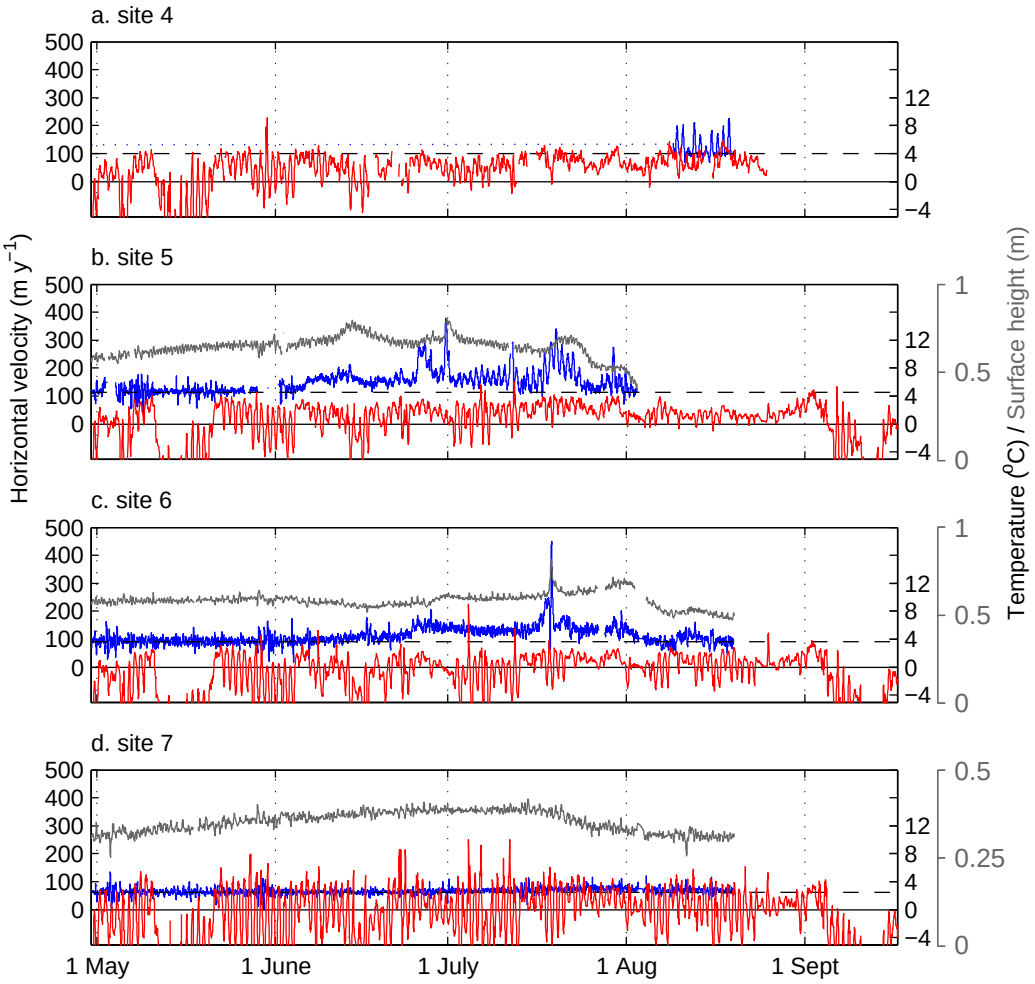

Figure 8.5: a-d. Ice velocity (blue), surface height profile (grey) and air temperature (red) at sites 4 - 7 during the 2010 summer melt season. The surface height profile is shown relative to an arbitrary datum and has a linear, surface parallel, trend removed. Winter background ice velocity (black dashes) is determined from displacement of the GPS sites during winter 2009/2010.

drainage system for a short time (Figures 8.2 & 8.4). In some cases, however, ice velocities are raised for a number of days in the absence of high temperatures. For example, in 2009 velocities are raised at sites 1 - 3 between July 3rd - 8th , which was a period of colder temperatures (Figure 8.2), although the event is still associated with ice surface uplift and a temporary increase in discharge at Leverett Glacier. The hydrological signature of this meltwater pulse indicates drainage of large volumes of stored water from the ice sheet surface, which was delivered to the ice sheet margin via the ice-bed interface (*Bartholomew et al.*, 2011a), in a manner similar to the spring-

events. The likely source for this water was identified, using satellite imagery, as a supraglacial lake within the Leverett Glacier catchment (*Bartholomew et al.*, 2011a).

The highest velocity events at sites 4, 5 and 6 in both 2009 and 2010 are also not closely linked to warm air temperatures and we suggest that these are also caused by sudden drainage of stored water from the ice sheet surface. Satellite imagery from 2009 shows lake drainage events, where supraglacial ponds disappear from the ice sheet surface in consecutive images, in close proximity to these sites at times which correspond to the velocity events (*Bartholomew et al.*, 2011b). Further, in 2010 we captured the rapid drainage of a lake which had accumulated less than 2 km from site 6 using timelapse photography. Drainage of this lake coincided with a 400 % increase in ice velocity on July 17th and uplift of the ice sheet surface of 0.3 m in less than 24 hours (Figure 8.6). Both variations in temperature and periodic drainage of meltwater which has accumulated at the ice sheet surface can therefore cause ice acceleration by raising meltwater input to the drainage system over a period of a few days.

8.5 Diurnal velocity cycles

The detailed velocity records also reveal clear daily cycles in ice motion at a number of the sites. These daily cycles are most clear at sites 2, 3 and 4 and their amplitude ranges from less than 50 m y^{-1} to over 300 m y^{-1}, ~300 % of winter background rates. At these sites, the total motion due to diurnal acceleration makes up a significant portion of the seasonal acceleration signal, particularly in the latter part of the melt season. They are also evident at site 1, although the relatively slow background velocity and technical problems with the GPS receiver mean that they are harder to resolve. In 2010, which was a significantly warmer year than 2009 (*Nienow et al.*, submitted; *Chapter 7*), daily cycles in ice velocity develop at site 5 from early July until the beginning of August. There are no daily cycles in either year, however, at site 6 or 7.

Daily cycles in ice velocity develop at sites 2 - 4 in 2009 following the beginning of locally-forced acceleration. The behaviour is very similar in 2010, although ice velocities are dramatically reduced at sites 1 and 2 after the spring-event due to a period of sub-freezing temperatures. When temperatures rise again, there is another multi-day

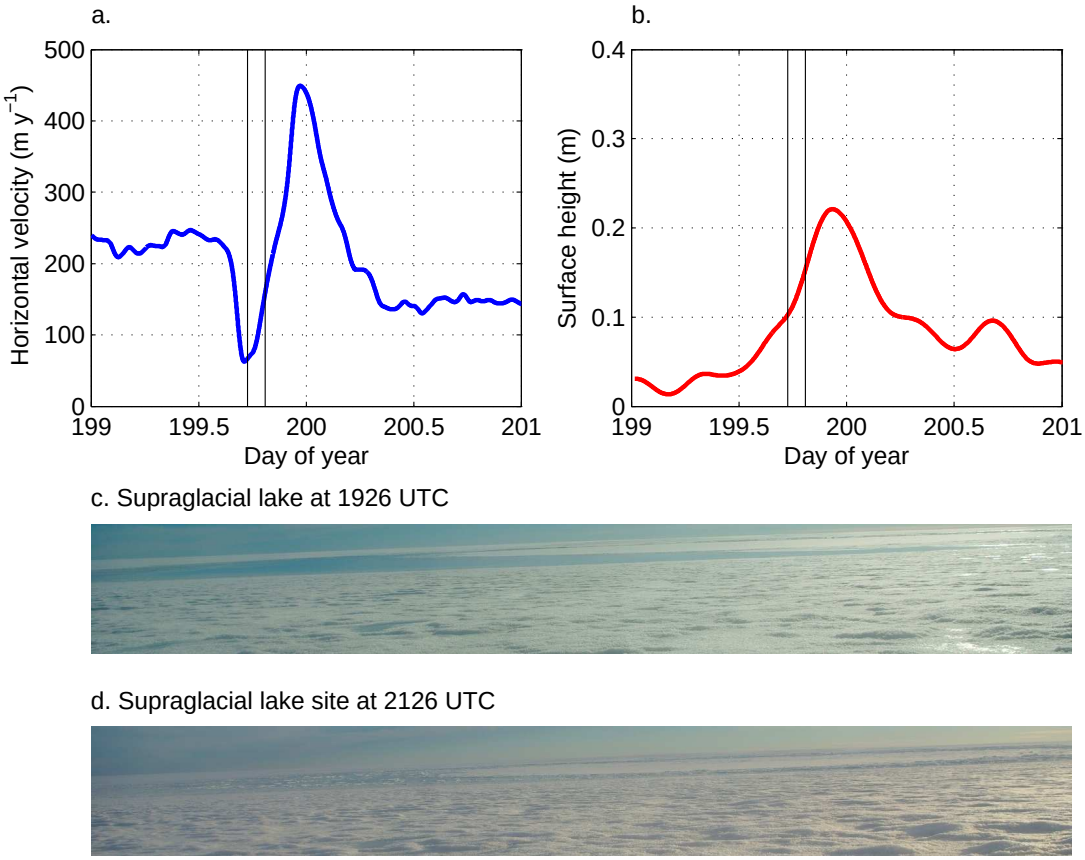

Figure 8.6: a. Surface velocity at site 6 during the lake drainage event which occurred <2 km from the GPS receiver on July 18th 2010. b. Surface height profile during the lake drainage event. c & d. Before and after images of the supraglacial lake drainage event taken by a timelapse camera mounted on the support pole at site 6. The time at which the photos were taken is marked on the velocity and height profiles by vertical black lines.

acceleration following which daily cycles begin. The daily velocity cycles at site 5 in 2010 develop later in the melt season, around June 24th, and their magnitude is from around 50 - 150 m y^{-1}, slightly lower than those nearer the ice sheet margin. Once developed, these extremely rapid variations in ice velocity appear to be superimposed on the seasonal velocity signal, and, in the absence of other events, ice velocity consistently returns to around winter background rates on a diurnal basis (Figures 8.2 - 8.5). At sites 2 and 3 in 2009, for which we have the longest ice velocity and discharge records it is clear that the cycles become subdued when discharge rapidly declines after August 18th.

Where daily cycles in ice velocity are evident, their timing is closely related to variations in both local temperatures and discharge from Leverett Glacier (Figure

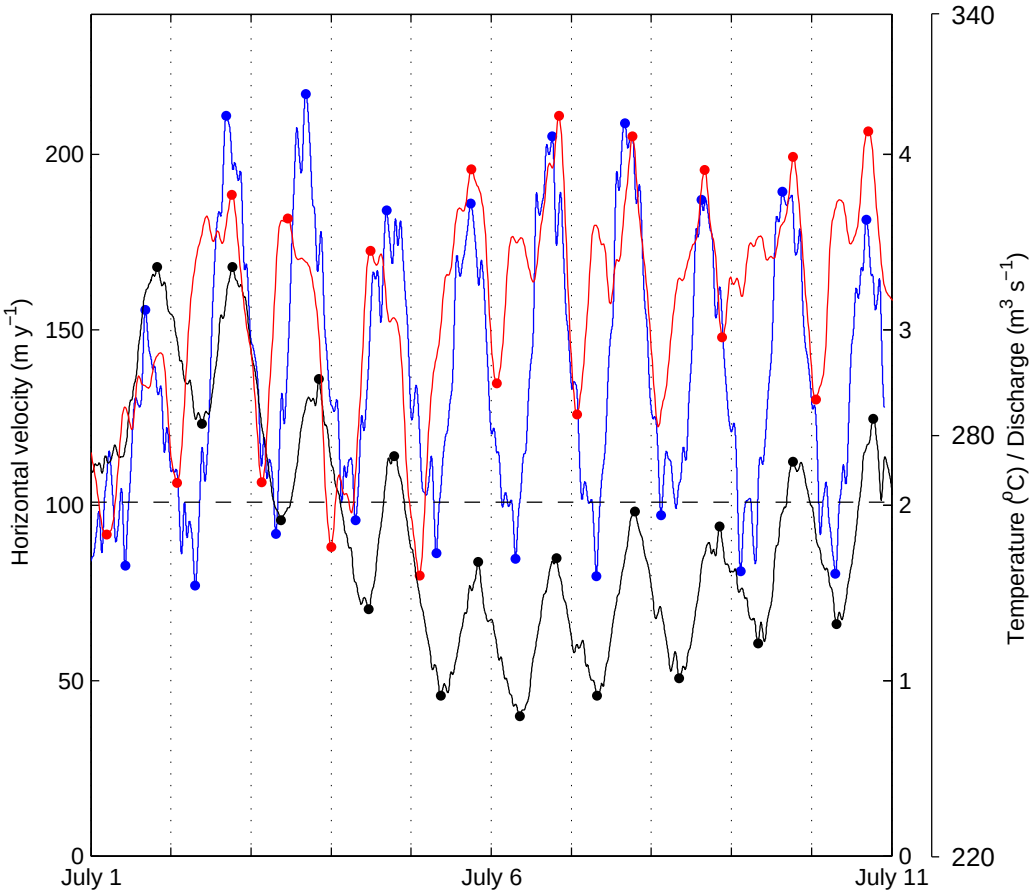

Figure 8.7: Detailed record showing the temporal relationship between diurnal cycles in ice velocity (blue), air temperature (red) and proglacial discharge (black) at site 2 between July 1 and July 10, 2010. Daily peaks and troughs are marked by coloured dots. Winter background ice velocity is indicated by a black dashed line.

8.7). By taking the mean difference in time between daily peaks in velocity and local temperature peak at each site we find that velocity lags temperature by 2 - 4 hours. This pattern is consistent across both years and between all of sites which experience daily cycles, although there is some variability on a day-to-day basis, as evidenced in Figure 8.7. Despite this variability in the lag between peak daily velocity and peak daily temperature, there is no discernible seasonal pattern. Previous studies found a similar delay and have suggested that this reflects a plausible transit time for supraglacial meltwater to collect and drain into the englacial drainage system before reaching the ice-bed interface (*Shepherd et al.*, 2009; *Bartholomew et al.*, 2011b). A couple of factors complicate this observation, however, and may explain the variability we see on a short-

term basis. Firstly, the resolution of the data makes it difficult to identify the timing of daily peaks in all variables (Figure 8.7). Secondly, the timing of the temperature peak does not necessarily coincide with peak melt, as melt rates are strongly influenced by local variations in incoming solar radiation (e.g. *Hock*, 2003).

By contrast with the temperature signal, daily peaks in ice velocity at sites 1, 2 and 3 precede the daily discharge peak at Leverett Glacier by 2.5, 1.6 and 1.2 hours on average respectively. This pattern is also consistent across both years and there is no seasonal signal. Daily velocity cycles at Site 4 in 2009 are almost in phase with discharge and at site 5 in 2010 the peak in ice velocity follows the peak in discharge. Since these sites lie outside of the Leverett Glacier hydrological catchment, however, there is little reason to imply cause and effect.

In common with longer term variations in ice velocity, therefore, daily cycles appear to be forced by increased meltwater flux through the subglacial drainage system. Although we cannot unequivocally resolve daily cycles in the surface uplift record, we argue that the sheer magnitude of these velocity variations suggests that they are forced locally and are not due to coupling to ice further downglacier. We can find no systematic relationship, however, between the magnitude of the daily cycles and daily range, peak or mean values in either temperature or discharge. Tentatively, we find the largest amplitude cycles in ice velocity at sites 2 and 3 in the early part of the melt season in both years, although there are some periods in the latter half of the season when the magnitude of daily velocity variations can still exceed 150% of winter background.

8.6 Discussion - velocity, temperature, discharge & drainage

Our data show that the ice velocity records at sites 1 - 3 in 2009 and 2010 are comprised of four main components which integrate to form the seasonal acceleration:

i. Slight acceleration, in the absence of surface uplift, which is attributed to coupling of faster moving ice further downglacier.

ii. Locally-forced velocity variations initiate with a spring-event, in a manner similar to Alpine and High Arctic glaciers, which indicates initial access of surface meltwater to the subglacial drainage system.

iii. Further events occur where ice velocity is raised above winter background rates for a number of days, particularly in the early part of the summer melt season. These events are forced by increased meltwater delivery to the subglacial drainage system, due either to increased surface ablation, or drainage of stored water which has accumulated at the ice sheet surface.

iv. Large diurnal variations in ice velocity which develop early in the melt-season, typically following initial access of surface meltwater to the ice-bed interface, persist for nearly all of the melt season until melting stops. Temporal association with daily cycles in air temperature and discharge from Leverett Glacier indicates that these are also forced by variations in meltwater delivery to the subglacial drainage system, although there is no clear correlation between the magnitude of daily velocity changes and variability in either of these variables.

In the short-term, changes in ice velocity, and therefore water pressure in the subglacial drainage system, are in phase with meltwater discharge from the Leverett Glacier snout. Over the full melt-season, however, this is not the case. Mean ice velocities are lower in late summer, following peak discharge, than in early summer. If we assume that the subglacial drainage system is distributed and inefficient prior to the spring-events, following the winter period, this observation indicates that the drainage system becomes channelised at some point during the melt season, and that this limits the overall summer acceleration (*Bartholomew et al.*, 2010, 2011b; *Sundal et al.*, 2011; *Nienow et al.*, submitted; *Chapter 7*).

Inspection of the detailed structure of the ice velocity records from sites 1 - 3 reveals that the discrepancy between early and late summer velocities (*Nienow et al.*, submitted; *Chapter 7*) is due to the the absence of multi-day speed-up events in the latter part of the summer melt season. They dominate the early season velocity records but do not appear once discharge has peaked and/or stabilised, while daily cycles in ice velocity are evident through most of the melt season (Figures 8.2 and 8.4). In late summer, therefore, either the signal which forces short-term variations in ice motion is different from early summer, or the drainage system has developed to become less responsive to the same forcing.

Two observations suggest the former. Firstly, multi-day events are associated with steep rises in proglacial discharge which are largely absent in the late season. The hydrological study from this catchment in 2009 showed that an efficient subglacial drainage system expands upglacier from the ice sheet margin, at the expense of the inefficient winter drainage configuration, in response to inputs of meltwater from higher elevations as the melt season progresses (*Bartholomew et al.*, 2011a). Increasing proglacial discharge therefore represents not only increasing temperatures, but an expanding area of the ice sheet surface from which meltwater is delivered, via the subglacial drainage system, to the ice sheet margin. Hydrological parameters such as ion-concentration and suspended sediment concentration also indicate that this process results in continued evolution of the drainage system until the catchment reaches its full inland extent (presumably meltwater from higher elevations drains through a different outlet glacier), at which point the drainage system reaches a more stable state (*Bartholomew et al.*, 2011a). We suggest, therefore, that the multi-day events on the rising limb of discharge are the consequence of pressure increases in a subglacial drainage system which is continually expanding to accommodate extra sources of meltwater. Once the drainage system has fully expanded, the discharge becomes more stable and these events are less likely to occur. Secondly, the large daily cycles indicate that velocity *is* still responsive to variations in meltwater input on a short-term basis, even once the subglacial drainage system has become channelised. This suggests that large pulses of meltwater, derived from increased surface melting over a wider area or drainage of stored supraglacial water, would still have the capacity to cause a large increase in ice velocity should they occur.

The observations from sites 1 - 3 are not easily explained by a transition from a predominantly distributed drainage system to a channelised one (cf. *Sundal et al.*, 2011). Preliminary dye-tracing experiments performed in 2010 indicate channelised drainage conditions between site 2 and the ice sheet margin on May 31st, and from 14 km along the transect on June 2nd (T. Cowton, pers. comm). Ice velocities at site 2 exceeded 500 m y^{-1} on June 5th and 18th of that summer, however, during the peaks of two separate multi-day acceleration events. This indicates that transition from a distributed to channelised drainage system does not inhibit the large multi-day events

which our data have revealed as the cause for the difference between early and late summer velocities. It is likely that pressure within the channelised drainage system *does* become less sensitive to variations in meltwater input over the course of the melt season, to some extent. As discharge into the system increases, subglacial channels will get larger and more water will be required to over-pressurise them. Since this effect is not pronounced in our dataset, however, variability in the forcing signal appears to exert the greatest control on changes in ice velocity.

At sites which are at higher elevations along the transect (>1000 m), the velocity record is also marked by hydrologically-forced acceleration in the same manner as identified in the record at sites 1 - 3, which make up the pattern of summer acceleration. Consistently raised ice velocities follow initial uplift of the ice sheet surface for all sites except site 7. At these sites there are locally-forced multi-day velocity events in both 2009 and 2010. Daily cycles in ice velocity occur at site 5 in 2010 from June 25th, although they do not appear in 2009 when air temperatures were cooler. There are no daily-cycles in ice velocity, however, that can be resolved by our GPS records at sites 6 or 7.

The thicker ice at higher elevation sites means that more water is required in order to initiate drainage to the ice-bed interface (*Van der Veen*, 2007; *Krawczynski et al.*, 2009) and observations from our field experience indicate that moulins are more scarce at higher elevations. Drainage of meltwater occurs in dramatic events which result in rapid channelisation of the subglacial drainage system (e.g. *Das et al.*, 2008). Lower melt rates also mean that, following drainage of a reservoir of stored water from the ice sheet surface, subsequent meltwater drainage is not sufficient to maintain high pressure within the now channelised drainage system and ice velocities are reduced again (*Bartholomew et al.*, 2011b).

The pattern of sporadic high velocity events, superimposed on slightly raised background velocity, suggests a cycle of intermittent local drainage events (*Das et al.*, 2008) which overwhelm the subglacial drainage system, combined with steady drainage to the ice-bed interface and coupling to faster moving ice downglacier (*Price et al.*, 2008). Daily cycles in ice velocity at lower sites appear to be caused by over-filling and drainage of a channelised subglacial drainage system in response to time-varying meltwater input

(*Bartholomew et al.*, 2011b). Diurnal variation in meltwater delivery to moulins at higher elevation sites is likely to be muted because moulins are spaced further apart and the snowpack remains for most of the summer making supraglacial travel times very long (*Nienow and Hubbard*, 2006; *Campbell et al.*, 2006). In the longer-term, following initial drainage of meltwater to the ice-bed interface, steady delivery of meltwater to the subglacial drainage means that the capacity of the system is in balance with inputs and short-term over-pressurisation is less likely to occur.

Our data do not show whether the drainage system beneath higher elevation sites remains channelised following initial drainage of meltwater. Although thicker ice increases creep closure rates in subglacial conduits, supraglacial streams can be large (>5 m^3 s^{-1}) and could conceivably maintain efficient conduits. If an efficient system cannot be sustained, however, lower ice velocities might be explained because the forcing is not great enough to raise water pressure over a wide enough area to have a significant impact on ice velocity (e.g. *Iken and Bindschadler*, 1986). The presence of daily cycles in ice velocity at site 5 in 2010 appears, therefore, to be caused by higher rates of surface melting. This favours early removal of the snowpack, allowing greater diurnal variability in meltwater supply to moulins. In addition, higher volumes of meltwater are also able to over-pressurise the drainage system more easily.

8.7 Subglacial conduit model

The basic physics of subglacial conduits can be described by a single equation for their cross-sectional area, S, which captures both cavity and R-channel behaviour (*Schoof*, 2010):

$$\frac{\partial S}{\partial t} = c_1 Q \frac{\partial \phi}{\partial s} + u_b h - c_2 N^n S \tag{8.1}$$

where Q is the water discharge, $\frac{\partial \phi}{\partial s}$ is the hydraulic gradient along the conduit and $N = p_i - p_w$ is the effective pressure in the conduit (ice overburden, p_i, minus water pressure, p_w). The first term on the right-hand side in equation 8.1 is the rate of conduit opening due to wall melting, the second term is opening due to horizontal sliding (at speed u_b) past bedrock obstacles (with height h) and the third is conduit closure due to

collapse under the weight of overlying ice. c_1 is a constant which is related to the latent heat of fusion for ice, L, by $c_1 = 1/(\rho_i/L)$, where ρ_i is the density of ice (910 kg m^{-3}). c_2 is equal to An^{-n} where A is Glen's flow law coefficient and $n = 3$ is the exponent in Glen's flow law for ice. Q can be related to S and $\frac{\partial \phi}{\partial s}$ by the Darcy-Weisbach law:

$$Q = \sqrt{\frac{8}{\rho_w f}} A^{3/2} \frac{\partial \phi}{\partial s}^{1/2} W^{-1/2} \tag{8.2}$$

where A is the filled cross-sectional area, W is the channel wetted perimeter, ρ_w is the density of water (1000 kg m^{-3}) and f is the Darcy-Weisbach friction factor. Equation 8.2 is a general case of the equation which was applied by *Schoof* (2010) for a full semicircular conduit. Analysis of equation 8.1 by *Schoof* (2010) demonstrates, for steady-state, that N decreases with Q below a critical threshold in Q, while at higher discharge N increases with Q, reflecting the transition from cavity to channel-like behaviour.

We present a simple model which uses Schoof's equation (our equation 8.1) to describe the behaviour of a subglacial conduit in response to time-varying water input in a configuration which is inspired by the approach used by *Cutler* (1998). In this model, a subglacial conduit is directly connected to a moulin that drains from the glacier surface to the ice sheet bed (*Catania and Neumann*, 2010). The moulin is subject to influx of meltwater from the ice sheet surface and a single, straight conduit, with semi-circular cross section, then drains from the moulin base to the ice margin (Figure 8.8). The model differs slightly from that used by *Cutler* (1998) in that we do not attempt to account for changes in the shape of the channel cross-section. By employing equation 8.1, however, we are able to incorporate both cavity and R-channel type behaviour (*Schoof*, 2010).

The moulin is considered to be a vertical circular pipe with constant radius, r_m which is fed by a supraglacial stream for which the discharge, Q_{in}, can be prescribed. A reservoir of depth h_r and radius r_r, sits at the top of the moulin and represents a small supraglacial pond which allows water to collect at the ice sheet surface if the moulin should overflow. The height of the moulin is then equal to the ice thickness, H, minus d_r at its top, and the channel radius at the moulin base (Figure 8.8).

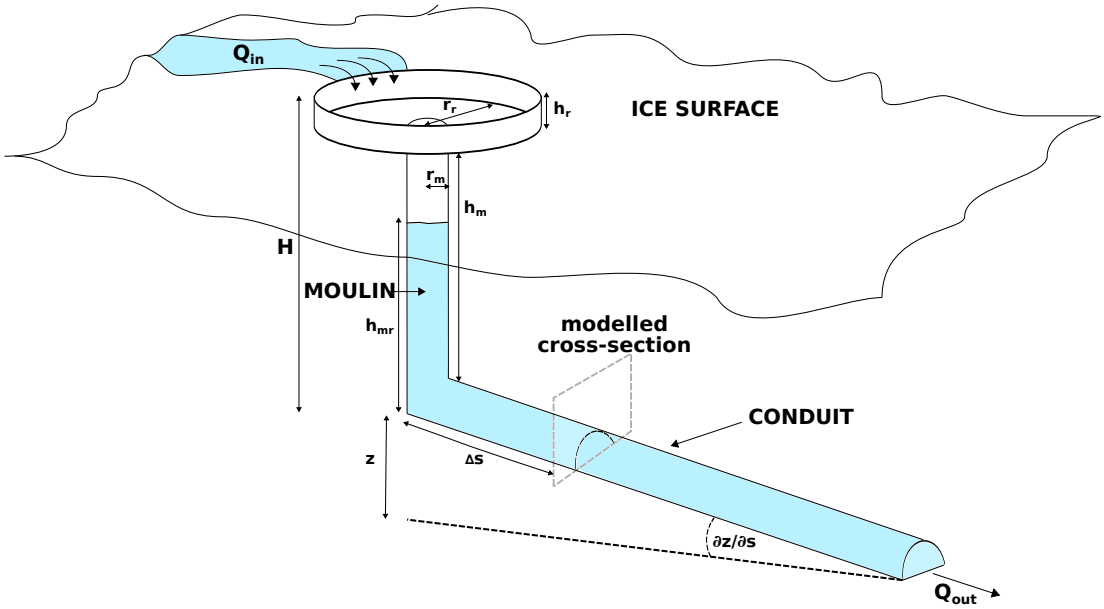

Figure 8.8: Schematic showing the model configuration. The drawing is not to scale. Symbols are defined in the text.

Water flow through the conduit is calculated using equation 8.2. The conduit has a uniform gradient, $\frac{\partial z}{\partial s}$ over its complete length, s. $\frac{\partial \phi}{\partial s}$, which drives water flow, results from a combination of both $\frac{\partial z}{\partial s}$ and $\frac{\partial h_{mr}}{\partial s}$, where h_{mr} is a function of hydraulic head in the moulin/reservoir section of the system. It is also assumed that $\frac{\partial \phi}{\partial s}$ is constant along the conduit and that water emerges at the glacier margin at atmospheric pressure.

We use the model to simulate channel cross-section evolution at a distance Δs from the base of the moulin (Figure 8.8). We assume that ice thickness is constant in the vicinity of the cross-section, negating the effect of glacier geometry on hydraulic potential (cf. *Shreve*, 1972). In addition, in this model the conduit rests on bedrock (i.e. no water is lost into a subglacial aquifer) and there is no energy transfer between the water and the channel bed.

At each time step, water volume within the system is determined in accordance with the conservation of mass:

$$\frac{\partial V}{\partial t} = Q_{in} - Q_{out} \tag{8.3}$$

which allows us to calculate the hydraulic head within the the moulin/reservoir. If there is no water stored in the moulin then open-channel flow occurs and the hydraulic

gradient is simply a function of $\frac{\partial z}{\partial s}$. If no water is backed up in the conduit, Q_{out} falls to be equal to Q_{in}. In the case of open-channel flow, melting is concentrated only on the wetted perimeter of the channel. In order to simplify the model, however, this melting is distributed across the whole channel boundary in the $\frac{\partial S}{\partial t}$ calculation, which retains the semi-circular cross-section (cf. *Cutler*, 1998). Equations 8.1 and 8.3 are solved numerically using the Matlab ode15s stiff differential equation solver (*Shampine and Reichelt*, 1997), producing timeseries of the conduit evolution, discharge and pressure characteristics in response to a time-varying water input signal.

The model described above contains a number of important assumptions which are introduced for the sake of computational simplicity. Firstly, that the pressure gradient is uniform along the entire conduit. In reality, the effect of glacier geometry and bed elevation, as well as channel morphology, will alter this gradient. In addition, changes in discharge may occur at different points downstream due to additional inputs of meltwater, either at the base of further moulins or confluences with other conduits. Secondly, we prescribe constant rates of basal sliding, u_b, which contributes to opening of conduits by horizontal motion past bedrock obstacles. A more sophisticated model would couple increases in water pressure with the rate of basal motion through a sliding law, which may hasten the transition from cavity to R-channel type behaviour. It is also assumed that water is able to penetrate straight to the ice bed on entering the moulin, meaning that water can only back up in the moulin if Q_{in} is greater than Q_{out}. Water storage at the ice surface, either in lakes or by filling of crevasses prior to the establishment of a hydraulic connection between the ice surface and its bed, is only replicated by specifying an initial water height in the moulin/reservoir.

The justification for the model structure, where we envisage a single conduit rather than attempting to simulate the evolution of a spatially distributed network, is provided by field observations which suggest that delivery of meltwater to the subglacial drainage system from the ice sheet surface typically occurs at discrete locations, through moulins or crevasses. This may mean that seasonal development of the subglacial drainage system is concentrated in relatively few conduits that interact with the pre-existing spatially distributed drainage system. The volume of meltwater produced at the ice sheet surface is more than an order of magnitude greater than is generated at the ice-bed

interface, meaning that the behaviour of these conduits is likely to force, rather than respond to, behaviour in the remainder of the system. There is no explicit interaction between the conduit which is modelled and a surrounding drainage system (*Hubbard et al.*, 1995). As a result, in the following simulations, water pressure is able to exceed ice overburden pressure. In reality, over-pressurisation of a subglacial conduit would set up lateral pressure gradients, driving water away from the conduit and increasing water pressure in the surrounding drainage system (*Hubbard et al.*, 1995; *Hubbard and Nienow*, 1997). If this is the case then interaction between conduits which are fed by a direct connection with the ice sheet surface and the rest of the drainage system is likely to govern more widespread increases in ice velocity (*Fountain*, 1994; *Hubbard et al.*, 1995; *Hubbard and Nienow*, 1997; *Bartholomaus et al.*, 2007; *Palmer et al.*, 2011).

In light of these limitations, the purpose of this study is not to provide a comprehensive treatment of subglacial drainage system behaviour, nor to tune the model results to fit a set of observations. Rather we hope to assess whether a simple model of subglacial conduit behaviour, as it responds to time-varying meltwater input, can reproduce patterns of subglacial water pressure that might explain the features of the seasonal acceleration signal which were described in the first part of this paper.

8.7.1 Equilibrium solution

From equations 8.1 and 8.2, the equilibrium solution for a subglacial conduit is:

$$N^n = \frac{c_1 Q \frac{\partial \phi}{\partial s} + u_b h}{c_2 c_3 Q^{\frac{4}{5}} \frac{\partial \phi}{\partial s}^{-\frac{2}{5}}} \tag{8.4}$$

where $c_3 = \frac{1}{2}\pi^{-\frac{1}{5}}(\pi+2)^{\frac{2}{5}}(\rho_w f)^{\frac{2}{5}}$.

Figure 8.4a uses the equilibrium solution to show, for a fixed hydraulic gradient, that our equations satisfy the steady-state behaviour described by *Schoof* (2010), where N increases with Q up until a critical threshold at which the relationship is reversed. In figure 8.4b, we use a steady meltwater input to the model to show that this behaviour is replicated by our numerical solution.

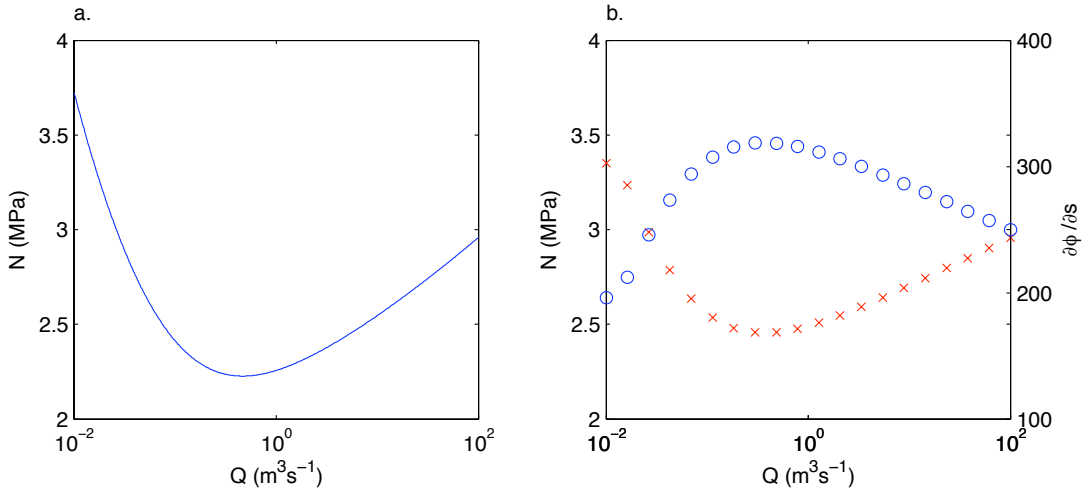

Figure 8.9: a. Steady-state N versus Q, with fixed hydraulic gradient $\frac{\partial \phi}{\partial s} = 250\ Pam^{-1}$ b. Modelled N versus Q with steady drainage into the system (red crosses, left axis). The right axis shows how the hydraulic gradient also varies with discharge $\frac{\partial \phi}{\partial s}$ (blue circles)

8.7.2 Experiment 1: model testing

In our first experiment we test the response of the conduit model to a forcing signal which simulates the key features of seasonal meltwater delivery to the subglacial drainage system that were identified in the first part of this paper. The model setup is based on a moulin which is located ~500 m south of site 2. Site 2 is 7.3 km along our transect from the ice sheet margin and the ice thickness is 375 m (Figure 8.1; *Bamber et al.*, 2001; *Krabill*, 2010). Based on field observations of this moulin, values of $r_m = 3$ m, $r_r = 250$ m and $d_r = 5$ m were adopted.

The model is run for 100 days with a meltwater signal which comprises: (i) a seasonal component which peaks at 4 $m^3\ s^{-1}$; (ii) daily cycles in meltwater production, with amplitude of 1 $m^3\ s^{-1}$ which are superimposed on the seasonal signal; and (iii) three pulses of meltwater which last two days each and have peak discharge of 5 $m^3\ s^{-1}$ (Figure 8.10a). We specify an initial conduit cross-sectional area of 0.005 m^2 to reflect the fact that conduits are likely to fall in the range for cavity-type behaviour following the winter period. The full list of model parameters is provided in Table 8.1.

Inspection of Figure 8.10 indicates that the model is able to reproduce key features of the seasonal subglacial drainage system behaviour reasonably well. When water drains into the conduit initially, the small conduit size restricts Q_{out} to be much smaller

Parameter	Symbol	Value	Units
Ice thickness at the moulin	H	375	m
Moulin radius	r_m	3	m
Reservoir radius	r_r	250	m
Reservoir depth	h_r	5	m
Conduit slope	$\frac{\partial z}{\partial s}$	0.02	-
Conduit length	s	7300	m
Distance of cross-section from moulin	Δs	500	m
Melt opening parameter	c_1	$\frac{1}{\rho_i L}$	-
Darcy-Weisbach friction factor	f	3.75 x 10^{-2}	-
Latent heat of fusion	L	3.35 x 10^5	J kg^{-1}
Density of water	ρ_w	1000	kg m^{-3}
Density of ice	ρ_i	910	kg m^{-3}
Conduit closure parameter	c_2	An^{-n}	-
Glen's flow law coefficient	A	6 x 10^{-24}	Pa^{-3} s^{-1}
Glen's flow law exponent	n	3	-
Basal sliding velocity	u_b	30	m yr^{-1}
Bedrock obstacle height	h	0.1	m

Table 8.1: Parameter values used during the model experiments

than Q_{in} and water backs up in the moulin. High water level, which fills the moulin but does not cause the reservoir to overflow, causes high subglacial water pressure and an increase in the hydraulic gradient, $\frac{\partial \phi}{\partial s}$. Increased $\frac{\partial \phi}{\partial s}$ forces higher discharge through the conduit, which leads to rapid growth of the cross-section. A positive feedback between conduit size and discharge then develops, and both Q_{out} and S continue to increase rapidly until the conduit has become large enough to drain all the water stored in the moulin. At this point, which occurs after ~5 days, pressure in the conduit drops rapidly as the meltwater input is not sufficient to fill the expanded conduit. The weight of overlying ice causes the conduit to adjust in size, until S and Q_{in} are more or less in balance after a period of a few days. Following the development of the conduit in response to initial meltwater input, the conduit size continues to adjust to changes in water input and short-term variations in the forcing signal cause large fluctuations in both water pressure and conduit size. This is evident both in response to the diurnal cycles in the meltwater signal, as well as the three pulses which occur on days 15, 30 and 45 (Figure 8.10).

Figure 8.11 shows that channel opening is forced nearly entirely by melting of

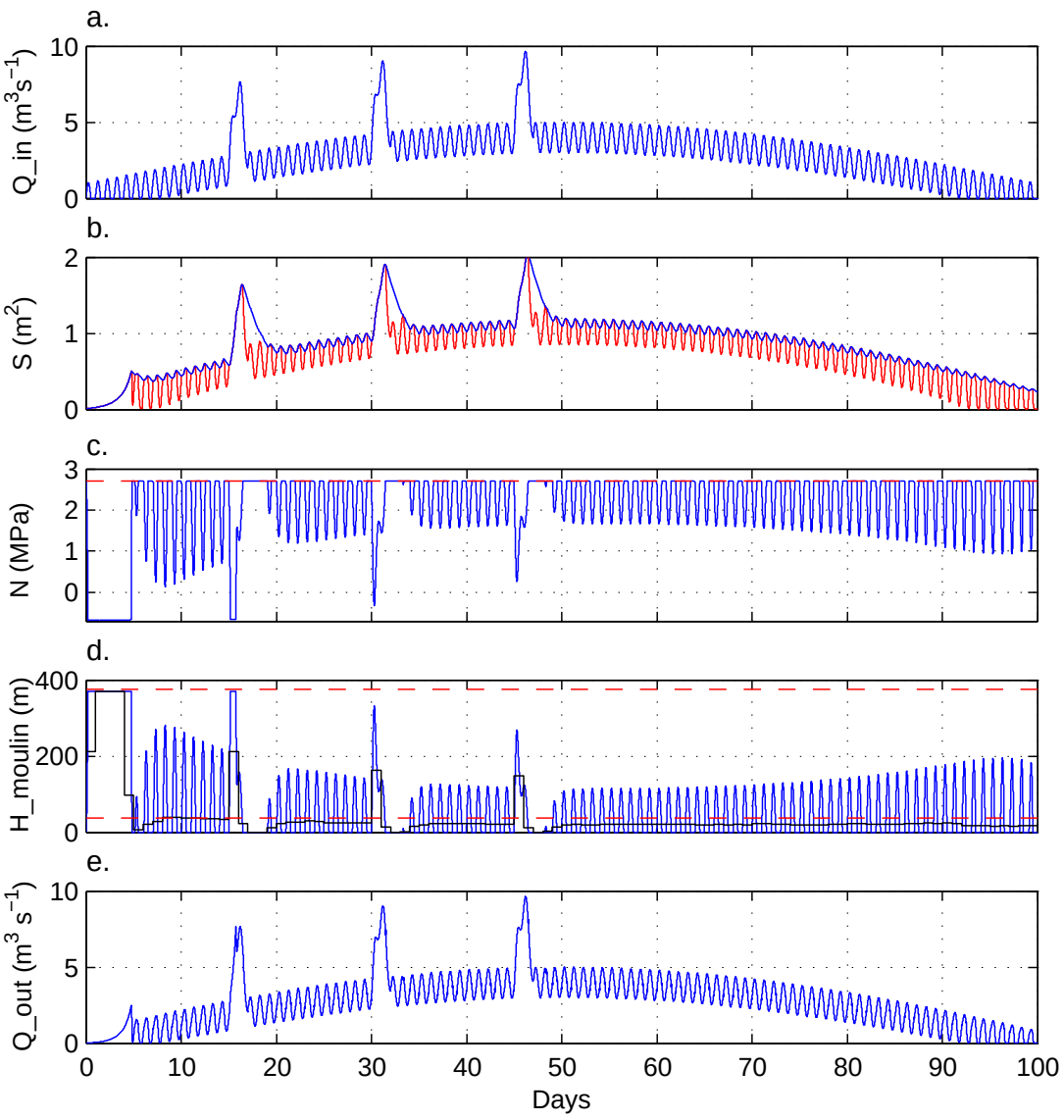

Figure 8.10: Simulation of channel-cross section evolution in response to a time-varying water input signal. a. Inflow to the system, Q_{in}. b. Conduit cross-sectional area, S (blue) and filled cross-sectional area (red) under open-channel conditions. c. Effective pressure, $N = p_i - p_w$ (blue), at the modelled cross-section. Maximum N is equal to p_i (red dashes). d. Water height in the moulin/reservoir system (blue), which drives variation in the hydraulic head gradient. Mean water height is shown for 24h periods (black steps) and the whole model run (lowest red dashes). Ice thickness, H is indicated by the upper red dashes. e. Outflow from the system, Q_{out}.

channel walls. Creep closure is the only component of equation 8.1 which is capable of causing both conduit opening and closure although we find that it acts primarily to close the conduit. During the pulses of meltwater, negative pressure in the conduit does contribute slightly to rates of conduit growth, although the overall impact is minimal.

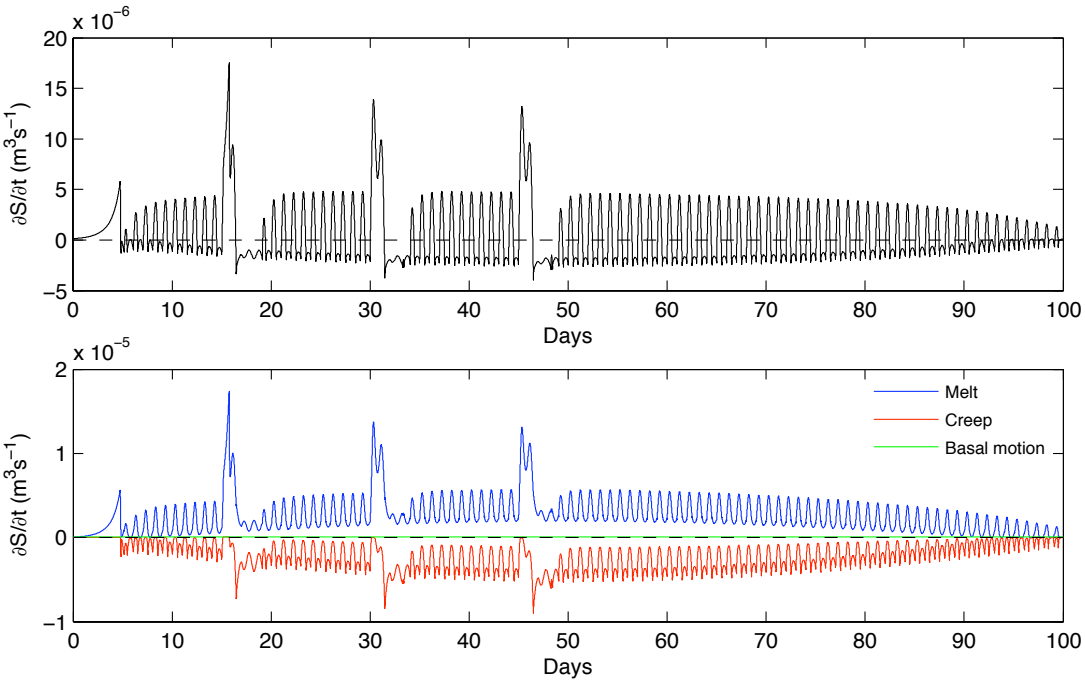

Figure 8.11: a. Rate of conduit cross-sectional area change through the first simulation forced by an artificial signal (see figure 8.10. b. Contribution of different components of equation 8.1 to the rate of conduit cross-sectional area change.

The behaviour which occurs in the first five days of the model run provides a good representation of the characteristics of a 'spring-event', where an inefficient, low volume drainage system is subject to comparatively large inputs of meltwater from the ice sheet surface. Since the drainage system is not able to evacuate all of this meltwater, it backs up in the englacial drainage system which causes high subglacial water pressure and growth of subglacial conduits. The drainage system continues to develop in capacity until there is no longer enough water in the englacial system to sustain growth, at which point discharge rapidly declines and conduits shrink again.

The short-term events which follow also reflect temporary imbalance between the water supply, Q_{in}, and the capacity of the conduit to evacuate the water. The capacity to remove water is governed by equation 8.2 which states that a larger conduit and increased hydraulic gradient both lead to higher discharge. At the same time, however, increased hydraulic gradient and larger discharge also causes an increase in conduit size. In our model, fluctuations in water pressure occur when the meltwater input signal overfills the conduit more quickly than the rate of wall melting can increase the conduit

size in order to accommodate the extra water, leading to the imbalance between Q_{out} and Q_{in}. Under these conditions water is stored in the englacial system increasing the hydraulic gradient and subglacial water pressure. The high pressure lasts until the water supply drops, at which point the conduit is larger than is necessary to evacuate the incoming meltwater and open channel flow occurs, presumably at atmospheric pressure, while the conduit slowly reduces in size again. The pulse events demonstrate that high water pressure can be sustained in the conduit for periods of more than one day, so long as Q_{in} keeps rising. These events cause the conduit to reach its greatest size and also maintain the highest mean water pressures outside of the spring-event. Following the pulse events, however, daily cycles in water pressure are suppressed while the conduit size adjusts more slowly to the reduction in meltwater input.

The conduit response to the seasonal component of the Q_{in} signal, however, is very different. Because Q_{in} varies only gradually on the longer-term the conduit is able to shrink and contract on the same timescales without a sharp rise in water pressure (*Schoof*, 2010). Running the model with the same parameters, but removing the short-term components of the Q_{in} signal, we find that mean water pressure in the conduit changes steadily with the water supply and is inversely related to Q_{in} (Figure 8.12). This pressure-discharge relationship is consistent with the behaviour of an R-channel in steady-state (*Schoof*, 2010).

Diurnal variations in water pressure are greatest at the beginning and end of the model run, when the size of the daily cycles in meltwater supply are greater as a proportion of the daily mean Q_{in} (Figure 8.10). The same also applies to the pulse events: the first pulse on day 15 achieves the highest water pressure, while the third pulse, which occurs on day 45 near the peak of seasonal water input, is more subdued. This behaviour highlights an important link between short-term variations in meltwater input and the longer-term evolution of the conduit. Since the conduit size is broadly in equilibrium with the longer-term signal of meltwater input, S is largest in the middle part of the model run, near the peak of the 'seasonal' signal. The larger channel has greater capacity to evacuate meltwater, therefore more water is required to overfill it and pressurise the conduit than earlier in the season when the conduit was smaller. In this way, the ratio between mean Q_{in} and the rate and magnitude of short-term

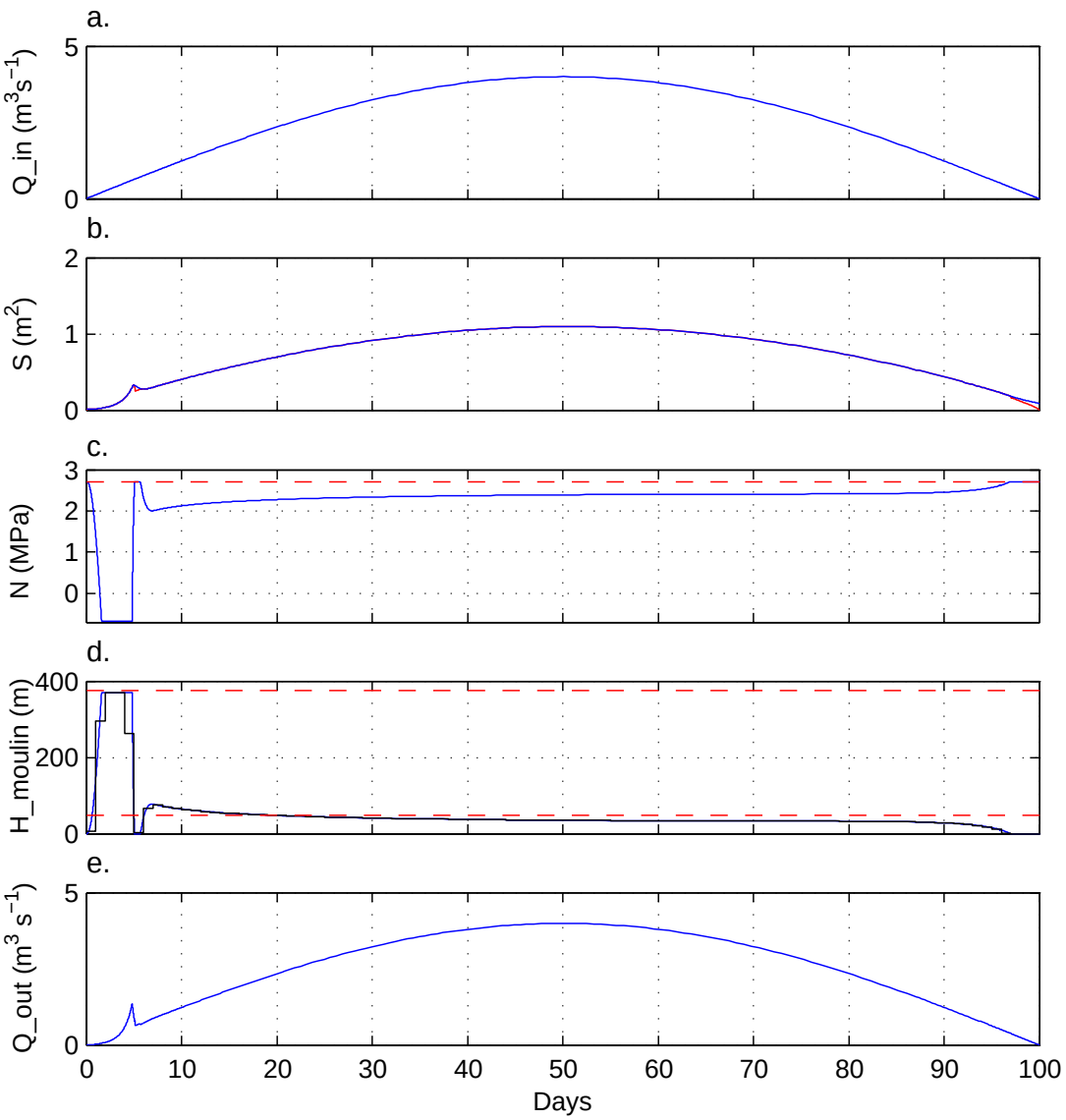

Figure 8.12: Simulation of channel-cross section evolution in response to a gradually-varying water input signal. a. Inflow to the system, Q_{in}. b. Conduit cross-sectional area, S (blue) and filled cross-sectional area (red) under open-channel conditions. c. Effective pressure, $N = p_i - p_w$ (blue), at the modelled cross-section. Maximum N is equal to p_i (red dashes). d. Water height in the moulin/reservoir system (blue), which drives variation in the hydraulic head gradient. Mean water height is shown for 24h periods (black steps) and the whole model run (lowest red dashes). Ice thickness, H is indicated by the upper red dashes. e. Outflow from the system, Q_{out}.

changes in Q_{in} controls the magnitude of short-term spikes in water pressure within the conduit. Overall, this suggests that a larger seasonal meltwater input signal may act to limit the size of short-term variations in water pressure while larger short-term variations in meltwater supply, relative to mean meltwater input, would favour greater

changes in water pressure.

The preceding discussion suggests that not only does this simple model successfully reproduce key features of the subglacial pressure response to inputs of meltwater from the ice sheet surface, but that the behaviour can be explained in terms of time-varying water input to a subglacial conduit without invoking the transition from cavity to R-channel type steady-state behaviour. For a full semicircular conduit, *Schoof* (2010) derived the following equation for the critical discharge value at which a switch from cavity to R-channel type behaviour in steady-state would occur:

$$Q_c = \frac{u_b h}{c_1(1-\alpha)\frac{\partial \phi}{\partial s}} \tag{8.5}$$

where $\alpha = 5/4$ is a constant. Under full and steady-state conditions, assuming a fixed hydraulic gradient, the critical discharge for the conduit modelled here is 0.59 $m^3\ s^{-1}$, which corresponds to a cross-sectional area of 0.16 m^2. Our model suggests, therefore, that the Q_c is easily exceeded very early in the initial growth phase. Figure 8.10 shows, however, that water pressure continues to rise during the spring-event even once the conduit has become 'channelised'.

In an experiment to investigate the impact which initial conduit size has on conduit evolution we ran the model again but with a starting conduit size of 0.2 m^2. The results of this experiment are shown in Figure 8.13 and indicate that with a larger initial conduit size the prolonged period of high pressure and conduit size adjustment seen in the first experiment is absent. Once the adjustment phase has taken place, however, then the conduit evolution is the same. The absence of the 'spring-event' in this experiment suggests that the larger conduit is not overwhelmed by the initial input of meltwater in the same way as a smaller one. A larger conduit has greater wetted-perimeter and greater discharge which allows faster melting of the conduit walls. On the basis of these results, therefore, we suggest that the significance of a transition from a winter-type inefficient drainage system to a summer channelised one is restricted to the early part of the melt season and is responsible for the high magnitude spring-events that occur when water first drains from the ice sheet surface to its bed.

Overall, this set of simulations has shown that, with an input signal which varies on

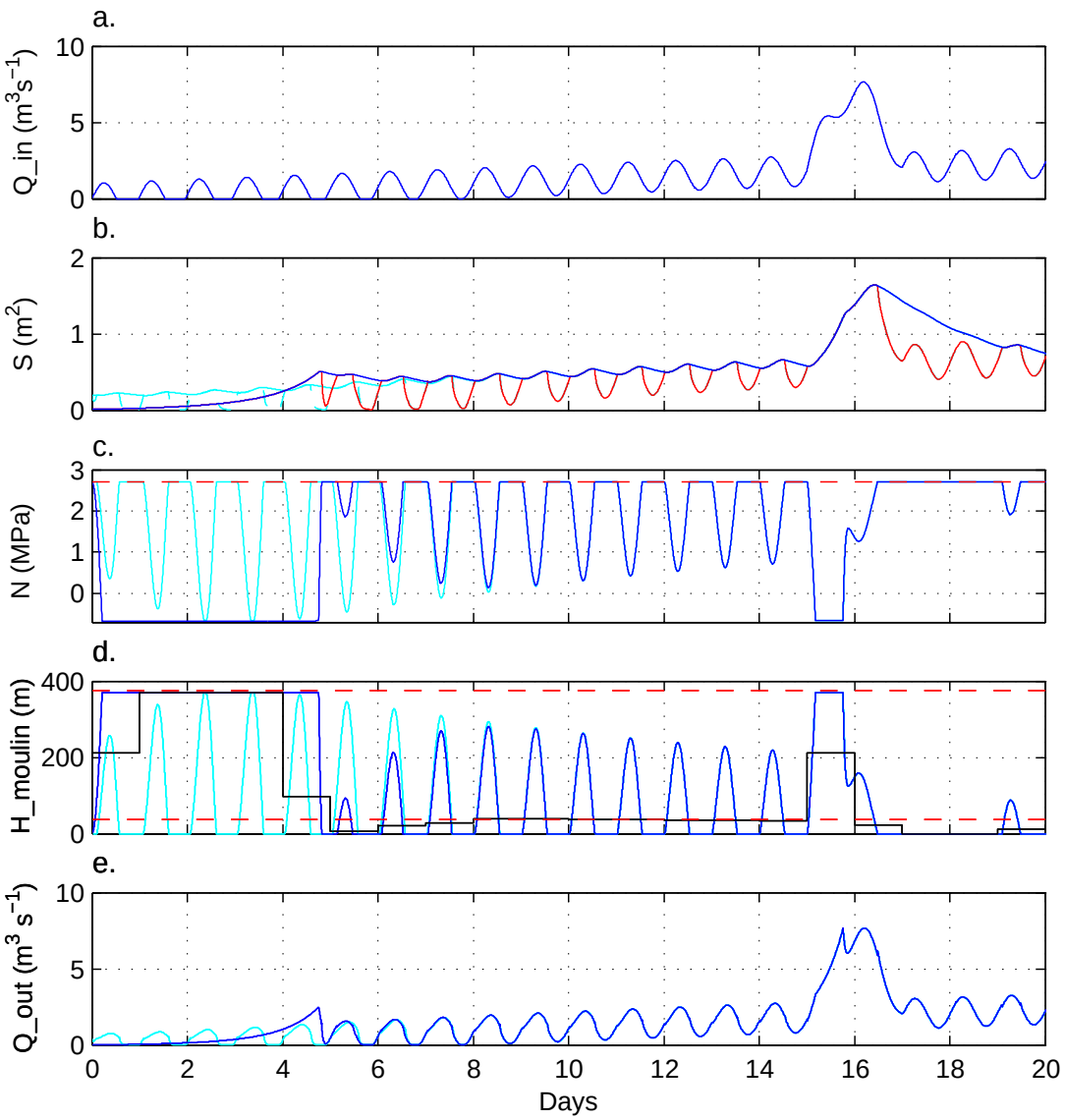

Figure 8.13: Comparison of simulated of channel-cross section evolution in response to a time-varying water input signal with different starting conduit size, S_0. In the initial experiment (1) S_0=0.01 m^2, which is compared with a second experiment (2) where S_0=0.2 m^2. a. Inflow to the system, Q_{in}. b. Conduit cross-sectional area, S ((1)blue & (2)cyan) and filled cross-sectional area ((1)red & (2)cyan dashes) under open-channel conditions. c. Effective pressure, $N = p_i - p_w$ ((1)blue & (2)cyan), at the modelled cross-section. Maximum N is equal to p_i (red dashes). d. Water height in the moulin/reservoir system ((1)blue & (2)cyan), which drives variation in the hydraulic head gradient. Mean water height is shown for experiment (1) for 24h periods (black steps) and the whole model run (lowest red dashes). Ice thickness, H is indicated by the upper red dashes. e. Outflow from the system, Q_{out} ((1)blue & (2)cyan).

short timescales, the subglacial conduit does not reach steady state. This results in short-term pressure variations within the conduit, which, should high pressure in the conduit cause increases in pressure over a wider area by interaction with a distributed drainage

system, could plausibly integrate to explain the seasonal velocity signal observed at sites 1 - 3 in the first part of the paper. In addition to over-pressurisation, open-channel flow in the conduit occurs regularly, on the falling limb of daily cycles in meltwater production and following meltwater pulses.

8.7.3 Experiment 2: forcing with realistic input signal

We now use field observations of temperature and surface ablation from site 2 in 2010 to generate a more realistic meltwater signal to drive conduit evolution. Runoff was estimated using a simple temperature-melt index model (*Hock*, 2003) applied to a 1 x 3 km rectangular catchment with a surface gradient of 0.025. This estimated catchment area is based on field observations of the spacing of moulins in the Leverett Glacier catchment during traverses by helicopter and on foot, and on obervations of mean discharge into moulins at this elevation. The surface gradient was was calculated using surface elevation data from a recent airborne survey (Figure 8.1; *Krabill*, 2010). A measurement of seasonal surface ablation was then used to calculate a degree-day factor for the period 1 May - 1 August (*Hock*, 2003). Applying a fixed lapse rate of -0.9°C per 100 m elevation, calculated using temperature from sites 2 and 3 in May and June, we then used the temperature data to estimate runoff for a period of 92 days, from 1 May until 1 August, at which point the temperature sensor at site 2 failed. In order to capture the daily variations in meltwater production, the daily signal in our runoff estimate was also amplified by a factor of 2. Since water did not access the ice bed interface until May 7 at site 2 (*Nienow et al.*, submitted; *Chapter 7*), melt generated prior to this date was artificially backed up in the moulin and used to calculate an initial water height. We then ran the conduit model from May 7th until August 1st with this initial water height and conduit evolution was driven by the remainder of the estimated runoff signal (Figure 8.14a).

Running the model with this meltwater signal results in similar conduit behaviour to that modelled in response to the artificial signal (Figure 8.14). A period of high subglacial water pressure and rapid conduit growth occurs when water first drains into the conduit. Following this, water pressure drops and the conduit reduces in size. For the rest of the melt season, the conduit continues to evolve in response to short-term

variations in meltwater input. This is evident both in daily-cycles in water pressure and conduit growth as well as longer-term periods of increased meltwater input, on the order of a few days, which sustains higher water pressures for longer and marked conduit growth. For example, a period of higher meltwater input from 22 - 28 May causes the conduit to reach its greatest size outside of the spring-event and high mean water pressure is sustain for 3 - 4 days. Daily-cycles in water pressure, where the conduit is over-pressurised during the day and operates under open-channel conditions when meltwater input starts to fall are persistent for most of the model run.

As with the velocity observations presented in the first part of this paper, there is no clear relationship between the magnitude of daily cycles in the input signal and the pressure response within the subglacial conduit. We suggest that this reflects the strong time-dependence of the relationship between meltwater supply and subglacial water pressure. For example, if larger diurnal variations in meltwater supply increase the size of the conduit, it will be over-filled for a shorter period of the day and require greater amounts of water to achieve the same water pressure. In this way the water pressure is highly sensitive to the recent development of the system.

Comparing the modelled conduit development with the observed velocity record from site 2 (Figure 8.14c) yields striking results which bear out this reasoning. High ice velocities are well matched with growth of the conduit, which is indicative of sustained high water pressure. The highest velocities are associated with sharpest rises in conduit cross-sectional area and begin to reduce again when water input declines and the conduit shrinks in size. Over daily timescales, high velocity occurs when the channel is overfilled and low velocities, which often return to winter background levels, occur during periods of open-channel flow.

In common with the previous experiments, the conduit reaches R-channel size during the spring-event and remains above the critical value through the remainder of the model run. After the spring-event Q_{out} roughly matches Q_{in} suggesting longer-term variability in meltwater input is easily accommodated by evolution of the conduit.

Our results suggest that efforts to derive a relationship between water pressure within a conduit and ice velocity might reasonably focus on developing an understanding of the pressure behaviour of the surrounding drainage system and its relationship to

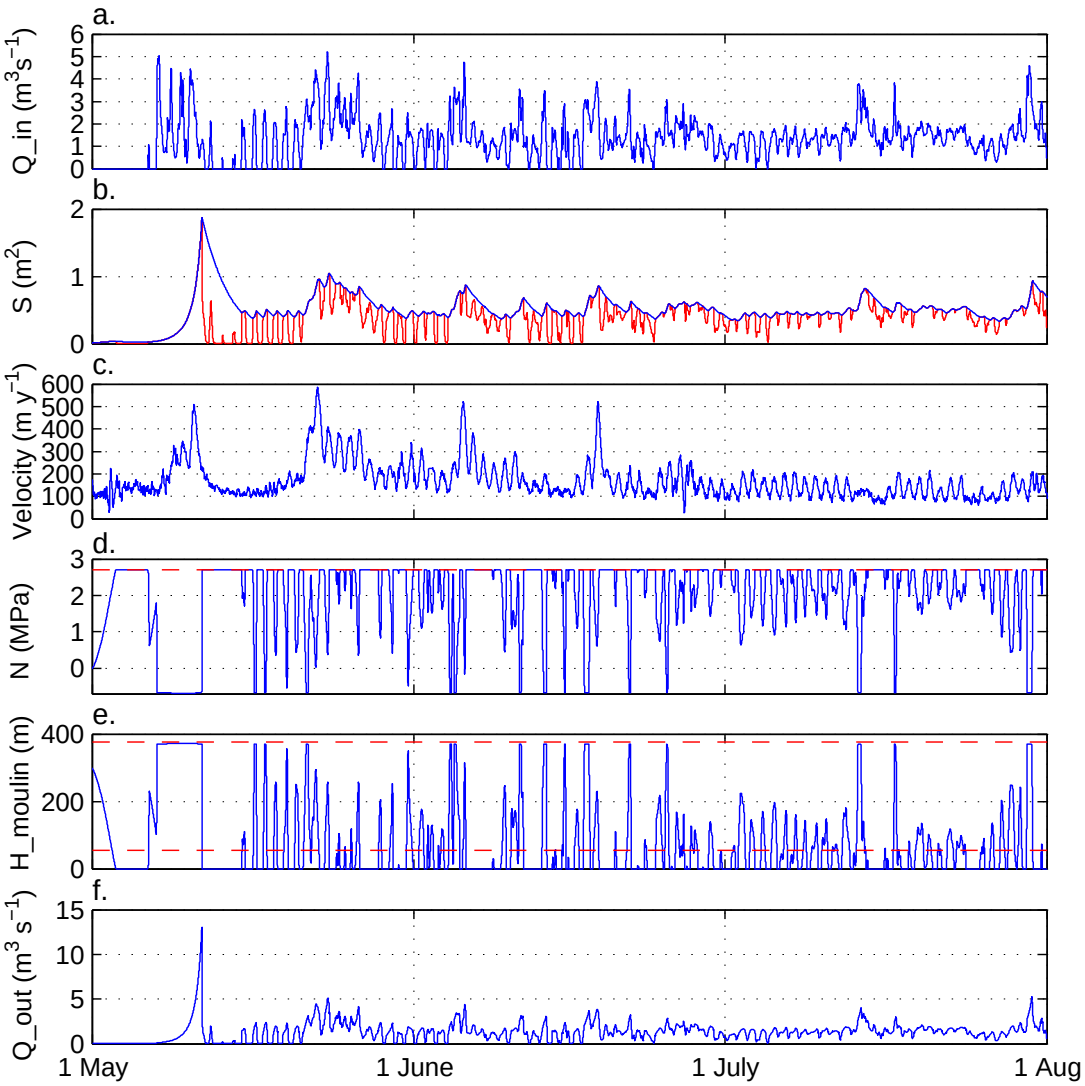

Figure 8.14: Simulation of channel-cross section evolution in response to a realistic water input signal generated from temperature data at site 2 in 2010, compared with the record of ice velocity. a. Inflow to the system, Q_{in}. b. Conduit cross-sectional area, S (blue) and filled cross-sectional area (red) under open-channel conditions. c. Ice velocity at site 2 during the 2010 summer melt season. d. Effective pressure, $N = p_i - p_w$ (blue), at the modelled cross-section. Maximum N is equal to p_i (red dashes). e. Water height in the moulin/reservoir system (blue), which drives variation in the hydraulic head gradient. Mean water height is shown for 24h periods (black steps) and the whole model run (lowest red dashes). Ice thickness, H is indicated by the upper red dashes. f. Outflow from the system, Q_{out}.

conduit water pressure. We suggest a conceptual model where over-pressurisation of a conduit causes excess discharge to be transferred into adjacent areas of the ice sheet bed. Such an investigation would require development of a model similar to the one employed here to include an extra water storage component to represent the distributed drainage system and a method for determining the area of the bed over which pressure

might be affected.

8.8 Discussion

Both the field observations and modelling experiments support the idea that discharge through the subglacial drainage system and water pressure are in phase over short timescales (<∼1 week), due to an imbalance between the capacity of the subglacial drainage system to evacuate meltwater and variations in meltwater input (*Röthlisberger*, 1972; *Cutler*, 1998; *Schoof*, 2010). When drainage into the system rises more quickly than conduits can expand to accommodate the extra water, water is backed up in the englacial system increasing subglacial water pressure. Over longer timescales, however, an increase in the hydraulic capacity of the subglacial drainage system allows higher discharge at lower pressures than earlier in the summer (*Bartholomew et al.*, 2010, 2011b; *Sundal et al.*, 2011).

The detailed record of ice velocity at sites near the ice sheet margin shows that the summer acceleration signal is dominated by short-term velocity events, which are forced by temporal variations in water input to the subglacial drainage system. Using a simple model of subglacial conduit evolution forced by a time-varying meltwater input signal, we are able to successfully reproduce the key features of the seasonal conduit development and pressure behaviour over both seasonal and short-term timescales. In the experiment where we force the conduit development with a realistic input signal, derived from the temperature record at site 2, the pattern of ice velocity changes can be explained by periods of high subglacial water pressure and conduit growth which are forced by short-term variations in meltwater input to an efficient drainage system. Our investigation suggests, therefore, that the total summer acceleration signal is plausibly interpreted as the integrated effect of numerous short-term events, rather than a transition from a period of consistently high ice velocities in early summer which are then reduced in late summer. In this context, the observation that mean ice velocities are higher in early summer compared with late summer is explained in two ways: firstly, the meltwater forcing signal levels off or declines in line with seasonal trends in air temperature (Figure 8.2d and 8.4d) and the subglacial drainage system stabilises having

reached its maximum spatial extent (*Bartholomew et al.*, 2011a); secondly, the drainage system has evolved to accommodate more water than earlier in the season and greater variations in meltwater input are required to overwhelm the system than earlier in the summer.

Many authors have appealed to the pressure-discharge characteristics of subglacial conduits in steady-state to suggest that the transition from an inefficient drainage system, where discharge is positively related to subglacial water pressure, to an efficient, channelised, drainage system, where higher discharge leads to lower water pressure, is responsible for the discrepancy between early and late summer mean velocities in land-terminating sections of the GrIS. We find no evidence in either the field observations or our modelling experiments to support this interpretation. Firstly, we find that conduit growth during the initial spring-event is likely to be sufficient to effect a change from cavity to R-channel size conduits soon after initial drainage of meltwater to the ice-bed interface. This finding is supported by preliminary dye tracing experiments (T.Cowton, pers. comm.) and the hydrological study conducted in 2009 (*Bartholomew et al.*, 2011a). Following the spring-events, however, mean velocities remain high until much later in the summer. The good agreement between the model of the development of a single conduit and observations of ice velocity, which is likely to represent subglacial water pressures over a wider area (*Kamb et al.*, 1994), implies that pressure within a discrete channelised drainage system which is fed by meltwater from the ice sheet surface causes interaction with a distributed drainage system when overfilled to raise pressure over a wider area (*Hubbard et al.*, 1995; *Hubbard and Nienow*, 1997; *Nienow et al.*, 2005). Secondly, the detailed ice velocity record does not reveal two modes of flow where ice velocity is positively related to temperature for the first part of the summer and then declines in late summer. The prevalence of short-term variations in ice velocity suggests very strongly that steady-state conditions rarely occur in practice in this section of the GrIS margin. Coupled with the success of the model experiments in reproducing both the long-term and short-term behaviour of the subglacial drainage system we argue that the variations in subglacial water pressure are better understood in terms of the response to time-varying meltwater input. In light of these findings it is extremely important to draw a distinction between 'channelisation' of the drainage system, which implies

a reversal in pressure-discharge characteristics, and development of a conduit system to accommodate larger volumes of water which reduces its sensitivity to variations in meltwater supply.

Previous studies from this transect have shown that increased summer ablation does not necessarily lead to a reduction in annual ice velocities (*Bartholomew et al.*, 2011b; *Nienow et al.*, submitted; *Chapter 7*). Our investigation substantiates the arguments put forward that variability in the *rate*, rather than absolute volume, of meltwater delivery to the subglacial drainage system is an important control on patterns of subglacial water pressure. In a warmer climate, therefore, we would expect the summer acceleration signal at lower elevations to be sustained by variability in meltwater delivery to the ice-bed interface, particularly in early summer while the system is continually adjusting to larger and larger inputs of meltwater.

Behaviour at higher elevations, where overall seasonal acceleration is lower, appears to be controlled strongly by supraglacial and englacial hydrology. In the first instance, accumulation and sudden drainage of stored water from the ice sheet surface control the timing of hydrologically forced ice acceleration (*Bartholomew et al.*, 2011b). Two previous studies have shown that higher melt rates result in greater seasonal acceleration because meltwater can drain to the ice-bed interface earlier in the season, increasing the time for velocity variations to occur (*Bartholomew et al.*, 2011b; *Nienow et al.*, submitted; *Chapter 7*). Following the initial drainage event, long supraglacial transit times mean that short-term cycles in meltwater inputs to the ice sheet bed are subdued. When there is more meltwater, however, the input signal can vary more quickly over shorter timescales and the record at site 5 shows that the behaviour of higher elevation sites becomes more like those nearer the ice sheet margin. At these sites, a warmer climate therefore favours increased seasonal acceleration on two counts, by increasing the length of time for which meltwater can reach the bed, and by increasing the short-term variability in that supply by removing the smoothing effect of the winter snowpack earlier in the summer.

8.9 Conclusions

High resolution measurements of ice velocity in a land-terminating section of the GrIS reveal that the seasonal acceleration signal is dominated by short-term variations in ice velocity. These short-term variations in ice velocity are forced by rapid variations in meltwater input to the subglacial drainage system from the ice sheet surface. The absence of short-term cycles in ice velocity at higher elevation sites reflects different patterns of meltwater input to the ice-bed interface, which are controlled by supraglacial and englacial hydrology. At these sites the velocity signal reflects more gradual variations in meltwater input, punctuated by events where large volumes of stored meltwater drain to the ice-bed interface.

We find that an efficient drainage system is likely to be established shortly after initial access of meltwater to the ice bed interface, which occurs at progressively higher elevations through the melt season. Large velocity variations can continue to occur, however, even once the drainage system has become channelised. Using a simple model of subglacial conduit behaviour we show that the record is best understood in terms of a time-varying water input to a channelised subglacial drainage system. Our investigation substantiates the arguments that variability in the *rate*, rather than absolute volume, of meltwater delivery to the subglacial drainage system is an important control on patterns of subglacial water pressure. These findings resolve the failure of steady-state analyses of subglacial drainage system behaviour to explain inter-annual variations in summer acceleration in this part of the GrIS margin.

In the context of predictions about the impact of increased meltwater production on ice dynamics and therefore on the future mass balance of the GrIS, we find no reason to expect a reduction in summer acceleration at sites near the ice sheet margin where water easily drains to the ice bed interface. At sites further inland, increased rates of surface melting favours greater summer acceleration both because water will drain to the ice-bed interface earlier each year and because earlier snowpack removal will lead to greater melt supply variability.

While we suggest that atmospheric forcing has the potential to increase rates of dynamic mass loss from the GrIS in a warmer climate, our findings call for a reassessment

of the role that the subglacial drainage system plays in moderating the relationship between surface melting and ice velocity (cf. *Van de Wal et al.*, 2008; *Shepherd et al.*, 2009; *Schoof*, 2010; *Sundal et al.*, 2011; *Pimentel and Flowers*, 2011).

8.10 Appendix: model sensitivity testing

In order to test the sensitivity of our model to variations in key unknown parameters, we performed a series of sensitivity tests. The key parameters which affect rates of conduit opening and closure are f in the Darcy-Weisbach equation and B in Glen's flow law respectively. In addition, due to uncertainty about drainage concentration at the ice sheet bed, we also tested variations in meltwater input to our conduit model. The results of these simulations are presented in figures 8.15 - 8.18. Overall, these simulations show that the values chosen for the parameters and inputs exert strong control over absolute values for modelled effective pressures and conduit size. In the context of the research presented in this chapter, however, the patterns of variability in conduit size, discharge and effective pressure remain similar within plausible limits for the parameters.

8.10.1 Darcy friction factor

The Darcy friction factor, f, controls rates of energy loss through friction at the channel walls in both pipe and open channel flow. In addition to our initial simulation, we performed experiments using values of 0.1 and 0.2 for f, to cover the range typically used for subglacial tunnels (e.g. *Clarke*, 1996; *Schoof*, 2010, Figure 8.15). Increasing f in our model reduces the conduit discharge for a given S. Initial rates of conduit opening are lower with increased f, but ultimately the conduit reaches a greater size in order to carry the same amount of water (Figure 8.15b). The slower rate of conduit opening applied in these sensitivity tests also leads to larger short-term variations in effective pressure (Figure 8.15c).

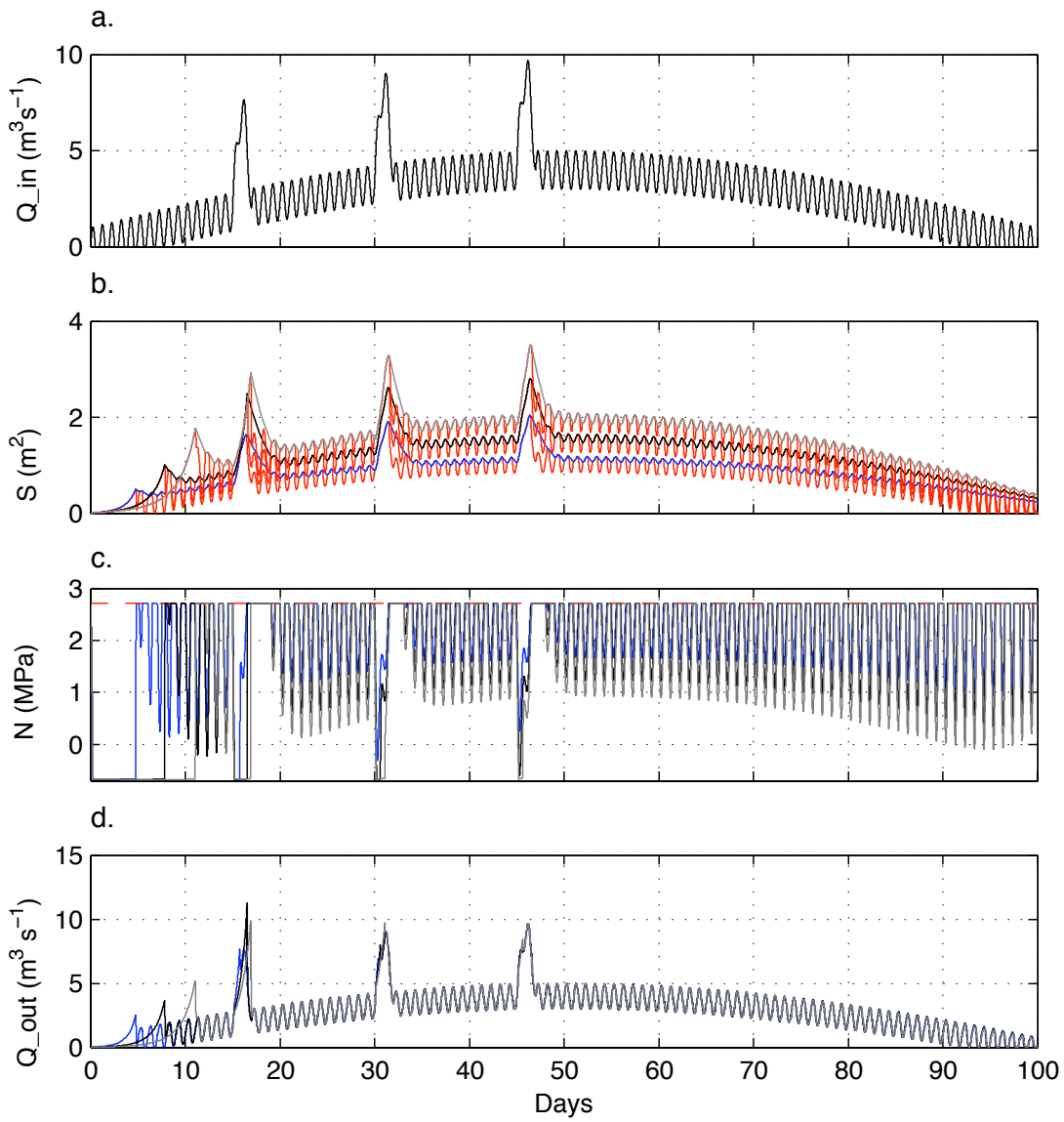

Figure 8.15: Simulation of channel-cross section evolution in response to a time-varying water input signal with different values for f. a. Inflow to the system, Q_{in}. b. Conduit cross-sectional area, S (f=0.0375, blue; f=0.1, black, f=0.2, grey) and filled cross-sectional area (red) under open-channel conditions. c. Effective pressure, $N = p_i - p_w$ (f=0.0375, blue; f=0.1, black, f=0.2, grey), at the modelled cross-section. Maximum N is equal to p_i (red dashes). d. Outflow from the system, Q_{out} (f=0.0375, blue; f=0.1, black, f=0.2, grey).

8.10.2 Flow law parameter

The parameter B in Glen's flow law controls the stiffness of ice and is strongly related to ice temperature (*Paterson*, 1994). Higher values of B represent softer ice, allowing faster rates of conduit closure for a given effective pressure. A lower value for B leads to stiffer ice and slower conduit closure rates. Figure 8.16 shows that reducing B leads

to a larger conduit size, but reduced daily variations in N, while increasing B leads to a slightly reduced conduit size and greater daily variations in N.

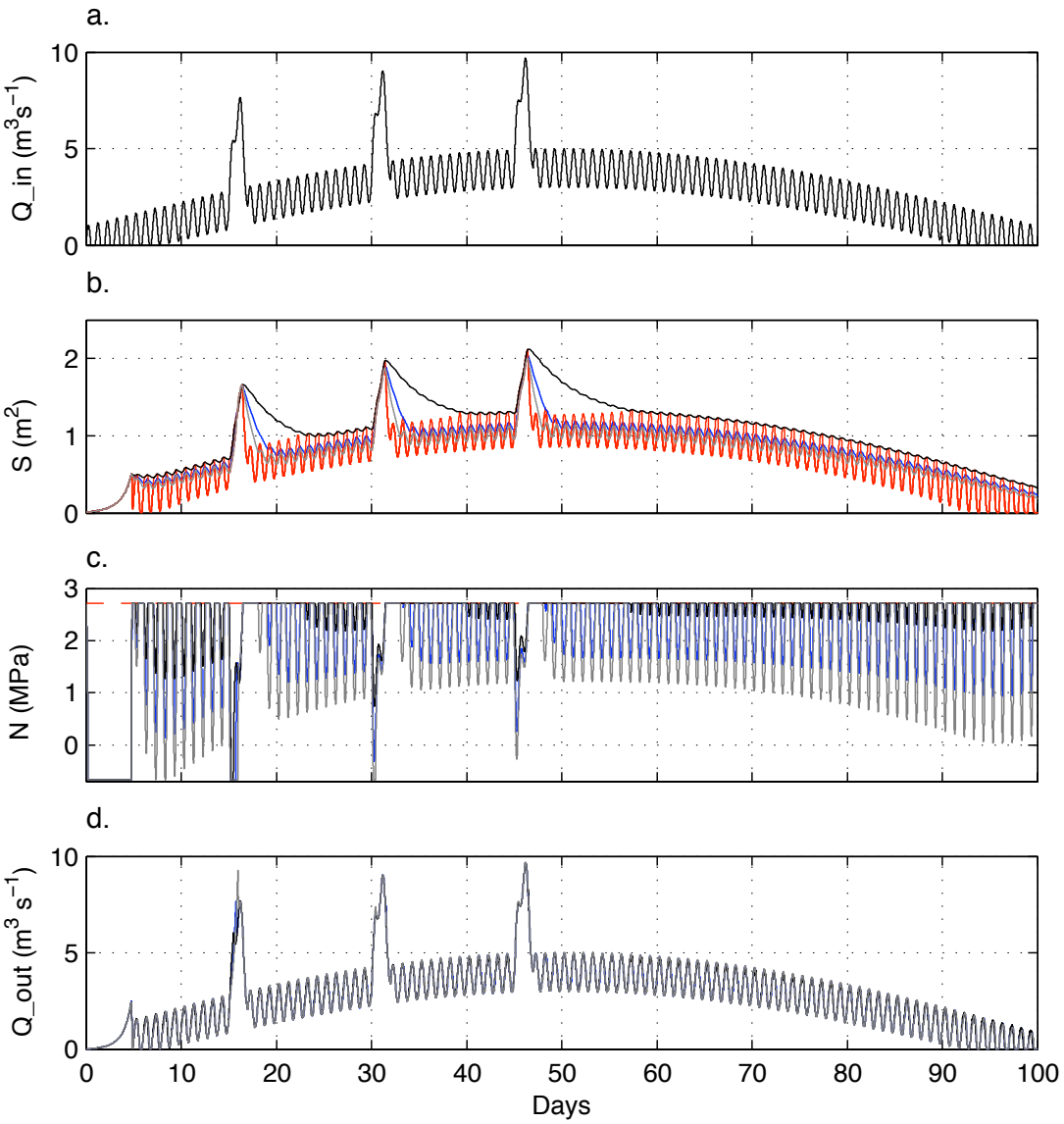

Figure 8.16: Simulation of channel-cross section evolution in response to a time-varying water input signal with different values for the flow law parameter B. a. Inflow to the system, Q_{in}. b. Conduit cross-sectional area, S (B=6x10^{-24}, blue; B=3x10^{-24}, black, B=9x10^{-24}, grey) and filled cross-sectional area (red) under open-channel conditions. c. Effective pressure, $N = p_i - p_w$ (B=6x10^{-24}, blue; B=3x10^{-24}, black, B=9x10^{-24}, grey), at the modelled cross-section. Maximum N is equal to p_i (red dashes). d. Outflow from the system, Q_{out} (B=6x10^{-24}, blue; B=3x10^{-24}, black, B=9x10^{-24}, grey).

8.10.3 Meltwater inputs

Finally, we performed experiments where we changed the magnitude of the overall meltwater input signal and the amplitude of daily cycles (Figures 8.17 and 8.18). Results for Qx2 and Qx4 are shown in figure 8.17. While the overall size reached by the

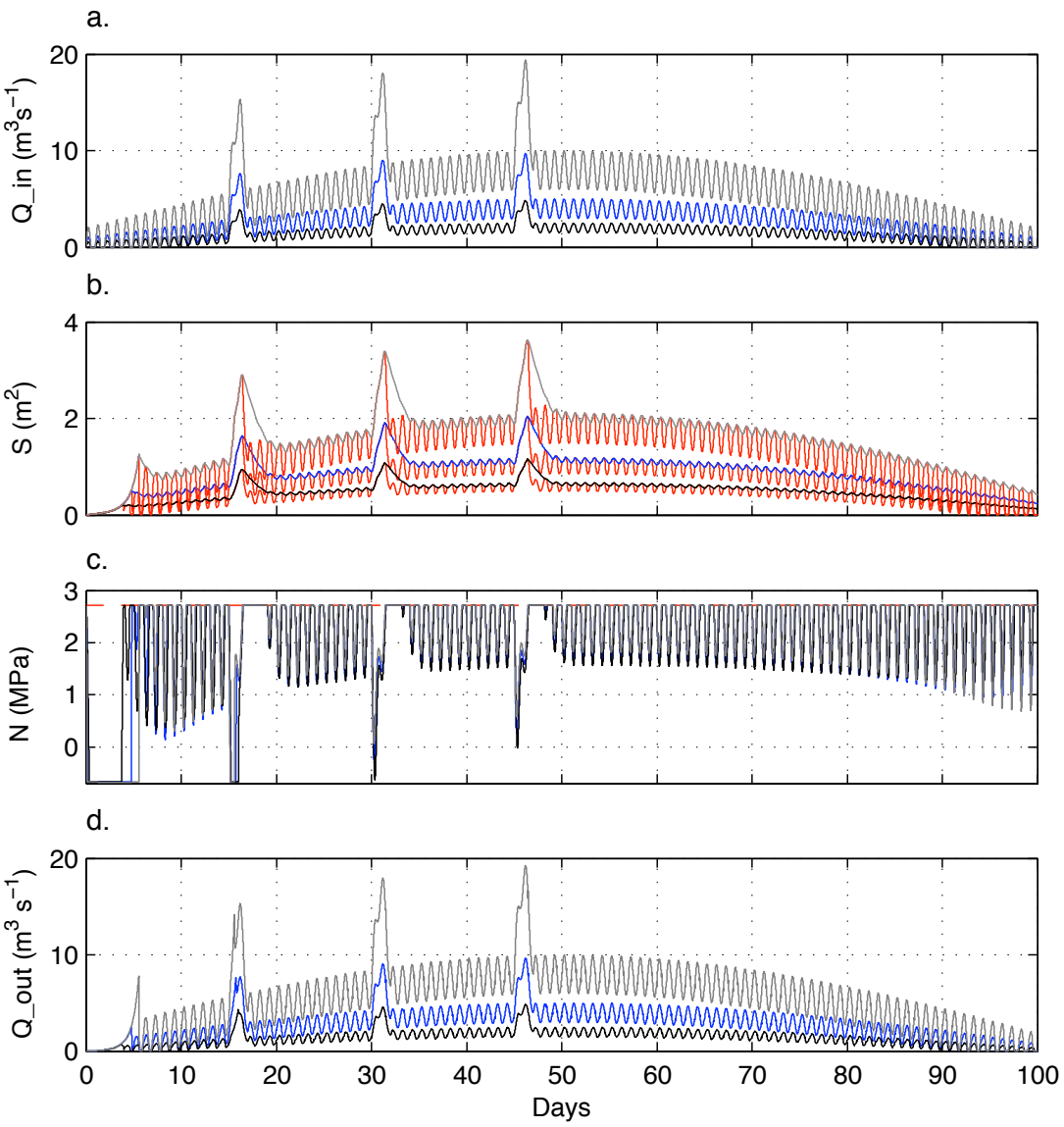

Figure 8.17: Simulation of channel-cross section evolution in response to a time-varying water input signal with different magnitude meltwater scenarios. a. Inflow to the system, Q_{in} (blue = Q_{in}; black = Q_{in} x2; grey = Q_{in} x4) . b. Conduit cross-sectional area, S (blue = Q_{in}; black = Q_{in} x2; grey = Q_{in} x4) and filled cross-sectional area (red) under open-channel conditions. c. Effective pressure, $N = p_i - p_w$ (blue = Q_{in}; black = Q_{in} x2; grey = Q_{in} x4), at the modelled cross-section. Maximum N is equal to p_i (red dashes). d. Outflow from the system, Q_{out} (blue = Q_{in}; black = Q_{in} x2; grey = Q_{in} x4).

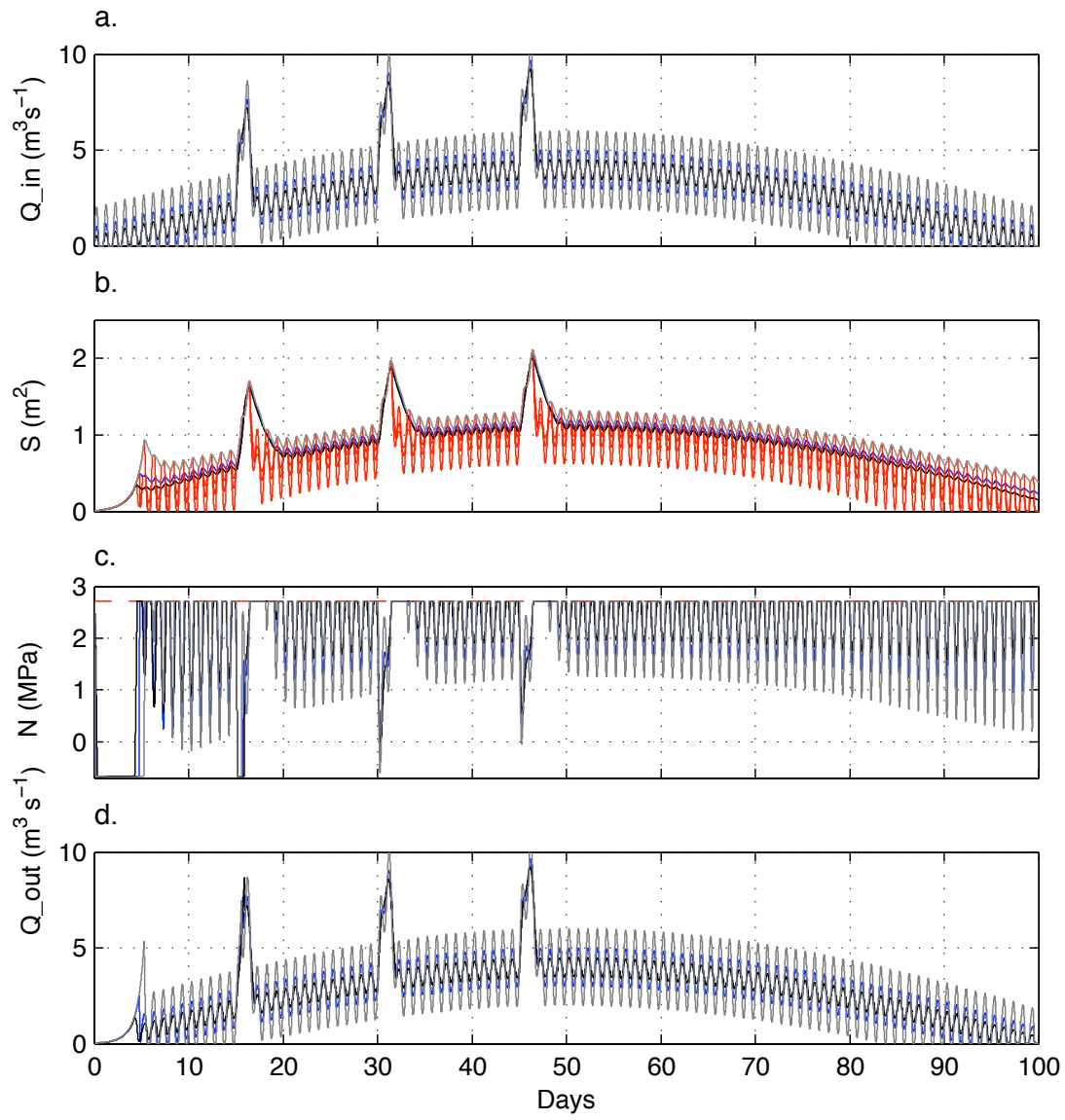

Figure 8.18: Simulation of channel-cross section evolution in response to a time-varying water input signal with different daily cycle scenarios. a. Inflow to the system, Q_{in} (blue = 2 m^3 s^{-1} amplitude; black = 1 m^3 s^{-1} amplitude; grey = 4 m^3 s^{-1} amplitude). b. Conduit cross-sectional area, S (blue = 2 m^3 s^{-1} amplitude; black = 1 m^3 s^{-1} amplitude; grey = 4 m^3 s^{-1} amplitude) and filled cross-sectional area (red) under open-channel conditions. c. Effective pressure, $N = p_i - p_w$ (blue = 2 m^3 s^{-1} amplitude; black = 1 m^3 s^{-1} amplitude; grey = 4 m^3 s^{-1} amplitude), at the modelled cross-section. Maximum N is equal to p_i (red dashes). d. Outflow from the system, Q_{out} (blue = 2 m^3 s^{-1} amplitude; black = 1 m^3 s^{-1} amplitude; grey = 4 m^3 s^{-1} amplitude).

conduit scales with the magnitude of the meltwater input signal (Figure 8.17a,b), daily cycles in effective pressure are much less sensitive (Figure 8.17). As discussed in this chapter, we obtain this result because variations in effective pressure are controlled more strongly by short-term variability in meltwater drainage which leads to an imbalance

between conduit capacity and meltwater inputs. In experiments presented in figure 8.18, therefore, we changed the magnitude of daily cycles in meltwater inputs while keeping the longer term signal the same. Increasing the daily variations in meltwater drainage leads to similar conduit growth, but much greater daily variations in N, while reducing the magnitude of daily cycles in meltwater drainage has the opposite effect.

CHAPTER 9

Conclusions

The aim of this thesis has been to investigate the relationship between surface meltwater production and seasonal variations in ice velocity in a land-terminating outlet glacier in west Greenland. The investigations were motivated by uncertainty about the effect of meltwater on rates of ice flow in the GrIS and the possibility that hydrologically forced changes in ice velocity might increase mass loss from the ice sheet significantly in response to climate warming.

The link between subglacial water pressure and variations in the basal sliding component of glacier motion has been long recognised in temperate glaciers (e.g. *Iken et al.*, 1983; *Iken and Bindschadler*, 1986) and a number of authors had suggested that Alpine glaciers, where the relationship between surface melting and ice motion depends on variations in the structure, hydraulic-capacity and efficiency of the subglacial drainage system (*Iken et al.*, 1983), may provide an appropriate analogue for the relationship between meltwater and ice velocity in the GrIS (e.g. *Bartholomaus et al.*, 2007; *Shepherd*

et al., 2009). Until now, however, limited datasets have been unable to assess this hypothesis for the GrIS and it is not clear whether our understanding of the behaviour of smaller glaciers can be scaled-up to large ice sheet systems.

The research presented in this thesis is based on field observations of the hydrology and dynamics of Leverett Glacier, a land-terminating outlet glacier at ∼67.10° N in west Greenland. We used a suite of different field observations in order to compare temporal and upglacier variability in the relationship between surface meltwater production, subglacial drainage system development and ice velocity over the course of three melt seasons. The primary field datasets were supplemented by use of satellite data and simple modelling.

In chapter 4 we compared seasonal records of ice velocity at four GPS sites in a transect which extended up to ∼35 km inland with variations in air temperature. We found that summer acceleration occurred at each of these sites, first near the ice sheet margin and progressively upglacier following the onset of surface melting. Observations of temperature and coincident changes in horizontal and vertical motion at each site, suggest a local, temperature-related, forcing mechanism for the seasonal changes in ice-motion. These summer velocity variations lead to an increase in annual ice motion of 6 - 14 %.

Comparison with records of air temperature indicated, however, that a temporally consistent relationship between surface melt and ice velocity does not exist once a hydraulic connection has been made and increases in ice velocity became less sensitive to surface melt rates later in the melt season. These results are interpreted to show that development in the structure and efficiency of the subglacial drainage system causes a reduction in basal water pressure in late summer, in a manner similar to Alpine glaciers. A more efficient subglacial drainage system can evacuate large volumes of water in discrete channels which operate at a lower steady-state water pressure, thereby reducing the basal lubrication effect of external meltwater inputs (e.g. *Röthlisberger*, 1972; *Kamb*, 1987; *Iken and Truffer*, 1997; *Schoof*, 2010; *Pimentel and Flowers*, 2011).

The hydrological study in chapter 5 substantiated the arguments made in chapter 4. Using proglacial records of discharge, EC and SSC we found that an efficient subglacial drainage system expanded upglacier, at the expense of the inefficient winter

drainage system, as the melt season progressed. This development was forced by inputs of meltwater from the ice sheet surface. We proposed that the model is similar to Alpine systems where the drainage system becomes increasingly efficient as hydraulic connections between the surface and bed are established further inland, evacuating large volumes of meltwater and sediment. It is notable, therefore, that the channelised subglacial drainage system is sustained in the GrIS where ice thicknesses are much greater. This implies that the high volumes of meltwater input are sufficient to offset increased channel closure potential by deformation of thicker ice.

The hydrological records revealed outburst of discrete pulses of stored water from the terminus of Leverett Glacier. These observations indicate that upglacier expansion of the efficient drainage system took place in a stepwise manner as water drained to the bed further and further inland. Satellite imagery suggests that supraglacial lake drainage events play a key role in establishing hydraulic connections between the ice sheet surface and bed, helping to drive evolution of the subglacial drainage system. Lake drainage events, which have the potential to concentrate surface meltwaters into large enough reservoirs to propagate fractures through ice that is >1000 m thick (*Alley et al.*, 2005b; *Das et al.*, 2008; *Krawczynski et al.*, 2009), may be especially important at higher elevations.

The seasonal and spatial increase in subglacial hydraulic efficiency supported arguments that have been advanced by previous authors to question the existence of positive feedback between climate warming and annual ice velocity of the GrIS (*Truffer et al.*, 2005; *Van de Wal et al.*, 2008). Although we do not claim that this process is responsible for the lack of correlation between seasonal ablation rates and velocity changes observed in the long-term study of ice motion in the Leverett Glacier region by *Van de Wal et al.* (2008), the findings presented in chapter 4 lead some to argue, by extension, that summer and therefore annual mean ice velocities at a given site on the GrIS could be *lower* in high ablation years than in low ablation years because channelisation of the subglacial hydrological system would occur more quickly (*Truffer et al.*, 2005; *Van de Wal et al.*, 2008; *Schoof*, 2010; *Pimentel and Flowers*, 2011; *Sundal et al.*, 2011).

Such reasoning ignores two crucial aspects of this problem: Firstly, the initiation of

hydrologically-forced ice velocity variations is dependent on the development of a conduit from the ice sheet surface to allow surface meltwater to access the ice-bed interface. In a warmer climate we expect summer melting of the GrIS to be more intense, affecting a wider area for a longer time period than is currently the case (*Hanna et al.*, 2008), providing greater volumes of surface meltwater. It is likely, then, that seasonal velocity variations in the GrIS will propagate further inland in response to climate warming. In addition, while diurnal ice velocity variations had been observed up to 72 km from the GrIS margin in a short-term study (*Shepherd et al.*, 2009), lack of comprehensive datasets meant that it was not clear that patterns in hydrologically-forced dynamic behaviour observed near the ice sheet margin are replicated at higher elevations.

In chapter 6 we presented ice velocity data from a transect which extended across the entire ablation zone and reached up to ∼1700 m elevation. At higher elevations (>1000 m), where the ice is thicker and temperatures are colder, there was a significant time lag between the onset of surface melting, as inferred from both positive degree-days and MODIS-derived albedo values, and the establishment of a hydraulic connection between the ice sheet surface and its bed as inferred from uplift of the ice surface. This means that significant velocity enhancement occurs for a much shorter time period than at lower elevations. Comparison of satellite observations of supraglacial lake drainage with ice velocity records indicates that drainage of stored surface water is a key factor in initiating hydrologically-forced ice acceleration at these higher elevation sites.

We found a strong positive correlation between rates of annual ablation and changes in annual ice velocity along the entire transect, with sites nearest the ice sheet margin experiencing greater increases in annual motion (15 - 18 %) than those above 1000 m elevation (3 - 8 %). At sites in the upper ablation zone, timing of meltwater drainage to the ice-bed interface appears to be the main control on the the overall magnitude of summer acceleration. In the lower ablation zone, the overall contribution of variations in ice motion to annual flow rates is limited by evolution in the structure of the subglacial drainage system. The positive relationship between temperature and seasonal acceleration across the lower elevation sites is explained, however, by variations in the rate, rather than the absolute volume, of meltwater production and delivery to the ice-bed interface.

Importantly, the data presented in chapter 6 indicate that short-term variations in ice velocity can still occur even once the subglacial drainage system has become channelised. Short-term variations in the rate of meltwater delivery to the ice-bed interface cause a temporary imbalance between the volume of water and the capacity of the subglacial drainage system to evacuate this water without an increase in pressure over a wide enough area to significantly affect basal motion (*Kamb et al.*, 1994). We find that hydrologically-forced ice acceleration is greatest on the rising limb of the seasonal runoff hydrograph when the hydraulic capacity of the subglacial drainage system is consistently exceeded and suggest that short-term variability in meltwater supply can sustain significant velocity variations for a large part of the summer.

Steady-state analysis of subglacial drainage system behaviour does not explain the positive correlation between rates of annual ablation and changes in annual ice velocity along the transect particularly well; sites near the ice sheet margin, which experience the highest rates of surface ablation, do not experience a smaller acceleration that those several kilometres upglacier. Although channelised drainage conditions do allow a reduction in subglacial water pressures in late summer, this appears to not be sufficient to cause a general reduction in ice velocities, which are sustained by time-varying meltwater inputs to the subglacial drainage system. These observations suggest that the timing of a transition from distributed to channelised drainage is not the main control on inter-annual variations in ice velocity at a particular site. Combined with the data from higher elevation sites, these findings lead us to hypothesise that inland propagation of hydrologically-forced velocity variations will induce greater dynamic mass loss in land-terminating sections of the GrIS in years with higher melting, as ice motion is sustained at sites near the ice sheet margin and water reaches the ice sheet bed earlier in the summer and at sites further inland.

In chapter 7 we had the opportunity to test this hypothesis. Regional scale data showed that summer temperatures near to the transect were approximately the same in 2009 as the 1960 - 2010 average, while 2010 was $\sim$2.5°C warmer. The regional temperature difference between 2009 and 2010 was reflected in the local measurements of air temperature at our sites, where the average difference in May-August mean temperature was 2.1°C. Local measurements of surfacing lowering at each GPS site also

show that total summer ablation was 22 - 220% greater in 2010 than 2009, while the runoff observations from Leverett Glacier glacier show that cumulative bulk discharge was approximately twice as great in 2010 compared with 2009.

Significantly, comparison of annual motion data from 2009 and 2010 shows, with the exception of site 2, that annual mean velocities along the transect were greater in 2010 than in 2009. On average, velocity variations in 2010 contributed an extra 2 % increase in annual motion on top of winter background rates compared with 2009. In addition, increases in ice velocity at our highest elevation GPS sites indicate that ice velocity variations also propagated further into the ice sheet in the warmer year of 2010. Combining data from 2009 and 2010 these data show that there is a direct and positive relationship between the seasonal rates of local ablation and the percentage increase in annual motion due to summer acceleration at each site.

Finally, in Chapter 8 we used high temporal resolution GPS data to reveal the detailed structure of the seasonal velocity record across our transect. These data are coupled with a simple model of subglacial conduit behaviour in response to a time-varying meltwater input signal in order to investigate the role of short-term variability in meltwater production on seasonal patterns of ice motion.

Both the field observations and modelling experiments support the idea that discharge through the subglacial drainage system and water pressure are in phase over short timescales ($<\sim$1 week), due to an imbalance between the capacity of the subglacial drainage system to evacuate meltwater and variations in meltwater input. Over longer timescales, however, an increase in the hydraulic capacity of the subglacial drainage system allows higher discharge at lower pressures than earlier in the summer.

The summer acceleration signal at sites near the ice sheet margin is dominated by short-term velocity variations on timescales ranging from a few hours to several days, which are forced by variations in air temperature or drainage of stored water from the ice sheet surface. The largest ice velocity events are absent, however, in the second part of the summer and we find that the reduction in mean late summer velocity at these sites is primarily due to stabilisation in the meltwater input signal.

Behaviour at higher elevations, where overall seasonal acceleration is lower, appears to be controlled strongly by supraglacial and englacial hydrology. In the first instance,

accumulation and sudden drainage of stored water from the ice sheet surface controls the timing of hydrologically forced ice acceleration. Following the initial drainage event, however, short-term cycles in meltwater inputs to the ice sheet bed are subdued. At these elevations meltwater input locations are more widely spaced and the snowpack remains for much of the summer, leading to long supraglacial transit times which damp diurnal and other short-term variations in meltwater deliver. At these sites the velocity signal reflects the more gradual variations in meltwater input, and is punctuated by high velocity events where large volumes of stored meltwater drain to the ice-bed interface. The record from site 5 in 2010 shows, however, that warmer temperatures can encourage short-term variability in the meltwater input signal and that behaviour of higher elevation sites has the potential to become more like sites nearer the ice sheet margin.

Using a simple model of subglacial conduit evolution forced by a time-varying meltwater input signal, we are able to successfully reproduce the key features of the seasonal conduit development and pressure behaviour over both seasonal and short-term timescales. Our investigation suggests, therefore, that the total summer acceleration signal is plausibly interpreted as the integrated effect of numerous short-term events, rather than a transition from a period of consistently high ice velocities in early summer which are then reduced in late summer. Overall, our investigation substantiates arguments that variability in the *duration* and *rate*, rather than absolute volume, of meltwater delivery to the subglacial drainage system is an important control on seasonal patterns of subglacial water pressure, and therefore ice velocity.

The research presented in this thesis was motivated by uncertainty about the effect of hydrologically-forced ice acceleration on the future mass balance of the GrIS. Drainage of surface meltwater to the ice sheet bed has the potential to allow GrIS dynamics to respond to atmospheric forcing on timescales of decades or less (*Parizek and Alley*, 2004). Initial field observations had suggested that there is a direct and positive relationship between rates of surface melting and ice velocity (*Zwally et al.*, 2002) and a subsequent numerical simulation applied this relationship to suggest that the widespread effect of increased surface melting on ice velocities would lead to an additional sea level rise of 0.15 - 0.4 m by 2500 AD (*Parizek and Alley*, 2004).

Our investigations suggest that higher rates of seasonal ablation would lead to increased hydrologically-forced dynamic mass loss in land-terminating sections of the GrIS. Higher surface ablation will allow hydrologically-forced velocity variations to propagate over larger sections of the GrIS as sufficient meltwater to force a hydraulic connection to the ice-bed interface is generated over a wider area. In addition, meltwater drainage will occur earlier at those sites in the upper ablation zone where the delay in the onset of seasonal acceleration currently limits the overall speed-up. At sites near the ice sheet margin, where abundant meltwater already reaches the bed each summer, variability in the meltwater input signal can sustain the high levels of acceleration that we have observed. Insights from the new datasets that were collected show, however, that interaction between patterns of meltwater drainage to the ice-bed interface and behaviour of the subglacial drainage system make this problem more complex than was captured by the initial observations made by *Zwally et al.* (2002) and the simulations performed by *Parizek and Alley* (2004).

We believe, then, that the research presented in this thesis offers an improved conceptual basis on which to understand the relationship between surface melting and ice dynamics in land-terminating sections of the GrIS. In addition, the data can be a valuable resource for numerical studies of hydro-dynamic behaviour in the GrIS. In the first instance we advocate attempts to use the positive relationship between seasonal rates of local ablation and the percentage increase in annual velocity reported in chapter 7 to constrain basal processes empirically in, for example, an ice flow-line model. This can then be used to perform similar experiments to *Parizek and Alley* (2004) to assess the potential impact of hydrologically-forced ice acceleration on the future mass balance of the GrIS in a range of anticipated climate scenarios. In the longer-term, we hope that insights from this work can help researchers in the glaciological modelling community improve representation of hydrologically-forced acceleration and subglacial drainage processes in more physically-based ice sheet models which are used to predict future sea-level change. Such models do exist for smaller domains(*Pimentel and Flowers*, 2011, e.g) as well as schemes for the inclusion of basal hydrology into ice flow models (e.g. *Creyts and Schoof*, 2009). It is clear, however, that this is not a straightforward task. A particular challenge is to represent detailed and complex physical processes on

appropriate temporal and spatial scales within the limits imposed by computational efficiency (*Alley et al.*, 2005a; *Parizek*, 2010). This problem is currently being worked on by a large number of groups and represents a focus for large collaborative projects such as the European Union funded Ice2sea initiative. In a more practical sense the data are also of value for calibration and testing of such models.

At the outset we identified that Alpine glaciers may provide an appropriate analogue for hydro-dynamic behaviour in the GrIS. We find that the basic processes operate in a very similar way: local drainage of meltwater to the ice bed interface causes surface uplift and horizontal acceleration of the ice, the hydrological system develops in efficiency, both spatially and temporally, over the course of the melt season and development in the structure of subglacial drainage system has a limiting effect on ice velocities. There are important differences, however, between an Alpine glacier setting and the marginal zone of the GrIS which complicate the analogy. Firstly, thicker ice found in the GrIS influences patterns in the timing and manner of meltwater delivery to the ice-bed interface, particularly at high elevation sites. The hydrofracture mechanism is critical in propagating fractures through the thick cold ice, in a manner similar to that observed on high Arctic polythermal glaciers (e.g. *Boon and Sharp*, 2003; *Bingham et al.*, 2003). In particular, drainage of supraglacial lakes, during which large volumes of meltwater drain in a discrete pulse, may play a key role in spatial and temporal development of subglacial drainage at higher elevations and as the ablation zone expands upglacier. Secondly, the larger catchment sizes that are possible for moulins in the GrIS alters patterns in meltwater delivery to the ice-bed interface, affecting short-term variability in ice motion. This appears to be particularly important at sites where the winter snowpack remains for most of the summer. Finally, we have identified that the rising limb of seasonal runoff and variability associated with upglacier evolution of the drainage system play a key role in sustaining ice velocities at sites lower in the ablation zone. Compared with Alpine glaciers where the spatial extent of surface melting is limited by the size of the glacier, in the GrIS there is effectively an unlimited upglacier extent over which surface melting can occur. Meltwater production can therefore keep rising as a result of increased temperatures over a wider and wider area over the course of a summer, perhaps being able to sustain increasing rate of discharge for longer than

is possible in Alpine glaciers.

An important consequence of this study, which used more detailed datasets than had been available previously, has been to cast doubt on the application of steady-state analysis of subglacial drainage system behaviour to understand the role of subglacial drainage in mediating the relationship between meltwater production and ice velocity (e.g. *Van de Wal et al.*, 2008; *Schoof*, 2010; *Pimentel and Flowers*, 2011; *Sundal et al.*, 2011). This idea has gained momentum recently within the glaciological community, because it provides an explanation for the observations that late summer velocity is lower than in the spring while melt rates remain high. It is a conceptually attractive explanation which turns the original hypothesis on its head (*Sundal et al.*, 2011). Channelisation of the subglacial drainage system has often been invoked to explain late summer slow-down in the same way in Alpine and Alaskan glaciers (e.g. *Mair et al.*, 2002b; *Anderson et al.*, 2004; *Bartholomaus et al.*, 2007), although it has been shown that short-term fluctuations in ice velocity can still occur (e.g. *Nienow et al.*, 2005).

Such reasoning has, however, ignored crucial aspects of this problem. For example, the focus on behaviour at a particular site (e.g. *Van de Wal et al.*, 2008; *Sundal et al.*, 2011) fails to account for inland propagation of the seasonal acceleration signal. In addition, it has not been known whether behaviour observed at lower elevations is replicated upglacier. Critically, our investigations suggest that the subglacial drainage system in the ablation zone of the GrIS rarely appears to operate under steady-state conditions. While this last finding undermines recent hypotheses about the impact of hydrologically-forced ice acceleration on future mass loss from the GrIS, its likelihood was put forward by *Röthlisberger* (1972) in his seminal paper on subglacial drainage nearly 40 years ago. While this might be a contentious observation, we suggest that, since observations in Greenland are difficult to obtain, investigators have at times been required to utilise temporally or spatially limited datasets, resulting in the reporting of potentially ambiguous signals with respect to their particular argument.

In many ways, the research presented in this study is preliminary and therefore provides the impetus for future work at Leverett Glacier and on other outlet glaciers in the GrIS. For example, we have highlighted that the timing, location and variability of seasonal meltwater drainage to the ice-bed interface are extremely important in

controlling the overall magnitude of summer acceleration, suggesting a need for detailed investigations of supraglacial and englacial hydrology in the GrIS and how it might evolve in the future. In particular this includes spatial and temporal controls on supraglacial lake development and drainage, crevasse and moulin formation, removal of the seasonal snowpack and spacing of supraglacial streams. Many of these questions are already being investigated by researchers within the glaciological community (e.g. *Sundal et al.*, 2009; *Krawczynski et al.*, 2009; *Catania and Neumann*, 2010).

At Leverett Glacier, the detailed datasets from three field seasons make it a good test site for catchment scale modelling experiments and for more detailed investigations which focus on spatial and temporal variability in subglacial drainage behaviour and ice velocity. The model of a single subglacial conduit presented in chapter 8 is rudimentary and only designed to demonstrate the behaviour of the equations which describe the physics of subglacial conduit development (*Schoof*, 2010). The next step is to generate a more sophisticated and spatially distributed version of this model, and to couple this with improved meltwater input data. In addition, while upglacier and temporal variability in seasonal drainage system development and changes in ice velocity have been investigated along the transect, further studies which investigate lateral variability in both of these processes on a range of scales would help us to understand how widespread or restricted the effect of acceleration in outlet glaciers might be (e.g. *Palmer et al.*, 2011). In addition, we currently lack direct observations of subglacial water pressures with which to compare our records of ice velocity and meltwater production. These could be captured using borehole drilling studies and would provide valuable information to verify the hypotheses made here about subglacial drainage system behaviour, and to constrain the relationship between basal water pressure and glacier sliding (e.g. *Harper et al.*, 2010).

The overall aim of this thesis has been to provide insights about hydrologically-forced dynamic behaviour in a land-terminating section of the GrIS margin, in order to help improve our ability to make predictions about the future mass balance of the ice sheet. Our observations have been made at a single glacier for a relatively short period of time. Although there is no reason that the findings presented here cannot be generalised across the whole ice sheet, it is not certain to be the case. Extending similar studies

to outlet glaciers at different latitudes and other regions of the GrIS margin will help address this shortcoming. Finally, continuous long-term records of ice velocity from Leverett Glacier can provide valuable datasets to investigate the longer-term controls on inter-annual variations in hydrologically-forced ice acceleration in land-terminating glaciers and to provide data to the glaciological community for model validation and testing.

While this thesis has focused on land-terminating glaciers, the significance of the results must be considered in the context of marine-terminating glaciers, not least because of their importance for the mass balance of the GrIS (*Rignot and Kanagaratnam*, 2006). Marine-terminating outlet glaciers have generally displayed less sensitivity to variations in meltwater forcing (*Echelmeyer and Harrison*, 1990; *Joughin et al.*, 2008a) and seasonal flow variations have been explained by changes in ice calving rates due to processes occurring at the ice front (e.g. *Howat et al.*, 2007; *Joughin et al.*, 2008b; *Nick et al.*, 2009; *Amundson et al.*, 2010). Subglacial hydrology has, however, been shown to exert strong control on the dynamics of marine-terminating glaciers in Alaska (e.g. *Kamb et al.*, 1994; *O'Neel et al.*, 2001). Furthemore, a number of recent observations suggest that meltwater forcing and glacier hydrology may also play an important role in the dynamics of marine-terminating outlet glaciers in the GrIS (*Joughin et al.*, 1996; *Andersen et al.*, 2010; *Howat et al.*, 2010; *Sole et al.*, 2011).

Sole et al. (2011) point out that most observations of seasonal flow variations in GrIS marine-terminating glaciers come from close to their termini (<30 km) where calving is likely to be the principal control on ice flow (*Joughin et al.*, 2008b). Their data show that, further into the ice sheet interior, seasonal and shorter-term variations in ice flow are controlled principally by surface melt-induced changes in subglacial hydrology rather than by changes at the calving front. It is not clear however, that the impact of meltwater forcing on marine-terminating glaciers results in the same acceleration signal as has been observed in land-terminating sections (*Joughin et al.*, 1996; *Andersen et al.*, 2010; *Howat et al.*, 2010; *Sole et al.*, 2011).

Although the relative importance of calving and hydrology on the dynamics of marine-terminating outlet glaciers is uncertain (e.g. *Andersen et al.*, 2010), these studies suggest that it is important to investigate the role of hydrological forcing on ice acceleration in

marine-terminating settings, particularly further from the glacier terminus. In addition, *Thomas et al.* (2009) shows that the greatest recent acceleration of marine-terminating outlet glaciers is restricted only to those with the deepest marine troughs. The impact of ice front processes on marine-terminating glacier dynamics may therefore become diminished if marine-terminating glaciers continue their retreat into shallower water (e.g. *Howat et al.*, 2008), or retreat further to become land-terminating (*Bamber et al.*, 2001; *Sole et al.*, 2008), leading to an increased role for hydrologically-forced ice dynamic processes in the future mass balance of the GrIS.

Bibliography

Alley, R. (1989), Water-pressure coupling of sliding and bed deformation: I. Water system, *Journal of Glaciology*, *35*(119), 108--118.

Alley, R., D. Blankenship, S. Rooney, and C. Bentley (1989), Water-pressure coupling of sliding and bed deformation: III. application to Ice Stream B, Antarctica, *Journal of Glaciology*, *35*(119), 130--139.

Alley, R., K. Cuffey, E. Evenson, J. Strasser, D. Lawson, and G. Larson (1997), How glaciers entrain and transport basal sediment: Physical constraints, *Quaternary Science Reviews*, *16*(9), 1017--1038.

Alley, R., P. Clark, P. Huybrechts, and I. Joughin (2005a), Ice-sheet and sea-level changes, *Science*, *310*(5747), 456.

Alley, R., T. Dupont, B. Parizek, and S. Anandakrishnan (2005b), Access of surface meltwater to beds of sub-freezing glaciers: preliminary insights, *Annals of Glaciology*, *40*(1), 8--14.

Amundson, J., M. Fahnestock, M. Truffer, J. Brown, M. Lüthi, and R. Motyka (2010), Ice mélange dynamics and implications for terminus stability, Jakobshavn Isbræ, Greenland, *Journal of Geophysical Research*, *115*, F01005.

Andersen, M., T. Larsen, M. Nettles, P. Elosegui, D. van As, G. Hamilton, L. Stearns, J. Davis, A. Ahlstrøm, J. de Juan, et al. (2010), Spatial and temporal melt variability at Helheim Glacier, East Greenland, and its effect on ice dynamics, *Journal of Geophysical Research*, *115*(F4), F04041.

Anderson, R., S. Anderson, K. MacGregor, E. Waddington, S. O'Neel, C. Riihimaki, and M. Loso (2004), Strong feedbacks between hydrology and sliding of a small alpine glacier, *Journal of Geophysical Research*, *109*.

Andreasen, J. (1985), Seasonal surface-velocity variations on a sub-polar glacier in West Greenland, *Journal of Glaciology*, *31*(109), 319--323.

Arnold, N., and M. Sharp (2002), Flow variability in the Scandinavian ice sheet: modelling the coupling between ice sheet flow and hydrology, *Quaternary Science Reviews*, *21*(4-6), 485--502.

Bamber, J., R. Layberry, and S. Gogineni (2001), A new ice thickness and bed data set for the Greenland ice sheet: I. Measurement, data reduction, and errors, *Journal of Geophysical Research. D. Atmospheres*, *106*, 33.

Bamber, J., D. Baldwin, and S. Gogineni (2003), A new bedrock and surface elevation dataset for modelling the greenland ice sheet, *Annals of Glaciology*, *37*(1), 351--356.

Bamber, J., R. Alley, and I. Joughin (2007), Rapid response of modern day ice sheets to external forcing, *Earth and Planetary Science Letters*, *257*(1-2), 1--13.

Bartholomaus, T., R. Anderson, and S. Anderson (2007), Response of glacier basal motion to transient water storage, *Nature Geoscience*, *1*(1), 33--37.

Bartholomew, I., P. Nienow, D. Mair, A. Hubbard, M. King, and A. Sole (2010), Seasonal evolution of subglacial drainage and acceleration in a Greenland outlet glacier, *Nature Geoscience*, *3*, 408--411.

Bartholomew, I., P. Nienow, A. Sole, D. Mair, T. Cowton, S. Palmer, and J. Wadham (2011a), Supraglacial forcing of subglacial hydrology in the ablation zone of the Greenland Ice Sheet, *Geophysical Research Letters*, *38*, L08502, doi:10.1029/2011GL047063.

Bartholomew, I., P. Nienow, A. Sole, D. Mair, T. Cowton, S. Palmer, and M. King (2011b), Seasonal variations in Greenland Ice Sheet motion: inland extent and behaviour at higher elevations, *Earth and Planetary Science Letters*, *307*, 271--278, doi:10.1016/j.epsl.2011.04.014.

Bindoff, N., J. Willebrand, V. Artale, A. Cazenave, J. Gregory, S. Gulev, K. Hanawa, C. Le Quere, S. Levitus, Y. Nojiri, L. Shum, C nad Talley, and A. Unnikishnan (2007), Observations: oceanic climate change and sea level, in *Climate change 2007: the physical science basis. Contribution of Working Group I to the Fourth Assessment Report of the Intergovernmental Panel on Climate Change*, edited by S. Solomon, D. Qin, M. Manning, Z. Chen, M. Marquis, K. Averyt, M. Tignor, and H. Miller, Cambridge University Press, Cambridge.

Bindschadler, R. (1983), The importance of pressurized subglacial water in separation and sliding at the glacier bed, *Journal of Glaciology*, *29*(101), 3--19.

Bingham, R., P. Nienow, and M. Sharp (2003), Intra-annual and intra-seasonal flow dynamics of a High Arctic polythermal valley glacier, *Annals of Glaciology*, *37*(1), 181--188.

Bingham, R., P. Nienow, M. Sharp, and L. Copland (2006), Hydrology and dynamics of a polythermal (mostly cold) high arctic glacier, *Earth Surface Processes and Landforms*, *31*(12), 1463--1479.

Bingham, R., A. Hubbard, P. Nienow, and M. Sharp (2008), An investigation into the mechanisms controlling seasonal speedup events at a High Arctic glacier, *Journal of Geophysical Research*, *113*(F2), F02006.

Blake, E., U. Fischer, and G. Clarke (1994), Direct measurement of sliding at the glacier bed, *Journal of Glaciology*, *40*, 595--599.

Bogen, J. (1996), Erosion rates and sediment yield of glaciers, *Annals of Glaciology*, *22*, 48--52.

Boon, S., and M. Sharp (2003), The role of hydrologically-driven ice fracture in drainage system evolution on an Arctic glacier, *Geophysical Research Letters*, *30*(18), 1916.

Boulton, G., and R. Hindmarsh (1987), Sediment deformation beneath glaciers: rheology and geological consequences, *Journal of Geophysical Research*, *92*(B9), 9059--9082.

Boulton, G., P. Dongelmans, M. Punkari, and M. Broadgate (2001), Palaeoglaciology of

an ice sheet through a glacial cycle:-the European ice sheet through the Weichselian, *Quaternary Science Reviews*, *20*(4), 591--626.

Box, J., and K. Ski (2007), Remote sounding of Greenland supraglacial melt lakes: implications for subglacial hydraulics, *Journal of Glaciology*, *53*(181), 257--265.

Box, J., J. Cappelen, D. Decker, X. Fettweis, T. Mote, M. Tedesco, and R. van de Wal (2010), Greenland, *Arctic Report Card 2010, http://www.arctic.noaa.gov/reportcard*.

Braithwaite, R. (1995), Positive degree-day factors for ablation on the greenland ice sheet studied by energy-balance modelling, *Journal of Glaciology*, *41*(137), 153--160.

Braithwaite, R., and O. Olesen (1989), Calculation of glacier ablation from air temperature, west Greenland, in *Glacier fluctuations and climatic change*, *Glaciology and Quaternary Geology*, vol. 6, edited by J. Oerlemans, pp. 219--233, Springer.

Braithwaite, R., and O. Olesen (1990), Response of the energy balance on the margin of the Greenland ice sheet to temperature changes, *Journal of Glaciology*, *36*(123), 217--221.

Brennand, T. (2000), Deglacial meltwater drainage and glaciodynamics: inferences from Laurentide eskers, Canada, *Geomorphology*, *32*(3), 263--293.

Brennand, T., and J. Shaw (1994), Tunnel channels and associated landforms, south-central Ontario: their implications for ice-sheet hydrology, *Canadian Journal of Earth Sciences*, *31*(3), 505--522.

Brown, G. (2002), Glacier meltwater hydrochemistry, *Applied Geochemistry*, *17*(7), 855--883.

Campbell, F., P. Nienow, and R. Purves (2006), Role of the supraglacial snowpack in mediating meltwater delivery to the glacier system as inferred from dye tracer investigations, *Hydrological Processes*, *20*(4), 969--985.

Catania, G., T. Neumann, and S. Price (2008), Characterizing englacial drainage in the ablation zone of the Greenland ice sheet, *Journal of Glaciology*, *54*(187), 567--578, doi:10.3189/002214308786570854.

Catania, G. A., and T. A. Neumann (2010), Persistent englacial features in the Greenland Ice Sheet, *Geophysical Research Letters*, *37*(2), L02501.

Chen, G. (1999), GPS kinematic positioning for the airborne laser altimetry at Long Valley, California, Ph.D. thesis, Massachusetts Institute of Technology.

Chen, J., C. Wilson, and B. Tapley (2006), Satellite gravity measurements confirm accelerated melting of Greenland ice sheet, *Science*, *313*(5795), 1958.

Church, J., J. Gregory, P. Huybrechts, M. Kuhn, K. Lambeck, M. Nhuan, D. Qin, and P. Woodworth (2001), Changes in Sea Level, in *Climate change 2001: The Scientific Basis. Contribution of Working Group I to the Third Assessment Report of the Intergovernmental Panel on Climate Change*, edited by J. Houghton, Y. Ding, D. Griggs, M. Noguer, P. van der Linden, X. Dai, K. Maskell, and C. Johnson, pp. 639--693, Cambridge University Press.

Clark, P., and J. Walder (1994), Subglacial drainage, eskers, and deforming beds beneath the Laurentide and Eurasian ice sheets, *Bulletin of the Geological Society of America*, *106*(2), 304.

Clarke, G. (1987), Subglacial till: a physical framework for its properties and processes, *Journal of Geophysical Research*, *92*(B9), 9023--9036.

Clarke, G. (1996), Lumped-element analysis of subglacial hydraulic circuits, *Journal of Geophysical Research*, *101*(B8), 17,547--17.

Clifford, N., K. Richards, R. Brown, and S. Lane (1995a), Scales of variation of suspended sediment concentration and turbidity in a glacial meltwater stream, *Geografiska Annaler. Series A. Physical Geography*, *77*(1), 45--65.

Clifford, N., K. Richards, R. Brown, and S. Lane (1995b), Laboratory and field assessment of an infrared turbidity probe and its response to particle size and variation in suspended sediment concentration, *Hydrological Sciences*, *40*(6), 771--791.

Collins, D. (1979), Hydrochemistry of meltwaters draining from an Alpine glacier, *Arctic and Alpine Research*, *11*(3), 307--324.

Collins, D. (1990), Seasonal and annual variations of suspended sediment transport in meltwaters draining from an Alpine glacier, *Hydrology in Mountainous Regions. I. Hydrological Measurements; the Water Cycle*, *193*, 439--446.

Collins, D. (1996), A conceptually based model of the interaction between flowing meltwater and subglacial sediment, *Annals of Glaciology*, *22*, 224--232.

Copland, L., M. Sharp, and P. Nienow (2003), Links between short-term velocity variations and the subglacial hydrology of a predominantly cold polythermal glacier, *Journal of Glaciology*, *49*(166), 337--348.

Cowton, T., P. Nienow, A. Sole, I. Bartholomew, and D. Mair (in review), Rapid erosion beneath the Greenland Ice Sheet, *Geology*.

Creyts, T., and C. Schoof (2009), Drainage through subglacial water sheets, *Journal of Geophysical Research*, *114*, F04008.

Cubasch, U., G. Meehl, G. Boer, R. Stouffer, M. Dix, A. Noda, C. Senior, S. Raper, and K. Yap (2001), Projections of future climate change, in *Climate change 2001: The Scientific Basis. Contribution of Working Group I to the Third Assessment Report of the Intergovernmental Panel on Climate Change*, edited by J. Houghton, Y. Ding, D. Griggs, M. Noguer, P. van der Linden, X. Dai, K. Maskell, and C. Johnson, pp. 526--582, Cambridge University Press.

Cutler, P. (1998), Modelling the evolution of subglacial tunnels due to varying water input, *Journal of Glaciology*, *44*(148), 485--497.

Das, S., I. Joughin, M. Behn, I. Howat, M. King, D. Lizarralde, and M. Bhatia (2008), Fracture propagation to the base of the Greenland Ice Sheet during supraglacial lake drainage, *Science*, *320*(5877), 778.

Dasgupta, S., B. Laplante, C. Meisner, D. Wheeler, and J. Yan (2009), The impact of sea level rise on developing countries: a comparative analysis, *Climatic Change*, *93*(3), 379--388.

Denner, J., D. Lawson, G. Larson, E. Evenson, R. Alley, J. Strasser, and S. Kopczynski

(1999), Seasonal variability in hydrologic-system response to intense rain events, Matanuska Glacier, Alaska, USA, *Annals of Glaciology*, *28*(1), 267--271.

Denton, G., and D. Sugden (2005), Meltwater features that suggest Miocene ice-sheet overriding of the Transantarctic Mountains in Victoria Land, *Geografiska Annaler: Series A, Physical Geography*, *87*, 67--85.

Di Baldassarre, G., and A. Montanari (2009), Uncertainty in river discharge observations: a quantitative analysis, *Hydrology and Earth System Sciences*, *13*(6), 913--921.

Dickson, R., and J. Brown (1994), The production of North Atlantic Deep Water: sources, rates, and pathways, *Journal of Geophysical Research*, *99*(C6), 12,319--12.

Echelmeyer, K., and W. Harrison (1990), Jakobshavns Isbræ, West Greenland: Seasonal variations in velocity-or lack thereof, *Journal of Glaciology*, *36*, 82--88.

Echelmeyer, K., T. Clarke, and W. Harrison (1991), Surficial glaciology of Jakobshavns Isbræ, West Greenland: Part I. Surface morphology, *Journal of Glaciology*, *37*(127), 368--382.

Fenn, C. (1987), Electrical Conductivity, in *Glacio-fluvial Sediment Transfer: an Alpine Perspective*, edited by A. Gurnell and M. Clark, pp. 377--414, Wiley, Chichester.

Fichefet, T., C. Poncin, H. Goosse, P. Huybrechts, I. Janssens, and H. Le Treut (2003), Implications of changes in freshwater flux from the greenland ice sheet for the climate of the 21st century, *Geophysical Research Letters*, *30*(17), 1911.

Fischer, U., and G. Clarke (1997), Stick-slip sliding behaviour at the base of a glacier, *Annals of Glaciology*, *24*, 390--396.

Fischer, U., and G. Clarke (2001), Review of subglacial hydro-mechanical coupling: Trapridge Glacier, Yukon Territory, Canada, *Quaternary International*, *86*(1), 29--43.

Flowers, G., and G. Clarke (2002), A multicomponent coupled model of glacier hydrology: 1. Theory and synthetic examples, *Journal of Geophysical Research*, *107*(2287), 10--1029.

Fountain, A. (1994), Borehole water-level variations and implications for the subglacial hydraulics of South Cascade Glacier, Washington State, USA, *Journal of Glaciology*, *40*(135).

Fountain, A., and J. Walder (1998), Water flow through temperate glaciers, *Reviews of Geophysics*, *36*(3), 299--328.

Fowler, A. (1986), A sliding law for glaciers of constant viscosity in the presence of subglacial cavitation, *Proceedings of the Royal Society of London. A. Mathematical and Physical Sciences*, *407*(1832), 147.

Gordon, S., M. Sharp, B. Hubbard, C. Smart, B. Ketterling, and I. Willis (1998), Seasonal reorganization of subglacial drainage inferred from measurements in boreholes, *Hydrological Processes*, *12*(1), 105--133.

Greuell, W., B. Denby, R. van de Wal, and J. Oerlemans (2001), Correspondence. 10 years of mass-balance measurements along a transect near Kangerlussuaq, central West Greenland, *Journal of Glaciology*, *47*, 157--158.

Gudmundsson, G. (2003), Transmission of basal variability to a glacier surface, *Journal of Geophysical Research*, *108*(B5), 2253.

Gumley, L., J. Descloitres, and J. Schmaltz (2003), Creating reprojected true color modis images: A tutorial, *University of Wisconsin-Madison*.

Gurnell, A. (1987), Fluvial sediment yield from Alpine, glacierized catchments, in *Glaciofluvial sediment transfer: an Alpine perspective*, edited by A. Gurnell and M. Clark, pp. 415--420, Wiley, Chichester.

Gurnell, A. (1995), Sediment yield from alpine glacier basins, *Sediment and Water Quality in River Catchments*, pp. 407--435.

Gurnell, A., and J. Warburton (1990), The significance of suspended sediment pulses for estimating suspended sediment load and identifying suspended sediment sources in Alpine glacier basins, *Hydrology of Mountainous Regions*, *1*, 463--470.

Hall, D., S. Nghiem, C. Schaaf, N. DiGirolamo, and G. Neumann (2009), Evaluation of surface and near-surface melt characteristics on the greenland ice sheet using modis and quikscat data, *Journal of Geophysical Research*, *114*, F04006.

Hall, G., D.K. Riggs, and V. Salomonson (2009), MODIS/Aqua Snow Cover Daily L3 Global 500m Grid, V005, *Boulder, CO, USA: National Snow and Ice Data Center.*, *Digital media*.

Hanna, E., P. Huybrechts, K. Steffen, J. Cappelen, R. Huff, C. Shuman, T. Irvine-Fynn, S. Wise, and M. Griffiths (2008), Increased runoff from melt from the Greenland Ice Sheet: a response to global warming, *Journal of Climate*, *21*(2), 331--341.

Hanson, B., R. Hooke, and E. Grace Jr (1998), Short-term velocity and water-pressure variations down-glacier from a riegel, Storglaciären, Sweden, *Journal of Glaciology*, *44*(147), 359--367.

Harbor, J., M. Sharp, L. Copland, B. Hubbard, P. Nienow, and D. Mair (1997), Influence of subglacial drainage conditions on the velocity distribution within a glacier cross section, *Geology*, *25*(8), 739.

Harper, J., N. Humphrey, J. Johnson, T. Meierachtol, D. Brinkerhoff, and C. Landowski (2010), Integrating borehole measurements with modeling of englacial and basal conditions, western Greenland, Abstract C42A-03 presented at 2010 Fall Meeting, AGU, San Francisco, California 13-17 December.

Herschy, R. (1995), *Streamflow Measurement*, Taylor & Francis.

Hinze, H., and G. Seeber (1988), Ice-motion determination by means of satellite positioning systems, *Annals of Glaciology*, *11*, 36--41.

Hock, R. (2003), Temperature index melt modelling in mountain areas, *Journal of Hydrology*, *282*(1-4), 104--115.

Holland, D., R. Thomas, B. De Young, M. Ribergaard, and B. Lyberth (2008), Acceleration of Jakobshavn Isbræ triggered by warm subsurface ocean waters, *Nature Geoscience*, *1*(10), 659--664.

Hooke, R., P. Calla, P. Holmlund, M. Nilsson, and A. Stroeven (1989), A 3 year record of seasonal variations in surface velocity, Storglaciaren, Sweden, *Journal of Glaciology*, *35*(120), 235--247.

Hooke, R., T. Laumann, and J. Kohler (1990), Subglacial water pressures and the shape of subglacial conduits, *Journal of Glaciology*, *36*(122).

Hooke, R., et al. (1984), On the role of mechanical energy in maintaining subglacial water conduits at atmospheric pressure, *Journal of Glaciology*, *30*(105), 180--187.

Howat, I., I. Joughin, S. Tulaczyk, and S. Gogineni (2005), Rapid retreat and acceleration of Helheim Glacier, east Greenland, *Geophysical Research Letters*, *32*(22).

Howat, I., I. Joughin, and T. Scambos (2007), Rapid changes in ice discharge from Greenland outlet glaciers, *Science*, *315*(5818), 1559.

Howat, I., I. Joughin, M. Fahnestock, B. Smith, and T. Scambos (2008), Synchronous retreat and acceleration of southeast Greenland outlet glaciers 2000-06: ice dynamics and coupling to climate, *Journal of Glaciology*, *54*(187), 646--660.

Howat, I., J. Box, Y. Ahn, A. Herrington, and E. McFadden (2010), Seasonal variability in the dynamics of marine-terminating outlet glaciers in Greenland, *Journal of Glaciology*, *56*(198), 601--613.

Hubbard, B., and N. Glasser (2005), *Field techniques in glaciology and glacial geomorphology*, Wiley.

Hubbard, B., and P. Nienow (1997), Alpine subglacial hydrology, *Quaternary Science Reviews*, *16*(9), 939--955.

Hubbard, B., M. Sharp, I. Willis, M. Nielsen, and C. Smart (1995), Borehole water-level variations and the structure of the subglacial hydrological system of Haut Glacier d'Arolla, Valais, Switzerland, *Journal of Glaciology*, *41*(139), 572--583.

Humphrey, N., and C. Raymond (1994), Hydrology, erosion and sediment production in a surging glacier: Variegated Glacier, Alaska, 1982-83, *Journal of Glaciology*, *40*(136), 539--552.

Huybrechts, P., and J. de Wolde (1999), The dynamic response of the Greenland and Antarctic ice sheets to multiple-century climatic warming, *Journal of Climate*, *12*(8), 2169--2188.

Huybrechts, P., A. Letreguilly, and N. Reeh (1991), The Greenland ice sheet and greenhouse warming, *Global and Planetary Change*, *3*(4), 399--412.

Iken, A. (1981), The effect of the subglacial water pressure on the sliding velocity of a glacier in an idealized numerical model, *Journal of Glaciology*, *27*, 407--421.

Iken, A., and R. Bindschadler (1986), Combined measurements of subglacial water pressure and surface velocity of Findelengletscher, Switzerland: conclusions about drainage system and sliding mechanism, *Journal of Glaciology*, *32*, 110.

Iken, A., and M. Truffer (1997), The relationship between subglacial water pressure and velocity of Findelengletscher, Switzerland, during its advance and retreat, *Journal of Glaciology*, *43*(144), 328--338.

Iken, A., H. Rothlisberger, A. Flotron, and W. Haeberli (1983), The uplift of Unteraargletscher at the beginning of the melt season, a consequence of water storage at the bed?, *Journal of Glaciology*, *29*(101), 28--47.

IPCC (2007), *Climate Change 2007: the physical science basis. Contribution of Working Group I to the Fourth Assessment Report of the Intergovernmental Panel on Climate Change*, Cambridge University Press.

Iverson, N., B. Hanson, R. Hooke, and P. Jansson (1995), Flow mechanism of glaciers on soft beds, *Science*, *267*(5194), 80.

Iverson, N., R. Baker, R. Hook, B. Hanson, and P. Jansson (1999), Coupling between a glacier and a soft bed: I. A relation between effective pressure and local shear stress determined from till elasticity, *Journal of Glaciology*, *45*(149), 31--40.

Jansson, P., R. Hock, and T. Schneider (2003), The concept of glacier storage: a review, *Journal of Hydrology*, *282*(1-4), 116--129.

Joughin, I., S. Tulaczyk, M. Fahnestock, and R. Kwok (1996), A mini-surge on the Ryder Glacier, Greenland, observed by satellite radar interferometry, *Science*, *274*(5285), 228--230.

Joughin, I., W. Abdalati, and M. Fahnestock (2004), Large fluctuations in speed on Greenlands Jakobshavn Isbræ glacier, *Nature*, *432*, 608--610.

Joughin, I., S. Das, M. King, B. Smith, I. Howat, and T. Moon (2008a), Seasonal Speedup Along the Western Flank of the Greenland Ice Sheet, *Science*, *320*(5877), 781--783, doi:10.1126/science.1153288.

Joughin, I., I. Howat, M. Fahnestock, B. Smith, W. Krabill, R. Alley, H. Stern, and M. Truffer (2008b), Continued evolution of Jakobshavn Isbræ following its rapid speedup, *Journal of Geophysical Research*, *113*(F4), F04006.

Joughin, I., B. Smith, I. Howat, T. Scambos, and T. Moon (2010), Greenland flow variability from ice-sheet-wide velocity mapping, *Journal of Glaciology*, *56*(197), 415--430.

Kalnay, E., M. Kanamitsu, R. Kistler, W. Collins, D. Deaven, L. Gandin, M. Iredell, S. Saha, G. White, J. Woollen, et al. (1996), The NCEP/NCAR 40-year reanalysis project, *Bulletin of the American Meteorological Society*, *77*(3), 437--471.

Kamb, B. (1987), Glacier surge mechanism based on linked cavity configuration of the basal water conduit system, *Journal of Geophysical Research*, *92*(B9), 9083--9100.

Kamb, B., C. Raymond, W. Harrison, H. Engelhardt, K. Echelmeyer, N. Humphrey, M. Brugman, and T. Pfeffer (1985), Glacier surge mechanism: 1982-1983 surge of Variegated Glacier, Alaska, *Science*, *227*(4686), 469--479.

Kamb, B., H. Engelhardt, M. Fahnestock, N. Humphrey, M. Meier, and D. Stone (1994), Mechanical and hydrologic basis for the rapid motion of a large tidewater glacier 2. Interpretation, *Journal of Geophysical Research*, *99*(B8), 15,231.

Kessler, M., and R. Anderson (2004), Testing a numerical glacial hydrological model using spring speed-up events and outburst floods, *Geophysical Research Letters*, *31*(18), L18503.

Kilpatrick, F., and E. Cobb (1984), *Measurement of discharge using tracers*, *USGS Techniques of Water-Resources Investigations*, vol. 3, chap. A-16.

King, M. (2004), Rigorous GPS data-processing strategies for glaciological applications, *Journal of Glaciology*, *50*(171), 601--607.

King, R., and Y. Bock (2006), Documentation for the GAMIT GPS analysis software, version 10.3, *Massachusetts Institute of Technology, Cambridge*.

Knap, W., and J. Oerlemans (1996), The surface albedo of the Greenland ice sheet: Satellite-derived and in situ measurements in the Sondre Stromfjord area during the 1991 melt season, *Journal of Glaciology*, *42*(141), 364--674.

Krabill, W. (2010), IceBridge ATM L2 Icessn Elevation, Slope, and Roughness, [8.5.2010], *Boulder, Colorado USA: National Snow and Ice Data Center*, *Digital Media*.

Krabill, W., W. Abdalati, E. Frederick, S. Manizade, C. Martin, J. Sonntag, R. Swift, R. Thomas, W. Wright, and J. Yungel (2000), Greenland ice sheet: High-elevation balance and peripheral thinning, *Science*, *289*(5478), 428.

Krabill, W., E. Hanna, P. Huybrechts, W. Abdalati, J. Cappelen, B. Csatho, E. Frederick, S. Manizade, C. Martin, J. Sonntag, et al. (2004), Greenland ice sheet: increased coastal thinning, *Geophysical Research Letters*, *31*(10.1029).

Krawczynski, M., M. Behn, S. Das, and I. Joughin (2009), Constraints on the lake volume required for hydro-fracture through ice sheets, *Geophysical Research Letters*, *36*(10), L10501.

Lang, H., and L. Braun (1990), On the information content of air temperature in the context of snow melt estimation, in *Hydrology of mountainous areas, Proceedings of the Strbske Pleso Symposium 1990: International Association of Scientific Hydrology*, vol. 190, edited by L. Molnar, pp. 347--354.

Leick, A. (2004), *GPS satellite surveying*, Wiley.

Lliboutry, L. (1968), General theory of subglacial cavitation and sliding of temperate glaciers, *Journal of Glaciology*, *7*(49), 21--58.

Luckman, A., and T. Murray (2005), Seasonal variation in velocity before retreat of Jakobshavn Isbræ, Greenland, *Geophysical Research Letters*, *32*(8), L08501.

Luckman, A., T. Murray, R. De Lange, and E. Hanna (2006), Rapid and synchronous ice-dynamic changes in East Greenland, *Geophysical Research Letters*, *33*(3), L03503.

MacGregor, K., C. Riihimaki, and R. Anderson (2005), Spatial and temporal evolution of rapid basal sliding on Bench Glacier, Alaska, USA, *Journal of Glaciology*, *51*(172), 49--63.

Mair, D., P. Nienow, I. Willis, and M. Sharp (2001), Spatial patterns of glacier motion during a high-velocity event: Haut Glacier d'Arolla, Switzerland, *Journal of Glaciology*, *47*(156), 9--20.

Mair, D., M. Sharp, and I. Willis (2002a), Evidence for basal cavity opening from analysis of surface uplift during a high-velocity event: Haut Glacier d'Arolla, Switzerland, *Journal of Glaciology*, *48*(161), 208--216.

Mair, D., P. Nienow, M. Sharp, T. Wohlleben, and I. Willis (2002b), Influence of subglacial drainage system evolution on glacier surface motion: Haut Glacier dArolla, Switzerland, *Journal of Geophysical Research*, *107*(B8), 2175.

Mair, D., I. Willis, U. Fischer, B. Hubbard, P. Nienow, and A. Hubbard (2003), Hydrological controls on patterns of surface, internal and basal motion during three ''spring events'': Haut Glacier d'Arolla, Switzerland, *Journal of Glaciology*, *49*(167), 555--567.

Marshall, S. (2005), Recent advances in understanding ice sheet dynamics, *Earth and Planetary Science Letters*, *240*(2), 191--204.

McMillan, M., P. Nienow, A. Shepherd, T. Benham, and A. Sole (2007), Seasonal evolution of supra-glacial lakes on the Greenland Ice Sheet, *Earth and Planetary Science Letters*, *262*.

Meehl, G., T. Stocker, W. Collins, P. Friedlingstein, A. Gaye, J. Gregory, A. Kitoh, R. Knutti, J. Murphy, A. Noda, S. Raper, I. Watterson, W. A, and Z. Zhao (2007),

Global Climate Projections, in *Climate change 2007: the physical science basis. Contribution of Working Group I to the Fourth Assessment Report of the Intergovernmental Panel on Climate Change*, edited by S. Solomon, D. Qin, M. Manning, Z. Chen, M. Marquis, K. Averyt, M. Tignor, and H. Miller, Cambridge University Press.

Muller, F., and A. Iken (1973), Velocity fluctuations and water regime of Arctic valley glaciers, in *Symposium on the Hydrology of Glaciers, Cambridge, 7-13 Sept. 1969*, 94-95, p. 165, International Association of Scientific Hydrology.

Murray, T., and G. Clarke (1995), Black-box modelling of the subglacial water system, *Journal of Geophysical Research*, *100*(B7), 10,231.

Nicholls, R., P. Wong, V. Burkett, J. Codignotto, J. Hay, R. McLean, S. Ragoonaden, and C. Woodroffe (2007), Coastal systems and low-lying areas, in *Climate Change 2007: Impacts, Adaptation and Vulnerability. Contribution of Working Group II to the Fourth Assessment Report of the Intergovernmental Panel on Climate Change*, edited by M. Parry, O. Canziani, J. Palutikof, P. van der Linden, and C. Hanson, pp. 315--356, Cambridge University Press.

Nick, F., A. Vieli, I. Howat, and I. Joughin (2009), Large-scale changes in Greenland outlet glacier dynamics triggered at the terminus, *Nature Geoscience*, *2*(2), 110--114.

Nienow, P., and B. Hubbard (2006), *Surface and Englacial Drainage of Glaciers and Ice Sheets*, Encyclopedia of Hydrological Sciences, John Wiley & Sons.

Nienow, P., M. Sharp, and I. Willis (1998), Seasonal changes in the morphology of the subglacial drainage system, Haut Glacier d'Arolla, Switzerland, *Earth Surface Processes and Landforms*, *23*(9), 825--843.

Nienow, P., A. Hubbard, B. Hubbard, D. Chandler, D. Mair, M. Sharp, and I. Willis (2005), Hydrological controls on diurnal ice flow variability in valley glaciers, *Journal of Geophysical Research*, *110*, F04002.

Nienow, P., I. Bartholomew, A. Sole, D. Mair, T. Cowton, and M. King (submitted),

Acceleration of a land-terminating margin of the Greenland Ice Sheet in contrasting melt years, *Nature Geoscience*.

Nye, J. (1953), The flow law of ice from measurements in glacier tunnels, laboratory experiments and the Jungfraufirn borehole experiment, *Proceedings of the Royal Society of London. Series A. Mathematical and Physical Sciences*, *219*(1139), 477--489.

Oerlemans, J. (1991), The mass balance of the Greenland ice sheet: sensitivity to climate change as revealed by energy-balance modelling, *The Holocene*, *1*(1), 40.

Ohmura, A. (2001), Physical basis for the temperature-based melt-index method, *Journal of Applied Meteorology*, *40*(4), 753--761.

O'Neel, S., K. Echelmeyer, and R. Motyka (2001), Short-term flow dynamics of a retreating tidewater glacier: LeConte Glacier, Alaska, U.S.A., *Journal of Glaciology*, *47*(159), 567--578.

Palmer, S., A. Shepherd, and P. Nienow (2008), Greenland Ice Sheet seasonal speedup coupled with surface hydrology, in *Eos, Transactions, American Geophysical Union. Fall Meeting Supplement*, vol. 89, pp. C31C--0508, AGU.

Palmer, S., A. Shepherd, P. Nienow, and I. Joughin (2011), Seasonal speedup of the Greenland Ice Sheet linked to routing of surface water, *Earth and Planetary Science Letters*, *302*, 423--428.

Parizek, B. (2010), Glaciology: Sliding to Sea, *Nature Geoscience*, *3*(6), 385--386.

Parizek, B., and R. Alley (2004), Implications of increased Greenland surface melt under global-warming scenarios: ice-sheet simulations, *Quaternary Science Reviews*, *23*(9-10), 1013--1027.

Paterson, W. (1994), *The Physics of Glaciers*, Butterworth-Heinemann.

Pfeffer, W., M. Meier, and T. Illangasekare (1991), Retention of Greenland runoff by refreezing: implications for projected future sea level change, *Journal of Geophysical Research*, *96*(C12), 22,117.

Phillips, T., H. Rajaram, and K. Steffen (2010), Cryo-hydrologic warming: A potential mechanism for rapid thermal response of ice sheets, *Geophysical Research Letters*, *37*(20), L20,503.

Pimentel, S., and G. Flowers (2010), A numerical study of hydrologically driven glacier dynamics and subglacial flooding, *Proceedings of the Royal Society A: Mathematical, Physical and Engineering Science*, *doi:10.1098/rspa.2010.0211*.

Pimentel, S., and G. Flowers (2011), A numerical study of hydrologically driven glacier dynamics and subglacial flooding, *Proceedings of the Royal Society A: Mathematical, Physical and Engineering Science*, *467*(2126), 537.

Price, S., A. Payne, G. Catania, and T. Neumann (2008), Seasonal acceleration of inland ice via longitudinal coupling to marginal ice, *Journal of Glaciology*, *54*(185), 213--219.

Pritchard, H., R. Arthern, D. Vaughan, and L. Edwards (2009), Extensive dynamic thinning on the margins of the Greenland and Antarctic ice sheets, *Nature*, *461*(7266), 971--975.

Rabus, B., and K. Echelmeyer (1997), The flow of a polythermal glacier: McCall Glacier, Alaska, USA, *Journal of Glaciology*, *43*(145), 522--536.

Rahmstorf, S. (1995), Bifurcations of the Atlantic thermohaline circulation in response to changes in the hydrological cycle, *Nature*, *378*, 9.

Rantz, S. (1982), Measurement and computation of streamflow: volume 2. Computation of discharge, *USGS Water-Supply Paper*, *2175*.

Raymond, C., R. Benedict, W. Harrison, K. Echelmeyer, and M. Sturm (1995), Hydrological discharges and motion of Fels and Black Rapids Glaciers, Alaska, USA: implications for the structure of their drainage systems, *Journal of Glaciology*, *41*(138), 290--304.

Richards, K. (1982), *Rivers, form and process in alluvial channels*, vol. 771, Routledge Kegan & Paul.

Richards, K. (1984), Some observations on suspended sediment dynamics in Storbregrova, Jotunheimen, *Earth Surface Processes and Landforms*, *9*(2), 101--112.

Rignot, E., and P. Kanagaratnam (2006), Changes in the velocity structure of the Greenland Ice Sheet, *Science*, *311*(5763), 986.

Rignot, E., J. Box, E. Burgess, and E. Hanna (2008), Mass balance of the greenland ice sheet from 1958 to 2007, *Geophysical Research Letters*, *35*(20), L20502.

Rignot, E., I. Velicogna, M. Van den Broeke, A. Monaghan, and J. Lenaerts (2011), Acceleration of the contribution of the greenland and antarctic ice sheets to sea level rise, *Geophysical Research Letters*, *38*(5), L05503.

Rippin, D., I. Willis, N. Arnold, A. Hodson, J. Moore, J. Kohler, and H. Björnsson (2003), Changes in geometry and subglacial drainage of Midre Lovénbreen, Svalbard, determined from digital elevation models, *Earth Surface Processes and Landforms*, *28*(3), 273--298.

Röthlisberger, H. (1972), Water pressure in intra- and subglacial channels, *Journal of Glaciology*, *11*(62), 177--203.

Röthlisberger, H., and H. Lang (1987), Glacial hydrology, in *Glacio-fluvial Sediment Transfer: an Alpine Perspective*, edited by A. Gurnell and M. Clark, pp. 207--274, Wiley, Chichester.

Schoof, C. (2005), The effect of cavitation on glacier sliding, *Proceedings of the Royal Society A: Mathematical, Physical and Engineering Science*, *461*(2055), 609.

Schoof, C. (2010), Ice-sheet acceleration driven by melt supply variability, *Nature*, *468*(7325), 803--806.

Seaberg, S., J. Seaberg, R. Hooke, and D. Wiberg (1988), Character of the englacial and subglacial drainage system in the lower part of the ablation area of Storglaciären, Sweden, as revealed by dye-trace studies, *Journal of Glaciology*, *34*, 217--227.

Shampine, L., and M. Reichelt (1997), The Matlab ODE suite, *SIAM Journal on Scientific Computing*, *18*(1), 1--22.

Sharp, M., J. Gemmell, and J. Tison (1989), Structure and stability of the former subglacial drainage system of the Glacier de Tsanfleuron, Switzerland, *Earth Surface Processes and Landforms*, *14*(2), 119--134.

Shepherd, A., and D. Wingham (2007), Recent Sea-Level Contributions of the Antarctic and Greenland Ice Sheets, *Science*, *315*(5818), 1529--1532, doi: 10.1126/science.1136776.

Shepherd, A., A. Hubbard, P. Nienow, M. King, M. McMillan, and I. Joughin (2009), Greenland Ice Sheet motion coupled with daily melting in late summer, *Geophysical Research Letters*, *36*(1), L01501.

Shreve, R. (1972), Movement of water in glaciers, *Journal of Glaciology*, *11*(62), 205--214.

Skidmore, M., and M. Sharp (1999), Drainage system behaviour of a High-Arctic polythermal glacier, *Annals of Glaciology*, *28*(1), 209--215.

Sneed, W., and G. Hamilton (2007), Evolution of melt pond volume on the surface of the greenland ice sheet, *Geophysical Research Letters*, *34*(3), L03501.

Sole, A., T. Payne, J. Bamber, P. Nienow, and W. Krabill (2008), Testing hypotheses of the cause of peripheral thinning of the Greenland Ice Sheet: is land-terminating ice thinning at anomalously high rates, *The Cryosphere*, *2*, 673--710.

Sole, A., D. Mair, P. Nienow, I. Bartholomew, M. King, M. Burke, and I. Joughin (2011), Seasonal speed-up of a Greenland marine-terminating outlet glacier forced by surface melt-induced changes in subglacial hydrology, *Journal of Geophysical Research*, *116*, F03014, doi:10.1029/2010JF001948.

Spring, U. (1980), *Intraglazialer Wasserabfluss, Theorie und Modellrechnungen*, 48, Versuchsanstalt für Wasserbau, Hydrologie und Glaziologie.

Stearns, L., and G. Hamilton (2007), Rapid volume loss from two East Greenland outlet glaciers quantified using repeat stereo satellite imagery, *Geophysical Research Letters*, *34*(5), 5503.

Stone, D., and G. Clarke (1996), In situ measurements of basal water quality and pressure as an indicator of the character of subglacial drainage systems, *Hydrological Processes*, *10*(4), 615--628.

Stroeve, J., J. Box, and T. Haran (2006), Evaluation of the MODIS (MOD10A1) daily snow albedo product over the Greenland Ice Sheet, *Remote Sensing of Environment*, *105*(2), 155--171.

Sugden, D., and B. John (1976), *Glaciers and landscape: A geomorphological approach*, Edward Arnold.

Sundal, A., A. Shepherd, P. Nienow, E. Hanna, S. Palmer, and P. Huybrechts (2009), Evolution of supra-glacial lakes across the Greenland Ice Sheet, *Remote Sensing of Environment*, *113*, 2164--2171.

Sundal, A., A. Shepherd, P. Nienow, E. Hanna, S. Palmer, and P. Huybrechts (2011), Melt-induced speed-up of Greenland Ice Sheet offset by efficient subglacial drainage, *Nature*, *469*(7331), 521--524.

Swift, D., P. Nienow, N. Spedding, and T. Hoey (2002), Geomorphic implications of subglacial drainage configuration: rates of basal sediment evacuation controlled by seasonal drainage system evolution, *Sedimentary Geology*, *149*(1-3), 5--19.

Swift, D., P. Nienow, T. Hoey, and D. Mair (2005), Seasonal evolution of runoff from Haut Glacier d'Arolla, Switzerland and implications for glacial geomorphic processes, *Journal of Hydrology*, *309*(1-4), 133--148.

Tedesco, M., X. Fettweis, M. van den Broeke, R. van de Wal, C. Smeets, W. van de Berg, M. Serreze, and J. Box (2011), The role of albedo and accumulation in the 2010 melting record in Greenland, *Environmental Research Letters*, *6*, 014,005.

Thomas, R. (2004), Force-perturbation analysis of recent thinning and acceleration of Jakobshavn Isbrae, Greenland, *Journal of Glaciology*, *50*(168), 57--66.

Thomas, R., E. Frederick, W. Krabill, S. Manizade, and C. Martin (2009), Recent changes on Greenland outlet glaciers, *Journal of Glaciology*, *55*(189), 147--162.

Thomsen, H., L. Thorning, and R. Braithwaite (1988), Glacier-hydrological conditions on the inland ice north-east of Jakobshavn/Ilulissat, West Greenland, *Rapport Gronlands Geologiske Undersogelse*, *138*.

Tranter, M., G. Brown, R. Raiswell, M. Sharp, and A. Gurnell (1993), A conceptual model of solute acquisition by Alpine glacial meltwaters, *Journal of Glaciology*, *39*(133), 573--581.

Truffer, M., W. Harrison, and R. March (2005), Record negative glacier balances and low velocities during the 2004 heatwave in Alaska, USA: implications for the interpretation of observations by Zwally and others in Greenland, *Journal of Glaciology*, *51*(175), 663.

Tulaczyk, S., W. Kamb, and H. Engelhardt (2000), Basal mechanics of ice stream B, West Antarctica 1. Till mechanics, *Journal of Geophysical Research*, *105*(B1), 463--481.

Turner Designs Inc. (2011), Application notes: Fluorescent Tracer Studies, http://www.turnerdesigns.com/t2/doc/appnotes/tracer_dye.html.

Van de Wal, R., and J. Oerlemans (1994), An energy balance model for the Greenland ice sheet, *Global and Planetary change*, *9*(1-2), 115--131.

Van de Wal, R., and A. Russell (1994), A comparison of energy balance calculations, measured ablation and meltwater runoff near Søndre Strømfjord, West Greenland, *Global and Planetary change*, *9*(1-2), 29--38.

Van de Wal, R., R. Bintanja, W. Boot, M. Van den Broeke, L. Conrads, P. Duynkerke, P. Fortuin, E. Henneken, W. Knap, O. J, M. Portanger, and H. Vugts (1995), Mass balance measurements in the Søndre Strømfjord area in the period 1990-1994, *Zeitschrift für Gletscherkunde und Glazialgeologie*, *31*, 57--63.

Van de Wal, R., W. Greuell, M. van den Broeke, C. Reijmer, and J. Oerlemans (2005), Surface mass-balance observations and automatic weather station data along a transect near Kangerlussuaq, West Greenland, *Annals of Glaciology*, *42*, 311--316.

Van de Wal, R., W. Boot, M. Van den Broeke, C. Smeets, C. Reijmer, J. Donker, and J. Oerlemans (2008), Large and rapid melt-induced velocity changes in the ablation zone of the Greenland Ice Sheet, *Science*, *321*(5885).

Van den Broeke, M., P. Smeets, J. Ettema, C. Van der Veen, R. Van de Wal, and J. Oerlemans (2008), Partitioning of melt energy and meltwater fluxes in the ablation zone of the west Greenland ice sheet, *The Cryosphere*, *2*, 179--189.

Van Den Broeke, M., J. Bamber, J. Ettema, E. Rignot, E. Schrama, W. Van de Berg, E. Van Meijgaard, I. Velicogna, and B. Wouters (2009), Partitioning recent Greenland mass loss, *Science*, *326*(5955), 984.

Van der Veen, C. (1998), Fracture mechanics approach to penetration of bottom crevasses on glaciers, *Cold Regions Science and Technology*, *27*(3), 213--223.

Van der Veen, C. (1999), *Fundamentals of Glacier Dynamics*, Balkema.

Van der Veen, C. (2007), Fracture propagation as means of rapidly transferring surface meltwater to the base of glaciers, *Geophysical Research Letters*, *34*(1), L01501.

Van der Veen, C., J. Plummer, and L. Stearns (2011), Controls on the recent speed-up of Jakobshavn Isbræ, West Greenland, *Journal of Glaciology*, *57*(204), 770.

Van Tatenhove, F., C. Roelfsema, G. Blommers, and A. van Voorden (1995), Change in position and altitude of a small outlet glacier during the period 1943-92: Leverett Glacier, West Greenland, *Annals of Glaciology*, *21*, 251--258.

Velicogna, I., and J. Wahr (2006), Acceleration of greenland ice mass loss in spring 2004, *Nature*, *443*(7109), 329--331.

Walder, J. (1986), Hydraulics of subglacial cavities, *Journal of Glaciology*, *32*(112), 439--445.

Walder, J., and A. Fowler (1994), Channelized subglacial drainage over a deformable bed, *Journal of Glaciology*, *40*(134), 3--15.

Walder, J., and B. Hallet (1979), Geometry of former subglacial water channels and cavities, *Journal of Glaciology*, *23*(89), 335--346.

Weertman, J. (1957), On the sliding of glaciers, *Journal of Glaciology*, *3*, 33--38.

Weertman, J. (1972), General theory of water flow at the base of a glacier or ice sheet, *Reviews of Geophysics*, *10*(1), 287--333.

Weertman, J. (1973), Can a water-filled crevasse reach the bottom surface of a glacier, in *Proceedings of Symposium on the hydrology of glaciers, September 7-13, 1969, Cambridge, England*, vol. 95, pp. 139--145, International Association of Scientific Hydrology.

Weertman, J. (1979), The unsolved general glacier sliding problem, *Journal of Glaciology*, *23*(89), 97--115.

Zwally, H., W. Abdalati, T. Herring, K. Larson, J. Saba, and K. Steffen (2002), Surface melt-induced acceleration of Greenland ice-sheet flow, *Science*, *297*(5579), 218.

Zwally, H., M. Giovinetto, J. Li, H. Cornejo, M. Beckley, A. Brenner, J. Saba, and D. Yi (2005), Mass changes of the Greenland and Antarctic ice sheets and shelves and contributions to sea-level rise: 1992 - 2002, *Journal of Glaciology*, *51*(175), 509--527.

Appendix 1

nature geoscience

LETTERS

PUBLISHED ONLINE: 9 MAY 2010 | DOI: 10.1038/NGEO863

Seasonal evolution of subglacial drainage and acceleration in a Greenland outlet glacier

Ian Bartholomew[1]*, Peter Nienow[1], Douglas Mair[2], Alun Hubbard[3], Matt A. King[4] and Andrew Sole[2]

The Greenland ice sheet contains enough water to raise sea levels by 7 m. However, its present mass balance and future contribution to sea level rise is poorly understood[1]. Accelerated mass loss has been observed near the ice sheet margin, partly as a result of faster ice motion[2–4]. Surface melt waters can reach the base of the ice sheet and enhance basal ice motion[5,6]. However, the response of ice motion to seasonal variations in meltwater supply is poorly constrained both in space and time. Here we present ice motion data obtained with global positioning system receivers located along a ~35 km transect at the western margin of the Greenland ice sheet throughout a summer melt season. Our measurements reveal substantial increases in ice velocity during summer, up to 220% above winter background values. These speed-up events migrate up the glacier over the course of the summer. The relationship between melt and ice motion varies both at each site throughout the melt season and between sites. We suggest that these patterns can be explained by the seasonal evolution of the subglacial drainage system similar to hydraulic forcing mechanisms for ice dynamics that have been observed at smaller glaciers.

Recent studies have focused on the role that seasonal changes in hydrological forcing have on ice motion of the Greenland ice sheet[3–5,7,8] (GrIS) and suggest that surface melting generates large enough volumes of melt water to lubricate basal flow should it reach the bed[9]. This process has the potential to create a positive feedback between climate warming and ice velocity that has not been considered in ice sheet models that predict sea level rise[1]. A theoretical mechanism of hydrofracture[10,11] proposes how surface melt water can penetrate to the bed through cold ice >1,000 m thick and has been invoked to explain changes in vertical and horizontal components of ice motion in response to a lake drainage event[5]. Simultaneous measurements of ice velocity and air temperature have established, over short timescales, a correlation between local surface melting and velocity fluctuations over a widespread area[4,8,9]. However, it has been shown that higher annual ablation does not necessarily lead to increased annual ice velocities[8] and the importance of this relationship for large-scale dynamic behaviour of the GrIS remains equivocal. It is suggested[9] that alpine glaciers may provide an appropriate analogue for the evolution of the GrIS in a warming climate. In alpine and high Arctic polythermal valley glaciers, ice motion depends on variations in the structure, hydraulic capacity and efficiency of the subglacial drainage system[12], each of which evolves spatially and temporally on a seasonal basis[13–17]. Until now, limited data sets have been unable to confirm this hypothesis for the GrIS.

We used global positioning system (GPS) observations to provide continuous ice velocity measurements, from 7 May, during the 2008 melt season and the subsequent winter at four sites along a land-terminating transect in the ablation zone of the western margin of the GrIS at ~67.10° N (Fig. 1). Simultaneous measurements of air temperature were made at each site.

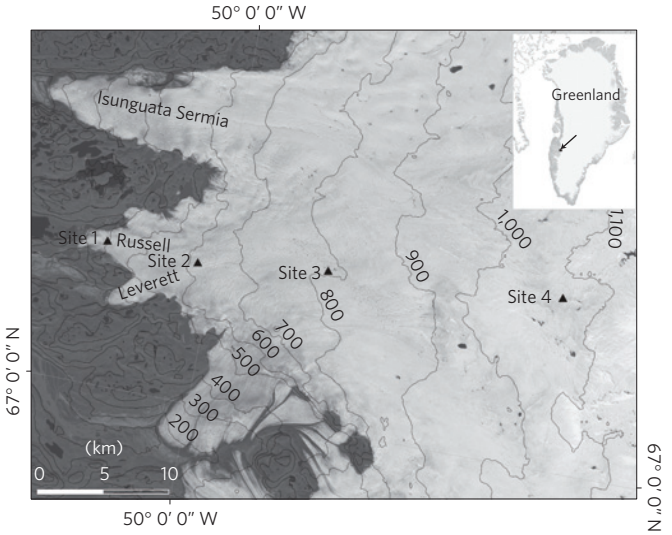

Figure 1 | Location of the GPS transect on the western margin of the GrIS. The four GPS sites are located in the ablation zone of the GrIS across an altitudinal range of 395–1,060 m a.s.l., contours show altitude where ice thickness ranges from ~270–920 m (ref. 29) and are located along a flowline from the ice sheet interior as determined by interferometric synthetic aperture radar observations[30]. Simultaneous measurements of air temperature were made at each site to constrain surface melt rates.

The GPS observations show that each site experienced changes in daily ice velocity that were >110% above winter motion over the course of our survey (Fig. 2). This variability is consistent with, but much stronger than, previously reported observations[6,8,9]. When our survey began, melt had commenced near the ice margin and site 1 was already experiencing motion above winter background level. At sites 2, 3 and 4 a common pattern of seasonal ice velocity variation is characterized by an initial period of slow flow at winter levels, followed by a 70–100% increase in horizontal velocity, following the onset of melt, that marks a change in the dynamic regime to higher mean velocities. These sites gradually return to velocities below their winter values by the end of the summer, although individual high-velocity events occur throughout the summer. Average rates of ice motion at sites 1, 3 and 4, following the seasonal increase in horizontal velocity, were 114, 132 and 142 m yr^{-1}, respectively. The net increases in ice motion above winter background motion, owing to these summer

[1]University of Edinburgh, School of Geosciences, Edinburgh, EH8 9XP, UK, [2]University of Aberdeen, School of Geosciences, Aberdeen, AB24 3UF, UK, [3]University of Aberystwyth, Institute of Geography & Earth Sciences, Aberystwyth, SY23 3DB, UK, [4]Newcastle University, School of Civil Engineering and Geosciences, Newcastle upon Tyne, NE1 7RU, UK. *e-mail: ian.bartholomew@ed.ac.uk.

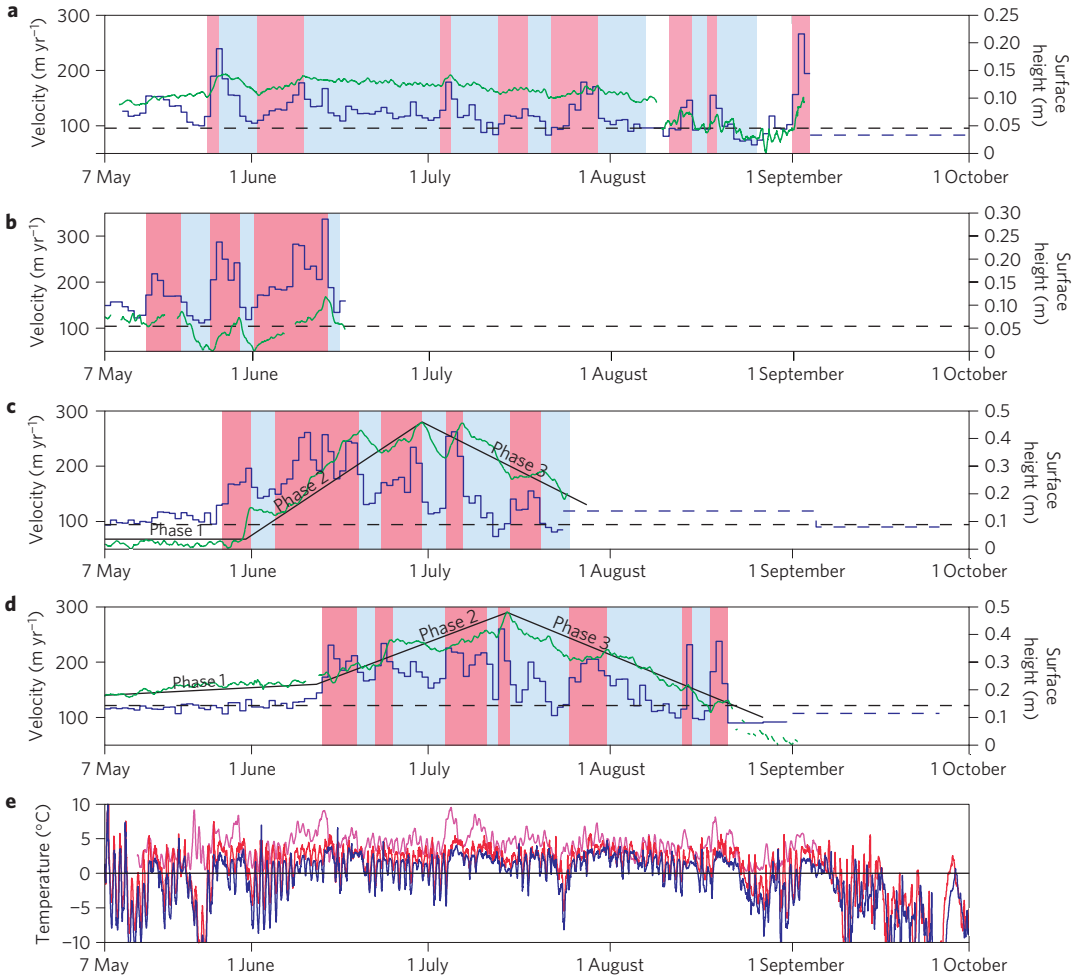

Figure 2 | Seasonal development of melt-induced ice velocity variations. a–d, 24-h horizontal velocity (blue) and surface height (green) at GPS site 1 (395 m a.s.l.) (**a**), site 2 (618 m a.s.l.) (**b**), site 3 (795 m a.s.l.) (**c**) and site 4 (1,063 m a.s.l.) (**d**). The surface height is shown relative to an arbitrary datum with a linear, surface-parallel, slope removed. The dashed lines show winter background velocity (black) and velocities from periods with sparse data (blue). The shaded sections identify periods of ice acceleration associated with ice-surface uplift (red), and slower ice motion associated with a decrease in surface height (blue). The solid lines indicate different phases of longer-term ice velocity versus surface uplift relationship. **e**, Temperature record from sites 1 (magenta), 3 (red) and 4 (blue).

variations, are 19%, 40% and 17%, equating to an increase in annual ice flux of 8%, 14% and 6%. In addition, the data reveal an up-glacier evolution in the onset of horizontal acceleration, and in the subsequent slowdown. Site 2 began to speed up on 15 May and sites 3 and 4 followed on 27 May and 11 June, respectively.

At all sites, the highest horizontal velocities coincide with uplift of the ice sheet surface, up to 12 cm in a single event, and reductions in velocity occur when the surface is lowering or stable. The highest daily horizontal velocities occur during periods of rapid uplift, rather than at peak elevation. Clear longer-term seasonal changes in surface elevation are associated with variations in the horizontal flow regime, particularly at sites 3 and 4, and can be categorized into three phases. Phase 1 is characterized by no enhanced surface uplift and low horizontal velocities (7–30 May at site 3; 7 May–10 June at site 4), and the slow-flowing inland ice (sites 3 and 4) seems to be unaffected by the faster ice downstream (sites 1 and 2). During phase 2, the rate of uplift increases, as do the horizontal velocities (31 May–19 June at site 3; 11 June–14 July at site 4), and in phase 3, surface elevations gradually decrease towards (site 3) and below (site 4) their early season levels (20 June–21 July at site 3; 15 July–29 August at site 4) but can fluctuate by ~0.05 m d^{-1}.

We used air temperature data to derive positive degree days (PDDs) at each site to investigate relationships between surface melt (as inferred from PDDs) and ice velocity. For the melt season as a whole, there was a weak but significant correlation between PDD and daily ice velocity at each site but there is no link between the intensity of seasonal melting and the mean horizontal velocity increase (Fig. 3a).

Studies of hydromechanical coupling at alpine and subpolar glaciers reveal that intra-seasonal changes in the hydraulic efficiency of the subglacial drainage system are a principal control on the sensitivity of ice motion to meltwater inputs[13–17]. Our data show that: (1) phase 1 (pre-melt) velocities are low and show no relationship to PDD (Fig. 3c,d); (2) phase 2 (enhanced surface uplift) mean velocities are high (>50% above winter background) and positively correlated with PDD (Fig. 3b–d); and (3) during phase 3 (surface lowering), the sensitivity of the relationship between PDD and velocity changes such that only periods of most intense melting (that is, high PDDs; Fig. 3b–d) are associated with substantial enhanced surface velocity (>50% above winter background). This accounts for the gradual decline in ice velocities, but explains the sporadic high-velocity events.

From the association between the onset of surface melting, surface uplift and enhanced horizontal velocities, we infer rapid delivery of surface melt water to the ice sheet bed following the establishment of a hydraulic connection[5,6,8,9]. This melt water increases

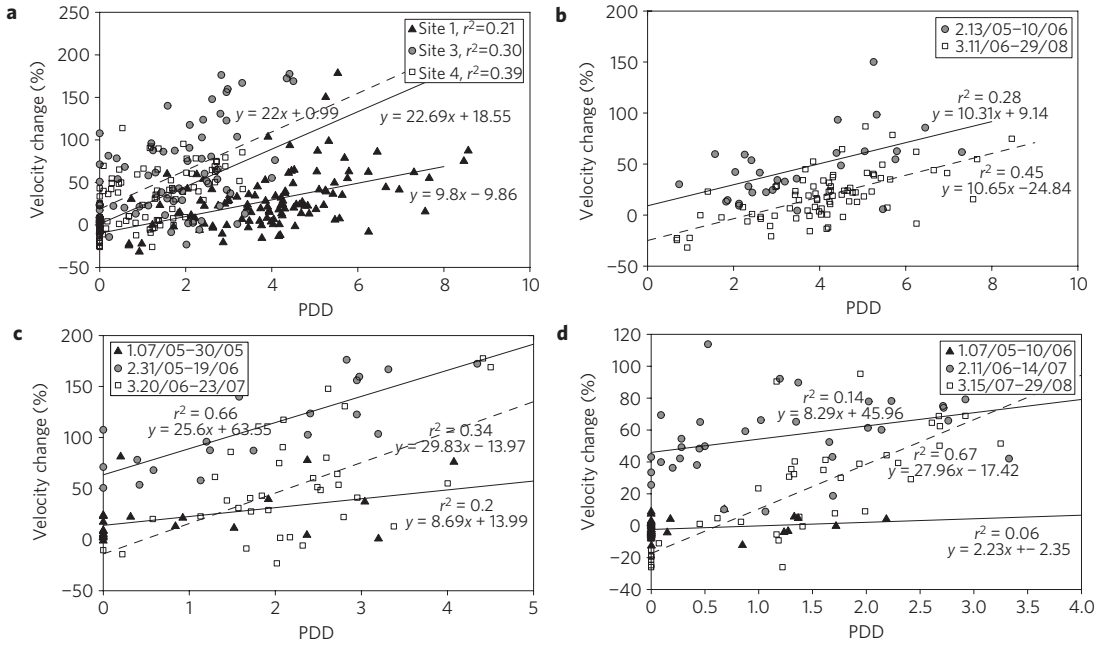

Figure 3 | Intra-seasonal changes in surface melting versus ice velocity relationships. a, Positive degree day (PDD) versus velocity change at sites 1, 3 and 4 for the whole season. 24-h velocities are shown as percentage change relative to winter background. **b**–**d**, PDD versus velocity for different phases of ice velocity versus uplift relationship—1. 'pre-melt', 2. 'enhanced surface uplift' and 3. 'surface lowering'—at GPS site 1 (**b**), site 3 (**c**) and site 4 (**d**).

basal sliding by reducing friction between overlying ice and its bed, probably through hydraulic jacking or cavitation[15,18]. Although changes in surface elevation can also result from changes in bedrock topography and strain rates[19], the patterns we observe cannot be attributed to these effects alone. We would expect acceleration of downstream ice to cause thinning upstream, yet observe the opposite, and would not expect bedrock obstacles to be expressed at the ice sheet surface on the length scales of the changes in our data. The coincidence of highest velocities with rate of uplift, rather than peak elevation, suggests 'stick–slip' behaviour similar to that observed in an alpine-type glacier[15,18,20], whereby separation of the ice and bed allows the immediate release of built-up stresses in the overlying ice.

Our observations of temperature and the pattern of changes in horizontal and vertical motion at each site, suggest a local, temperature-related, forcing mechanism for the seasonal changes in ice motion. As also observed at alpine and high Arctic polythermal glaciers[14,15,17], the initiation of summer velocity changes is dependent on the establishment of a hydraulic connection between the ice surface and bed, which occurs first in the lowest parts of the ablation zone, through thinner ice, and migrates progressively up-glacier (Fig. 2). However, our results from Greenland suggest that a temporally consistent relationship between surface melt and ice velocity does not exist once a hydraulic connection has been made. Instead, the relationship evolves both at a point and develops up-glacier. When melt first accesses the bed, the onset of high surface velocities and uplift (phase 2; Fig. 3) is indicative of an inefficient basal hydraulic system in which basal water pressures are highly sensitive to relatively small inputs of water[13]. During the last part of the melt season (phase 3), the gradual surface lowering and ice slow down indicates a more efficient channelized system in which basal water pressures are generally lower[13]. Only during very high meltwater inputs are basal water pressures raised enough to reduce basal friction significantly and enhance surface velocity[21]. This categorization is complicated by a small number of examples of high horizontal velocity in our data in the absence of high temperatures (for example, site 4 on 14 August (Fig. 2)), which may be caused by rapid drainage of surface lakes to the ice sheet bed[5,6].

Sites 3 and 4 do not show velocity increases to above winter values even when sites downstream have started accelerating (Fig. 2), suggesting that longitudinal coupling is not effective over >10 km at these locations. Although numerical studies have suggested that it may be possible for seasonal acceleration of inland ice to be explained through longitudinal coupling to marginal ice[22], and our data do not preclude its effectiveness in other parts of the GrIS, we do not observe that process here at length scales of >10 km. Therefore, enhanced surface velocity is primarily a consequence of local hydrological forcing at each site and the efficiency of the hydrological system.

Thus, the ice sheet exhibits a transient dynamic response to seasonal melting at each site[3,4,18]. We find that, in addition to surface melt rates, a key control on the magnitude and location of enhanced basal sliding is the structure and efficiency of the subglacial drainage system, which evolves seasonally, in a similar manner to alpine glaciers[15,18,23]. The seasonal and spatial increase in subglacial hydraulic efficiency is probably responsible for the lack of correlation between seasonal ablation rates and velocity changes that has caused previous authors to question the existence of positive feedback between climate warming and annual ice velocity of the GrIS (refs 8,24). Using a more extensive data set, we find that the relationship between melt rate and ice motion evolves through time at each site and with distance up-glacier, suggesting that its significance lies at higher elevations. Although our data extend only up to 1,000 m altitude, further ground-based observations have also detected ice-motion variations during late summer that are strongly associated with changes in surface hydrology, at elevations above 1,400 m in the same region[9].

In a warming climate, with longer and more intense summer melt seasons, we would expect that water will reach the bed farther inland[25] and a larger portion of the ice sheet will experience summer velocity changes. Modelling studies have suggested that the enhancement of summer ice motion is critical in drawing down ice from the accumulation zone, thereby reducing the surface elevation of the ice sheet, exposing more of the ice sheet to surface ablation[7]. Furthermore, the low gradient of the GrIS interior ensures that a small rise in temperature will induce melt across

a spatially extensive area and substantial melt at elevations above 1,600 m is already evident in the presence of supraglacial lakes[26,27]. Our findings emphasize the importance of both surface melting and seasonal evolution of the subglacial drainage system on ice motion in marginal regions of the GrIS and will help parameterize numerical models that predict the future evolution of the GrIS.

Methods

Each GPS antenna was mounted on a support pole drilled several metres into the ice, which froze in subsequently, providing measurements of ice motion that are independent of ablation. The GPS receivers collected data that were processed kinematically using a Precise Point Positioning approach (sites 2, 3 and 4 at 300 s intervals), and relative to a local (<2.5 km, 10 s intervals) base station for site 1 (ref. 28). Estimates of the uncertainty associated with positioning are ±1.5 cm in the horizontal direction and ±2.5 cm in the vertical direction. The precision and resolution of the data set is therefore sufficient to study changes along the flowline on seasonal and shorter (<1 day) timescales. Daily horizontal velocities reported in this letter are calculated by differencing 1-h mean positions every 24 h. Vertical profiles are generated by filtering the whole data set to suppress noise without over-smoothing the time series.

The GPS units were powered by solar panels. The GPS receiver at site 2 lost power on 16 June and our analysis is focused mainly on the three remaining sites. The receiver at site 1 was installed 3 days later than the others on 10 June. We also experienced power problems later in the season at site 3 and data from the beginning of September onwards is sporadic. This means that the detail of the ice motion record is unavailable at the very end of the melt season and through the subsequent winter. However, using occasional GPS positions (Fig. 2a–d, dashed blue lines), horizontal ice motion can still be calculated over longer periods, allowing us to assess the net velocity increase in summer compared with winter. The values for net summer velocity over winter background reported in this paper are calculated on the basis of ice motion from the onset of speed-up (the beginning of the survey period in the case of site 1) until the end of summer, when melting has finished at all sites and the effect of 'slower than winter' motion that we observe in late summer has been incorporated—as such they may be considered minimum estimates of summer velocity.

The values for background velocities are derived from the displacement of each site over the subsequent winter, following the end of the summer melting period (between 11 October and 27 February at Site 1, 26 September and 2 May at site 2, 26 September and 8 May at site 3 and 11 October and 8 May at site 4). The reported contribution to annual ice flux from the hydrologically forced summer ice velocity variations is the percentage by which the observed displacement exceeds that which would occur if the ice flowed at calculated winter rates all year round. At sites 3 and 4, the pre-speed-up velocities bear close agreement with over-winter velocities, however, are not included in the calculations to retain consistency between the approach adopted for each site.

Measurements of air temperature were made using shielded HOBO air temperature sensors. PDDs, used as a proxy for rates of surface melting, are derived using mean daily air temperature. A lack of ablation data meant that it was not possible to obtain degree-day factors, which vary for ice and snow. However, accumulation rates are low in this part of Greenland and snow depths when the GPSs were deployed at the beginning of May were less than 20 cm.

Received 5 October 2009; accepted 12 April 2010; published online 9 May 2010

References

1. *IPCC Climate Change 2007: The Physical Science Basis: Contribution of Working Group 1 to the Fourth Assessment Report of the Intergovernmental Panel of Climate Change* (Cambridge Univ. Press, 2007).
2. Krabill, W. *et al.* Greenland ice sheet: Increased coastal thinning. *Geophys. Res. Lett.* **31,** L24402 (2004).
3. Rignot, E. & Kanagaratnam, P. Changes in the velocity structure of the Greenland ice sheet. *Science* **311,** 986–990 (2006).
4. Joughin, I. *et al.* Seasonal speedup along the western flank of the Greenland ice sheet. *Science* **320,** 781–783 (2008).
5. Das, S. B. *et al.* Fracture propagation to the base of the Greenland ice sheet during supraglacial lake drainage. *Science* **320,** 778–781 (2008).
6. Zwally, H. J. *et al.* Surface melt-induced acceleration of Greenland ice-sheet flow. *Science* **297,** 218–222 (2002).
7. Parizek, B. R. & Alley, R. B. Implications of increased Greenland surface melt under global-warming scenarios: Ice-sheet simulations. *Quat. Sci. Rev.* **23,** 1013–1027 (2004).
8. van de Wal, R. S. W. *et al.* Large and rapid melt-induced velocity changes in the ablation zone of the Greenland ice sheet. *Science* **321,** 111–113 (2008).
9. Shepherd, A. *et al.* Greenland ice sheet motion coupled with daily melting in late summer. *Geophys. Res. Lett.* **36,** L01501 (2009).
10. Van der Veen, C. J. Fracture propagation as a means of rapidly transferring surface meltwater to the base of glaciers. *Geophys. Res. Lett.* **34,** L01501 (2007).
11. Alley, R. B., Dupont, T. K., Parizek, B. R. & Anandkrishnan, S. Access of surface meltwater to beds of subfreezing glacier: Preliminary insights. *Ann. Glaciol.* **40,** 8–14 (2005).
12. Iken, A., Röthlisberger, H., Flotron, A. & Haeberli, W. The uplift of Unteraargeltscher at the beginning of the melt season—a consequence of water storage at the bed? *J. Glaciol.* **29,** 28–47 (1983).
13. Kamb, B. Glacier surge mechanism based on linked cavity configuration of the basal water conduit system. *J. Geophys. Res.* **92,** 9083–9100 (1987).
14. Bingham, R. G., Nienow, P. W. & Sharp, M. J. Intra-annual and intra-seasonal flow dynamics of a high Arctic polythermal valley glacier. *Ann. Glaciol.* **37,** 181–188 (2003).
15. Anderson, R. S. *et al.* Strong feedbacks between hydrology and sliding of a small alpine glacier. *J. Geophys. Res.* **109,** F03005 (2004).
16. Kessler, M. A. & Anderson, R. S. Testing a numerical glacial hydrological model using spring speed-up events and outburst floods. *Geophys. Res. Lett.* **31,** L18503 (2004).
17. Mair, D., Nienow, P., Sharp, M., Wohlleben, T. & Willis, I. Influence of subglacial drainage system evolution on glacier surface motion: Haut Glacier d'Arolla, Switzerland. *J. Geophys. Res.* **107,** B82175 (2002).
18. Iken, A. The effect of subglacial water pressure on the sliding velocity of a glacier in an idealized numerical model. *J. Glaciol.* **27,** 407–421 (1981).
19. Gudmundsson, G. H. Transmission of basal variability to a glacier surface. *J. Geophys. Res.* **108,** B52253 (2003).
20. Fischer, U. H. & Clarke, G. K. C. Stick-slip sliding behaviour at the base of a glacier. *Ann. Glaciol.* **24,** 390–396 (1997).
21. Iken, A. & Bindschadler, R. A. Combined measurements of subglacial water-pressure and surface velocity of Findelenglescher Switzerland: Conclusions about drainage system and sliding mechanism. *J. Glaciol.* **42,** 564–575 (1986).
22. Price, S., Payne, A. J., Catania, G. & Neumann, T. A. Seasonal acceleration of inland ice via longitudinal coupling to marginal ice. *J. Glaciol.* **54,** 213–219 (2008).
23. Nienow, P. W., Sharp, M. J. & Willis, I. Seasonal changes in the morphology of the subglacial drainage system, Haut Glacier d'Arolla, Switzerland. *Earth Surf. Process. Landf.* **23,** 825–843 (1998).
24. Truffer, M., Harrison, W. D. & March, R. S. Record negative glacier balances and low velocities during the 2004 heatwave in Alaska, USA: Implications for the interpretation of observations by Zwally and others in Greenland. *J. Glaciol.* **51,** 663–664 (2005).
25. Hanna, E. *et al.* Increased runoff from melt from the Greenland ice sheet: A response to global warming. *J. Clim.* **21,** 331–341 (2008).
26. Sundal, A. V. *et al.* Evolution of supra-glacial lakes across the Greenland ice sheet. *Remote Sens. Environ.* **113,** 2164–2171 (2009).
27. Pritchard, H. D., Arthern, J. D., Vaughan, D. G. & Edwards, L. A. Extensive dynamic thinning on the margins of the Greenland and Antarctic ice sheets. *Nature* **461,** 971–975 (2009).
28. King, M. Rigorous GPS data-processing strategies for glaciological applications. *J. Glaciol.* **50,** 601–607 (2004).
29. Bamber, J. L., Layberry, R. L. & Gogineni, S. P. A new ice thickness and bed data set for the Greenland ice sheet: 1. Measurement, data reduction, and errors. *J. Geophys. Res.* **106,** 773–780 (2001).
30. Palmer, S. J., Shepherd, A. & Nienow, P. W. Greenland ice sheet seasonal speedup coupled with surface hydrology. *Eos Trans. AGU (Fall Meeting Suppl.)* **89,** abstr. C31C-0508 (2009).

Acknowledgements

We thank for financial support: UK Natural Environment Research Council (NERC, through a studentship to I.B. and grants to P.N./D.M.), Edinburgh University Moss Centenary Scholarship (I.B.), Edinburgh University Small Project Grants (P.N.), Carnegie Foundation (D.M.), SKB Sweden (A.H.), Royal Geographical Society Dudley Stamp Memorial Award (I.B.), Research Councils UK Academic Fellowship (M.A.K.), Aberystwyth University Research Award (A.H.), Royal Society Research Grant and Royal Geographical Society Gilchrist Fieldwork Grant (A.H.). GPS equipment and training were provided by the NERC Geophysical Equipment Facility. We also thank B. Anderson for thoughtful comments that helped improve the manuscript.

Author contributions

All authors contributed extensively to the work presented in this letter. P.N. and D.M. conceived the project. M.A.K. processed the GPS data. I.B., P.N., D.M., A.H. and A.S. collected the field data. I.B. wrote the manuscript. All authors discussed the results and implications and commented on the manuscript.

Additional information

The authors declare no competing financial interests. Reprints and permissions information is available online at http://npg.nature.com/reprintsandpermissions. Correspondence and requests for materials should be addressed to I.B.

Appendix 2

Supraglacial forcing of subglacial drainage in the ablation zone of the Greenland ice sheet

Ian Bartholomew,[1] Peter Nienow,[1] Andrew Sole,[1] Douglas Mair,[2] Thomas Cowton,[1] Steven Palmer,[3] and Jemma Wadham[4]

Received 8 February 2011; revised 5 March 2011; accepted 16 March 2011; published 21 April 2011.

[1] We measure hydrological parameters in meltwater draining from an outlet glacier in west Greenland to investigate seasonal changes in the structure and behaviour of the hydrological system of a large catchment in the Greenland ice sheet (GrIS). Our data reveal seasonal upglacier expansion and increase in hydraulic efficiency of the subglacial drainage system, across a catchment >600 km^2, to distances >50 km from the ice-sheet margin. This expansion occurs episodically in response to the drainage of surface meltwaters into a hitherto inefficient subglacial drainage system as new input locations become active progressively further upglacier; this system is similar to Alpine glaciers. These observations provide the first synopsis of seasonal hydrological behaviour in the ablation zone of the GrIS. **Citation:** Bartholomew, I., P. Nienow, A. Sole, D. Mair, T. Cowton, S. Palmer, and J. Wadham (2011), Supraglacial forcing of subglacial drainage in the ablation zone of the Greenland ice sheet, *Geophys. Res. Lett.*, *38*, L08502, doi:10.1029/2011GL047063.

1. Introduction

[2] In land-terminating sections of the GrIS, meltwater production enhances ice motion through seasonal velocity variations that are initiated when surface meltwaters gain access to the ice-bed interface [*Zwally et al.*, 2002]. A positive feedback between surface melting and ice velocities would accelerate mass loss from the GrIS in a warmer climate [*Zwally et al.*, 2002; *Parizek and Alley*, 2004; *Shepherd et al.*, 2009]. On the basis of correlations between ice motion and surface melting, however, it has been shown that a key control on the relationship between surface melting and ice velocity variations is the structure and hydraulic efficiency of the subglacial drainage system, which develops spatially and temporally on a seasonal basis [*Bartholomew et al.*, 2010]. A more efficient subglacial drainage system can conduct large discharges in discrete channels which operate at a lower steady-state water pressure, thereby reducing the basal lubrication effect of external meltwater inputs [*Kamb*, 1987; *Pimentel and Flowers*, 2011; *Schoof*, 2010; *Sundal et al.*, 2011].

[3] Despite the clear link between rates of ice motion and the structure of the subglacial drainage system, predictions about the future extent and magnitude of hydrologically-forced ice velocity changes in the GrIS remain uncertain [*Van de Wal et al.*, 2008]. To address this, we need to understand how spatial and temporal changes in surface melting of the GrIS force development of an efficient subglacial drainage system on a seasonal basis [*Pimentel and Flowers*, 2011; *Schoof*, 2010]. Here we present observations from Leverett Glacier, a land-terminating outlet glacier at ~67°N in west Greenland (Figure 1) in 2009, that elucidate seasonal development of the drainage system of a large catchment in the ablation zone of the GrIS.

2. Data and Methods

[4] Drainage from Leverett Glacier occurs through one large portal on the North side of the glacier snout, which grows in size over the melt season and is the outlet for runoff from a large subglacial conduit. Water stage, electrical conductivity (EC) and turbidity were monitored continuously in the proglacial stream at a stable bedrock section ~2 km downstream from the glacier terminus from May 18th 2009, before melting had started, until September 3rd. Stage was converted into discharge (Q) using a rating curve (r = 0.92) derived from 29 repeat dye-dilution gauging tests conducted in the proglacial stream across the full range of discharges. Uncertainty in the discharge record is the result of measurement error and application of a rating curve, and is estimated to be ±15%. A relationship between turbidity and suspended sediment concentration (SSC) was derived by calibration against 49 manual gulp sediment samples (r = 0.91). Uncertainties in the SSC and EC record are estimated to be ±7% and ±10% respectively. Our monitoring station was located in a single channel close to the ice margin that did not overflow at peak discharge. During a 2 week period simultaneous measurements of SSC and EC were taken within 50 m of the glacier snout, showing that the hydrological parameters we measured did not change significantly following emergence of the meltwaters from the glacier terminus.

[5] A surface digital elevation model [*Palmer et al.*, 2011] was used to derive a first approximation of the Leverett Glacier hydrological catchment (Figure 1). Although there is uncertainty in this approach, lack of appropriate bed elevation data prevents an estimate of catchment geometry based on calculations of subglacial hydraulic potential [*Shreve*, 1972]. We used satellite observations from the Moderate-resolution Imaging Spectrometer (MODIS) to study the development and drainage of supraglacial lakes within the Leverett catchment [*Sundal et al.*, 2009; *Box and Ski*, 2007]. 40 MODIS images were used spanning the period 31st May to 18th August, representing all days when lake identification was not impeded by cloud cover.

[1]School of Geosciences, University of Edinburgh, Edinburgh, UK.
[2]School of Geosciences, University of Aberdeen, Aberdeen, UK.
[3]School of Earth and Environment, University of Leeds, Leeds, UK.
[4]School of Geographical Sciences, University of Bristol, Bristol, UK.

0094-8276/11/2011GL047063

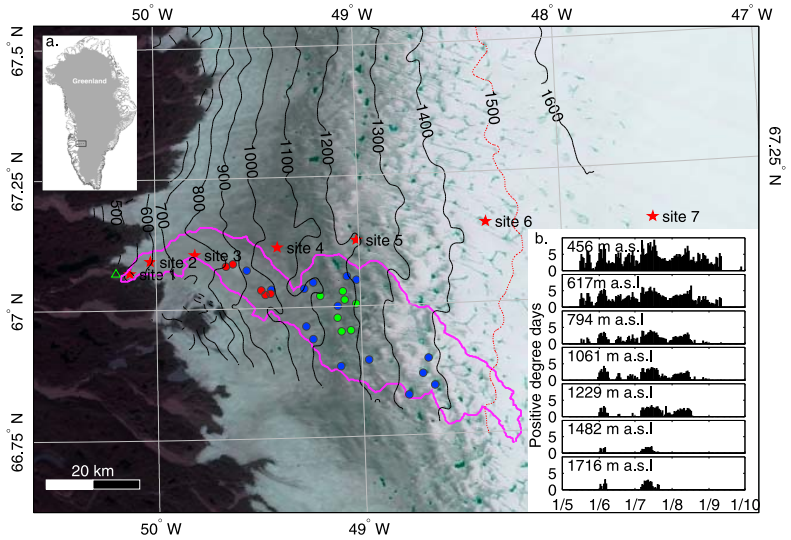

Figure 1. (a) Map showing the location of Leverett Glacier, a catchment derived from the surface DEM (purple), and locations of temperature measurements (red stars). Lakes that drain during the survey period are denoted by circles, colour-coded to show drainage events that coincide with meltwater pulses P2 (red) and P4 (green). Lakes which drain during the survey period but are not clearly associated with pulses in the discharge record are coloured blue. The location of the bedrock section where stage, EC and turbidity were measured is shown by the green triangle. (b) Positive degree-days at each of the temperature measurement locations (sites 1–7).

There is significant uncertainty in applying a depth-retrieval algorithm based on surface reflectance to find the depth of GrIS supraglacial lakes shallower than 2.5 m [*Box and Ski*, 2007]. Therefore, we used a modelled estimate [*McMillan et al.*, 2007] of the average depth of supraglacial lakes obtained within this region to estimate volumes of lakes that drain from the ice sheet surface. Continuous measurements of air temperature were made at seven sites, from 450–1700 m altitude (Figure 1). Ablation rates were also monitored using measurements of surface lowering from ultrasonic depth gauges in order to constrain a temperature-melt index model which we used to predict volumes of runoff generated from the catchment during our survey period.

3. Hydrological Observations

[6] The proglacial runoff hydrograph (Figure 2a) shows that, prior to June 1st, discharge was <6 m^3 s^{-1} during a period of ~20 days of above-zero temperatures extending up to 1400 m altitude (Figure 2d). Discharge then increased rapidly over 3 days to 46 m^3 s^{-1} on June 4th and continued to grow episodically before rising dramatically, by 220 m^3 s^{-1} in 10 days, to a peak of 317 m^3 s^{-1} on July 16th. Following this peak, discharge declined gradually but remained 3–4 times greater than early-season levels until late August. Proglacial runoff showed clear diurnal cycles which had greatest amplitude (~25 m^3 s^{-1}) later in the season, after July 16th, and were more subdued (~6 m^3 s^{-1}) earlier in the summer.

[7] The rising limb of the seasonal hydrograph is also marked by four distinct pulses of water, superimposed on the general pattern of runoff growth. These pulses each last a few days, and contribute between 4.9–11.8 × 10^6 m^3 of water to the total runoff. These pulses are also defined by coincident spikes in the EC and SSC records (Figures 2a–2c). The first pulse of water (P1 on June 3rd) marks the start of significant runoff growth. It was followed by further pulses (P2–P4) starting on June 7th, June 17th and July 3rd (Figure 2a).

[8] Maximum EC (69.9 μS cm^{-1}) occurred while discharge was still low at the beginning of the season and declined in a stepwise fashion to a minimum of 9.9 μS cm^{-1} on July 3rd, immediately prior to P4 (Figure 2b). There is a negative relationship between EC and discharge over the whole melt season (R^2 = 0.27). Following P4 EC remains low (<20 μS cm^{-1}) and the daily cycles of Q and EC develop a characteristic inverse relationship [*Fenn*, 1987] with clear stable hysteresis where EC is highest on the rising limb of the diurnal hydrograph (auxiliary material).[1] However, the relationship is not consistent throughout the survey period (Figure 2e), and early in the season can fluctuate between strong positive and strong negative relationships over short time-scales (<1 week). In particular, P1, P2 and P4 are characterized by pronounced conductivity peaks (Figure 2b) that show a strong positive relationship with increasing Q on their rising limbs (Figure 2e). During P2, EC increases from 17–42 μS cm^{-1} in 9 hours as Q increases from 40–59 m^3 s^{-1} and, during P4, EC increases from 10–40 μS cm^{-1} in 6 hours as Q increases from 74–140 m^3 s^{-1}. In these pulses, an EC peak shortly precedes maximum discharge, and EC returns to pre-pulse levels within a few days (Figure 2b). By contrast, there is no large peak in EC associated with P3.

[9] Suspended sediment concentration ranged from less than 0.2 kg m^{-3} to greater than 18 kg m^{-3}, beyond the range of our sensor, and increased gradually but episodically throughout the season (Figure 2c). In common with the pattern in electrical conductivity and discharge, there are

[1] Auxiliary materials are available in the HTML. doi:10.1029/2011GL047063.

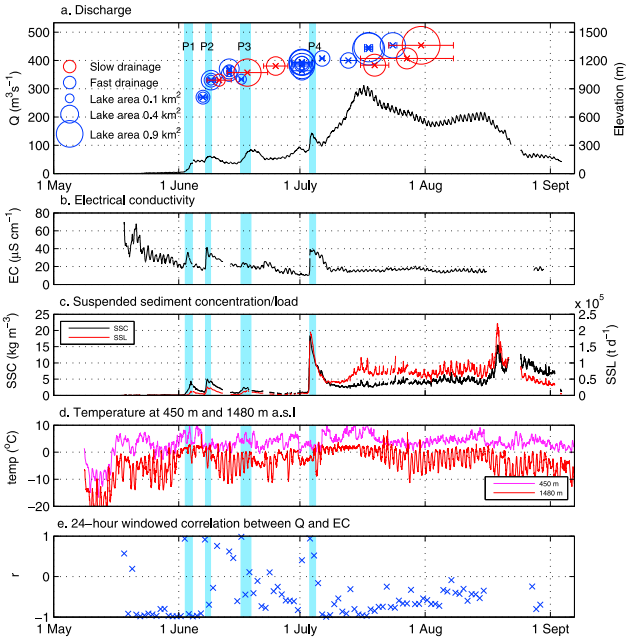

Figure 2. (a) Proglacial meltwater stream discharge ($m^3\ s^{-1}$; black line; shaded blue sections show the pulses of meltwater (P1–P4) which are superimposed on the rising limb of the seasonal runoff hydrograph). Timing, area and elevation of lake drainage events. Each circle represents a single lake drainage event, based on change in surface area on MODIS images. Horizontal bars represent the time period in which drainage took place. Red circles are lakes that drained slowly over several images while blue circles drained in a discrete event between two images. (b) Electrical conductivity ($\mu S\ cm^{-1}$). (c) suspended sediment concentration ($kg\ m^{-3}$; left-axis, black) and suspended sediment load ($t\ d^{-1}$; right-axis, red). (d) Temperature measurements from 450 m and 1480 m elevation. (e) 24-hour windowed correlation coefficient between Q and EC.

large spikes in SSC during P1, P2 and P4, and to a lesser extent, P3. These spikes precede the local discharge peaks and are characterized by a steep rise followed by a more gradual return to lower values. The SSC peak at P4 is the most dramatic and jumps from 2–>18 $kg\ m^{-3}$ within 6 hours. The suspended sediment load (SSL) also grows throughout the season, and is significantly greater in the latter part of the season (Figure 2c). Prior to P4, SSL ranges from $0–4 \times 10^4\ t\ d^{-1}$, and following P4 ranges from $4–20 \times 10^4\ t\ d^{-1}$. The total suspended sediment flux for the survey period is $\sim 4.7 \pm 0.74 \times 10^6$ t.

4. Discussion

[10] The delay in the onset of significant runoff, following ~20 days with above-zero temperatures, can be explained by refreezing of an initial fraction of the surface melt in cold snow until the firn becomes isothermal [*Pfeffer et al.*, 1991] and observed ponding of surface meltwater. Prior to P1, low runoff volume and high EC indicate that water in the proglacial stream was derived substantially from leakage of basal meltwater from an inefficient winter drainage system beneath Leverett Glacier [*Collins*, 1979; *Skidmore and Sharp*, 1999].

[11] Using a temperature-index model [*Hock*, 2003] of surface melt within the catchment, calibrated with *in situ* measurements of initial snow depth and ablation, we found that the seasonal discharge volumes we observe cannot be explained by an increase in melt intensity within a stable catchment area (auxiliary material). Instead, the discharge observed at Leverett glacier can only be accounted for by progressive upglacier expansion of the catchment to include runoff from higher elevations through the melt season, indicating delivery of surface-generated meltwater from a progressively larger area of the ice sheet as the melt season develops. The required development and expansion of the contributing hydrological catchment, up to 800 melevation by June 6th, and to 1000 m by July 9th, eventually delivers surface meltwater from an area of over 600 km^2 that extends higher than 1200 m elevation and to a distance of >50 km from the ice margin by July 21st. The dramatic rise in runoff observed in the first half of July is driven, therefore, by a combination of high temperatures (Figure 2d) and recent expansion of the area of the ice sheet which delivers water to the ice margin via Leverett Glacier.

[12] The EC of meltwater can be used crudely to differentiate runoff components and hydrological pathways through a glacial catchment [*Collins*, 1979]. The basic pattern of decline from high to low solute concentration that we observe is typical of Alpine and High Arctic glaciers [*Collins*, 1979; *Skidmore and Sharp*, 1999] as the drainage system becomes more efficient and a greater proportion of water is transported rapidly through the glacier, limiting the potential for solute acquisition. Therefore, along with the upglacier expansion of the catchment in response to surface melt inputs, our data suggest a concomitant increase in its hydraulic efficiency throughout the melt-season.

[13] High suspended sediment concentrations indicate that meltwater emerging from Leverett Glacier has been routed from the ice sheet surface, where it was generated, via the ice sheet bed. Rates of basal sediment evacuation are controlled by the hydraulic efficiency of the subglacial drainage system, but can be limited by the availability of source material [*Alley et al.*, 1997; *Swift et al.*, 2002]. A sustained increase in subglacial hydraulic efficiency, and ongoing expansion of the subglacial drainage system, is consistent with the continued increase in SSC, even while runoff diminishes following peak discharge on July 16th [*Alley et al.*, 1997]. In addition, SSC shows no sign of supply exhaustion, suggesting that expansion of the efficient basal hydraulic system provides continual access to an extensive reservoir of basal sediment [*Swift et al.*, 2002].

[14] Spatial expansion of efficient subglacial drainage at the expense of a hydraulically inefficient distributed system explains temporal instability in the correlation between EC and Q on the rising limb of the seasonal discharge hydrograph. Upglacier expansion of supraglacial melt extent results in the upglacier expansion of the efficient subglacial drainage system through the delivery of surface meltwater to the glacier bed [*Nienow et al.*, 1998]. These surface waters initially drain into a hydraulically inefficient drainage system causing channel sections to grow in a downglacier direction until they connect with existing channels further downstream. Reduction of mean water pressure in the channels, relative to the distributed drainage system, is probably responsible for drawing out stored basal waters. Temporal and spatial evolution of the efficiency of the drainage system

therefore complicates the relationship between surface melting and proglacial runoff, especially during the period of each year when the subglacial system is becoming established. The stable hysteresis pattern that develops with EC peaking on the rising limb of the diurnal flow hydrograph, and the constant inverse relationship between EC and Q (Figure 2e), demonstrate that the hydrological system has reached a more stable and uniform configuration by July 16th.

[15] Observations on the GrIS have shown that moulins essentially comprise vertical conduits which transport water from the ice sheet surface to its bed [*Das et al.*, 2008; *Catania and Neumann*, 2010]. While there may be some lateral transport of water via englacial channels, in order to explain the trends in Q, EC and SSC we argue that opening of moulins at progressively higher elevations allows surface generated meltwater to be delivered to the ice sheet bed further inland through the melt season. Growth of the efficient subglacial system therefore follows upglacier development of supraglacial drainage and proceeds in a stepwise fashion as new input points become active 1998. This proposed model is analogous to one previously proposed for Alpine glacier drainage systems [*Nienow et al.*, 1998]. It is notable, therefore, that the channelized subglacial drainage system is sustained in the GrIS where ice thicknesses are much greater, implying that the high volumes of meltwater delivered to the glacier bed are sufficient to offset the increased potential for channel closure by deformation of thicker ice.

[16] Large rises in EC associated with P1, P2 and P4 suggest that a significant component of these flood-waters has a subglacial provenance and indicates the displacement of solute-rich stored water from an inefficient drainage system [*Skidmore and Sharp*, 1999]. Large sediment flushes (Figure 2c) also confirm interaction of meltwaters with the basal environment. They indicate sudden access of water to areas of subglacially stored sediments and a dramatic increase in the capacity of subglacial waters to mobilise and evacuate them [*Swift et al.*, 2002]. Rapid return to low EC values following each of the meltwater pulses implies that the hydraulic system downglacier already has the capacity to transport water quickly and efficiently.

[17] We suggest that P1, when the rise in EC is less dramatic than during P2 and P4, is the result of initial access of meltwater to the subglacial drainage system through moulins and crevasses low down on the glacier following the onset of spring melting. This is supported by observations of meltwater ponded in crevasses and supraglacial channels prior to P1, the drainage of which causes mixing with subglacially stored water and flushing of sediments from the winter drainage system as new channel sections develop. P3 is not accompanied by a dramatic rise in EC and therefore appears to be driven by changes in temperature-driven runoff feeding into the existing drainage system.

[18] P2 and P4 are superimposed on the rising limb of the seasonal hydrograph (Figure 2a) and cannot be explained by trends in surface melting (Figure 2d) as they occur during periods of low or zero ablation within the catchment. From the MODIS satellite images, we find that the timing of supraglacial lake drainage events, the size and elevation of the lakes (Figure 2a), and their location within the proposed catchment of Leverett Glacier (Figure 1), suggest that they are likely candidates for the source of the pulses of water during P2 and P4. In particular, P2 is associated with the drainage of five lakes between 800–1000 m, and P4 coincides with seven drainage events from lakes located between 1100–1200 m.

[19] Previous studies have found that MODIS classification of GrIS supraglacial lakes is robust when compared with higher resolution satellite data [*Sundal et al.*, 2009] and has an approximate error of 0.22 km^2. Estimation of lake area (Figure 2a), based on manual pixel counting of classified images [*Sundal et al.*, 2009], indicates that the lakes that drain at P2 have areas between 0.13 and 0.49 km^2 and those that drain at P4 are between 0.25 and 0.88 km^2. Using an average lake depth of 2.7 m (a value determined [*McMillan et al.*, 2007; *Shepherd et al.*, 2009] for ~150 lakes in this region in summer 2001), we find that the volume of water in each pulse (4.9 and 7.2 × 10^6 m^3 respectively) can be accounted for by the drainage of multiple lakes in a single event. Since there is uncertainty about the depth of individual lakes we are unable to determine which, or how many, of the lakes could contribute to each meltwater pulse. It is clear, however, that coincident with the observed pulses of meltwater (P2 and P4) a commensurate volume of meltwater drains from a number of lakes on the surface of the ice sheet within the catchment of Leverett glacier.

[20] We have observed active moulins at elevations of at least 1100 m in this region and supraglacial lakes that have drained through large crevasses in their centre at elevations up to 1450 m. A key role of these features in GrIS hydrology appears to be their contribution to the expansion of the subglacial area that is subject to inputs of surface meltwater and seasonal reorganization. Supraglacial lake drainage at high elevations may be particularly important for two reasons. Firstly it provides a mechanism for water to penetrate through thick, cold ice [*van der Veen*, 2007]. Secondly, concentration of surface meltwater into lakes may be critical to provide the volumes of water required to force evolution of a channelized drainage system beneath thick ice where overburden pressures are large.

[21] Our findings of seasonal upglacier-directed seasonal expansion of evolution in the subglacial drainage system and its conversion from a distributed to channelized system are supported by observations of ice-motion [*Bartholomew et al.*, 2010] and upglacier evolution in the timing of lake drainage [*Sundal et al.*, 2009] in this section of the ice sheet. Given recent focus within the glaciological community on the impact of channelized subglacial drainage on ice motion [*Schoof*, 2010; *Sundal et al.*, 2011] our findings provide a conceptual model of subaerial and supraglacial forcing of subglacial drainage development which can be incorporated in numerical experiments designed to investigate the relationship between surface melting and ice velocity in the GrIS [*Schoof*, 2010; *Pimentel and Flowers*, 2011].

5. Conclusions

[22] Our observations provide the first synopsis of the seasonal hydrological behaviour of a large (>600 km^2) catchment in the ablation zone of the GrIS, showing how surface meltwater production drives spatial and temporal changes in the subglacial drainage system. These observations show the development and expansion of a drainage system that delivers water from the ice surface, via the ice-sheet bed, to the margin. This system expands progressively throughout the ablation season to >50 km from the ice

margin. We propose a model that is similar to one proposed for Alpine systems, where the drainage system becomes increasingly efficient as hydraulic connections between the surface and bed are established further inland, evacuating large volumes of meltwater and sediment.

[23] **Acknowledgments.** We thank for financial support: UK Natural Environment Research Council (NERC, through a studentship to IB and grants to PN/DM), Edinburgh University Moss Centenary Scholarship (IB). ERS SAR data, for the surface DEM, were provided by the European Space Agency VECTRA project (SP).

[24] The Editor thanks Martin Sharp and an anonymous reviewer for their assistance in evaluating this paper.

References

Alley, R., K. Cuffey, E. Evenson, J. Strasser, D. Lawson, and G. Larson (1997), How glaciers entrain and transport basal sediment: Physical constraints, *Quat. Sci. Rev.*, *16*(9), 1017–1038.

Bartholomew, I., P. Nienow, D. Mair, A. Hubbard, M. King, and A. Sole (2010), Seasonal evolution of subglacial drainage and acceleration in a Greenland outlet glacier, *Nat. Geosci.*, *3*, 408–411.

Box, J., and K. Ski (2007), Remote sounding of Greenland supraglacial melt lakes: Implications for subglacial hydraulics, *J. Glaciol.*, *53*(181), 257–265.

Catania, G. A., and T. A. Neumann (2010), Persistent englacial drainage features in the Greenland ice sheet, *Geophys. Res. Lett.*, *37*, L02501, doi:10.1029/2009GL041108.

Collins, D. (1979), Hydrochemistry of meltwaters draining from an alpine glacier, *Arct. Alp. Res.*, *11*(3), 307–324.

Das, S., I. Joughin, M. Behn, I. Howat, M. King, D. Lizarralde, and M. Bhatia (2008), Fracture propagation to the base of the Greenland ice sheet during supraglacial lake drainage, *Science*, *320*(5877), 778.

Fenn, C. (1987), Electrical conductivity, in *Glacio-fluvial Sediment Transfer: An Alpine Perspective*, edited by A. M. Gurnell and M. J. Clark, pp. 377–414, John Wiley, Chichester, U. K.

Hock, R. (2003), Temperature index melt modelling in mountain areas, *J. Hydrol.*, *282*(1–4), 104–115.

Kamb, B. (1987), Glacier surge mechanism based on linked cavity configuration of the basal water conduit system, *J. Geophys. Res.*, *92*(B9), 9083–9100

McMillan, M., P. Nienow, A. Shepherd, T. Benham, and A. Sole (2007), Seasonal evolution of supra-glacial lakes on the Greenland Ice Sheet, *Earth Planet. Sci. Lett.*, *262*, 484–492.

Nienow, P., M. Sharp, and I. Willis (1998), Seasonal changes in the morphology of the subglacial drainage system, Haut Glacier d'Arolla, Switzerland, *Earth Surf. Processes Landforms*, *23*(9), 825–843.

Palmer, S., A. Shepherd, P. Nienow, and I. Joughin (2011), Seasonal speedup of the Greenland ice sheet linked to routing of surface water, *Earth Planet. Sci. Lett.*, *302*, 423–428.

Parizek, B., and R. Alley (2004), Implications of increased Greenland surface melt under global-warming scenarios: Ice-sheet simulations, *Quat. Sci. Rev.*, *23*(9–10), 1013–1027.

Pfeffer, W. T., M. F. Meier, and T. H. Illangasekare (1991), Retention of Greenland runoff by refreezing: Implications for projected future sea level change, *J. Geophys. Res.*, *96*(C12), 22,117–22,124.

Pimentel, S., and G. Flowers (2011), A numerical study of hydrologically driven glacier dynamics and subglacial flooding, *Proc. R. Soc. A*, doi:10.1098/rspa.2010.0211, in press.

Schoof, C. (2010), Ice-sheet acceleration driven by melt supply variability, *Nature*, *468*(7325), 803–806.

Shepherd, A., A. Hubbard, P. Nienow, M. King, M. McMillan, and I. Joughin (2009), Greenland ice sheet motion coupled with daily melting in late summer, *Geophys. Res. Lett.*, *36*, L01501, doi:10.1029/2008GL035758.

Shreve, R. (1972), Movement of water in glaciers, *J. Glaciol.*, *11*(62), 205–214.

Skidmore, M., and M. Sharp (1999), Drainage system behaviour of a high-Arctic polythermal glacier, *Ann. Glaciol.*, *28*(1), 209–215.

Sundal, A., A. Shepherd, P. Nienow, E. Hanna, S. Palmer, and P. Huybrechts (2009), Evolution of supra-glacial lakes across the Greenland ice sheet, *Remote Sens. Environ.*, *113*, 2164–2171.

Sundal, A., A. Shepherd, P. Nienow, E. Hanna, S. Palmer, and P. Huybrechts (2011), Melt-induced speed-up of Greenland ice sheet offset by efficient subglacial drainage, *Nature*, *469*(7331), 521–524.

Swift, D., P. Nienow, N. Spedding, and T. Hoey (2002), Geomorphic implications of subglacial drainage configuration: rates of basal sediment evacuation controlled by seasonal drainage system evolution, *Sediment. Geol.*, *149*(1–3), 5–19.

Van de Wal, R., W. Boot, M. Van den Broeke, C. Smeets, C. Reijmer, J. Donker, and J. Oerlemans (2008), Large and rapid melt-induced velocity changes in the ablation zone of the Greenland ice sheet, *Science*, *321*(5885), 111.

van der Veen, C. J. (2007), Fracture propagation as means of rapidly transferring surface meltwater to the base of glaciers, *Geophys. Res. Lett.*, *34*, L01501, doi:10.1029/2006GL028385.

Zwally, H., W. Abdalati, T. Herring, K. Larson, J. Saba, and K. Steffen (2002), Surface melt-induced acceleration of Greenland ice-sheet flow, *Science*, *297*(5579), 218.

I. Bartholomew, T. Cowton, P. Nienow, and A. Sole, School of Geosciences, University of Edinburgh, Drummond Street, Edinburgh EH8 9XP, UK. (ian.bartholomew@ed.ac.uk; t.r.cowton@sms.ed.ac.uk; peter.nienow@ed.ac.uk; andrew.sole@ed.ac.uk)

D. Mair, School of Geosciences, University of Aberdeen, Elphinstone Road, Aberdeen AB24 3UF, UK. (d.mair@abdn.ac.uk)

S. Palmer, School of Earth and Environment, University of Leeds, Maths/Earth and Environment Building, Leeds LS2 9JT, UK. (s.j.palmer@leeds.ac.uk)

J. Wadham, School of Geographical Sciences, University of Bristol, University Road, Bristol BS8 1SS, UK. (j.l.wadham@bristol.ac.uk)

Appendix 3

Earth and Planetary Science Letters 307 (2011) 271–278

Contents lists available at ScienceDirect

Earth and Planetary Science Letters

journal homepage: www.elsevier.com/locate/epsl

Seasonal variations in Greenland Ice Sheet motion: Inland extent and behaviour at higher elevations

I.D. Bartholomew [a,*], P. Nienow [a], A. Sole [a], D. Mair [b], T. Cowton [a], M.A. King [c], S. Palmer [d]

[a] School of Geosciences, University of Edinburgh, Drummond Street, Edinburgh, EH8 9XP, UK
[b] School of Geosciences, University of Aberdeen, Aberdeen, AB24 3UF, UK
[c] School of Civil Engineering and Geosciences, Newcastle University, Newcastle upon Tyne, NE1 7RU, UK
[d] School of Earth and Environment, University of Leeds, Leeds, LS2 9JT, UK

ARTICLE INFO

Article history:
Received 8 December 2010
Received in revised form 5 April 2011
Accepted 14 April 2011
Available online 28 May 2011

Editor: P. DeMenocal

Keywords:
Greenland
GPS
ice dynamics
supraglacial lakes
subglacial hydrology

ABSTRACT

We present global positioning system observations that capture the full inland extent of ice motion variations in 2009 along a transect in the west Greenland Ice sheet margin. *In situ* measurements of air temperature and surface ablation, and satellite monitoring of ice surface albedo and supraglacial lake drainage are used to investigate hydrological controls on ice velocity changes. We find a strong positive correlation between rates of annual ablation and changes in annual ice motion along the transect, with sites nearest the ice sheet margin experiencing greater annual variations in ice motion (15–18%) than those above 1000 m elevation (3–8%). Patterns in the timing and rate of meltwater delivery to the ice–bed interface provide key controls on the magnitude of hydrologically-forced velocity variations at each site. In the lower ablation zone, the overall contribution of variations in ice motion to annual flow rates is limited by evolution in the structure of the subglacial drainage system. At sites in the upper ablation zone, a shorter period of summer melting and delayed establishment of a hydraulic connection between the ice sheet surface and its bed limit the timeframe for velocity variations to occur. Our data suggest that land-terminating sections of the Greenland Ice Sheet will experience increased dynamic mass loss in a warmer climate, as the behaviour that we observe in the lower ablation zone propagates further inland. Findings from this study provide a conceptual framework to understand the impact of hydrologically-forced velocity variations on the future mass balance of land-terminating sections of the Greenland Ice Sheet.

1. Introduction

Our ability to make robust predictions about the future mass balance of the Greenland Ice Sheet (GrIS), and therefore its contribution to sea-level change, is limited by uncertainty about how the dynamic component of mass loss (*i.e.* due to changes in ice motion) will respond to anticipated changes in atmospheric temperature (IPCC, 2007; Pritchard et al., 2009). In land-terminating sections of the GrIS, variations in ice velocity are initiated when surface meltwater gains access to the ice–bed interface, lubricating basal motion (Bartholomew et al., 2010; Joughin et al., 2008; Shepherd et al., 2009; Van de Wal et al., 2008; Zwally et al., 2002). This effect is both widespread (Joughin et al., 2008; Sundal et al., 2011) and persistent each summer (Sundal et al., 2011; Van de Wal et al., 2008; Zwally et al., 2002) near the ice sheet margin. Initial observations show that summer velocities in land-terminating sections of the GrIS can be 50% faster than in winter (Joughin et al., 2008; Van de Wal et al., 2008), and that summer velocity variations increase annual ice motion by 6–14% in the lower ablation zone (Bartholomew et al., 2010). A direct positive relationship between rates of surface melting and basal motion would create a mechanism to significantly increase rates of mass loss from the GrIS in a warming climate by drawing more ice to lower elevations where ablation rates are higher (Parizek and Alley, 2004). This process allows the dynamic component of the GrIS mass balance to respond to climatic variability within decades or less, yet is not considered in current sea-level projections made by the Intergovernmental Panel on Climate Change (IPCC).

Recent observations (Bartholomew et al., 2010; Sundal et al., 2011) and theoretical work (Pimentel and Flowers, 2010; Schoof, 2010) suggest, however, that the contribution of seasonal velocity variations to annual rates of ice motion at a particular site is limited by evolution in the structure of the subglacial drainage system. Each summer in the lower ablation zone, sustained inputs of meltwater from the ice sheet surface transform the subglacial hydrological system into an efficient network of channels that can evacuate large quantities of water rapidly (Bartholomew et al., 2011). This moderates the lubricating effect of meltwater on ice velocities by reducing the pressure within the hydrological system for a given

* Corresponding author.
E-mail address: ian.bartholomew@ed.ac.uk (I.D. Bartholomew).

0012-821X/$ – see front matter © 2011 Elsevier B.V. All rights reserved.
doi:10.1016/j.epsl.2011.04.014

volume of water (Kamb, 1987; Van de Wal et al., 2008). It has been observed that late summer velocities near the GrIS margin are lower for a given intensity of surface melting than earlier in the season (Bartholomew et al., 2010; Sundal et al., 2011). As a result, it is not expected that increased annual ablation rates at a specific location will necessarily stimulate faster ice flow than at present; in this respect the process could be seen as self-limiting (Van de Wal et al., 2008). By extension, it has been argued that summer, and therefore annual mean ice velocities at a given site on the GrIS could be *lower* in high ablation years than in low ablation years because channelisation of the subglacial hydrological system occurs more quickly (Pimentel and Flowers, 2010; Sundal et al., 2011; Truffer et al., 2005).

A key feature of hydrologically-forced velocity variations in the GrIS is also that they propagate inland from the ice sheet margin on a seasonal basis, in response to the onset of surface melting at successively higher elevations (Bartholomew et al., 2010). The initiation of hydrologically-forced ice velocity variations is dependent on the development of a conduit from the ice sheet surface to allow surface meltwater to access the ice–bed interface. In a warmer climate we expect summer melting of the GrIS to be more intense, affecting a wider area for a longer time period than is currently the case (Hanna et al., 2008), providing greater volumes of surface meltwater. The melt regime will be amplified because the hypsometry of the GrIS, which flattens inland, gives a non-linear expansion of the area of the GrIS experiencing melt in response to a rise in the equilibrium-line altitude (ELA). It is therefore possible that seasonal velocity variations in the GrIS will propagate further inland in response to climate warming. One mechanism to allow this is drainage of supraglacial lakes, which have the potential to concentrate surface meltwaters into large enough reservoirs to propagate fractures through ice that is >1000 m thick (Alley et al., 2005; Das et al., 2008; Krawczynski et al., 2009).

Current debates over whether increased melt rates across the GrIS will induce greater dynamic mass loss can therefore be reduced to whether increased mass loss due to inland propagation of velocity variations in warmer years will more than offset any potential reduction in mass loss due to earlier onset of channelisation in the lower ablation zone. However, uncertainty remains over the effect of increased meltwater production on dynamic behaviour in the lower ablation zone — observations to date do not show conclusively whether annual mean ice velocities will increase or decrease in a warmer climate (Bartholomew et al., 2010; Joughin et al., 2008; Sundal et al., 2011; Van de Wal et al., 2008) and a more detailed understanding of the response of the subglacial drainage structure to large inputs of surface meltwater is required. In addition, while diurnal ice velocity variations have been observed up to 72 km from the GrIS margin in a short-term study (Shepherd et al., 2009), it is not clear that patterns in hydrologically-forced dynamic behaviour observed near the ice sheet margin are replicated at higher elevations. While singular lake drainage events have been described in detail (Das et al., 2008), it has not been shown that the integrated effect of widespread meltwater generation and lake drainage (Box and Ski, 2007; McMillan et al., 2007; Sundal et al., 2009) is a significant and sustained increase in glacier flow speed at higher elevations.

A secondary effect of meltwater inputs to the glacier system on ice dynamics is 'cryo-hydrologic warming', whereby heat conduction from water within the englacial system causes ice temperatures to be raised (Phillips et al., 2010). Increased temperatures will reduce ice viscosity and thus contribute to faster ice flow. It has been suggested that, in a warmer climate, drainage of meltwater into the ice sheet across a wider area will also cause a rapid thermal response in deep layers of the GrIS, compounding the effect of meltwater drainage on ice velocities (Phillips et al., 2010).

The aim of this study is to provide a clearer understanding of the mechanisms which control the magnitude and extent of hydrologically-forced dynamic behaviour at elevations up to and beyond the current ELA *on a seasonal basis*. This is motivated by the need to incorporate these processes in numerical models which predict the future evolution of the GrIS and the current lack of comprehensive empirical data with which to inform them (Parizek, 2010). The thermal effect of meltwater, which affects ice deformation rates rather than basal motion, does not have a significant seasonal signal (Phillips et al., 2010) and is not considered here.

We present continuous ice velocity measurements, derived from global position system (GPS) observations, that capture the full inland extent of seasonal velocity variations along a land-terminating transect at ~67°N in western Greenland during the 2009 melt season (Fig. 1). Measurements were made at seven sites up to 1716 m elevation, which is ~115 km inland from the GrIS margin. The ice motion record is compared with *in situ* and satellite observations of air temperatures, surface melt characteristics and supraglacial lake evolution within the region of study, as well as with proglacial hydrological data (Bartholomew et al., 2011).

2. Data and methods

2.1. GPS data

We used dual-frequency Leica 500 and 1200 series GPS receivers to collect the season long records of ice motion at each site. Each GPS antenna was mounted on a pole drilled several metres into the ice, which froze in subsequently, providing measurements of ice motion that were independent of ablation. The GPS receivers collected data at 30 second intervals that were processed using a kinematic approach relative to an off-ice base station (King, 2004) using the Track 1.21 software (Chen, 1999; King and Bock, 2006). Conservative estimates of the uncertainty associated with positioning at each epoch are approximately ±1 cm in the horizontal direction and ±2 cm in the vertical direction. The data were smoothed using a Gaussian low-pass filter to suppress high-frequency noise without distorting the long-term signal. Daily horizontal velocities reported in this paper (Fig. 2a–g) are calculated by differencing the filtered positions every 24 h. Shorter-term variations in ice velocity were derived by differencing positions across a 6 hour sliding window, applied to the whole time series of filtered positions for each site. This window length was chosen in order to highlight short-term variations in the velocity records while retaining a high signal to noise ratio. Estimates of the magnitude of daily cycles in horizontal velocity are therefore minimum estimates. Unfortunately, the quality of the GPS data at site 1 was compromised by technical problems, and we are unable to resolve short-term variations in horizontal velocity at this site.

Uncertainties associated with the filtered positions are <0.5 cm in the horizontal and <1 cm in the vertical directions, corresponding to annual horizontal velocity uncertainties of $<3.7\ m\ yr^{-1}$ and $<14.6\ m\ yr^{-1}$ for the 24 hour and 6 hour velocity measurements respectively. We used the standard deviation of 24 hour and 6 hour sliding window velocities from site 7, which has the longest processing baseline and experienced negligible velocity variations, to estimate the noise floor in the GPS velocity records. The standard deviations for 24 hour and 6 hour velocities at site 7 are $5.6\ m\ yr^{-1}$ and $19.5\ m\ yr^{-1}$ respectively. These values compare well with the calculated uncertainties and represent conservative error estimates for our dataset.

The values for winter background ice-velocities are derived from the displacement of each GPS receiver between the end of the summer melt season and the following spring (Bartholomew et al., 2010). The reported contribution to annual ice flux from the hydrologically-forced summer ice velocity variations is the percentage by which the observed annual displacement exceeds that which would occur if the ice moved at winter rates all year round.

2.2. Air temperate and surface ablation

Simultaneous measurements of air temperature were made at each GPS site to constrain melt rates, and show that the velocity data

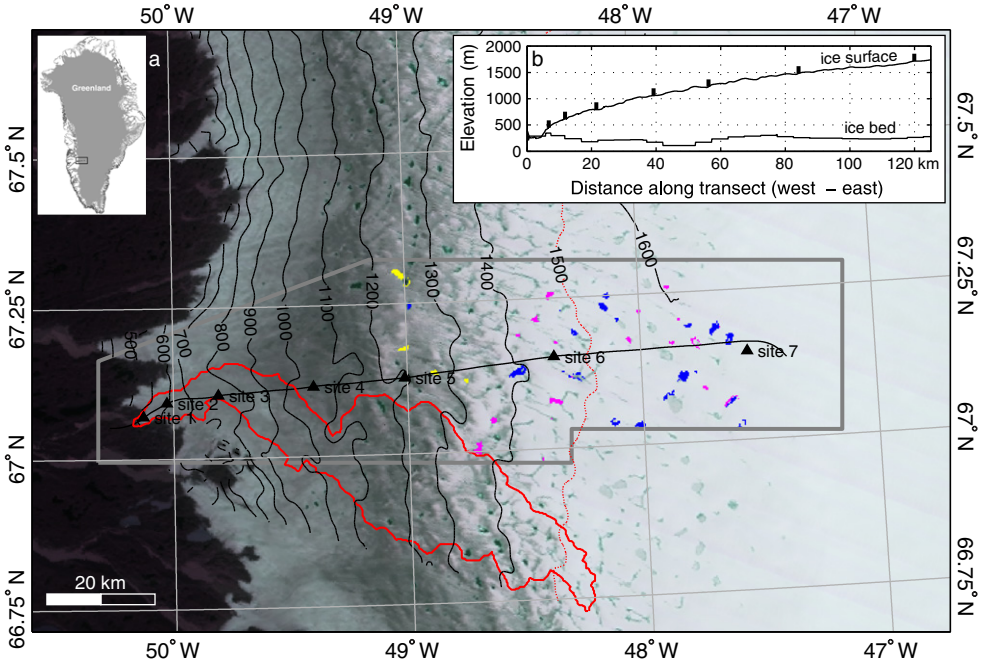

Fig. 1. a. Location of the study region on the western margin of the GrIS. The GPS sites are located along a transect across an altitudinal range of 450–1700 m.a.s.l. Simultaneous measurements of air temperature and seasonal measurements of ablation were made at each site. The ELA in this region is at 1500 m (Van de Wal et al., 2005). Contours are produced from a digital elevation model derived from InSAR (Palmer et al., 2011) at 100 m intervals. Lakes which drain in the interval between sequential MODIS satellite images during the survey period are denoted by coloured patches which represent their surface area immediately prior to drainage (yellow: July 11th–15th; red: July 19th–23rd; blue: July 26th–29th). The region in which lake drainage events were monitored is enclosed by the grey box and the catchment of the river which drains through Leverett glacier and which was also monitored in 2009 is shown in red (Bartholomew et al., 2011). b. Ice surface (Krabill, 2010) and bed elevation (Bamber et al., 2001) profiles along the transect (black line, main figure). The locations of the GPS sites are shown by black vertical marks.

cover the whole seasonal melt cycle. Measurements of air temperature were made using shielded Campbell Scientific T107 temperature sensors connected to Campbell Scientific CR800 data loggers (sites 1, 3 and 6) and shielded HOBO U21-004 temperature sensors (sites 2, 4, 5 and 7) at 15 minute intervals throughout the survey period. Seasonal melt totals were also measured using ablation stakes at each GPS site.

2.3. Proglacial discharge

We made continuous measurements of water stage in the proglacial stream that emerges from the terminus of Leverett Glacier. Proglacial discharge was derived from a continuous stage–discharge rating curve calibrated with repeated dye dilution gauging experiments throughout the melt-season as described in detail in Bartholomew et al. (2011).

2.4. Supraglacial lake evolution

We used satellite observations from the Moderate-resolution Imaging Spectrometer (MODIS) to study the development of supraglacial lakes within the region of our GPS transect (Fig. 1; delimited by the grey line). 20 MODIS images, spanning the period 31st May to 18th August 2009, were used, representing all the days when lake identification was not impeded by cloud cover. MODIS level 1B Calibrated Radiances (MOD02) were processed and projected as 250 m resolution true colour images in conjunction with the MODIS Geolocation product (MOD03), according to the methodology laid out by Gumley et al. (2003); see also Box and Ski (2007), and Sundal et al. (2009). Lakes were digitised manually in order to allow classification even on days of partial or thin cloud cover, producing a dataset with slightly higher temporal resolution than fully automated classification (Sundal et al., 2009). Drainage events were identified as occasions on which the area of a lake decreased to zero (or a very small fraction of its former size) without an intermediate period of refilling. Previous studies have found that MODIS classification of GrIS supraglacial lakes is robust when compared with higher resolution satellite data (Sundal et al., 2009) and has approximate error of 0.22 km^2 per lake. However, since the lakes within this region are relatively small (typically <1 km^2) and there is considerable uncertainty in using a depth-retrieval algorithm to determine the depth of individual lakes (Box and Ski, 2007) we do not estimate individual lake volume. We note, however, that on the basis of a recent theoretical study of supraglacial lake drainage in the western GrIS (Krawczynski et al., 2009), any lake which is large enough to be resolved on MODIS images (theoretically one 250 m $\times$ 250 m pixel (0.0625 km^2)) will contain enough water to drive a water-filled crack through 1 km of ice.

2.5. Ice sheet surface characteristics

We used the MYD10A1 1-day albedo product, part of the MODIS Aqua snow cover daily L3 global 500 m gridded product (Hall et al., 2009a,b), to map changes in the albedo of the ice sheet surface in this region of the GrIS through the survey period. These data are used to quantify the lowering of surface albedo associated with meltwater generation and retreat of the seasonal snowline through the survey period. This product provides albedo values for pixels identified as cloud free and snow-covered on a 500 m grid derived from a snapshot taken once per day (Stroeve et al., 2006). We used 70 days of data, from April 22nd to September 20th, representing all the days on which the image was not obscured by cloud cover. This time period covers the whole melt season, from before the onset of melt at the ice sheet margin in spring, to the period of refreezing and snowfall in the autumn. In order to integrate the albedo characteristics across the region surrounding the transect, mean albedo was calculated by 50 m elevation bands in the study region using a surface digital elevation model (Palmer et al., 2011). Albedo thresholds for snow (<0.45) and bare ice (>0.66) surfaces were used to classify pixels on the basis of

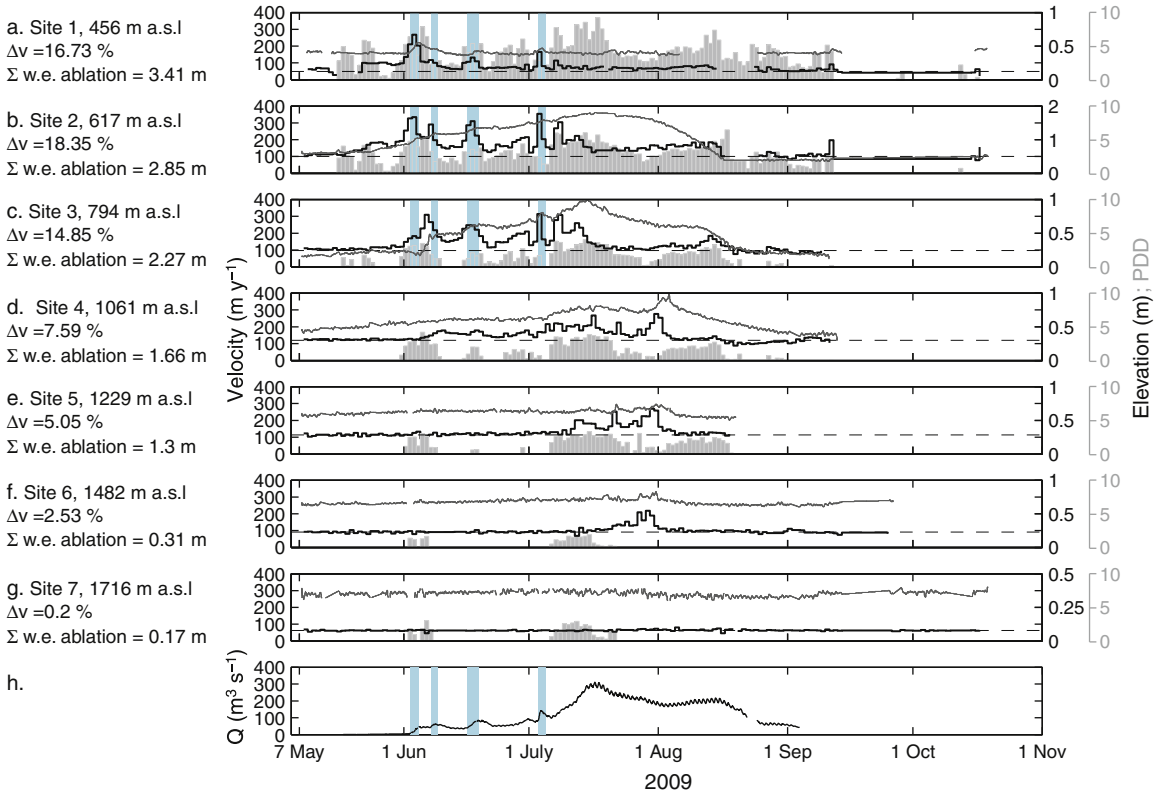

Fig. 2. a–g. 24-h horizontal velocity (black stairs), surface height (grey line) and positive-degree days (grey bars) at sites 1–7 for the survey period. The surface height is shown relative to an arbitrary datum, with a linear, surface-parallel, slope removed. Winter background velocity (black dashes) is determined by bulk movement of each GPS site over the subsequent winter. Text to the left of each panel shows the elevation, percentage annual velocity change due to summer velocity variations compared with values if the ice moved at winter rates all year and the total surface ablation in water equivalence at each site for the whole survey period. h. Discharge hydrograph (black; $m^3 s^{-1}$) from Leverett Glacier in 2009. The estimated catchment for this outflow channel (Bartholomew et al., 2011) is shown on Fig. 1 and contains GPS sites 1, 2 and 3. The blue shaded sections identify pulses of meltwater which are associated with dramatic reorganisation and expansion of the subglacial drainage system within the catchment.

field observations along the nearby K-transect (Knap and Oerlemans, 1996). A resulting transitional band between the two zones is assumed to comprise a mixture of snow, ice with surface water and slush surfaces and broadly delimits the transient snowline (Knap and Oerlemans, 1996).

3. Hydrological forcing of velocity variations

Sites 1–6 all experience velocity peaks that are over 100% higher than their winter background values (Fig. 2a–f). These variations begin nearest the margin on May 22nd, and propagate inland following the onset of surface melting up to a distance of 80 km from the GrIS margin in late July, at 1482 m elevation. Initial uplift of the ice sheet surface at each of these sites is interpreted to signal the establishment of a local hydraulic connection to the ice sheet bed (Anderson et al., 2004; Bartholomew et al., 2010; Das et al., 2008; Iken et al., 1983; Zwally et al., 2002). A high-velocity 'spring-event', accompanied by uplift of the ice sheet surface, characterises the start of locally-forced velocity variations at each of these sites in a manner similar to Alpine and High Arctic glaciers (Bingham et al., 2008; Iken et al., 1983; Iken and Bindschadler, 1986; Mair et al., 2001). This behaviour is consistent with inputs of meltwater to a subglacial hydrological system which is incapable of accommodating them without a great increase in pressure (Hooke et al., 1989; Iken et al., 1983; Iken and Bindschadler, 1986; Mair et al., 2001; Röthlisberger and Lang, 1987).

Although a small component of the coincident vertical and horizontal velocity changes is due to thickness changes resulting from longitudinal strain-rate or stress-gradient coupling, the signals we observe cannot be attributed to these effects alone. Based on motion of adjacent sites and ice thickness data (Fig. 1b; (Bamber et al., 2001; Krabill, 2010)), we calculate that the thickness changes originating due to longitudinal coupling are approximately an order of magnitude smaller than the elevation changes we have recorded. They also typically operate in the opposite direction as acceleration of downstream sites causes extension and thinning of ice upstream as opposed to the uplift observed. Throughout the summer, further speed-up events which are coincident with ice surface uplift confirm the role of surface generated meltwater in forcing seasonal changes in ice motion for this section of the GrIS. We also note that the evidence for hydraulically-forced enhanced basal motion implies that basal temperatures along this transect are at the pressure melting point.

Immediately prior to the spring events most sites also experience a short period of increased velocity in the absence of uplift of the ice surface, which we attribute to mechanical coupling to ice downglacier that is already moving more quickly (Price et al., 2008). At site 7, which is located at 1716 m elevation, 115 km from the margin, there is no surface uplift or significant ice acceleration indicating that surface generated meltwater did not penetrate to the bed this far inland (Fig. 2g). Site 7 does display a small, but clear, change in horizontal velocity (Fig. 3), however, which can likely be attributed to coupling to ice downstream. Since the magnitude of these changes is insignificant in terms of annual ice flux, site 7 delimits the inland extent of hydrologically forced velocity variations in 2009 for this transect.

3.1. Behaviour in the lower ablation zone

At sites 1–3, which are low in the ablation zone and experience the greatest acceleration, spring-events occur early in the melt-season,

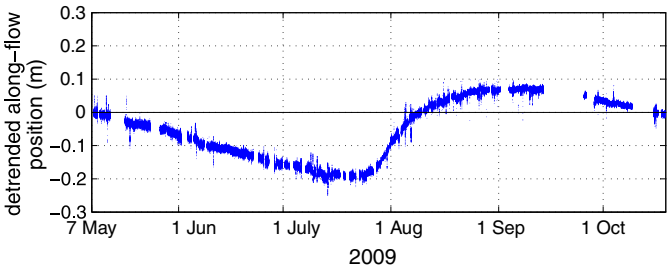

Fig. 3. Detrended along-flow position for the GPS at site 7. The residual value indicates the observed distance in metres of the GPS from the expected position if it flowed at its mean rate for the whole survey period. Negative slopes therefore occur when the velocity is slower than the survey period average and *vice versa*.

near the beginning of June, and ice velocity becomes less sensitive to air temperature variations as the melt season progresses (Fig. 2). This behaviour is explained by evolution in the structure of the subglacial drainage system in response to sustained inputs of meltwater from the ice sheet surface, consistent with previous observations and predictions of dynamic behaviour in this section of the GrIS (Bartholomew et al., 2010; Pimentel and Flowers, 2010).

A recent hydrological study (Bartholomew et al., 2011) supports the conclusion that evolution in the structure of the subglacial drainage system is responsible for limiting the magnitude of hydrologically-forced velocity variations at sites 1–3 later in the melt season. Observations of hydrological parameters from a catchment that drains through Leverett Glacier show that an efficient subglacial drainage system expands upglacier at the expense of an inefficient one as the summer progresses, a process that has been observed previously on Alpine glaciers (Nienow et al., 1998). Episodic increases in the runoff hydrograph (Fig. 2h), which are interpreted as evidence for dramatic re-organisation and expansion of the subglacial drainage system in response to new inputs of meltwater from the ice sheet surface, have a clear short-lived effect on the velocity records at sites 1, 2 and 3 (Fig. 2a–c,h). These events indicate, firstly, that sites 1–3 are within the hydrological catchment of the river and, secondly, that changes in the subglacial drainage system have a direct impact on ice velocity downglacier from where they initially occur. The large volumes of water exceed the capacity of the subglacial drainage system, causing pressurisation, and a concomitant reduction in basal drag (Iken and Bindschadler, 1986), as the water is transported to the ice sheet margin.

Clear daily-cycles in horizontal velocity occur at sites 2 and 3 following the spring events, and persist until mid-August. The magnitude of these cycles is typically between 100 and 150% of the mean daily velocity, and can be over 200% of winter background during periods of significantly enhanced motion (Fig. 4). Their existence indicates that over-pressurisation of the subglacial drainage system also happens regularly on diurnal timescales. The daily cycles in ice velocity appear to be closely related to variations in air temperature, with a typical lag between peak temperature and peak velocity of less than 3 h, suggesting that they occur in direct response to diurnal variations in meltwater production at the ice sheet surface and that surface and englacial transit times are short (Shepherd et al., 2009).

In addition to these short-lived events, ice velocities at sites 1, 2 and 3 are higher on the rising limb of the seasonal runoff hydrograph for Leverett Glacier, subdued following peak discharge on July 21st, and display a return to winter background rates in late August, when runoff is diminishing (Fig. 2a–c,h). 'Slower than winter' ice velocities are also observed for a short period at some sites once the summer melt has stopped, however this signal is not large enough to have a significant impact on rates of annual ice motion.

These findings from the lower ablation zone can be explained in physical terms. Although increased efficiency of the subglacial hydrological system reduces the dynamic response to absolute water input volume (Bartholomew et al., 2010), lake drainage and other singular high velocity events, as well as diurnal fluctuations in horizontal velocity testify that the system can still be overfilled by a large enough increase in meltwater input, causing an increase in subglacial water pressure (Das et al., 2008; Pimentel and Flowers, 2010; Schoof, 2010; Shepherd et al., 2009). Production of surface meltwater, and its delivery to the ice–bed interface, is inherently variable on timescales of hours, days, weeks and months. Since the capacity of the subglacial hydrological system reflects the balance between channel opening by melting of the channel walls, and closure due to deformation of the surrounding ice, and adjusts relatively slowly to changes in water flux (Röthlisberger, 1972; Schoof, 2010), the system never reaches steady-state. We argue, therefore, that once a conduit has been established to deliver surface meltwater to the glacier bed, large changes in the rate of meltwater delivery to the subglacial hydrological system will continue to force velocity variations.

This analysis explains why high-velocity events at sites 1, 2 and 3 occur on the rising limb of the discharge hydrograph, when the system is continuously challenged to evacuate larger and larger volumes of water. Later in the season, when a channelised drainage system has been established, and volumes of meltwater are diminishing, the drainage system is better able to evacuate meltwater without overfilling, explaining the reduction in magnitude of hydrologically-forced variations in ice motion. While ice velocities are subdued on the falling limb of the runoff hydrograph, velocities at sites 1–3 still exceed winter flow rates until mid-August. This appears to be the result of continued diurnal fluctuations in ice velocity (Fig. 4), which occur until there is a dramatic reduction in runoff volumes at Leverett glacier after August 15th (Bartholomew et al., 2011).

3.2. Behaviour in the upper ablation zone

At sites 4–6, which are higher in the ablation zone (>1000 m), the relationship between changes in the rate of horizontal motion and the rate of uplift of the ice sheet surfaces indicates that the forcing mechanism is the same as in the lower ablation zone. Mapping of surface albedo using satellite data shows that the observed spring-events at these sites follow the onset of surface melting above their respective elevations (Fig. 5), although both satellite and *in situ* observations showed that the snowpack was not fully removed at sites 5 and 6 by the end of the summer.

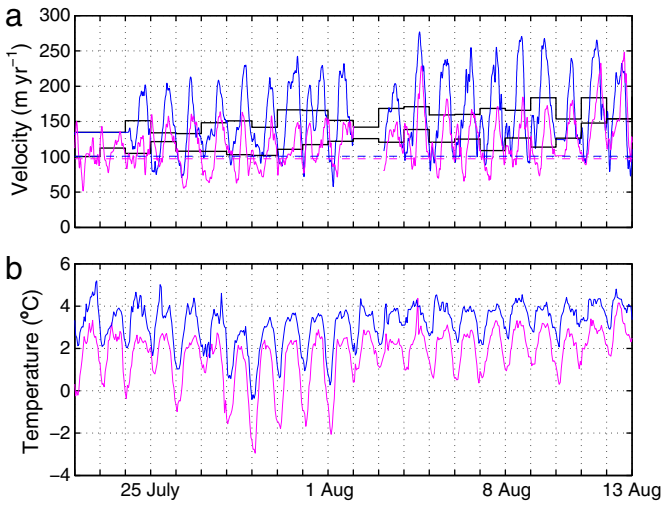

Fig. 4. a. Daily cycles in horizontal ice velocities at sites 2 (blue) and 3 (magenta) for ~3 weeks in late-July/early-August. 24-hour mean velocities are shown by black stairs and coloured lines indicate winter background velocities. b. Temperature record for sites 2 (blue) and 3 (magenta) for the same period.

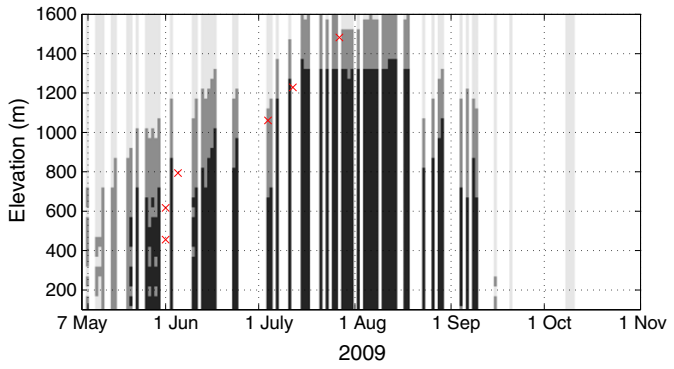

Fig. 5. Ice sheet surface conditions inferred using the MODIS MYD10A1 1-day albedo product. Thresholds for bare ice (<0.45; black) and snow (>0.66; light grey) are used to delimit zones across the study region by elevation (y-axis) throughout the survey period (x-axis). A transitional zone (dark grey) is assumed to comprise a mixture of snow, slush, surface water and bare ice surfaces and broadly delimits the altitudinal extent of surface albedo changes caused by melting of the ice sheet surface (Knap and Oerlemans, 1996). The timing and elevation of the onset of hydrologically forced velocity variations, which occur at sites 1–6 successively, are denoted by crosses.

A key difference from the lower ablation zone is that the spring events occur later in the melt season (Fig. 2a–g). There is also a significant time lag between the onset of surface melting, as inferred from both positive degree days (PDDs) and MODIS-derived albedo values, and the establishment of a hydraulic connection between the ice sheet surface and its bed as inferred from uplift of the ice surface. This means that significant velocity enhancement occurs for a much shorter time period than at lower elevations. At site 4, surface melting begins in early June, while coincident surface uplift and horizontal acceleration, which are diagnostic of local hydrological-forcing, are delayed until July 5th (Fig. 2d). Increased velocities prior to this date, which occur without accompanying surface uplift, are explained by coupling to downglacier ice and are not as large as those induced by local forcing at the sites nearer the margin. *In situ* measurements of air temperature and satellite observations of surface albedo show that sites 5 and 6 both experience prolonged surface melting from July 6th onwards, and experience locally-forced velocity variations from July 12th and July 27th respectively (Fig. 2e,f). Later spring events and the delay between the onset of surface melting and hydraulic connection between the ice surface and its bed are due in part to lower rates of surface melting. In addition greater volumes of water are required to propagate fractures through thicker ice (Alley et al., 2005; Van der Veen, 2007). These factors both increase the time required for the accumulation of sufficient volumes of meltwater to penetrate to the ice sheet bed.

Sites 4, 5 and 6 all experienced their highest velocities during a period of cooler temperatures from July 22nd to August 2nd (Fig. 2d–f), suggesting that drainage of stored surface water was a key factor in these hydrologically-forced events. Satellite images show surface meltwater accumulation in supraglacial lakes in this region from mid-June at elevations between 1000 and 1200 m, and from 1200 m to >1600 m from early July. This storage of surface meltwater is made possible by relatively low surface gradients, which reduce the tendency for water to runoff to lower elevations (Nienow and Hubbard, 2006), and allows concentration of the large volumes of water required to propagate fractures to the ice sheet bed through thick ice (Box and Ski, 2007; Das et al., 2008; McMillan et al., 2007; Sundal et al., 2009).

Using MODIS imagery, we identify a number of events where changes in horizontal and vertical movement at one or more of our GPS sites are coincident with the disappearance of supraglacial lakes from the ice sheet surface. In particular, the spring event at site 5 on July 12th is coincident with disappearance of three supraglacial lakes from between 1200 and 1350 m elevation (Fig. 1, yellow). Widespread drainage of supraglacial lakes at elevations up to 1500 m between July 19th and 23rd (Fig. 1, red) corresponds with increases in ice velocity at sites 4 and 5 of up to 100 m y^{-1} on July 21st and 22nd respectively. The peak in horizontal velocities at sites 4, 5 and 6 at the end of July also coincides with drainage of a lake at ~1400 m elevation and a number of lakes above ~1500 m between July 26th and July 29th (Fig. 1, blue). It is not possible to be certain, using optical imagery, that all lakes which disappear from the ice sheet surface drain directly into englacial conduits. For example, some lakes may drain superficially either into other lakes or to join with water input points that are already open further downglacier. However, the repeated coincidence of lake disappearance from the ice sheet surface with changes in ice velocities suggests strongly that a large number of these lakes drain to the ice–bed interface locally. Uplift of the ice surface indicates that this water is delivered to a subglacial drainage system which is unable to evacuate it without a large increase in water pressure, leading to the enhanced basal motion (Das et al., 2008).

Drainage of supraglacial lakes therefore appears to be responsible for the initiation of hydrologically forced velocity variations at both sites 5 and 6. It is not clear that the spring event at site 4, on July 5th, is caused directly by drainage of supraglacial lakes. This site is located by a large moulin which becomes active each year (Catania and Neumann, 2010), and it is likely that the spring event is associated with the re-opening of this moulin. A common factor in the upper ablation zone, however, is that by the time a hydraulic connection has been established between the ice sheet surface and its bed, facilitating hydrologically-forced velocity variations, air temperatures and proglacial runoff are already decreasing. Lake drainage events are known to be rapid, delivering large enough volumes of water to quickly transform the subglacial hydrological system into an efficient channelised network (Das et al., 2008). Under these circumstances, it is unlikely that the volumes of water generated at the ice sheet surface at these elevations following lake drainage events will be sufficient to sustain large velocity variations (Pimentel and Flowers, 2010). Accordingly, even though the temperature data show that considerable melting occurs at sites 4 and 5 until mid-August, we do not observe any changes in ice velocity at sites above 1000 m elevation beyond August 2nd.

3.3. Changes in annual motion

Annual mean ice velocities at sites 1–7 respectively are 16.7%, 18.4%, 14.8%, 7.6%, 5.1%, 2.5% and 0.2% greater than they would be if the ice flowed at winter rates all year round. We find a strong correlation between the magnitude of local ablation and the percentage changes in annual ice motion due to hydrologically-forced

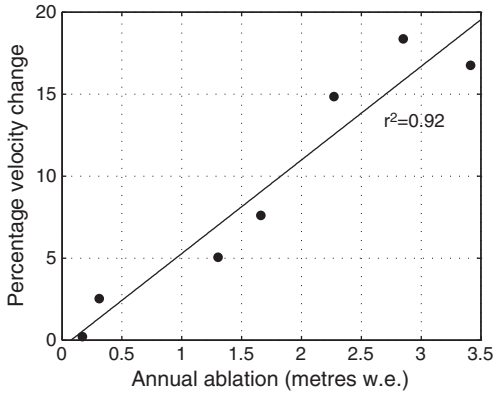

Fig. 6. Percentage change in mean annual ice velocity vs. total surface ablation (m w.e.) at the GPS sites. The increase in annual ice velocity is calculated as the percentage by which the observed annual displacement exceeds that which would occur if the ice moved at winter rates all year round.

velocity variations at each GPS site (Fig. 6). Sites 1, 2 and 3, which are nearest the margin and below 800 m elevation, experience the most surface melting and show significantly greater annual acceleration than those at higher elevations, with the effect attenuating inland. Data from 2008 also show increases in mean annual ice velocity of 13.5% and 5.6% at sites 3 and 4 respectively due to summer velocity variations (Bartholomew et al., 2010), indicating that the velocity changes that we observe in 2009 are a persistent feature of the dynamic behaviour of this part of the GrIS.

The relationship between rates of annual ablation and the amplitude of hydrologically-forced velocity change is not intuitive on the basis of previous theoretical work (Pimentel and Flowers, 2010) and observations (Van de Wal et al., 2008), which have suggested that higher volumes of surface meltwater production will ultimately reduce the impact of hydrological forcing on GrIS motion. Implicit in these arguments is a concept of 'optimum melt': too much meltwater and the hydrological system will become channelised earlier in the summer, making ice velocities less sensitive to the volumes of meltwater reaching the bed more quickly, reducing the impact of seasonal velocity variations on the annual displacement of the ice. However, it is important to consider that the hydrological forcing at each site is a product of both local melting *and* meltwater delivered through the subglacial drainage system from further upglacier. As a result, sites nearest the margin will receive disproportionately more meltwater per unit of local melting than those at higher elevations. Following this logic, previous theoretical work (Pimentel and Flowers, 2010) and observations (Van de Wal et al., 2008) expect sites nearest the margin, where the total flux of meltwater through the subglacial drainage system will be greatest, to show smaller overall velocity changes than sites further inland. However, despite significant differences in the local volume of meltwater delivered to the ice–bed interface, we see similar increases in annual ice motion at sites 1–3 (14.8–18.4%).

Our findings from the lower ablation zone are consistent with the numerical model of subglacial drainage proposed recently by Schoof (2010) and suggest that hydrologically-forced ice velocity variations are controlled more strongly by variations in the rate, rather than the absolute volume, of meltwater production and delivery to the ice–bed interface. In particular, this reflects a temporary imbalance between the volume of water within the subglacial drainage system, and its inability to evacuate this water without an increase in pressure over a wide enough area to significantly affect basal motion (Kamb et al., 1994). We argue that in a warmer climate, where greater volumes of surface meltwater are produced in the lower ablation zone, the seasonal rising limb and shorter-term variations in water delivery to the subglacial drainage system will continue to cause significant increases in annual ice motion despite the potential for an earlier 'switch' from a distributed to a channelised subglacial drainage system (Schoof, 2010). However, the overall magnitude of velocity variations will continue to be limited by evolution in the structure of the subglacial drainage system, which responds to inputs of surface meltwater over a longer period (Anderson et al., 2004; Bartholomew et al., 2010; Mair et al., 2002; Schoof, 2010).

While development in the efficiency of the subglacial drainage system also exerts some control on hydro-dynamic behaviour at higher elevations, the dominant limiting factor on the contribution of velocity variations to annual ice motion at sites in the upper ablation zone is the shorter duration and later establishment of the hydraulic connection between the ice sheet surface and its bed. The expectation that surface melting will be more intense, and spatially extensive, in a warmer climate (Hanna et al., 2008), leads us to suggest that, in future, sites at higher elevations are likely to experience velocity variations for a longer period of time, allowing a greater annual change in ice velocity. In particular, higher rates of meltwater production would allow lakes that fill and subsequently drain to reach the volume required to propagate cracks through thick, cold ice earlier in the summer season (Krawczynski et al., 2009). We therefore expect that the behaviour observed at sites 1–3 would be extended to higher elevations, creating a positive relationship between atmospheric warming and dynamic mass loss in land-terminating sections of the GrIS, albeit one that is modified by development in the structure of the subglacial drainage system.

We do not infer direct cause and effect between bulk volumes of surface ablation and changes in ice motion on the basis of the relationship shown in Fig. 6. Instead, our data show contrasting regimes in hydrologically-forced dynamic behaviour of the GrIS at different elevations within the ablation zone, which provide a compelling explanation for the relationship between total surface ablation and changes in annual ice motion. We therefore believe that our data provide a realistic basis for parameterisation of ice flow models that are used to predict the future evolution of the GrIS (Parizek and Alley, 2004).

4. Conclusions

Our data show that seasonal changes in horizontal ice velocity along an ~115 km transect in a land-terminating section of the western GrIS, are forced by the generation of surface meltwater which is able to reach the ice–bed interface. These velocity variations propagate inland from the ice sheet margin to progressively higher elevations in response to the onset of surface melting, and the creation of a hydraulic connection between the ice sheet surface and its bed. We find a positive relationship between rates of annual ablation and percentage changes in annual ice motion along the transect, with sites nearest the ice sheet margin experiencing greater annual variations in ice motion (15–18%) than those above 1000 m elevation (3–8%).

Patterns in the timing and rate of meltwater delivery to the ice–bed interface are key controls on the magnitude of hydrologically-forced velocity variations at each site. In the lower ablation zone (<800 m elevation), 'spring events' occur early in the melt season and the overall contribution of variations in ice motion to annual flow rates is limited by evolution in the structure of the subglacial drainage system (Bartholomew et al., 2010). At these sites, hydrologically-forced ice acceleration is greatest on the rising limb of the seasonal runoff hydrograph, when the hydraulic capacity of the subglacial drainage systems is consistently exceeded. However, we find that this behaviour is not replicated at sites in the upper ablation zone (>1000 m), where the period of summer melting is shorter, and the establishment of a hydraulic connection between the ice sheet surface and its bed is delayed, limiting the timeframe for velocity variations to occur.

In a warmer climate we expect seasonal melting of the GrIS surface to extend over a wider area, and to be more prolonged (Hanna et al., 2008). This makes it likely that volumes of meltwater sufficient to reach the ice–bed interface will accumulate further from the ice sheet margin and that the timing of meltwater input will occur earlier each summer (Krawczynski et al., 2009; Sundal et al., 2009). Our data therefore support the hypothesis that inland propagation of hydrologically-forced velocity variations will induce greater dynamic mass loss in land-terminating sections of the GrIS in a warmer climate, as patterns of hydro-dynamic behaviour observed in the lower ablation zone extend upglacier. These considerations provide a conceptual framework to understand the positive relationship between annual rates of surface ablation and percentage variations in annual ice velocity, and can be used to improve numerical simulations used for predicting the impact of hydrologically-forced variations in ice velocity on the future mass balance of the GrIS (Parizek, 2010).

Acknowledgements

We thank for financial support: UK Natural Environment Research Council (NERC, through a studentship to IB and grants to PN and DM),

Edinburgh University Moss Centenary Scholarship (IB). GPS equipment and training were provided by the NERC Geophysical Equipment Facility. MAK was funded by a RCUK Academic Fellowship. ERS SAR data, for the surface DEM, were provided by the European Space Agency VECTRA project (SP).

References

Alley, R., Dupont, T., Parizek, B., Anandakrishnan, S., 2005. Access of surface meltwater to beds of sub-freezing glaciers: preliminary insights. J. Glaciol. 40 (1), 8–14.
Anderson, R., Anderson, S., MacGregor, K., Waddington, E., O'Neel, S., Riihimaki, C., Loso, M., 2004. Strong feedbacks between hydrology and sliding of a small alpine glacier. J. Geophys. Res. 109.
Bamber, J., Layberry, R., Gogineni, S., 2001. A new ice thickness and bed data set for the Greenland ice sheet: I. measurement, data reduction, and errors. J. Geophys. Res.-Atmos. 106, 33.
Bartholomew, I., Nienow, P., Mair, D., Hubbard, A., King, M., Sole, A., 2010. Seasonal evolution of subglacial drainage and acceleration in a Greenland outlet glacier. Nat. Geosci. 3, 408–411.
Bartholomew, I., Nienow, P., Sole, A., Mair, D., Cowton, T., Palmer, S., Wadham, J., 2011. Supraglacial forcing of subglacial drainage in the ablation zone of the Greenland ice sheet. Geophys. Res. Lett 38. doi:10.1029/2011GL047063.
Bingham, R., Hubbard, A., Nienow, P., Sharp, M., 2008. An investigation into the mechanisms controlling seasonal speedup events at a High Arctic glacier. J. Geophys. Res. 113 (F2), F02006.
Box, J., Ski, K., 2007. Remote sounding of Greenland supraglacial melt lakes: implications for subglacial hydraulics. J. Glaciol. 53 (181), 257–265.
Catania, G.A., Neumann, T.A., 2010. Persistent englacial features in the Greenland Ice Sheet. Geophys. Res. Lett. 37 (2), L02501.
Chen, G., 1999. GPS kinematic positioning for the airborne laser altimetry at Long Valley, California. Ph.D. thesis, Massachusetts Institute of Technology.
Das, S., Joughin, I., Behn, M., Howat, I., King, M., Lizarralde, D., Bhatia, M., 2008. Fracture propagation to the base of the Greenland Ice Sheet during supraglacial lake drainage. Science 320 (5877), 778.
Gumley, L., Descloitres, J., Schmaltz, J., 2003. Creating Reprojected True Color Modis Images: a tutorial. University of Wisconsin, Madison.
Hall, D., Nghiem, S., Schaaf, C., DiGirolamo, N., Neumann, G., 2009a. Evaluation of surface and near-surface melt characteristics on the Greenland Ice Sheet using Modis and Quikscat data. J. Geophys. Res. 114, F04006.
Hall, D.K., Riggs, G., Salomonson, V., 2009b. MODIS/Aqua Snow Cover Daily L3 Global 500m Grid, V005. National Snow and Ice Data Center, Boulder, CO, USA. May to August.
Hanna, E., Huybrechts, P., Steffen, K., Cappelen, J., Huff, R., Shuman, C., Irvine-Fynn, T., Wise, S., Griffiths, M., 2008. Increased runoff from melt from the Greenland Ice Sheet: a response to global warming. J. Climate 21 (2), 331–341.
Hooke, R., Calla, P., Holmlund, P., Nilsson, M., Stroeven, A., 1989. A 3 year record of seasonal variations in surface velocity, Storglaciaren, Sweden. J. Glaciol. 35 (120), 235–247.
Iken, A., Bindschadler, R., 1986. Combined measurements of subglacial water pressure and surface velocity of Findelengletscher, Switzerland: conclusions about drainage system and sliding mechanism. J. Glaciol. 32, 110.
Iken, A., Rothlisberger, H., Flotron, A., Haeberli, W., 1983. The uplift of Unteraargletscher at the beginning of the melt season, a consequence of water storage at the bed? J. Glaciol. 29 (101), 28–47.
IPCC, 2007. Climate Change 2007: the Physical Science Basis: Contribution of Working Group I to the Fourth Assessment Report of the Intergovernmental Panel on Climate Change. Cambridge Univ Press.
Joughin, I., Das, S.B., King, M.A., Smith, B.E., Howat, I.M., Moon, T., 2008. Seasonal speedup along the western flank of the Greenland Ice Sheet. Science 320 (5877), 781–783.
Kamb, B., 1987. Glacier surge mechanism based on linked cavity configuration of the basal water conduit system. J. Geophys. Res. 92 (B9), 9083–9100.
Kamb, B., Engelhardt, H., Fahnestock, M., Humphrey, N., Meier, M., Stone, D., 1994. Mechanical and hydrologic basis for the rapid motion of a large tidewater glacier 2. Interpretation. J. Geophys. Res. 99 (B8), 15231.
King, M., 2004. Rigorous GPS data-processing strategies for glaciological applications. J. Glaciol. 50 (171), 601–607.
King, R., Bock, Y., 2006. Documentation for the GAMIT GPS Analysis Software, Version 10.3. Mass. Inst. of Technol., Cambridge.
Knap, W., Oerlemans, J., 1996. The surface albedo of the Greenland ice sheet: satellite-derived and in situ measurements in the Sondre Stromfjord area during the 1991 melt season. J. Glaciol. 42 (141), 364–674.
Krabill, W., 2010. IceBridge ATM L2 Icessn Elevation, Slope, and Roughness, [8.5.2010]. National Snow and Ice Data Center Digital Media, Boulder, Colorado USA.
Krawczynski, M., Behn, M., Das, S., Joughin, I., 2009. Constraints on the lake volume required for hydro-fracture through ice sheets. Geophys. Res. Lett. 36 (10), L10501.
Mair, D., Nienow, P., Willis, I., Sharp, M., 2001. Spatial patterns of glacier motion during a high-velocity event: Haut Glacier d'Arolla, Switzerland. J. Glaciol. 47 (156), 9–20.
Mair, D., Sharp, M., Willis, I., 2002. Evidence for basal cavity opening from analysis of surface uplift during a high-velocity event: Haut Glacier d'Arolla, Switzerland. J. Glaciol. 48 (161), 208–216.
McMillan, M., Nienow, P., Shepherd, A., Benham, T., Sole, A., 2007. Seasonal evolution of supra-glacial lakes on the Greenland Ice Sheet. Earth Planet. Sci. Lett. 262.
Nienow, P., Hubbard, B., 2006. Surface and englacial drainage of glaciers and ice sheets. Encyclopedia of Hydrological Sciences. John Wiley & Sons.
Nienow, P., Sharp, M., Willis, I., 1998. Seasonal changes in the morphology of the subglacial drainage system, Haut Glacier d'Arolla, Switzerland. Earth Surf. Proc. Land. 23 (9), 825–843.
Palmer, S., Shepherd, A., Nienow, P., Joughin, I., 2011. Seasonal speedup of the Greenland Ice Sheet linked to routing of surface water. Earth Planet. Sci. Lett. 302, 423–428.
Parizek, B., 2010. Glaciology: sliding to sea. Nat. Geosci. 3 (6), 385–386.
Parizek, B., Alley, R., 2004. Implications of increased Greenland surface melt under global-warming scenarios: ice-sheet simulations. Quaternary Sci. Rev. 23 (9–10), 1013–1027.
Phillips, T., Rajaram, H., Steffen, K., 2010. Cryo-hydrologic warming: a potential mechanism for rapid thermal response of ice sheets. Geophys. Res. Lett. 37 (20), L20503.
Pimentel, S., Flowers, G., 2010. A numerical study of hydrologically driven glacier dynamics and subglacial flooding. Proc. R. Soc. A Math. Phys. Eng. Sci. doi:10.1098/rspa.2010.0211.
Price, S., Payne, A., Catania, G., Neumann, T., 2008. Seasonal acceleration of inland ice via longitudinal coupling to marginal ice. J. Glaciol. 54 (185), 213–219.
Pritchard, H., Arthern, R., Vaughan, D., Edwards, L., 2009. Extensive dynamic thinning on the margins of the Greenland and Antarctic ice sheets. Nature 461 (7266), 971–975.
Röthlisberger, H., 1972. Water pressure in intra- and subglacial channels. J. Glaciol. 11 (62), 177–203.
Röthlisberger, H., Lang, H., 1987. Glacial hydrology. Glacio-Fluvial Sediment Transfer: an Alpine Perspective, pp. 207–274.
Schoof, C., 2010. Ice-sheet acceleration driven by melt supply variability. Nature 468 (7325), 803–806.
Shepherd, A., Hubbard, A., Nienow, P., King, M., McMillan, M., Joughin, I., 2009. Greenland Ice Sheet motion coupled with daily melting in late summer. Geophys. Res. Lett. 36 (1), L01501.
Stroeve, J., Box, J., Haran, T., 2006. Evaluation of the MODIS (MOD10A1) daily snow albedo product over the Greenland Ice Sheet. Remote Sens. Environ. 105 (2), 155–171.
Sundal, A., Shepherd, A., Nienow, P., Hanna, E., Palmer, S., Huybrechts, P., 2009. Evolution of supra-glacial lakes across the Greenland Ice Sheet. Remote Sens. Environ. 113, 2164–2171.
Sundal, A., Shepherd, A., Nienow, P., Hanna, E., Palmer, S., Huybrechts, P., 2011. Melt-induced speed-up of Greenland Ice Sheet offset by efficient subglacial drainage. Nature 469 (7331), 521–524.
Truffer, M., Harrison, W., March, R., 2005. Record negative glacier balances and low velocities during the 2004 heatwave in Alaska, USA: implications for the interpretation of observations by Zwally and others in Greenland. J. Glaciol. 51 (175), 663.
Van de Wal, R., Greuell, W., van den Broeke, M., Reijmer, C., Oerlemans, J., 2005. Surface mass-balance observations and automatic weather station data along a transect near Kangerlussuaq, West Greenland. Ann. Glaciol. 42, 311–316.
Van de Wal, R., Boot, W., Van den Broeke, M., Smeets, C., Reijmer, C., Donker, J., Oerlemans, J., 2008. Large and rapid melt-induced velocity changes in the ablation zone of the Greenland Ice Sheet. Science 321 (5885), 111.
Van der Veen, C., 2007. Fracture propagation as means of rapidly transferring surface meltwater to the base of glaciers. Geophys. Res. Lett. 34 (1), L01501.
Zwally, H., Abdalati, W., Herring, T., Larson, K., Saba, J., Steffen, K., 2002. Surface melt-induced acceleration of Greenland ice-sheet flow. Science 297 (5579), 218.

Appendix 4

Seasonal speedup of a Greenland marine-terminating outlet glacier forced by surface melt–induced changes in subglacial hydrology

A. J. Sole,[1,2] D. W. F. Mair,[2] P. W. Nienow,[1] I. D. Bartholomew,[1] M. A. King,[3] M. J. Burke,[4] and I. Joughin[5]

Received 9 December 2010; revised 12 May 2011; accepted 23 May 2011; published 23 August 2011.

[1] We present subdaily ice flow measurements at four GPS sites between 36 and 72 km from the margin of a marine-terminating Greenland outlet glacier spanning the 2009 melt season. Our data show that >35 km from the margin, seasonal and shorter–time scale ice flow variations are controlled by surface melt–induced changes in subglacial hydrology. Following the onset of melting at each site, ice motion increased above background for up to 2 months with resultant up-glacier migration of both the onset and peak of acceleration. Later in our survey, ice flow at all sites decreased to below background. Multiple 1 to 15 day speedups increased ice motion by up to 40% above background. These events were typically accompanied by uplift and coincided with enhanced surface melt or lake drainage. Our results indicate that the subglacial drainage system evolved through the season with efficient drainage extending to at least 48 km inland during the melt season. While we can explain our observations with reference to evolution of the glacier drainage system, the net effect of the summer speed variations on annual motion is small (~1%). This, in part, is because the speedups are compensated for by slowdowns beneath background associated with the establishment of an efficient subglacial drainage system. In addition, the speedups are less pronounced in comparison to land-terminating systems. Our results reveal similarities between the inland ice flow response of Greenland marine- and land-terminating outlet glaciers.

Citation: Sole, A. J., D. W. F. Mair, P. W. Nienow, I. D. Bartholomew, M. A. King, M. J. Burke, and I. Joughin (2011), Seasonal speedup of a Greenland marine-terminating outlet glacier forced by surface melt–induced changes in subglacial hydrology, *J. Geophys. Res.*, *116*, F03014, doi:10.1029/2010JF001948.

1. Introduction

[2] The Greenland Ice Sheet (GRIS), which contains sufficient water equivalent to raise global sea level by ~7 m [*Lemke et al.*, 2007], has experienced increased rates of mass loss over the last decade due to increased surface melt and runoff [*Tedesco*, 2007; *Tedesco et al.*, 2008; *van den Broeke et al.*, 2009] and accelerated ice discharge [*Rignot and Kanagaratnam*, 2006; *Rignot et al.*, 2008; *Pritchard et al.*, 2009]. Approximately half the current mass loss is through melt and runoff, while the remainder is due to ice discharge to the surrounding oceans [*Shepherd and Wingham*, 2007; *van den Broeke et al.*, 2009]. Two principal mechanisms by which climate could influence ice discharge have been proposed: (1) ice geometry and thickness changes at the calving fronts of marine-terminating glaciers reduce resistive forces, resulting in glacier acceleration and thinning or "drawdown" [*Thomas*, 2004; *Howat et al.*, 2005; *Luckman and Murray*, 2005; *Howat et al.*, 2007; *Nick et al.*, 2009], and (2) increased surface melt reaches the ice sheet bed locally, [*Das et al.*, 2008] enhancing basal sliding and lowering the ice sheet surface, exposing it to higher melt rates [*Zwally et al.*, 2002]. Although both effects have been modeled for individual glacier basins [e.g., *Price et al.*, 2008; *Pimentel and Flowers*, 2010; *Nick et al.*, 2009], their relative importance for the mass balance of the whole GRIS is at present unknown because continental-scale ice sheet models do not include the necessary physics to represent them [e.g., *Parizek and Alley*, 2004; *Huybrechts et al.*, 2004].

[3] The drainage of surface lakes to the bed via hydrofracture [*van der Veen*, 2007] enables subsequent rapid routing of surface melt to the glacier base [*Shepherd et al.*, 2009] and causes short-lived ice acceleration [*Das et al.*, 2008]. Acceleration is driven by a reduction in effective pressure, which promotes basal sliding at times when the

[1]School of Geosciences, University of Edinburgh, Edinburgh, UK.
[2]School of Geosciences, University of Aberdeen, Aberdeen, UK.
[3]School of Civil Engineering and Geosciences, Newcastle University, Newcastle upon Tyne, UK.
[4]Department of Geography, Simon Fraser University, Burnaby, British Columbia, Canada.
[5]Applied Physics Laboratory, University of Washington, Seattle, Washington, USA.

0148-0227/11/2010JF001948

input of surface meltwater to the bed exceeds the capacity of the subglacial drainage system [*Iken*, 1981; *Iken and Bindschadler*, 1986; *Kamb*, 1987; *Meier et al.*, 1994; *Anderson et al.*, 2004]. Following the establishment of local surface to bed conduits, land-terminating margins have been shown to respond rapidly to seasonal [*Bartholomew et al.*, 2010] and diurnal [*Shepherd et al.*, 2009] variations in surface meltwater generation with the net effect of increasing annual ice speed [*Joughin et al.*, 2008a; *Bartholomew et al.*, 2010]. A 17 year record from west Greenland found a weak negative correlation between ice speed and melting [*van de Wal et al.*, 2008], suggesting that in certain situations, other processes such as changing ice geometry might eclipse the importance of basal sliding. Inland expansion of the region experiencing melting, expected in a warming climate, will increase the area over which seasonal acceleration occurs and, thus, its potential impact on annual ice flux [*Sundal et al.*, 2009]. A positive relationship between surface melting and ice speed is important because it would initiate a positive feedback whereby in a warmer climate ice would flow increasingly quickly into the lower-elevation ablation area, thereby experiencing higher melt rates.

[4] In contrast, marine-terminating GRIS outlet glaciers have generally displayed less sensitivity to variations in meltwater forcing [*Echelmeyer and Harrison*, 1990; *Joughin et al.*, 2008a]. Instead, seasonal flow variations at such glaciers have been explained by changes in calving rate due to the breakup of the seasonal ice mélange (a mixture of fjord sea ice and recently calved ice) [*Joughin et al.*, 2008b; *Amundson et al.*, 2010] or the ungrounding of ice near the terminus [*Howat et al.*, 2007]. However, most observations of seasonal flow variations on GRIS marine-terminating glaciers come from close to their termini (<30 km) where calving is very likely to be the principal control on ice flow [*Joughin et al.*, 2008b]. On the other hand, a "minisurge" of Ryder Gletscher in northern Greenland, which experienced a 400% speedup over a 7 week period toward the end of the 1995 melt season, was likely related to changes in subglacial water pressure caused by the drainage of several large supraglacial lakes [*Joughin et al.*, 1996]. Similarly, *Andersen et al.* [2010] found a correlation (with a 1 day lag) between modeled surface melting and ice speed at Helheim Gletscher, east Greenland. The relationship was strongest for the heavily crevassed terminus region, but variations in flow were small compared to those attributed to calving front changes. *Howat et al.* [2010] found that close to the calving fronts of several marine-terminating outlet glaciers in west Greenland, ice speed decreased by 40% to 60% following the drainage of surface lakes in midsummer. Furthermore, subglacial hydrology has been shown to exert a strong control on the dynamics of large marine-terminating glaciers in Alaska [e.g., *Kamb et al.*, 1994; *O'Neel et al.*, 2001]. The relative importance of calving and subglacial hydrology on controlling ice flow of GRIS marine-terminating glaciers farther inland from their termini is not known. There is, therefore, a clear need to include both empirically constrained representations of basal hydrology and the long- and short-term effects of ice front changes and their transmission inland into models which aim to predict the future contribution of the GRIS to global sea level rise.

[5] Here we present subdaily ice flow measurements from Global Positioning System (GPS) sites located between 36 and 72 km from the calving front of a major marine-terminating GRIS outlet glacier spanning the 2009 melt season (May to August). These data show that far into the ice sheet interior, seasonal and shorter-term variations in ice flow are principally controlled by surface melt–induced changes in subglacial hydrology rather than by changes at the calving front.

2. Field Site and Methods

[6] Kangiata Nunata Sermia (KNS) is a large tidewater outlet glacier which terminates at the head of the ~175 km long Nuup Kangerlua Fjord in southwest Greenland at ~64.30°N (Figure 1a). The glacier, which flows at ~6000 m yr^{-1} at its calving front [*Joughin et al.*, 2010], drains an area of ~31,400 km^2 (see Figure 1c) toward a ~4.5 km wide calving front. KNS accelerated by 27% between 2000 and 2005 and retreated by 580 m between 2006 and 2007 [*Rignot and Kanagaratnam*, 2006; *Moon and Joughin*, 2008; *Joughin et al.*, 2010]. Surface lowering rates exceeded 10 m yr^{-1} between 1998 and 2001 within 10 km of the glacier's calving front and decreased to approximately zero 30 km inland [*Thomas et al.*, 2009] (Figure 1b).

[7] On 11 May (day 131), prior to the onset of runoff in 2009, four dual-frequency GPS receivers ("rovers") were deployed on a single flow line of KNS at sites 36 km (KNS1), 48 km (KNS2), 59 km (KNS3), and 72 km (KNS4) from the KNS calving front (Figure 1a and Table 1). Extensive crevassing precluded deploying GPS receivers closer to the terminus. Each on-ice GPS antenna was mounted on a support pole drilled into the ice (to 5 m depth for KNS1 and KNS2 and to 3 m depth for KNS3 and KNS4), which froze in place subsequently, providing measurements of ice motion that were independent of ablation. None of the poles tilted significantly during the survey period. A fifth GPS receiver acted as a reference station and was installed on bedrock overlooking the calving front of KNS. The maximum baseline between reference station and rover was ~70 km. The GPS data were sampled and recorded at 10 s intervals, with a continuous record obtained from 11 May (day 131) to 13 August (day 225) for KNS1 and to 23 August (day 235) for KNS2, KNS3, and KNS4. The data were processed in Track v1.21 [*Chen*, 1998; *Herring et al.*, 2010] relative to the off-ice reference station using a kinematic approach [see *King*, 2004] that utilized International Global Navigation Satellite Systems Service (IGS) precise orbits and loosely constrained site motion to be no more than 0.02 m per epoch. We estimated relative (base to rover) tropospheric zenith delay parameters which, if not estimated, could result in biased height time series. Site coordinates were produced for each measurement epoch, and these were then rotated to along- and across-flow directions, from which speeds were computed. Daily horizontal speeds were calculated by taking the difference of 1 h mean positions every 24 h. Uncertainties associated with mean hourly positioning are <0.5 cm in the horizontal and <1 cm in the vertical, corresponding to annual horizontal speed uncertainties of <3.7 m yr^{-1}. The determined vertical positions were detrended by removing a linear component assumed to represent bed-parallel motion to give residual vertical displacement, which includes horizontal (and ver-

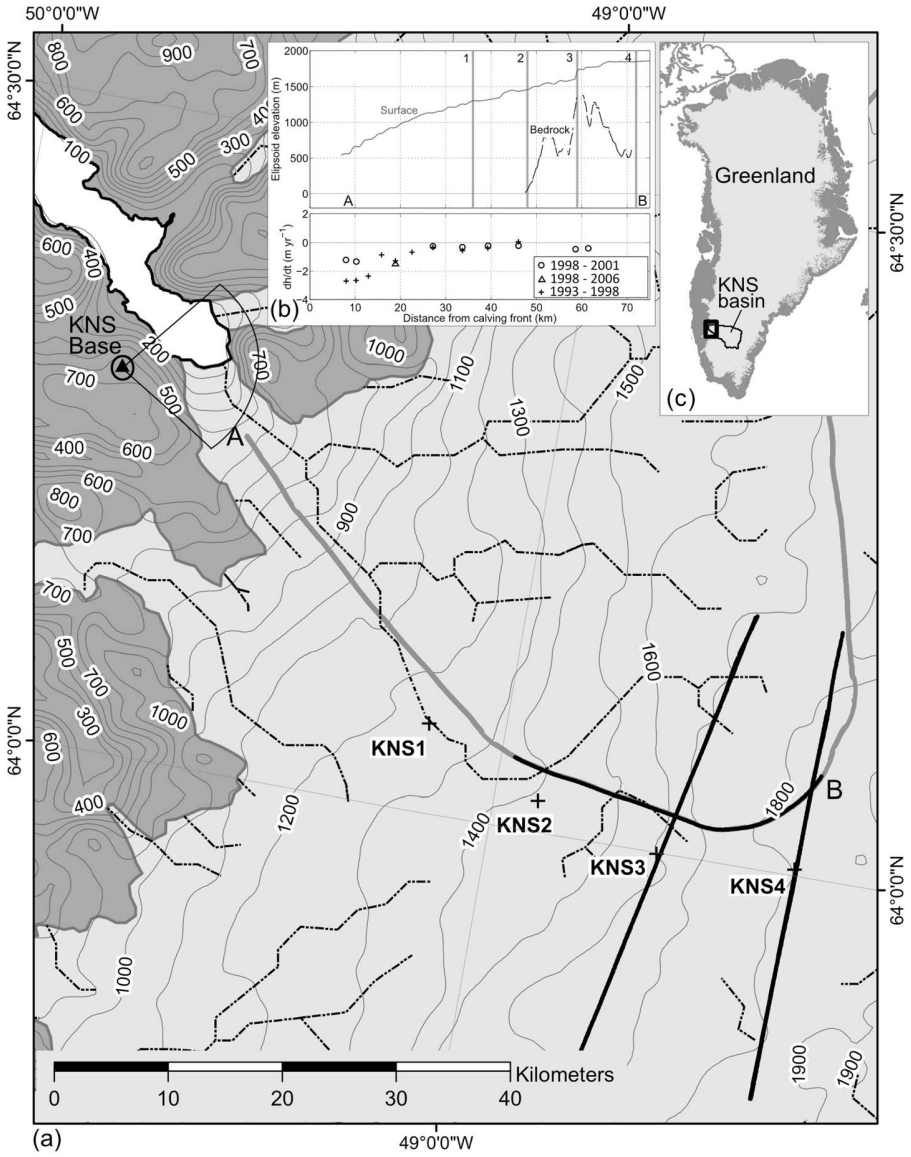

Figure 1. (a) Location of KNS and the GPS transect. GPS sites KNS1–KNS4 are represented as black crosses. Bold black lines show airborne radio echo sounding transects of bed topography, and the bold gray line shows the laser altimetry flight line for ice surface topography. Contours show ice sheet elevation above the geoid (m), and dot-dashed lines represent surface (and approximate subglacial) hydrological pathways. The location of the off-ice reference station (KNS Base) and time-lapse camera approximate field of view are also shown. (b) Bed and surface topography for KNS centerline (A–B) as well as surface elevation change rates for the along-flow flight line shown in Figure 1. (c) The location of the KNS surface drainage basin.

tical) strain rate as well as bed separation and till dilation [*Howat et al.*, 2008].

[8] At each GPS site, snow depth was measured before the onset of runoff, and mean surface lowering rate and air temperature were measured every 15 min using a Campbell SR50A ultrasonic depth gauge and a Campbell T107 shielded temperature sensor, respectively. The surface lowering data, combined with appropriate densities of snow and firn facies [*Parry et al.*, 2007], were used to estimate the potential water input to the subglacial drainage system. We

Table 1. GPS Site Characteristics

	Distance From Calving Front (km)	Elevation Above Geoid (m)	Approximate Ice Thickness (m)
KNS1	36	1282	unknown
KNS2	48	1443	1500
KNS3	59	1648	350
KNS4	72	1840	1200

Figure 2. Time-lapse images of (a) early season with fjord ice mélange intact, 12 May, day 132; (b) the breakup of seasonal fjord ice mélange, 4 June, day 155; (c) when a small ice-free area and turbid plume first became visible in the fjord at the KNS terminus, 11 July, day 192; and (d) when the ice-free area and turbid plume expanded significantly, 14 July, day 195.

acknowledge that initial snowmelt is likely to refreeze in the snowpack [*Pfeffer et al.*, 1991] but assume that the majority of measured surface lowering represents melting ice which does produce runoff. A time-lapse camera system was installed adjacent to the off-ice reference station with a field of view encompassing the calving terminus of KNS (Figure 1a) and obtained hourly photographs over the entire melt season (Figure 2). The resulting photographs allowed a qualitative analysis of water outflow from the glacier system [e.g., *O'Neel et al.*, 2001] and the timing of the ice mélange breakup.

[9] Supraglacial lake evolution was analyzed using Moderate Resolution Imaging Spectroradiometer (MODIS) level 1B calibrated radiances (MOD02QKM) of the catchment, which were corrected for atmospheric effects and orthorectified using the *Gumley et al.* [2007] method after *Sundal et al.* [2009]. Forty-seven MODIS images were used spanning the period 30 April to 27 August, representing all days when lake identification was not impeded by cloud cover. Band 3 data were upsampled from 500 to 250 m resolution using a resolution-sharpening algorithm [*Gumley et al.*, 2007] which bilinearly interpolates band 3 to the equivalent of 250 m resolution [*Sundal et al.*, 2009]. Supraglacial lakes were identified using membership functions of the ratio of band 1 to band 3 and band 1 radiances (band 1/(band 1 + band 3)) [*Sundal et al.*, 2009], and their areas (A) were subsequently calculated. Comparison between areas for 45 lakes automatically identified on three 250 m pixel size MODIS images and manually digitized on three concurrent 14 m pixel size Landsat images (days 173, 198, and 230) gives a correlation of 0.84 ($p < 0.05$) with a 1σ uncertainty (A_{err}) of 0.2 km^2 per lake. This is comparable

with the 1σ uncertainty of 0.22 km^2 per lake from a comparison of MODIS-derived and Advanced Spaceborne Thermal Emission and Reflection Radiometer (ASTER)–derived (15 m pixel size) lake areas from a similar region of the ice sheet [*Sundal et al.*, 2009]. Mean lake depths (D) were estimated from their relationship with band 1 reflectance after *Box and Ski* [2007],

$$D = \frac{0.716738}{(R + 0.036304)} + 0.701691, \quad (1)$$

where R is band 1 reflectance. This relationship has 1σ uncertainty D_{err} of 0.86 m [*Box and Ski*, 2007]. Lake volume V was simply estimated by multiplying D by A. The uncertainty V_{err} associated with estimating V for a single lake is therefore

$$V_{\mathrm{err}} = \left[\sqrt{\left(\frac{D_{\mathrm{err}}}{D}\right)^2 + \left(\frac{A_{\mathrm{err}}}{A}\right)^2}\right] V. \quad (2)$$

[10] We used the ASTER Global Digital Elevation Model (GDEM, http://www.ersdac.or.jp/GDEM/E/2.html) combined with the *Bamber et al.* [2001] 1 km resolution Digital Elevation Model (DEM, which has an accuracy of −0.33 ± 6.97 m for slopes 0.0° to 1°) farther inland to estimate the extent of KNS's surface drainage basin. Water at the ice sheet base is expected to flow normal to equipotential contours which, because of the density difference between water and ice, can be expected to be 11 times more sensitive to ice surface slope than bedrock slope [*Shreve*, 1972]. Despite this, it is possible that at several locations along our transect (see Figure 1b), bed topography is sufficiently steep to control subglacial water routing. However, there are no ice-marginal rivers large enough to evacuate runoff from the KNS basin visible in satellite imagery of the KNS margin, and so we assume the majority of runoff is injected directly into the Nuup Kangerlua Fjord. Therefore, in the absence of more extensive or accurate bed data, we also used the surface topography data to delineate the extent and likely flow paths of theoretical subglacial drainage (Figure 1).

3. Results

3.1. Horizontal Motion

[11] At the start of our survey period all the sites were flowing at steady background speeds (Figures 3a–3d). In the absence of GPS data spanning a winter season, background speed for each site was estimated by taking a mean early season value, prior to the start of melting and the breakup of the ice mélange. Following the onset of melting at each site, ice flow rate increased above background with a resultant up-glacier evolution of both the onset and peak of speed enhancement (Figures 3a–3d). Seasonal acceleration at KNS1, KNS2, KNS3, and KNS4 began on approximately days 156, 183, 190, and 198, respectively. Ice flow rate reached a maximum at KNS1 on day 191 (535 m yr^{-1}, 40% above background), at KNS2 on day 203 (271 m yr^{-1}, 25% above background), and at both KNS3 and KNS4 on day 213 (200 and 133 m yr^{-1}, 15% and 36% above background speed, respectively). Initially, at each site the acceleration was small (giving speeds generally <10% above background) but increased episodically toward a peak. After this, speeds varied considerably but gradually returned to values below or similar to background.

[12] Superimposed on the seasonal ice flow pattern were multiple short-lived speedup events lasting 1 to 15 days, some of which occurred at multiple sites. For the remainder of the paper, we refer to six of the more significant individual speedup events as S1 (days 156–170), S2 (days 177–184), S3 (days 189–195), S4 (days 201–204), S5 (days 212–214), and S6 (days 220–223) since these are synchronous across multiple sites (Figures 3a–3d). For example, during S3, the largest of these events at KNS1, speed increased by 33% of background (from 408 to 535 m yr^{-1}) in 3 days. At the same time at KNS2, speed increased from 221 to 259 m yr^{-1} (20%), while KNS3 accelerated from 174 to 183 m yr^{-1} (6%). There was no discernible concurrent speedup at KNS4.

[13] Following S4 at KNS1, ice flow decreased to consistently >6% below background for 9 days, while at KNS2 speed decreased to >1% below background for 5 days. This period of below-background flow was interrupted at both sites by S5, during which speed increased to 2% and 4% above background at KNS1 and KNS2, respectively. Immediately after S6, speeds at KNS2 decreased steadily, reaching a minimum of ~6% below background after 11 days, while at KNS1, speed decreased to ~10% below background over 3 days. A similar pattern of speedup followed by slowdown to below background speeds was also observed at KNS3 and KNS4. By the end of our survey, speeds at both KNS1 and KNS2 were ~5% below background, while at KNS3 and KNS4 speeds were 1% and 2% below their background values, respectively.

3.2. Vertical Motion

[14] At KNS1, the ice surface was raised by between 0.025 ± 0.01 and 0.140 ± 0.01 m coincident with these short-lived speedup events. During each event at KNS1, maximum horizontal speed coincided with maximum rate of vertical uplift rather than peak vertical displacement (e.g., day 191, Figure 3a). Indeed, for the whole survey period, horizontal ice speed is more strongly correlated with rate of vertical displacement ($r = 0.72$ and $p < 0.05$) than it is with vertical displacement itself ($r = 0.42$ and $p > 0.05$). After each speedup event, the ice surface subsided, at times (e.g., days 173–178 and days 205–212) to levels below those immediately prior to the speedup. The rate of subsidence was generally less than the rate of uplift (e.g., uplift of ~0.06 cm d^{-1} from days 155–160 and subsidence of ~0.02 cm d^{-1} from days 160–178). Sites KNS2–KNS4 showed smaller magnitude variations in vertical position, but maximum horizontal speed did not always coincide with maximum rate of vertical uplift (Figures 3b–3d).

3.3. Calving Front Changes

[15] The breakup of the seasonal ice mélange occurred on day 155 (vertical solid black line in Figures 3a–3f; compare Figures 2a and 2c), a day before the onset of seasonal acceleration at KNS1. A turbid plume first appeared in the time-lapse photographs on day 192 (vertical black dotted line in Figures 3a–3f), 1 day after maximum speed at KNS1. The plume grew dramatically on day 195 (vertical black dashed line in Figures 3a–3f), flushing remnant sea ice and

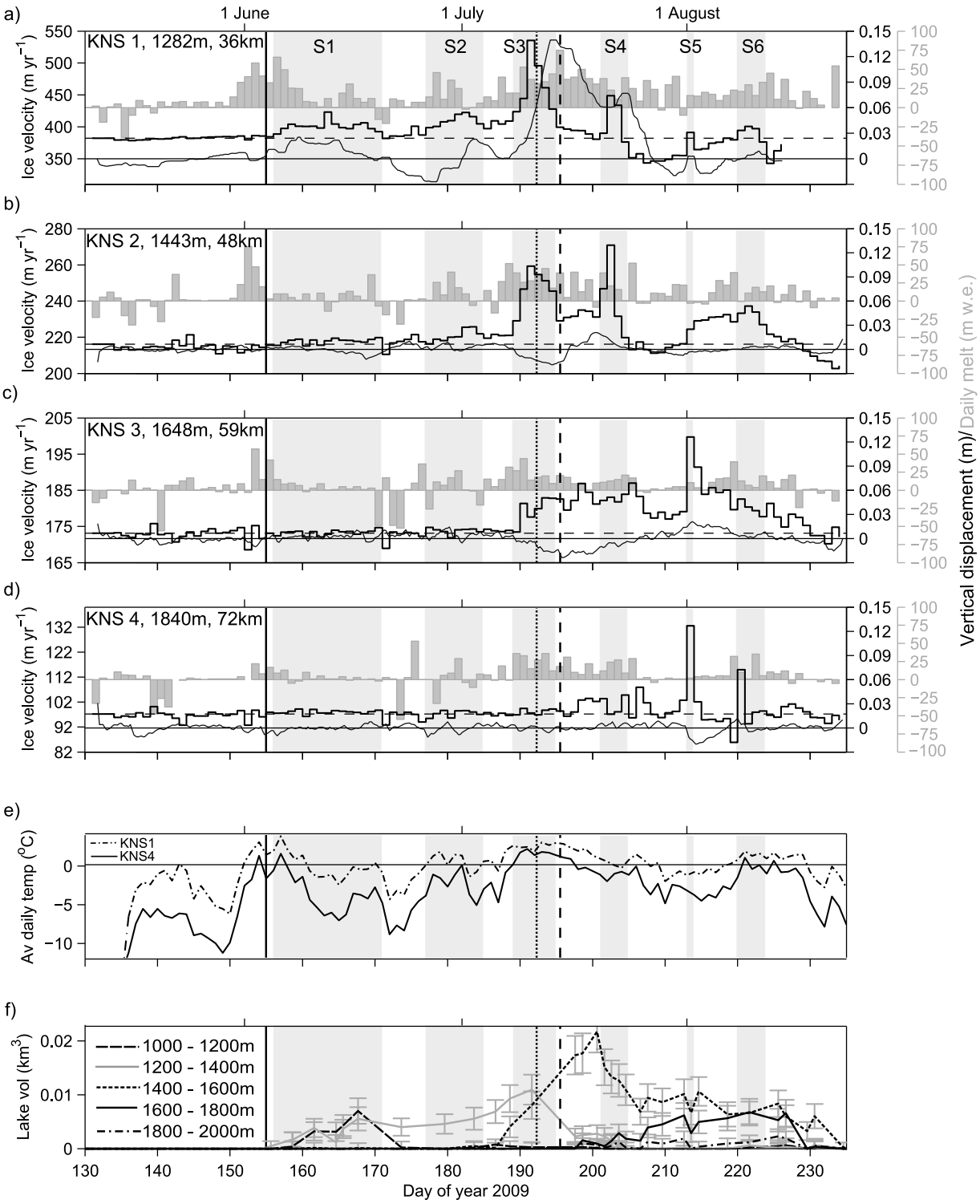

Figure 3. (a–d) Daily horizontal speed (stepped line), 6 hourly vertical displacement (smooth line), and daily water equivalent ice melt (gray bars) at KNS1–KNS4. The horizontal dashed lines represent respective background speeds, and shaded light gray areas display periods categorized as short-lived speedup events (S1–S6). (e) Daily mean temperature for KNS1 and KNS4. (f) Lake volume by 200 m elevation band derived from MODIS imagery and the relationship between radiance and lake depth from *Box and Ski* [2007]. The solid vertical black line in each plot shows the timing of the breakup of seasonal fjord ice mélange (day 155, 4 June), the dotted black vertical line indicates when a small ice-free area and turbid plume first became visible in the fjord at the KNS terminus (day 192, 11 July), and the dashed vertical black line shows when the ice-free area and turbid plume expanded significantly (day 195, 14 July).

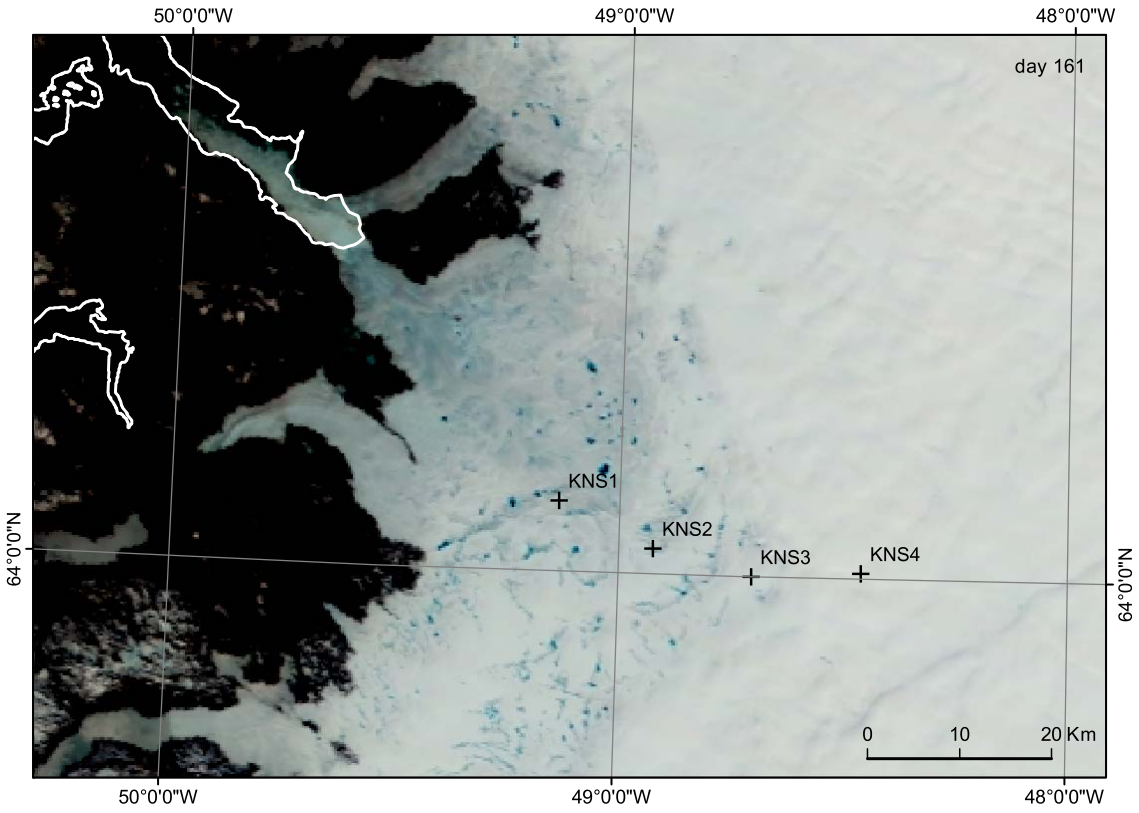

Figure 4. Example of a MODIS image showing surface lakes (dark blue on-ice patches) on 10 June, day 161.

recently calved glacier ice down fjord (Figure 2d). The plume persisted until day 209, after which it returned only sporadically. According to the time-lapse images, after the initial mélange breakup the calving front remained in approximately the same position for the entirety of our survey period.

3.4. Supraglacial Lake Drainage

[16] Surface lakes are clearly visible in MODIS imagery (e.g., Figure 4) of KNS from day 155, 2 days before the start of S1. MODIS imagery has a horizontal resolution of 0.25 by 0.25 km, and so all of the visible lakes (assuming a conical bathymetry [*Krawczynski et al.*, 2009] with a diameter-to-depth aspect ratio of 100:1 [e.g., *Sneed and Hamilton*, 2007; *Krawczynski et al.*, 2009]) contain sufficient water ($\sim 2 \times 10^{-5}$ km^3) to force hydrofracture through 1000 m of ice [*Krawczynski et al.*, 2009]. Figure 3f shows a time series of supraglacial lake volume for 200 m elevation bands within the KNS catchment with error bars for the 1σ uncertainty. The region with the greatest lake volume migrates up glacier through the season. The expansion of lake area within each elevation band is controlled by surface melting. Rapid decrease in lake area corresponds to lake drainage, probably initiated by hydrofracturing once sufficient water has gathered [*Krawczynski et al.*, 2009]. The largest of these drainage events within each elevation band coincide with the largest accelerations at the respective GPS sites but also affect adjacent sites. For example, the biggest 1200–1400 m lake drainage event (days 192–197) coincided with the biggest speedup (S3) at KNS1 and with S3 at KNS2. Similarly, the biggest 1400–1600 m lake drainage event (days 201–207) coincided with the biggest speedup (S4) at KNS2 and also with S4 at KNS1.

[17] Several lakes drained between days 201 and 205 coinciding with S4, the peak ice speed at KNS2. According to the surface (and by extension, bed) flow routing (dot-dashed lines in Figure 1a), these lakes are <8 km upstream of KNS2. The first lake (L1 at ~1500 m) drained over a 3 day period from day 200 to day 203 (Figures 5b and 5c). A second lake (L2 at ~1300 m) drained from day 201 to day 206, and several other up-glacier lakes (L3–L7 between ~1450 and 1650 m) decreased in size between days 204 and 207 but did not completely empty (Figure 5a). A time series of the combined discharge from L1 and L2 (and subsequent surface melt from these lake drainage basins) was estimated by linearly interpolating the reductions in MODIS-derived [*Box and Ski*, 2007] L1 and L2 volume through time (Figures 5b and 5c). The initiation of these lake drainages preceded the onset of S4 at KNS1 and KNS2 by approximately 24 h.

4. Discussion

[18] The synchroneity of the short-lived speedups at different sites suggests a common forcing which acts over length scales of at least ~11 km. There are two mechanisms that could be responsible for the observed synchronous behavior: (1) changes at the calving front could propagate

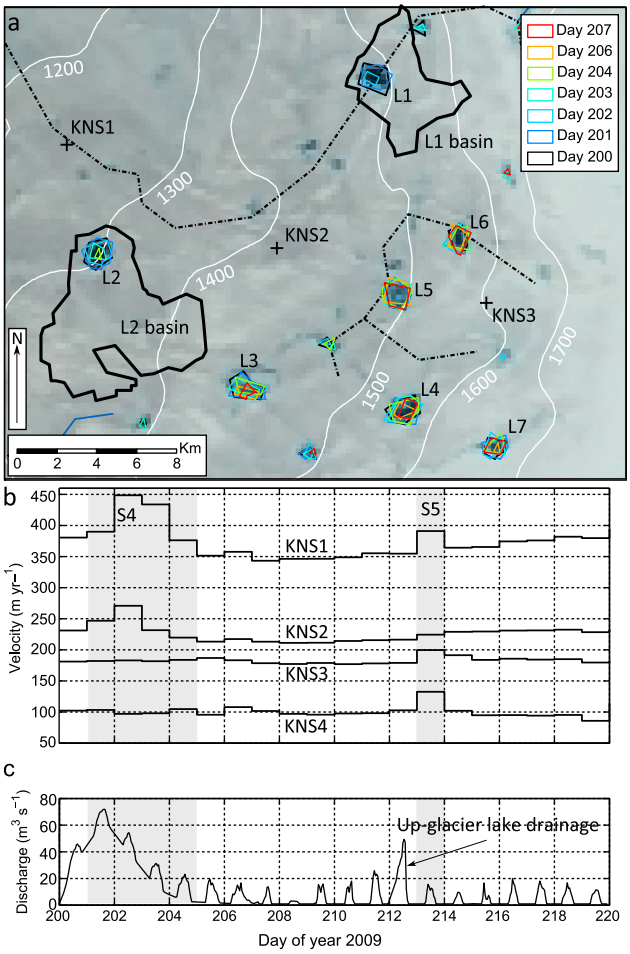

Figure 5. (a) Changes in lake area during S4. Dot-dashed black lines represent supraglacial or subglacial flow pathways, thick black lines delineate L1 and L2 drainage basins, and colored polygons show daily lake area. The GPS sites are marked with black crosses. (b) Daily horizontal surface speed and (c) combined discharge of lakes L1 and L2 and subsequent surface melt from the L1 and L2 drainage basins (delineated by the vertical black line). Shaded light gray areas display periods categorized as short-lived speedup events (S4 and S5).

up glacier via longitudinal stresses [*Nick et al.*, 2009] or (2) local changes in subglacial water pressure may initiate speed variations as observed on land-terminating margins of the GRIS [*Bartholomew et al.*, 2010].

4.1. Mechanism for Speed Variations

[19] If the observed speedups had been directly caused by changes at the calving front, we would expect the magnitude of the ice speed response to each event to decrease up glacier [*Nick et al.*, 2009] and the ice surface at KNS1 to have lowered as the ice was stretched by positive longitudinal strain rates [*Thomas*, 2004]. To examine the surface lowering which could be expected at KNS1 from an event such as S3, we obtained the speed at a point ~16 km down glacier from KNS1 prior to and after S3 from interferometric synthetic aperture radar (InSAR) data [*Joughin et al.*, 2010]. Our estimated acceleration between this point and KNS2 (a distance of ~28 km) would have produced additional longitudinal strain rates of ~+0.023 yr^{-1} at KNS1. Mean ice thickness for this region is not known, but on the basis of ice thickness for similar-sized marine-terminating outlet glaciers (e.g., ~600 m for Kangerdlugssuaq Gletscher near terminus and ~1900 m for ~30 km inland (using Center for Remote Sensing of Ice Sheets bed elevation data, https://www.cresis.ku.edu/data/greenland, and the 1 km Bamber GRIS surface DEM [*Bamber et al.*, 2001])), we employ a value of 1200 m. Using the above values of strain and ice thickness, ignoring any changes in ice thickness advection, and assuming that the cause of S3 originated at the calving front, we estimate that lowering rates at KNS1 would be approximately 0.13 m d^{-1} (0.054 m d^{-1} for 500 m ice thickness and 0.16 m d^{-1} for 1500 m ice thickness) [*Thomas*, 2004]. On the contrary, we observed synchronous vertical *uplift* at KNS1 during S3 of ~+0.03 m d^{-1} (Figure 3a), indicating that the speedup did not originate at the calving front.

[20] Uplift was also recorded at KNS1 during S2–S6, none of which coincided with major changes (i.e., visible in the time-lapse photographs) at the calving terminus. Furthermore, if the speedups measured across sites KNS1–KNS4 were all caused by perturbations at the calving front, we would expect KNS1 to display the greatest ice flow response to each event and the relative magnitude of each acceleration to decrease with distance up glacier [*Nick et al.*, 2009]. Instead, our data show that the maximum relative acceleration during each event occurred at sites farther up glacier as the melt season progressed, indicating a local cause. Although the arrival of the turbid plume at the terminus could also have affected the glacier's force balance by removing the ice mélange (which may inhibit calving [*Amundson et al.*, 2010]), it occurred after S3, suggesting that it was a consequence rather than a cause of the speedup and lake drainage observed farther up glacier. This indicates that there was no coupling between the terminus and KNS1 (36 km apart) at this stage of the melt season [cf. *Kamb and Echelmeyer*, 1986] and that the breakup of the ice mélange had little effect on ice flow. This lack of coupling between the terminus and ice ~36 km up glacier is in line with the observations of *Thomas et al.* [2009], who reported dynamic thinning of >10 m yr^{-1} between 1998 and 2001 within 10 km of the terminus decreasing to zero ~30 km inland.

[21] During each speedup event at KNS1, maximum horizontal speed coincided with maximum uplift rate. Such behavior is consistent with enhanced basal sliding as a consequence of high basal water pressures [*Iken et al.*, 1983; *Iken*, 1981]. The asymmetrical shape of the uplift and subsidence (steep uplift and more gradual subsidence) is also indicative of subglacial water pressure forcing and has been attributed to the (relatively) slow release of basal water trapped in cavities following the cessation of increased surface meltwater input [*Iken et al.*, 1983]. This "hydraulic jacking" has been well documented on temperate glaciers [*Iken et al.*, 1983; *Iken*, 1981; *Iken and Bindschadler*, 1986; *Mair et al.*, 2003] and has also been observed previously on the GRIS [*Zwally et al.*, 2002; *Das et al.*, 2008; *Shepherd et al.*, 2009; *Bartholomew et al.*, 2010].

[22] Further evidence for local hydrological forcing at KNS1 comes from temporal patterns of measured surface melt and lake drainage discharge (which we use as a proxy for water input to the subglacial system). Although surface

meltwater will initially percolate and refreeze in the snowpack, eventually the snowpack temperature reaches the pressure melting point and becomes saturated [*Pfeffer et al.*, 1991]. Once this occurs, surface meltwater can rapidly access the ice bed via existing moulins [*Catania and Neumann*, 2010] and crevasses and influence basal sliding. This is likely to have been the cause of S1 and S2 at KNS1 as both followed several days of above-freezing temperatures and consequent increased melt (Figures 3a–3e). The coincidence of other speedups (e.g., S3 and S4) with reductions in lake volume is strong evidence that they were caused by these lakes draining to the glacier bed. It is likely that these large volumes of meltwater were initially input to an inefficient distributed drainage system, creating episodes of high subglacial water pressure, hydraulic jacking, and enhanced basal sliding. Expansion of the efficient channelized subglacial system therefore follows up-glacier development of surface melting, lake formation, and hydrofracture and proceeds in a series of steps as new ice-bed connections are established [*Nienow et al.*, 1998].

4.2. Coupling of Ice Flow Over ~10 km

[23] At KNS2–KNS4 we observed speedups with different simultaneous patterns of surface uplift from those observed at KNS1 (Figures 3b–3d). For example, during S3 at KNS1 we observed vertical uplift of 0.14 m, while at KNS2 the ice surface lowered simultaneously by ~0.02 m. Indeed, we estimate surface lowering at KNS2 resulting from the relative accelerations at KNS1 and KNS3 during S3 (i.e., due to the additional horizontal strain imposed by the speedup event) to be ~0.02 m d^{-1}. Theoretical and field studies show that the stress coupling length, L, should range between 4 and 10 times the ice thickness (approximately 4 to >10 km along our transect) depending on glacier geometry and bed topography [*Balise and Raymond*, 1985; *Kamb and Echelmeyer*, 1986]. L is therefore comparable to the distance between our GPS sites, indicating that speedups could have resulted from longitudinal or lateral coupling to adjacent hydraulically induced faster flowing ice [*Price et al.*, 2008]. We note, however, that although S2 is observed at KNS2, S1 is not, and neither S1 nor S2 are measured at KNS3. The former suggests that longitudinal stress coupling over ~10 km is not possible until the bed is primed, for example, once basal water pressure has reached a critical proportion of overburden pressure [*Pimentel and Flowers*, 2010], while the latter indicates that sites ~20 km apart are not stress coupled.

[24] The coincidence of S4 at KNS1 and KNS2 with drainage of nearby lakes (Figure 5) suggests that this speedup was due to local coupling to areas of hydromechanical forcing. Simple modeling of subglacial channel expansion and closure (following *Spring and Hutter* [1981]; see auxiliary material)[1] suggests that the drainage of L1 and L2 (Figures 5b and 5c) would be sufficient to open large (~18 m^2) conduits at the bed and that water pressures within these channels would exceed ice overburden pressure for longer than 24 h. Thick overlying ice could reduce conduit diameter in less than a day, but the conduits would remain open because of surface melt–derived discharge assumed to reach the bed via moulins at the lake drainage sites [e.g., *Das et al.*, 2008]. A subsequent increase in discharge to the ice bed on day 213 (Figures 5b and 5c), caused by the drainage of several lakes between 1600 and 2000 m, would have been sufficient to increase basal water pressures above ice overburden pressure once again for a further 12 h during S5. This simple modeling approach produces qualitatively similar results to other simulations of supraglacial lake drainage such as those of *Pimentel and Flowers* [2010]. Supraglacial lake development is therefore important, because it provides sufficient water both to force hydrofracture through thick cold ice and to open efficient channels at the ice bed, forming a rapid surface-bed route for subsequent surface meltwater.

4.3. Slowdown Events

[25] At KNS1, following S3 and S4, horizontal speed decreased to values consistently lower than those immediately prior to the speedups. For S4 these values were also >6% below background speed. These "extra slowdowns" [*Meier et al.*, 1994] are probably the consequence of enlargement of the basal water conduits following increased surface water input. Less significant extra slowdowns are also observed at land-terminating margins [e.g., *Bartholomew et al.*, 2010]. Larger channels subsequently require greater water flux to become pressurized so that the basal resistance required to balance the driving stress can be achieved at lower speeds [*Meier et al.*, 1994]. The extra slowdowns that follow many of the later speedup events and the late season below-background speeds at each site therefore suggest that toward the end of our survey period an efficient subglacial drainage system had developed at distances of up to 48 km from the terminus [*Mair et al.*, 2002; *Anderson et al.*, 2004]. This reasoning is consistent with the findings of *Howat et al.* [2010], although slowdowns at our sites are relatively smaller, between 1% and 10% as opposed to 40% and 60%. We find that although establishment of an efficient drainage system reduces the sensitivity of the subglacial hydrological system to further meltwater inputs, it does not preclude subsequent speedups. This is demonstrated by the occurrence of S5 and S6 at KNS1 despite preceding extra slowdowns. The amount by which sensitivity is reduced depends on the balance between channel closure rates and basal water flux following channelization [*Pimentel and Flowers*, 2010; *Schoof*, 2010].

[26] The emergence of the large turbid fjord plume at the KNS calving front on day 195, indicative of the arrival of an efficient channelized subglacial system and consequent flushing of stored basal water and sediment [*Kamb et al.*, 1985], coincided with the slowdown at KNS1 after S3 (Figure 3a) and followed by less than 24 h reductions in lake area between 1200 and 1400 m (Figure 3f). A similar coincidence between ice deceleration and discharge from the basal water system was observed following the surge of Variegated Glacier, Alaska [*Kamb et al.*, 1985], and further supports a hydrological forcing mechanism for S3.

5. Conclusion

[27] Our data show that beyond 36 km up glacier of the terminus of Kangiata Nunata Sermia, a large marine-terminating outlet glacier in southwest Greenland, both seasonal and shorter-term ice flow variations are principally

[1] Auxiliary material files are available in the HTML. doi:10.1029/2010JF001948.

Table 2. The Net Effect of Seasonal Ice Flow Variations (Summer Speedup and Extra Slowdowns) on Annual Ice Speed for KNS1–KNS4[a]

	Defined Background Speed (m yr^{-1})	Mean Summer Speed (m yr^{-1})	Summer Versus Winter Percentage Difference	Percentage Annual Speed Change
KNS1	382	396	+3.7	+0.7
KNS2	216	226	+4.2	+0.9
KNS3	173	180	+3.7	+0.5
KNS4	97	99	+2.1	+0.3

[a]The summer period begins on day 155 for KNS1 and KNS2 and on day 180 for KNS3 and KNS4 and finishes at the end of our survey at each site. Ice speed for all nonsummer days is prescribed as the defined background speed.

controlled by local hydromechanical forcing rather than by changes at the calving front. At our transect, as has been demonstrated for land-terminating margins [e.g., *Bartholomew et al.*, 2010], surface melt forcing drives evolution of the subglacial drainage system, leading to uplift, acceleration, and subsequent slowdown following the establishment of an efficient channelized hydrological system [*Bartholomaus et al.*, 2008; *Das et al.*, 2008]. Lake drainages play a key role in forcing subglacial drainage evolution and often coincide with the largest speedup events. Our data support the conclusion that lakes provide sufficient accumulations of surface water to (1) force hydrofracture through thick cold ice, (2) pressurize the existing drainage system, and (3) develop efficient subglacial channels which reduce the sensitivity of the subglacial hydrological system to subsequent variations in meltwater flux. More generally, our data support previous observations [e.g., *Fudge et al.*, 2009] and modeling [e.g., *Schoof*, 2010] demonstrating that it is rapid variations in the meltwater supply to the subglacial drainage system that have the greatest effect on ice flow. In this sense, at distances >36 km from the calving front, KNS behaves similarly to other smaller glaciers elsewhere [*Iken*, 1981; *Kamb et al.*, 1994].

[28] However, as has been previously reported at locations closer to the margins of other marine-terminating glaciers [*Joughin et al.*, 2008a], the overall effect of observed seasonal flow variations on the annual motion of KNS is small compared to those reported for land-terminating glaciers [*Bartholomew et al.*, 2010] (Table 2). This in part is because the speedups are compensated for by slowdowns beneath background speed associated with the establishment of an efficient subglacial drainage system, which are greater than those reported at land-terminating margins. The short-lived speedups at KNS are also relatively small compared to those observed at land-terminating margins (up to 40% rather than 220% [*Bartholomew et al.*, 2010]). Fast flowing outlet glaciers, such as KNS, may be less sensitive to seasonal variations in surface meltwater input because basal shear heating already provides a supply of subglacial water that could maintain relatively high basal water pressures [*Joughin et al.*, 2008a] if the subglacial drainage system remains inefficient. Marine-terminating outlet glaciers tend to be deep and narrow so that lateral shear stress is likely to provide a greater proportion of the total resistance to ice flow, and changes in basal friction will have relatively less impact on ice speed [*Joughin et al.*, 2008a]. It is important to note, however, that our most down-glacier site (KNS1) is at a similar elevation to the most up-glacier site reported by *Bartholomew et al.* [2010], where the effect on annual ice speed of seasonal variations was 6%. Our results suggest that despite the above differences, sufficiently far inland from the calving front, the ice flow response of a large GRIS marine-terminating outlet glacier to variations in surface melting is similar to that of land-terminating outlet glaciers.

[29] **Acknowledgments.** We thank Tim Bartholomaus, two anonymous reviewers, and the Associate Editor for constructive comments that improved the paper. We thank U.K. Natural Environment Research Council (NERC, through a studentship to I.D.B. and grants to P.W.N., D.W.F.M., and M.A.K) and the Edinburgh University Moss Centenary Scholarship (I.D.B.) for financial support. M.A.K. was also funded by a RCUK academic fellowship. GPS equipment and training were provided by the NERC Geophysical Equipment Facility.

References

Amundson, J., M. Fahnestock, M. Truffer, J. Brown, M. Luthi, and R. Motyka (2010), Ice melange dynamics and implications for terminus stability, Jakobshavn Isbrae, Greenland, *J. Geophys. Res.*, *115*, F01005, doi:10.1029/2009JF001405.

Andersen, M. L., et al. (2010), Spatial and temporal melt variability at Helheim Glacier, east Greenland, and its effect on ice dynamics, *J. Geophys. Res.*, *115*, F04041, doi:10.1029/2010JF001760.

Anderson, R., S. Anderson, K. MacGregor, E. Waddington, S. O'Neel, C. Riihimaki, and M. Loso (2004), Strong feedbacks between hydrology and sliding of a small alpine glacier, *J. Geophys. Res.*, *109*, F03005, doi:10.1029/2004JF000120.

Balise, M., and C. Raymond (1985), Transfer of basal sliding variations to the surface of a linearly viscous glacier, *J. Glaciol.*, *31*, 308–318.

Bamber, J., S. Ekholm, and W. Krabill (2001), A new, high-resolution digital elevation model of Greenland fully validated with airborne laser altimeter data, *J. Geophys. Res.*, *106*, 6733–6745.

Bartholomaus, T. C., R. S. Anderson, and S. P. Anderson (2008), Response of glacier basal motion to transient water storage, *Nat. Geosci.*, *1*, 33–37.

Bartholomew, I., P. Nienow, D. Mair, A. Hubbard, M. King, and A. Sole (2010), Seasonal evolution of subglacial drainage and acceleration in a Greenland outlet glacier, *Nat. Geosci.*, *3*, 408–411, doi:10.1038/NGEO863.

Box, J., and K. Ski (2007), Remote sounding of Greenland supraglacial melt lakes: Implications for subglacial hydraulics, *J. Glaciol.*, *53*, 257–265.

Catania, G., and T. Neumann (2010), Persistent englacial drainage features in the Greenland Ice Sheet, *Geophys. Res. Lett.*, *37*, L02501, doi:10.1029/2009GL041108.

Chen, G. (1998), GPS kinematic positioning for the airborne laser altimetry at Long Valley, California, Ph.D. thesis, Mass. Inst. of Technol., Cambridge.

Das, S. B., I. Joughin, M. Behn, I. Howat, M. A. King, D. Lizarralde, and M. P. Bhatia (2008), Fracture propagation to the base of the Greenland Ice Sheet during supraglacial lake drainage, *Science*, *320*, 778–781, doi:10.1126/science.1153360.

Echelmeyer, K., and W. Harrison (1990), Jakobshavn Isbrae, west Greenland, seasonal variations in velocity—Or lack thereof, *J. Glaciol.*, *36*, 82–88.

Fudge, T., J. Harper, N. Humphrey, and W. Pfeffer (2009), Rapid glacier sliding, reverse ice motion and subglacial water pressure during an autumn rainstorm, *Ann. Glaciol.*, *50*, 101–108.

Gumley, L., J. Descloitres, and J. Schmaltz (2007), Creating reprojected MODIS true color images: A tutorial, version 1.0.1, Univ. of Wis.-Madison, Madison.

Herring, T., R. King, and S. McClusky (2010), Documentation for the GAMIT GPS analysis software, version 10.3, Mass. Inst. of Technol., Cambridge.

Howat, I., I. Joughin, S. Tulaczyk, and S. Gogineni (2005), Rapid retreat and acceleration of Helheim Glacier, east Greenland, *Geophys. Res. Lett.*, *32*, L22502, doi:10.1029/2005GL024737.

Howat, I., I. Joughin, and T. Scambos (2007), Rapid changes in ice discharge from Greenland outlet glaciers, *Science*, *315*, 1559–1561, doi:10.1126/science.1138478.

Howat, I., J. Box, Y. Ahn, A. Herrington, and E. McFadden (2010), Seasonal variability in the dynamics of marine-terminating outlet glaciers in Greenland, *J. Glaciol.*, *56*, 601–613.

Howat, I. M., S. Tulaczyk, E. Waddington, and H. Björnsson (2008), Dynamic controls on glacier basal motion inferred from surface ice motion, *J. Geophys. Res.*, *113*, F03015, doi:10.1029/2007JF000925.

Huybrechts, P., J. Gregory, I. Janssens, and M. Wild (2004), Modelling Antarctic and Greenland volume changes during the 20th and 21st centuries forced by GCM time slice integrations, *Global Planet. Change*, *42*, 83–105.

Iken, A. (1981), The effect of the subglacial water pressure on the sliding velocity of a glacier in an idealized numerical model, *J. Glaciol.*, *27*, 407–421.

Iken, A., and R. A. Bindschadler (1986), Combined measurements of subglacial water pressure and surface velocity of Findelengletscher, Switzerland: Conclusions about drainage system and sliding mechanism, *J. Glaciol.*, *32*, 101–119.

Iken, A., H. Rothlisberger, A. Flotron, and W. Haeberli (1983), The uplift of Unteraargletscher at the beginning of the melt season—A consequence of water storage at the bed?, *J. Glaciol.*, *29*, 28–47.

Joughin, I., S. Tulaczyk, M. Fahnestock, and R. Kwok (1996), A mini surge on the Ryder Glacier, Greenland, observed by satellite radar interferometry, *Science*, *274*, 228–230.

Joughin, I., S. Das, M. King, B. Smith, I. Howat, and T. Moon (2008a), Seasonal speedup along the western flank of the Greenland Ice Sheet, *Science*, *320*, 781–783, doi:10.1126/science.1153288.

Joughin, I., I. Howat, M. Fahnestock, B. Smith, W. Krabill, R. Alley, H. Stern, and M. Truffer (2008b), Continued evolution of Jakobshavn Isbrae following its rapid speedup, *J. Geophys. Res.*, *113*, F04006, doi:10.1029/2008JF001023.

Joughin, I., B. Smith, I. Howat, T. Scambos, and T. Moon (2010), Greenland flow variability from ice-sheet-wide velocity mapping, *J. Glaciol.*, *56*, 415–430.

Kamb, B. (1987), Glacier surge mechanism based on linked cavity configuration of the basal water conduit system, *J. Geophys. Res.*, *92*, 9083–9100.

Kamb, B., and K. A. Echelmeyer (1986), Stress-gradient coupling in glacier flow: 1. Longitudinal averaging of the influence of ice thickness and surface slope, *J. Glaciol.*, *32*, 267–298.

Kamb, B., C. Raymond, W. Harrison, H. Engelhardt, K. Echelmeyer, N. Humphrey, M. Brugman, and T. Pfeffer (1985), Glacier surge mechanism: 1982–1983 surge of Variegated Glacier, Alaska, *Science*, *227*, 469–479.

Kamb, B., H. Engelhardt, M. Fahenstock, N. Humphrey, M. Meier, and D. Stone (1994), Mechanical and hydrologic basis for the rapid motion of a large tidewater glacier: 2. Interpretation, *J. Geophys. Res.*, *99*, 14,231–15,244.

King, M. (2004), Rigorous GPS data-processing strategies for glaciological applications, *J. Glaciol.*, *50*, 601–607.

Krawczynski, M., M. Behn, S. Das, and I. Joughin (2009), Constraints on the lake volume required for hydro-fracture through ice sheets, *Geophys. Res. Lett.*, *36*, L10501, doi:10.1029/2008GL036765.

Lemke, P., et al. (2007), Observations: Changes in snow, ice and frozen ground, in *Climate Change 2007: The Physical Science Basis. Contribution of Working Group I to the Fourth Assessment Report of the Intergovernmental Panel on Climate Change*, edited by S. Solomon et al., chap. 4, pp. 337–384, Cambridge Univ. Press, New York.

Luckman, A., and T. Murray (2005), Seasonal variation in velocity before retreat of Jakobshavn Isbrae, Greenland, *Geophys. Res. Lett.*, *32*, L08501, doi:10.1029/2005GL022519.

Mair, D., P. Nienow, M. Sharp, T. Wohlleben, and I. Willis (2002), Influence of subglacial drainage system evolution on glacier surface motion: Haut Glacier d'Arolla, Switzerland, *J. Geophys. Res.*, *107*(B8), 2175, doi:10.1029/2001JB000514.

Mair, D., I. Willis, U. Fischer, B. Hubbard, P. Nienow, and A. Hubbard (2003), Hydrological controls on patterns of surface, internal and basal motion during three "spring events": Haut Glacier d'Arolla, Switerland, *J. Glaciol.*, *49*, 555–567.

Meier, M., S. Lundstrom, D. Stone, B. Kamb, H. Engelhardt, N. Humphrey, W. W. Dunlap, M. Fahnestock, R. M. Krimmel, and R. Walters (1994), Mechanical and hydrologic basis for the rapid motion of a large tidewater glacier: 1. Observations, *J. Geophys. Res.*, *99*, 15,219–15,229.

Moon, T., and I. Joughin (2008), Changes in ice front position on Greenland's outlet glaciers from 1992 to 2007, *J. Geophys. Res.*, *113*, F02022, doi:10.1029/2007JF000927.

Nick, F., A. Vieli, I. Howat, and I. Joughin (2009), Large-scale changes in Greenland outlet glacier dynamics triggered at the terminus, *Nat. Geosci.*, *2*, 110–114, doi:10.1038/ngeo394.

Nienow, P., M. Sharp, and I. Willis (1998), Seasonal changes in the morphology of the subglacial drainage system, Haut Glacier d'Arolla, Switzerland, *Earth Surf. Processes Landforms*, *23*, 825–843.

O'Neel, S., K. Echelmeyer, and R. Motyka (2001), Short-term flow dynamics of a retreating tidewater glacier: LeConte Glacier, Alaska, U.S.A., *J. Glaciol.*, *47*, 567–578.

Parizek, B., and R. Alley (2004), Implications of increased Greenland surface melt under global-warming scenarios: Ice sheet simulations, *Quat. Sci. Rev.*, *23*, 1013–1027.

Parry, V., P. Nienow, D. Mair, J. Scott, B. Hubbard, K. Steffen, and D. Wingham (2007), Investigations of meltwater refreezing and density variations in the snowpack and firn within the percolation zone of the Greenland Ice Sheet, *Ann. Glaciol.*, *46*, 61–68.

Pfeffer, W., M. Meier, and T. Illangasekare (1991), Retention of Greenland runoff by refreezing: Implications for projected future sea level change, *J. Geophys. Res.*, *96*, 22,117–22,124.

Pimentel, S., and G. Flowers (2010), A numerical study of hydrologically driven glacier dynamics and subglacial flooding, *Proc. R. Soc. A*, *467*, 537–558, doi:10.1098/rspa.2010.0211.

Price, S., A. Payne, G. Catania, and T. Neumann (2008), Seasonal acceleration of inland ice via longitudinal coupling to marginal ice, *J. Glaciol.*, *54*, 213–219.

Pritchard, H., R. Arthern, D. Vaughan, and L. Edwards (2009), Extensive dynamic thinning on the margins of the Greenland and Antarctic Ice Sheets, *Nature*, *461*, 971–975, doi:10.1038/nature08471.

Rignot, E., and P. Kanagaratnam (2006), Changes in the velocity structure of the Greenland Ice Sheet, *Science*, *311*, 986–990, doi:10.1126/science.1121381.

Rignot, E., J. Box, E. Burgess, and E. Hanna (2008), Mass balance of the Greenland Ice Sheet from 1958 to 2007, *Geophys. Res. Lett.*, *35*, L20502, doi:10.1029/2008GL035417.

Schoof, C. (2010), Ice-sheet acceleration driven by melt supply variability, *Nature*, *468*, 803–806, doi:10.1038/nature09618.

Shepherd, A., and D. Wingham (2007), Recent sea-level contributions of the Antarctic and Greenland Ice Sheets, *Science*, *315*, 1529–1532, doi:10.1126/science.1136776.

Shepherd, A., A. Hubbard, P. Nienow, M. King, M. McMillan, and I. Joughin (2009), Greenland Ice Sheet motion coupled with daily melting in late summer, *Geophys. Res. Lett.*, *36*, L01501, doi:10.1029/2008GL035758.

Shreve, R. (1972), Movement of water in glaciers, *J. Glaciol.*, *11*, 205–214.

Sneed, W. A., and G. S. Hamilton (2007), Evolution of melt pond volume on the surface of the Greenland Ice Sheet, *Geophys. Res. Lett.*, *34*, L03501, doi:10.1029/2006GL028697.

Spring, U., and K. Hutter (1981), Numerical studies of jökulhlaups, *Cold Reg. Sci. Technol.*, *4*, 227–244.

Sundal, A., A. Shepherd, P. Nienow, E. Hanna, S. Palmer, and P. Huybrechts (2009), Evolution of supra-glacial lakes across the Greenland Ice Sheet, *Remote Sens. Environ.*, *113*, 2164–2171.

Tedesco, M. (2007), Snowmelt over the Greenland and Antarctica Ice Sheets from spaceborne radiometric data: Extreme events and updated trends, *Geophys. Res. Lett.*, *34*, L02504, doi:10.1029/2006GL028466.

Tedesco, M., M. Serreze, and X. Fettweis (2008), Diagnosing the extreme surface melt event over southwestern Greenland in 2007, *Cryosphere*, *2*, 159–166.

Thomas, R. (2004), Force-perturbation analysis of recent thinning and acceleration of Jakobshavn Isbrae, Greenland, *J. Glaciol.*, *50*, 57–66.

Thomas, R., E. Frederick, W. Krabill, S. Manizade, and C. Martin (2009), Recent changes on Greenland outlet glaciers, *J. Glaciol.*, *55*, 147–162.

van de Wal, R., W. Boot, M. van den Broeke, C. Smeets, C. Reijmer, J. Donker, and J. Oerlemans (2008), Large and rapid melt-induced velocity changes in the ablation zone of the Greenland Ice Sheet, *Science*, *321*, 111–113, doi:10.1126/science.1158540.

van den Broeke, M., J. Bamber, J. Ettema, E. Rignot, E. Schrama, W. J. van de Berg, E. van Meijgaard, I. Velicogna, and B. Wouters (2009), Partitioning recent Greenland mass loss, *Science*, *326*, 984–986, doi:10.1126/science.1178176.

van der Veen, C. J. (2007), Fracture propagation as means of rapidly transferring surface meltwater to the base of glaciers, *Geophys. Res. Lett.*, *34*, L01501, doi:10.1029/2006GL028385.

Zwally, H., W. Abdalati, T. Herring, K. Larson, J. Saba, and K. Steffen (2002), Surface melt-induced acceleration of Greenland Ice Sheet flow, *Science*, *297*, 218–222, doi:10.1126/science.1072708.

I. D. Bartholomew, P. W. Nienow, and A. J. Sole, School of Geosciences, University of Edinburgh, Drummond Street, Edinburgh EH8 9XP, UK. (andrew.sole@ed.ac.uk)

M. J. Burke, Department of Geography, Simon Fraser University, Burnaby, BC V5A 1S6, Canada.

I. Joughin, Applied Physics Laboratory, University of Washington, 1013 NE 40th St., Seattle, WA 98105-6698, USA.

M. A. King, School of Civil Engineering and Geosciences, Newcastle University, Newcastle upon Tyne NE1 7RU, UK.

D. W. F. Mair, School of Geosciences, University of Aberdeen, Elphinstone Road, Aberdeen AB24 3UF, UK.